ANALYSIS AND BEHAVIOR OF PREEXISTING LANDSLIDES

BY

MANZOOR HUSSAIN

DISSERTATION

Submitted in partial fulfillment of the requirements
for the degree of Doctor of Philosophy in Civil Engineering
in the Graduate College of the
University of Illinois at Urbana-Champaign, 2010

Urbana, Illinois

Doctoral Committee:

Professor Timothy D. Stark, Chair
Associate Professor James H. Long
Assistant Professor Scott M. Olson
Professor Erol Tutumluer

ABSTRACT

The selection of shear strength parameters for the design and repair of landslide is important and difficult. Skempton (1964) concludes that if a failure has already occurred in clayey soils, any subsequent movement along the preexisting slip surface will be controlled by the drained residual strength. Skempton (1985) suggests that the strength of a clay also will be at or close to the residual value on slip surfaces in soliflucted slopes, bedding shears in folded strata, sheared joints or faults, and after an embankment failure. Therefore, the drained residual shear strength has been and still is being used for analysis of slopes that contain a preexisting shear surface.

Some recent research suggests that preexisting shear surfaces may exhibit a shear strength that is greater than the drained residual value after a period of time in which the slope remains stable, i.e., does not experience shear displacement. If so, strength recovery could impact landslide mitigation and remedial measures because the increased strength could result in savings to insurance companies and/or landslide mitigating agencies. Thus, it is important to determine if the shear strength after a long rest period during which no movement occurred still corresponds to the residual strength or has attained a strength that is greater than the residual value.

The main objectives of this research are to study the shear strength and long term behavior of landslides and in particular preexisting shear surfaces. The research involved laboratory testing to determine the strength recovery, if any, of cohesive soils with varying plasticity, effective normal stress, and the applicability of the recovered strength to remedial measures and the back-analysis of landslides. Some of the issues addressed include (a) if the shear strength increases from the residual value with time, (b) what is the maximum recovered strength, (c) how long does it take to reach the maximum recovered strength, (d) if the strength increases with time, does the strength return to the residual value with additional shear displacement and if so how much shear displacement is required to reduce the strength back to the residual value, and (d) what is the maximum shear strength that can be obtained from strength recovery and used for design purposes.

Back-analysis of landslides is important for evaluating the mobilized recovered strength and thus back-analysis procedures were reviewed and augmented. Empirical correlations for drained residual and fully softened friction angles are important in the back-analysis of landslides because they provide estimates for use in preliminary design and serve as a check for laboratory test and back-analysis results. The empirical correlations for drained residual and fully softened friction angles proposed by Stark et al. (2005a) in graphical form are widely used in geotechnical practice. To capture the stress dependent nature of the residual and fully softened failure envelopes, a trend line for an effective normal stress of 50 kPa was developed to better describe the stress dependent nature of the drained residual strength and data for seven additional soils were added to the database. In addition, mathematical equations were developed for each trend line and which can be used to estimate stress dependent failure envelopes for use in stability analyses. These mathematical expressions were incorporated in a spreadsheet that can be used to estimate the shear strength parameters of a soil using only two index properties, i.e., liquid limit and clay-size fraction. These mathematical expressions were also coded in Microsoft Visual Basic (VB 6.0) that may facilitate slope stability software developers incorporating the expressions in software to facilitate the use of stress dependent strength parameters in stability analyses.

To my parents

Whose lives have been and

always will be emblems of

total dedication and

unparalleled faith

In the Name of Allah, the Most Beneficent, the Most Merciful

ACKNOWLEDGEMENTS

All thanks and praises be to *Allah* (God), the Lord, the Creator, and the Sustainer of the Universe, *Who* taught knowledge to *His* human beings, and guided me to complete my research successfully.

I am indebted to the Government of Pakistan for the generous financial support for my studies in the United States.

I wish to express my sincere thanks and profound sense of gratitude to Professor Timothy D. Stark, my adviser and mentor, for his genuine concern, advice and enthusiastic encouragement throughout the course of this research. Indeed it has been a great learning experience to conduct research and write this thesis under his close supervision. I highly value my association with him.

My sincere gratitude and heartfelt thanks to the group of renowned scholars, Professor J. H. Long, Professor E. Tutumluer, and Professor S. M. Olson, for their willingness to serve on my dissertation committee. My special thanks to Professor Gholamreza Mesri for providing me initial guidance to perform direct shear tests for my research.

My special thanks to Brigadier Syed Muhammad Jamil, Ph.D., an alumnus of University of Illinois for his initial guidance and helping me to select this prestigious institution for pursuits of my academic goals. My special thanks to Brigadier Gulfam Alam, Ph.D. for providing all his administrative and moral support for entire duration of my studies.

My thanks to all the friends and colleagues for their encouragement and support during my research and stay at Illinois. I would like to thank my friends Aqeel Ahmed, Michigan State University, Colonel Ejaz Hussain, Dr. Muhammad Irfan, and Dr. Muhammad Bilal Khurshid, Purdue University, for their encouragement and support during my stay in the United States. I would also like to thank my friends Aamir Wali, Abdul Qudoos Khan, Sarfraz Ahmed, Kamran Akhtar, Adeel Zafar, Muhammad Kashif, Ali Tahir Kazmi, Jehanzeb Abbas, Kashif Manzoor, Salman Noshear Arshad, Usman Tariq, Qazi Aurangzeb, Azeem Sarwar, and many other, for providing me and my family a family environment during our stay in Urbana. I would also like

to thank the Central Illinois Mosque and Islamic Center for providing me congenial environment for fulfilling spiritual and religious obligations.

I am grateful to my brother Faiz Ahmad Faiz, for all his endeavors, encouragements and supports without which it would have been difficult for me to complete this research. His frequent visits have been source of motivation and helped me boosting my morale. I am also grateful to my other family members, brother and sisters, for always praying for my success and encouraging me to complete my studies.

I am grateful to my wife, Saima Manzoor, for her continued support and encouragement and my children, Qasim, Minahel, and Basim, for their patience and understanding during the course of this research.

A very special thanks is due to my parents for their best wishes and prayers which brought me all the successes in this life. I am forever indebted to their life long struggles and sacrifices for my wellbeing of all sorts. I wish they could have seen my success in their lives. May ***Allah*** (God) bless them, showers ***His*** bounties and bestows ***His*** blessings on them.

Table of Contents

CHAPTER 1: INTRODUCTION

1.1 Statement of the Problem

The selection of shear strength parameters for the design and repair of slopes in landslide prone areas is important and difficult. Skempton (1964) concludes that if a failure has already occurred in clayey soils, any subsequent movement along the preexisting slip surface will be controlled by the drained residual strength. Skempton (1985) suggests that the strength of a clay also will be at or close to the residual value on slip surfaces in soliflucted slopes, bedding shears in folded strata, sheared joints or faults, and after an embankment failure. Therefore, the drained residual shear strength has been and is still being used for analysis of slopes that contain a preexisting shear surface.

Some recent research suggests that preexisting shear surfaces may exhibit a higher shear strength than the drained residual value after a period of time in which the slope remains stable, i.e., does not experience shear displacement. If so, strength recovery could impact landslide mitigation and remedial measures because the increased strength could result in savings to insurance companies and/or landslide mitigating agencies. There are many ancient landslides that are stable and not undergoing any movement even though the residual strength had been reached at the end of sliding/movement. It is important to determine if the shear strength after a long rest period during which no movement occurred still corresponds to the residual strength or has attained a strength that is greater than the residual value. If some strength recovery occurs on a preexisting shear surface it may impact the back-analysis of ancient and recent landslides.

For low plasticity soils, with a small difference between the fully softened and residual strengths, the importance of strength recovery may not be significant. However, high plasticity soils exhibit a large difference between fully softened and residual strengths so the recovered shear strength, if any, may be significantly greater than the residual value. Therefore, it is important to determine the existence and magnitude of recovered shear strength of preexisting shear surfaces as a function of time. If a preexisting shear surface exhibits strength recovery in a short period of time, i.e., prior to remediation, it might be possible to design the remedial

measures using a shear strength greater than the drained residual strength for the problematic layer. This higher strength could reduce the cost of the remedial measures.

Back-analysis of slopes containing a preexisting shear surface is an effective method to evaluate the mobilized shear strength along the failure surface and assess the level of improvement required to make the slope safe. In the back-analysis of a landslide, conditions at the time of failure are assumed while assuming the factor of safety to be at or near unity. The most important assumptions in a back-analysis of a landslide are the shear strength parameters of the materials present along the failure surface and the phreatic surface at the time of failure yielding a factor of safety equal or near unity. Because monitoring of the phreatic surface or the porewater pressures is rarely performed before the slide, the phreatic surface at the time of failure is usually estimated. This allows the phreatic surface to be adjusted to obtain a factor of safety of unity. Even though back-analysis is assumed to yield a better shear strength estimate than laboratory tests because of sample disturbance, lack of a representative sample, and testing difficulties, there are uncertainties in a back-analysis. The important aspect of a back-analysis is that all assumptions that are conservative during slope design are usually unconservative in a back-analysis. For example, considering a high phreatic surface in the stability analysis is conservative but it is unconservative in the back-analysis because it will result in an overestimate of the back-calculated shear strength.

Empirical correlations for drained residual and fully softened friction angles are important in the back-analysis of landslides because they provide estimates for use in preliminary design and serve as a check for laboratory test results. The empirical correlations for drained residual and fully softened friction angles proposed by Stark et al. (2005a) in graphical form are widely accepted in geotechnical practice. To capture the stress dependent nature of the residual and fully softened failure envelopes, a 50 kPa trend line and additional data were added. In addition, mathematical equations were developed for each trend line and can be used to estimate stress dependent failure envelopes for use in stability analyses.

1.2 Research Objectives

The main objectives of this research are to study the shear strength and long term behavior of landslides and in particular preexisting shear surfaces. The research involves

laboratory testing to determine the strength recovery of cohesive soils with varying plasticity and applicability of the laboratory recovered shear strength to remedial measures and the back-analysis of landslides. Some of the issues addressed include (a) if the shear strength increases from the residual value with time, (b) how long does it take to reach the maximum recovered strength, (c) if the strength increases with time, does the strength return to the residual value with additional shear displacement and if so how much shear displacement is required to reduce the strength back to the residual value, and (d) the maximum shear strength that can be obtained from strength recovery and used for design purposes.

To accomplish these objectives, the study involved the following major tasks:

(1) Evaluation of existing literature on strength recovery along preexisting shear surfaces.

(2) Evaluate the suitability of laboratory shear devices for strength recovery tests.

(3) Development of laboratory test procedures to measure strength recovery along preexisting shear surfaces for a torsional ring shear and direct shear box device.

(4) Selection of soils for laboratory strength recovery testing covering a range of plasticity.

(5) Measurement of recovered shear strength in the laboratory using a torsional ring shear device and a direct shear box using proposed testing procedure.

(6) Analysis of laboratory strength recovery test results with a view to recommend recovered shear strength for design.

(7) Evaluating the probable causes of strength recovery along the preexisting shear surfaces.

(8) Analysis of field case histories involving preexisting shear surfaces that indicate of strength recovery during the period of no movement.

(9) Evaluation of uncertainties involved in the back-analysis of landslides.

(10) Development of a back-analysis procedure for preexisting/reactivated and first-time landslides.

(11) Evaluation of laboratory shearing devices and test procedures for measurement of drained residual and fully softened shear strength.

(12) Evaluation of existing empirical correlations for residual and fully softened shear strengths and/or friction angles.

(13) Evaluating the effect of sample preparation on index properties, i.e., LL and CF, and drained residual and fully softened friction angles.

(14) Development of an ASTM Test method for measuring fully softened shear strength in a torsional ring shear device.

(15) Development of a correlation between values of LL and CF estimated using ASTM standards and values of LL and CF estimated from a material processed through Number 200 sieve for highly overconsolidated clays with induration (aggregation).

(16) Development of mathematical expressions for drained residual and fully softened empirical correlations.

1.3 Scope

The thesis is divided into six chapters. Chapter 1 is this introduction and Chapter 2 presents a review of existing literature on strength recovery along preexisting shear surfaces. Evaluation of existing literature suggests the possibility of strength recovery based on laboratory test results and was used to determine and evaluate the type of laboratory shear devices and testing procedures used by different researchers.

Suitability of the available laboratory shear devices for performing strength recovery tests is presented in Chapter 3. Based on the suitability of available laboratory shear devices, a new strength recovery test procedure for a torsional ring shear device and a direct shear box were developed. The torsional ring shear strength recovery testing program for four soils is presented along with the evaluation of test results.

Chapter 3 presents direct shear strength recovery test results and analysis for one of the four soils tested using the torsional ring shear device and a comparison with the torsional ring shear strength recovery test results. The probable causes of shear strength recovery along the preexisting shear surfaces are also discussed in this chapter. Recommendations for the use of recovered shear strength in design are also presented in Chapter 3.

Chapter 4 presents the back-analyses of two case histories that suggest some strength recovery during the period of no movement. Detailed back-analyses performed using varying field conditions, the measured residual shear strength, and empirically derived recovered shear strength envelope from the strength recovery test results presented in Chapter 3 are also presented in Chapter 4.

The uncertainties involved in the back-analysis of landslides are discussed in Chapter 5 with a view to recommending a back-analysis procedure for preexisting/reactivated and first-time landslides. The uncertainties involved in a back-analysis are discussed in detail by providing examples from existing literature. Recommendations for applicable shear strengths for remedial design are also presented in this chapter.

Chapter 6 presents a review and analysis of available laboratory shearing devices and testing procedures for measuring drained residual and fully softened shear strength. Available empirical correlations for residual and fully softened friction angles are presented and analyzed in this chapter to determine the reliability of such existing empirical correlations. Chapter 6 also presents new empirical correlations for drained residual and fully softened friction angles based on additional data, trend-lines for an effective normal stress of 50 kPa, and mathematical expressions for each trend line. Chapter 6 also discusses the effect of sample preparation on basic index properties, i.e., LL and CF, and on engineering properties, i.e., drained residual and fully softened friction angles. Relationships between values of LL and CF estimated using ASTM test methods and values of LL and CF estimated using material processed through Number 200 sieve for highly overconsolidated clays with induration (aggregation) are also presented in this chapter. A spreadsheet developed herein using the mathematical equations is described in Chapter 6.

Finally, Chapter 7 presents the summary and conclusions of the research.

CHAPTER 2: LITERATURE REVIEW AND DISCUSSION - SHEAR STRENGTH IN PREEXISTING LANDSLIDES

2.1 Introduction

In landslide mitigation and planning of remedial measures, back-analysis is used to obtain a better estimate of the mobilized shear strength than the laboratory tests because of sample disturbance, lack of representative samples, and testing difficulties. However, there are many uncertainties involved in a back analysis which are discussed in Chapter 5. Two important uncertainties are; available shear strength of the other materials and location of phreatic surface at the time of failure. Because most natural slopes are not instrumented prior to failure, correct information on the location of the phreatic surface at the time of failure is usually not available. Even if the slope is being monitored for pore water pressures using piezometers, reliability of the data may be questionable due to the problems associated with the location, installation, operation, and response of the piezometers. Thus in a back-analysis of a landslide or slope failure, the phreatic surface can be varied to obtain a FS at or near unity using the drained residual shear strength of the weak layer along the failure surface and measured in the laboratory as suggested by Skempton (1964, 1970 and 1985). Varying the phreatic surface or average pore pressure ratio (r_u) to obtain a factor of safety equal or close to unity results in a range of back-calculated phreatic surface or shear strength for the landslide.

Based on the back-analysis of a landslide and laboratory test results, D'Appolonia et al. (1967) present the concept of healing of shear surfaces. Subsequently, Ramiah et al. (1973), Angeli et al. (1996 and 2004), Gibo et al. (2002), Stark et al. (2005a), and most recently Carrubba and Del Fabbro (2008) also suggest that preexisting shear surfaces in clay soils after obtaining a residual conditions may heal and show a strength greater than laboratory measured drained residual shear strength when subjected to a rest period during which no movement occurs. All of these researchers use different shear devices, shear displacement rates, test procedures, effective normal stresses, and rest periods to determine the strength gain in the clay soils. Furthermore, all of the researchers, except Gibo et al. (2002), report test results at effective normal stresses of 100 kPa or less. Gibo et al. (2002) conclude that strength recovery is possible

in soil with a large amount of silt and sand particles at effective normal stresses below 100 kPa whereas all other researchers determined a greater possibility of strength recovery in high plasticity soils. Because the peak strength reduces to a residual value with a small shear displacement, Angeli et al. (2004) and Stark et al. (2005) recommend using recovered strength in remedial design with great caution.

These studies also conflict with Skempton's (1964 and 1985) recommendation of using the drained residual strength for preexisting shear surfaces. The objective of this study is to address this conflict and develop recommendations for the shear strength of preexisting shear surfaces. This chapter summarizes the previous research on strength recovery and healing of preexisting shear surfaces.

2.2 Drained Residual Shear Strength in Landslides

Skempton (1964) suggests that the drained residual strength is mobilized along preexisting shear surfaces caused by previous landsliding and tectonic shearing. Skempton (1964) acknowledges some initial work on residual strength of clay soils by other authors e.g., Tiedmann (1937), Hvorslav (1937), Haefeli (1938 and 1950), and Turnbull (1952), but provides the first slope design recommendations using the residual shear strength.

Skempton and Petley (1967) report direct shear test results performed on intact specimens obtained from the principal slip surface and other surfaces containing joints and minor shears from various landslides. Skempton and Petley (1967) report that specimens obtained from principal shear surfaces in landslides and tectonic shear zones show a shear strength equal or close to the residual value; whereas surfaces containing joints and minor shears show a peak strength greater than the residual strength (Figure 2.1). This peak strength observed in specimens containing joints and minor shears was reduced to the residual value after small shear displacement thus exhibiting a brittle shear behavior. Skempton and Petley (1967) suggest that surfaces containing joints and minor shears may have not obtained a residual condition in the field due to insufficient shear displacement or movement that may have resulted in a strength greater than residual value. Skempton and Petley (1967) conclude that the strength along the principal slip surfaces and preexisting shear surfaces of reactivated landslides is considered to be

equal or close to the residual value and also suggest that this conclusion holds even if there is no new movement during the past 10,000 years or more, i.e., no healing.

Skempton (1970) affirms the use of the residual strength in the analysis of reactivated landslides in stiff fissured clays. Skempton (1970) concludes that in all clays the residual strength will be reached after a continuous principal shear surface has developed which appears to be attained typically after mass movements on the order of several feet.

Skempton (1985) suggests that "When tests are satisfactorily carried out on samples containing a fully developed slip surface or shear surface, the residual strength is recovered at virtually zero displacement." Skempton (1985) concludes that "Measurements of strength on natural shear surfaces agree, within the practical limits of variation, with values derived from back-analysis of reactivated landslides."

Chandler (1984) presents a study of reactivated landslides which shows the back-calculated friction angles are 2º to 3º greater than those measured using a ring shear device on slip surface specimens (see Figure 2.2). Chandler (1984) did not discuss the possibility of strength recovery of the preexisting shear surfaces and attributed the difference in friction angle to movement on a single shear plane in the ring shear device versus different shear surfaces or a shear zone in the field resulting in a high strength.

Chandler (1984) uses four case histories of landslides in London clay to compare back-calculated residual stress ratios with laboratory direct shear and ring shear measured residual stress ratios. The interesting aspect of the resulting comparison, shown in Figure 2.2, is the stress ratios determined from the back-calculated case histories and from the direct shear testing are in agreement but the ring shear stress ratios are lower. Direct shear test data obtained from Skempton (1984) through personal communication with Chandler (1984) shows large scatter (see Figure 2.2). Although some direct shear data points of Skempton (1984) and most of the Bromhead and Curtis (1983) direct shear data are in agreement with the ring shear test data, the majority of the direct shear data from Skempton (1984) lie above ring shear test data. No information is available on the direct shear tests or the samples used, e.g., sample obtained from the slip surface or not of these landslides. These direct shear tests may have been performed on London clay samples obtained from non-slip surface areas and yielded a strength greater than the

ring shear data because of problems trimming and orienting the specimens in the direct shear device. Furthermore, it is well known that direct shear devices usually yield higher residual stress ratios than a ring shear device (e.g., Stark and Eid, 1992) because of the limited shear displacement which can be imposed. The difference between the back-calculated and ring shear residual strengths may also be explained by the possibility of healing/strength recovery of preexisting shear surfaces. Therefore, during the present study the four London clay landslide case histories used by Chandler (1984) were evaluated to better explain the results shown in Figure 2.2. Uncertainties involved in the back-analysis, discussed in Chapter 5, were considered to investigate the reliability of the back-calculated stress ratios reported by Chandler (1984).

The landslide at Herne Bay analyzed by Bromhead (1978) is a deep-seated landslide which has limited applicability to strength recovery because significant strength gain was only observed at low effective normal stresses in the laboratory testing conducted during this study and discussed in Chapter 3. Although the landslide at Sudbury Hill analyzed by Skempton (1977) is a shallow landslide, uncertainties in post failure slope geometry, location of failure surface, and porewater pressures at the time failure exist which make the back-calculated residual stress ratios uncertain. For example, Skempton (1977) assumed a critical failure surface and a piezometric surface to perform a back-analysis because no piezometric data was available. The landslide at Hadleigh Cliff, discussed by Hutchinson and Gostelow (1976), is a retrogressive landslide and thus contains many uncertainties involved in locating the critical slide mass and failure surface. Because Chandler (1984) does not report the failure surface selected for the back-analysis, it is difficult to confirm Chandler's (1984) back-analysis.

The landslide at Stag Hill near Guildford, Surrey, studied by Skempton and Petley (1967), was used herein to verify the back-analysis results shown by Chandler (1984) in Figure 2.2. Using the post failure geometry, observed slip surface, and back-calculated residual stress relationship shown in Figure 2.2, a FS of unity (FS=1.0) was obtained for an average pore pressure ratio, r_u, of 0.3 (see Table 2.1). This value of r_u was selected based on a conclusion by Skempton (1977) that in the absence of reliable piezometric data at any given site containing London clay, a reasonable value of r_u is 0.3 for back-analysis and/or design. Skempton (1977) also suggested a range of r_u values from 0.25 to 0.35 for landslides in London clay. A back-analysis of Stag Hill landslide near Guildford was performed herein using the same slope

geometry, observed failure surface (see Figure 2.3), and a stress dependent failure envelope developed from the empirical correlation presented in Figure 6.24 using LL = 83% and CF=55% of London clay. This back-analysis yielded FS = 0.92 for r_u = 0.3, and FS = 1.0 for r_u = 0.23 (see Table 2.1). This failure envelope developed from the empirical correlation lies between the failure envelopes suggested by Chandler (1984) from the back-analysis and from the ring shear test results (see Figure 2.4). Thus, the failure envelope developed from the ring shear test results by Chandler (1984), shown in Figures 2.2 and 2.4, will yield a FS less than unity for r_u = 0.3 which may not be appropriate. The absence of reliable piezometric data at the time of failure results in uncertainty in this back-analysis.

In summary, the reevaluation of the four landslide case histories used by Chandler (1984) revealed uncertainties in the back-analysis input parameters which unfortunately prevent a complete explanation of the difference between the back-calculated and ring shear residual strengths shown in Figure 2.2.

2.3 Strength Recovery along Preexisting Shear Surfaces

Previous research on strength recovery/healing discussed herein is based on laboratory test results using three different types of shear devices, a direct shear device and two different types of ring shear devices, i.e., Bromhead (1979) and a Japanese ring shear device by Gibo (1994)). In direct shear, shearing occurs in the gap between top and bottom halves of the shear box. In the Bromhead ring shear device (Bromhead, 1979), shearing occurs at the top of a thin annular specimen, 5 mm thick (smear type shearing). In the Japanese ring shear device (Gibo, 1994) which is similar to the Bishop et al. (1971) ring shear device, shearing occurs near mid-height of an annular specimen.

Major work by some researchers (Ramiah et al., 1973, Angeli et al., 1996 and 2004, Gibo et al., 2002, Stark et al., 2005, and Carrubba and Del Fabbro, 2008) suggest strength recovery can occur along preexisting shear surfaces in reactivated landslides based on laboratory strength recovery tests. However, these suggestions are not supported or confirmed by field observation and/or back-analysis of case histories that show a strength recovery. Thus, the existence of strength recovery in the field is not known. Laboratory strength recovery test results presented by

various researchers are discussed in this chapter, whereas, some case histories suggesting/ supporting strength recovery/healing of shear surfaces are discussed in Chapter 4.

2.3.1 Strength Recovery using Direct Shear Tests

2.3.1.1 Direct Shear Tests on Intact/Undisturbed Shear Surface Specimen

The concept of "healing" of shear surfaces was presented by D'Appolonia et al. (1967) while investigating a colluvial slope in Weirton, West Virginia. The project involves an old landslide therefore the residual strength should have governed the slope stability. But the back-analyses of the landslide performed by D'Appolonia et al. (1967) suggests the soil along the failure surface exhibited a strength greater than the residual value measured in laboratory direct shear tests. They concluded that the strength gain prevented any renewal of movement along the preexisting failure surface. Detailed discussion on the landslide and its back-analysis is presented in Chapter 4 whereas discussion of the laboratory direct shear test results is presented herein.

D'Appolonia et al. (1967) located the preexisting slip surface by the presence of slickensides along the colluvium-alluvium interface to obtain representative block samples of the shear surface. The block samples obtained from the slip surface and used in the direct shear and triaxial compression tests have LL = 51%, PI = 25%, CF = 55% and natural water content, w_0 = 26%. D'Appolonia et al. (1967) established the drained and undrained soil strength parameters from consolidated-drained direct shear tests and consolidated undrained triaxial compression tests with pore pressure measurements on undisturbed and remolded block samples obtained from exposed slickensided surfaces at the top and toe of slope. Thus, these samples were obtained from shallow depths and exposed to a low effective normal stress.

The direct shear specimens were prepared by trimming the block samples, placing them in the direct shear apparatus, applying a normal stress at least twice the insitu effective overburden stress and submerging the specimens. The specimens were unloaded to the insitu effective normal stress and then sheared at a strain rate less than 0.127 mm/min. The specimens were sheared to a large displacement using the reversal procedure described by Skempton (1964) and the peak strengths were noted in each test. The results of the drained direct shear tests performed on samples obtained from the top and bottom of the slope, are shown with circles in

Figure 2.5a . Open circles/symbols denote peak strength whereas closed/solid circles/symbols denote the residual strength as shown in Figure 2.5a.

Because the intact specimens were obtained from the top and bottom of the slope and tested under insitu effective normal stress conditions less than 38 kPa, most of the specimens were exposed to a low effective normal stress. Only two tests were conducted at a greater effective normal stresses, one at 71.8 kPa (1500 psf) and the other at 105 kPa (2200 psf). Direct shear residual strength test results of using remolded specimens at effective normal stresses of 98 kPa (2050 psf) and 196 kPa (4100 psf) are shown with closed/solid triangles in Figure 2.5a.

D'Appolina et al. (1967) use a linear Mohr-Coulomb failure envelope to estimate the peak strength parameters of effective stress cohesion, c', of 7.66 kPa (160 psf) and drained peak friction angle, ϕ', of 20º and residual strength parameters $c' = 0$ and $\phi'_r = 16^o$ (see Figure 2.5a). Direct shear tests on remolded slide plane material also show $\phi'_r = 16^o$ which is in agreement with the drained residual friction angle values measured on intact specimens.

D'Appolonia et al. (1967) also performed triaxial compression tests using isotropically consolidated specimens, subjected to a back pressure to ensure 100% saturation and undrained shearing with pore pressure measurements. The peak and residual shear strengths were established in triaxial compression tests and are $c' = 9.58$ kPa (200 psf) and $\phi' = 19^o$ whereas the large axial strain, i.e., near residual strength parameters are $c' = 0$ and $\phi'_r = 16.5^o$. D'Appolina et al. (1967) acknowledge that triaxial compression tests cannot be extended to the large strains required to develop a residual strength condition but the close agreement of the values suggests that a ϕ'_r of 16º as determined from the direct shear test is a good estimate of the residual friction angle. The peak strength parameters as determined in the undrained triaxial tests (shown in Figure 2.5b) are in agreement with the peak strength parameters determined in the direct shear tests on similar samples.

Peak strength measured in direct shear and triaxial compression tests on preexisting shear surface specimens are higher than the drained residual strength of the soil. Thus, D'Appolonia et al. (1967) conclude "since all samples were taken from old slide planes, a shear strength greater than the residual strength could have not developed unless "healing" had occurred."

D'Appolonia et al. (1967) suggest two possible mechanisms that might cause the soil to increase in strength after the residual strength is attained which are desiccation and natural cementation.

D'Appolonia et al. (1967) attempted to artificially induce healing by overconsolidation but no tests to determine the possibility of cementation were performed. The researchers established the residual strength conditions and then consolidated the specimens to pressures up to eight times the effective normal stress employed during shear. The samples were then unloaded to overconsolidation ratios from 2 to 8 and then sheared again. D'Appolonia et al. (1967) observed no increase in the effective stress parameters upon re-shearing. To observe the effect of desiccation on the strength parameters, D'Appolonia et al. (1967) allowed two specimens to dry after establishing the residual strength conditions. Subsequently, the specimens were saturated and allowed to swell under constant normal stress prior to re-shearing. It was observed that one of these samples developed a strength greater than residual but the other did not.

Thus D'Appolonia et al. (1967) conclude that the strength on the preexisting failure surface in the colluvial slope increased to a value somewhat greater than the residual strength, suggesting that healing occurred along this shear surface. D'Appolonia et al. (1967) performed direct shear tests on undisturbed specimens obtained from shallow depths (from the top and bottom of slope) and at effective normal stresses equal to the insitu overburden pressure (< 100 kPa). These tests exhibited peak strengths greater than the residual strength values at the same effective normal stresses. D'Appolonia et al. (1967) postulate healing occurred along the shear surfaces based on direct test results performed at effective normal stresses equal to 100 kPa or less. Although the test results show the possibility of strength recovery/healing at shallow depths or shallower parts of the landslide, D'Appolonia et al. (1967) do not conclude that healing is a function of landslide depth or effective normal stress.

2.3.1.2 Direct Shear Tests on Reconstituted/Remolded Shear Surface Specimens

2.3.1.2.1 Ramiah et al. (1973) Study

Ramiah et al. (1973) investigated the effect of thixotropy on residual strength of remolded normally consolidated commercially available kaolinite and bentonite clay from Bangalore, India. The kaolinite has LL = 66%, PL = 43.4%, PI = 22.6%, and CF = 11% whereas

the bentonite has LL = 400%, PL = 45.75%, PI = 354.25%, and CF = 71%. Ramiah et al. (1973) prepared the specimens for reversal direct shear tests at an initial water content greater than the liquid limit of each soil, allowed the specimens to hydrate for seven days, and then consolidated the specimens in increments to the selected effective normal stresses of 29.4, 58.8, and 98.1 kPa, separately. Although the researchers do not mention how the samples were prepared, it is assumed that the material passing Number 40 sieve was used for the direct shear tests. After consolidation, each specimen was trimmed and loaded in a direct shear box under normally consolidated conditions. Each specimen was allowed to come to equilibrium in the shear box before shearing. Each specimen was sheared at a displacement rate of 0.0127 mm/min during first forward cycle and then at a displacement rate of 0.0254 mm/min for all subsequent forward and reverse cycles.

Drained residual friction angle(s) (ϕ'_r) measured by Ramiah et al. (1973) at an effective normal stress of 29.4 kPa for kaolinite is 24.2º and at effective normal stresses of 29.4, 58.8, and 98.4 kPa for bentonite are 12.7º, 9.4º and 7.5º respectively. Drained residual friction angle measured by Ramiah et al (1973) for kaolinite are in agreement with empirical correlations by Stark et al. (2005). The bentonite residual friction angles are not in agreement with updated empirical correlation shown in Figure 6.24 because these are too high which may be caused by problems with specimen preparation, testing procedures, and/or measurements of the index properties.

After establishing the residual strength condition, the kaolinite specimens were subjected to a rest period of 96 hours (4 days) at three effective normal stresses i.e., 29.4, 58.8, and 98.4 kPa, whereas, the bentonite specimens were subjected to different rest periods of 12, 24, 48, and 96 hours (0.5, 1, 2, and 4 days) at the same three effective normal stresses i.e., 29.4, 58.8, and 98.4 kPa. The specimens were re-sheared after each rest period. Ramiah et al. (1973) show a strength gain for high plasticity soil (bentonite) even with a short rest period whereas low plasticity soil (kaolinite) did not show a strength increase in any test.

Figure 2.6 shows the test results after 96 hours (4 days) of a bentonite specimen at an effective normal stress of 29.4 kPa. Upon restarting the test after 96 hours (4 days), a peak strength is observed and then the strength drops to a lower value during the travel of the shear

box. The peak friction angle observed after 96 hours (4 days) equals 15.1º which is greater than the measured drained residual friction angle by 2.4º within 4 days. Furthermore, after measuring the peak, the strength did not return to the initial residual value (12.7º) instead it dropped to a friction angle of 14.2º and remained almost constant for the entire cycle (see Figure 2.6 at a displacement of 54mm).

Figure 2.7 shows the relationships between strength ratio (ratio between recovered and residual shear strengths) and rest period/recovery time measured by Ramiah et al. (1973). Ramiah et al. (1973) suggest that this increase in shear strength above the residual value after a rest period for bentonite may be attributed to thixotropic behavior of high plasticity soils. Ramiah et al. (1973) conclude that the increase in strength ratio due to thixotropy is greater at low effective normal stresses and lower at higher effective normal stresses. Furthermore, Ramiah et al. (1973) conclude that the increase in shear strength above the residual value may not be significant at higher effective normal stresses or at high consolidation pressures.

Ramiah et al. (1973) used normally consolidated specimens to study the effect of thixotropy on the residual strength of two soils using direct shear tests. A normally consolidated specimen is expected to undergo vertical settlement due to secondary compression. Settlement due to secondary compression, if it is pronounced, may cause the shear surface to move below the top of the bottom half of the direct shear box. This may result in shearing along a new shear surface when the test is restarted after the rest period. Because high plasticity soil (bentonite) has a higher initial void ratio than low plasticity soil (kaolinite) and is usually more compressible, it is likely to undergo more secondary compression. Therefore there is a greater likelihood that the shear surface will move down below the top of the bottom half of the direct shear box with bentonite than kaolinite. Furthermore, when the direction of shearing in the direct shear box is changed at the end of each cycle, the clay particles reorient to align along the shear surface in the new direction of shear. Because of this reorientation of clay particles, a peak on the shear stress-displacement relationship is usually observed at the start of each cycle or reversal and then it drops towards the residual value if the specimen has already obtained the residual strength condition. Although Ramiah et al. (1973) do not specify the test procedure in detail, review of the test results shown in Figure 2.6 show that the specimen was stopped at the end of a reverse movement of the shear box and changed the direction before the restart of movement. It is

anticipated that upon restarting the test after a rest period, the peak strength observed may have been caused by particle reorientation because shearing was restarted at the start of shear box reversal. This may have resulted in a large increase in strength above the residual value because of particle reorientation. Because the contribution of secondary compression and particle reorientation cannot be accurately assessed from the test results presented by Ramiah et al. (1973), it is difficult to estimate the strength gain above the residual value for the soils tested due to factors other than particle reorientation.

2.3.1.2.2 Angeli et al. (1996) Study

Angeli et al. (1996) describe the Alver`a landslide in the area of Cortina d'Ampezzo located in northeastern Italy. Alver`a landslide is a start-stop slide, that consists of clays resulting from the weathering of marls and shales. This case is discussed in detail in Chapter 4 because a back-analysis of the slide was performed and discussed.

Angeli et al. (1996) found a large variation in material present in the slide. Two samples from the slip surface yielded LL = 91.5, 99.1%, PI = 45.5-51.1%, CF = 68-71%, and $\phi'_r = 15.9^o$ measured in ring shear tests that are not described in detail. Angeli and Silvano (2004) report a range of index properties measured on four slip surface samples as LL = 69.3-99.1%, PI = 29.6-51.1%, CF = 56-71% and $\phi'_r = 9.0^o$ -15.9^o measured in ring shear tests but the tests are not described. Angeli and his coworkers have not reported the effective stress at which these ring shear tests were performed but Deganutti and Gasparetto (1992) also report $\phi'_r = 15.9^o$ measured in ring shear test at an effective normal stress of 100 kPa using the same two slip surface specimens which indicates that Angeli and his coworkers are using $\phi'_r = 15.9^o$ as a standard. It was determined that the samples collected from the slip surface essentially consist of montmorillonitic clay.

At an effective normal stress of 100 kPa the empirical correlation for drained residual friction angle presented by Stark et al. (2005a) and also in Figure 6.24 shows $\phi'_r = 16^o$ for LL = 69.3% and CF = 56% and $\phi'_r = 9.5^o$ for LL= 99.1% and CF = 71 % which are agreement with the values of ϕ'_r (9.0^o -15.9^o) reported by Angeli and Silvano (2004). Angeli et al. (1996) do not mention whether the same soil was used in both direct and ring shear tests or if the direct shear test results are in agreement with the ring shear test results.

Angeli et al. (1996) report an approximate upper and lower threshold groundwater level for the start and stop of slope movement as 0.9 and 1.3 m below ground surface, respectively. For long periods, there was no slope movement and the longer the landslide was "stationary", the higher the piezometric change necessary to restart movement. The authors concluded that the higher piezometric change was evidence of strength regain on stationary slip surfaces containing montmorillonitic clays according to Angeli et al. (1996 and 1999) based on the direct shear strength recovery tests performed.

Angeli et al. (1996) present direct shear strength recovery test results performed on slip surface samples of the of Alver`a landslide. The direct shear tests used material passing Number 40 sieve (<0.42 mm) for effective normal stresses equal to the field stresses. Figure 2.8a shows the direct shear test results on Alver`a landslide slip surface material at possible effective normal stress of 71 kPa because Angeli et al. (1996) mention s_n=71 kPa in the figure caption but not the text. The specimen was sheared at a displacement rate of 0.0609 mm/min. Angeli et al. (1996) do not report the residual strength of the soil measured in the direct shear test. As discussed earlier, Angeli et al. (1996) report $\phi'_r = 15.9^o$ for the slip surface samples measured during the ring shear test but it is not mentioned whether the direct shear test results are in agreement with the ring shear test results or not. Later Angeli and Sivano (2004) report a range of drained residual friction angles, $\phi'_r = 9.0^o$-15.9^o which creates further ambiguity in the direct shear test results reported by Angeli et al. (1996) and makes it difficult to compare the direct shear and ring shear test results.

The researchers report the strength gain above the residual value for material obtained from the slip surface of Alver`a landslide after rest periods of 54, 166, 925, and 6860 mins [54 min – 114 hrs (≈ 5days)] as shown in Figure 2.8(a). The peak strength observed after each rest period corresponds to the shear strength regain during that rest period. Although the strength gain of 6 kPa above the residual value after almost 5 days is reported, the recovered strength cannot be estimated without knowing the residual strength prior to stopping the test which is the reference strength. Anglei et al. (1996) do not provide details of direct shear specimen preparation and its consolidation before shearing. Considering an effective normal stress of 71 kPa and $\phi'_r = 15.9^o$, the value of recovered shear stress will be 20.2 kPa. This corresponds to an increase in the drained friction angle of 4.35º after a rest period of almost 5 days as reported by

Angeli et al. (1996). However, this increase appears too high based on the ring shear data developed herein and discussed in Chapter 4. Figure 2.8(a) also shows that the peak strength observed after almost 5 days was lost after a small shear displacement and the strength drops to the residual value after a shear displacement of only 0.6 mm. Angeli et al. (1996) relate this strength regain to thixotropy of the montmorillonite present along Alver`a landslide slip surface. Using the data shown in Figure 2.8(a), the relationship between strength ratio (τ_{Rec}/τ_r) and rest time shown in Figure 2.8(b) was developed.

Angeli et al. (1996) use normally consolidated specimens, but do not report the drained residual strength measured in the direct shear or detail about the displacement at which the rest period is started. Hence the contribution of specimen secondary compression during the rest period, movement of shear surface away from the gap between the top and bottom halves i.e., below the top of the bottom half of shear box, and/or reorientation of clay particles upon reversing the direction of shear/movement as discussed earlier, cannot be determined. Therefore, the strength gain above the residual value, if any, is difficult to estimate for these tests. Furthermore, lack of information on the drained residual shear strength measured in the direct shear test also makes it difficult to comment on the strength regain above the residual value measured by Angeli et al. (1996).

Thus, the direct shear strength recover test results reported by Angeli et al. (1996) are not sufficient to make an estimate of strength regain along the preexisting shear surface and reach at a conclusion but suggest a need for further investigation into the healing phenomenon.

2.3.2 Japanese Ring Shear Tests on Reconstituted/Remolded Specimen

2.3.2.1 Gibo et al. (2002) Study

Gibo et al. (2002) used ring shear tests to measure the strength recovery from the residual value for soil sample obtained from two different reactivated landslides. Gibo et al. (2002) used a Japanese ring shear device designed and discussed by Gibo (1994) which is similar to the Bishop et al. (1971) ring shear device. In both of these devices shearing occurs at or near a mid-height of the specimen instead of at the top (smear type) like in the Bromhead ring shear apparatus. The Japanese ring shear device has inner and outer diameters of 60 mm and 100 mm, respectively.

One soil sample was obtained from the Xuechengzhen landslide in Sichuan, China. The sample obtained from the fractured soil mass is composed of the black phyllite colluvium of the Silurian and Devonian periods. The Xuechengzhen soil sample has LL = 32%, PL = 17%, and CF = 10% with mica as the principal clay mineral in the clay size fraction. The other soil sample was obtained from the slip surface at a depth of 69 m of the Kamenose landslide in Kashiwara-shi, Osaka, Japan. This slide had been stabilized by extensive control work and the slip surface was located in a strongly argillised layer dominated by smectite. The Kamenose soil sample has LL = 114%, PL = 50%, and CF = 73% with smectite as the principal clay mineral in the clay size fraction.

The ring shear tests performed by Gibo et al. (2002) used soil passing Number 420 μm sieve (Number 40 sieve). Separate reconstituted and remolded specimens were normally consolidated in the ring shear device at selected effective normal stresses before shearing. The Xuechengzhen specimens were consolidated at effective normal stresses ranging from 30 to 300 kPa whereas the Kamenose specimens were consolidated at effective normal stresses ranging from 50 to 400 kPa. Each specimen was sheared at a displacement rate of 0.01 mm/min until the residual strength condition was established and then "reconsolidated" or healed (probably under the same effective normal stress because Gibo et al. (2002) do not provide this information) for two days. After two days, the specimens were re-sheared to observe the strength gain, if any, and the test continued until the strength dropped to the initial residual value. Gibo et al. (2002) measured $\phi'_r = 28^o$ for the Xuechengzhen material and $\phi'_r = 10^o$ for the Kamenose material at an effective normal stress of 100 kPa. These values of ϕ'_r are in agreement with the values obtained from updated empirical correlation presented in Figure 6.24 corresponding to the LL and CF of these two soils.

Summary of the test results and strength envelopes on both the soils are shown in Figure 2.9. The Xuechengzhen specimens (which are silt and sand dominated) show a strength recovery whereas the Kamenose specimens (which are smectite dominated) do not (see Figure 2.9). This contradicts the finding of Ramiah et al. (1973) which indicate bentonitic soil exhibit higher strength gain. The strength recovery observed in the Xuechengzhen specimens is greater at effective normal stresses of 100 kPa or less and almost negligible at effective normal stresses of 200 kPa or greater. Gibo et al. (2002) conclude from their strength recovery test results that it is

reasonable to consider the recovered strength in the stability analysis of a reactivated landslide dominated by silt and sand particles and at effective normal stress less than 100 kPa. Gibo et al. (2002) postulate that at low effective stresses, clay particles may not be sufficiently aligned at the residual condition which may have allowed rearrangement and/or bonding during the rest period and a strength gain upon re-shearing. It is also concluded by Gibo et al. (2002) that the rate of strength recovery increased with decreasing normal stress but the strength did not recover to the fully softened level in any case.

In summary, Gibo et al. (2002) conclude basing on their strength recovery test results that it is reasonable to consider the recovered strength in stability analyses of reactivated landslides dominated by silt and sand particles and under low effective normal stresses, i.e., landslides with a shallow depths.

Gibo et al. (2002) use a ring shear device in which shearing occurs at or near specimen mid-height, which is expected to give a better estimate of the strength recovery because shearing is occurring at a soil-soil interface not near the porous stone/bronze interface as is in the Bromhead ring shear device. However, the use of normally consolidated specimens and short duration of the tests (just two days) may not be sufficient to reach such conclusion. Also the strength recovery observed for normally consolidated Xuechengzhen specimens may be caused by some silt or sand particles being present along the shear surface (material passing Number 40 sieve was used) which may have penetrated the shear surface or zone during secondary compression of the ring shear specimen and provided some additional shear resistance. Although Gibo et al. (2002) conclude that the Kamenose soil with high clay minerals (smectite) did not show any strength recovery, Figure 2.9 shows a small peak strength that exceeds the residual value after only two days. This strength gain may have been more pronounced if Gibo et al. (2002) had used a longer rest period. Because the residual shear strength in preexisting landslides are more common in overconsolidated soils and rest periods longer than two days are relevant to field conditions, additional strength gain may have occurred if Gibo et al. (2002) had used overconsolidated specimens and longer rest periods.

2.3.3 Bromhead Ring Shear Tests on Reconstituted/Remolded Shear Surface Specimen

2.3.3.1 Angeli et al. (2004) Study

Anglei et al. (2004) present an extension of the Angeli et al. (1996) study using Bromhead ring shear tests to study the strength gain in other clayey soils. The study uses a Bromhead ring shear apparatus modified for stress controlled tests. This modification allows application of a constant shear stress on the test specimen during a rest period using dead weights applied by a wire. Anglei et al. (2004) present the results of seven tests on five different soils at effective normal stresses ranging from 98-220 kPa. Anglei et al. (2004) use three clayey soils from Italy which are low to medium plasticity with highly soluble minerals such as calcite and one soil from Britain which is high plasticity, i.e., London clay (from coastal cliffs at Warden Point, Sheppey, UK), without much soluble minerals. Anglei et al. (2004) present detailed results of ring shear strength recovery tests on Tessina clay from the Tessina landslide of northeastern Italy as shown in Figure 2.10(a). The information on the index properties of all soils tested including Tessina clay is not reported by Angeli et al. (2004). No information is provided on specimen preparation, consolidation, shearing rate, and type of the bronze porous stones used although use of distilled and deionized water during testing is mentioned. Anglei et al. (2004) show the drained residual strength of Tessina clay equals 42 kPa at an effective normal stress of 100 kPa (see Figure 2.10(a)) which corresponds to $\phi'_r = 22.8^o$. Using $\phi'_r = 22.8^o$ at an effective normal stress of 100 kPa, updated empirical correlation shown in Figure 6.24 yields a LL = 43% with CF < 50 %, whereas, the empirical correlation by Mesri and Shahien (2003) yields a PI = 20-30%. Angeli et al. (2000) report index properties for the Tessina clay of LL = 38.5-52.5%, PI = 16.2-24.7% and $\phi'_r = 19.9^o$-26.1^o however the procedure used to measure these properties has not been specified.

Angeli et al. (2004) consider three different healing test procedures for establishing the initial residual strength conditions, stopping shear displacement, and then subjecting the specimen to one of the following rest periods:

- Zero Shear Stress (ZSS): Removing the shear stress from the specimen during the rest period.

- Constant Shear Stress (CSS): Applying a shear stress less than the residual strength of the soil during the rest period.
- Removing the shear stress and increasing the normal stress during the rest period.

Angeli et al. (2004) recommend using the CSS procedure because it represents field conditions and they used this procedure to investigate the strength recovery of Tessina clay. Figure 2.10(a) shows the strength gain above the residual value after 9 days (12950 mins) is about 8.8 kPa which corresponds to an increase in drained friction angle above ϕ'_r of 4.1° after 9 days. Using this data, the relationship between strength ratio (τ_{Rec}/τ_r) and rest time/period was developed and is shown in Figure 2.10(b).

Although a range of effective normal stress from 98 to 220 kPa was used by Angeli et al. (2004), the absence of index properties for the soils tested and their residual shear strengths makes analysis of the results difficult.

Based on the test results shown in Figure 2.10(a), Angeli et al. (2004) conclude that strength recovery is possible but the regained strength is lost after a small shear displacement and reduced to the residual strength value after about 0.6 mm of shear displacement. Although Angeli et al. (2004) recognize the strength recovery in clay soils at low effective normal stresses, they suggest that the application of the recovered strength to design of stabilization measures should be done with great caution.

In the ring shear device the entire specimen is likely to compress/settle uniformly but the shear surface may undergo some non-uniform micro level changes due to secondary compression that may contribute to strength gain. Furthermore, the absence of index properties of the soil samples tested by Angeli et al. (2004) prevents conclusions about strength gain/recovery. In addition, the presence of calcites in the soil and changes in pore water chemistry may have some effects on strength recovery which should be investigated before conclusions are drawn.

2.3.3.2 Stark et al. (2005a) Study

Stark et al. (2005a) present a study to investigate the possibility of healing of shear surfaces in a low and a high plasticity soil at a single effective normal stress of 100 kPa. This study was motivated by a 1991 consulting project in which the possibility of strength gain was

postulated to reduce repair costs for a landslide near Seattle, Washington. Surface features indicated presence of an ancient landslide that was reactivated in 1990. The 1990 movement involved less than 0.6 m of lateral movement. A consultant proposed that the cohesive colluvium responsible for the slide had gained strength, i.e., healed, during the inactive or dormant period prior to 1990. As a result, it was concluded that the slide was less stable than before the 1990 movement because the shear strength increase due to healing was removed because of the less than 0.6 m of lateral displacement. The small amount of movement did not significantly change the driving or resisting forces. In other words, the strength gain that occurred from the time that the ancient landslide occurred until 1990 was not available after the 1990 movement and thus the slope was less stable after 1990 than before 1990 because the slope geometry had not changed significantly. If so, a large stabilization effort was required to restore the slope to pre-movement stability condition as required by the homeowners insurance coverage. Dr. Stark was asked to investigate the possible strength to determine whether or not the insurance company had to restore the slope to a stability condition that reflected some strength gain. This project initiated the testing reported in Stark et al. (2005a).

Stark et al. (2005a) use a modified Bromhead ring shear device (Stark and Eid, 1993) to study healing along preexisting shear surfaces in the laboratory. Stark et al. (2005a) use two natural soils i.e., Duck Creek shale from Fulton, IL and Otay bentonitic shale from San Diego, CA, obtained from slip surfaces. Duck Creek shale is a low plasticity soil with LL = 37%, PL = 25%, and CF = 19% , whereas, Otay bentonitic shale is a high plasticity soil with LL = 112%, PL = 53%, and CF = 73%. The ring shear device uses a reconstituted and remolded soil specimen prepared from soil passing Number 200 sieve by mixing with water at initial water contents more than the liquid limit of the soil and hydrating it for a week in a moisture controlled room. The soil specimen is then transferred to the ring shear specimen container with an initial thickness of 5 mm, consolidated in the ring shear under increment loading as described by Stark and Eid (1993 and 1994) and ASTM D6467. The specimen is consolidated to 700 kPa which will corresponds to overconsolidation ratio (OCR) of 7 after unloading to 100 kPa, consolidation settlement was removed prior to shearing using the Stark and Eid (1993 and 1994) procedure and the specimen was then loaded to an effective normal stress of 100 kPa. The specimen was presheared at a fast shear displacement rate to develop a shear surface. After dissipation of porewater pressures developed during preshearing, the specimen is sheared at a shear

displacement rate of 0.018 mm/min until the residual strength condition is reached. After establishing the drained residual strength condition, Stark et al. (2005a) stopped the test, removed the shear stress by disengaging the torque couple so that no shear stress was exerted on the shear surface by the proving rings during the rest period. Thus the specimen was subjected to the applied effective normal stress of 100 kPa but no shear stress during the rest period. After the first rest period, shearing was restarted to observe a strength gain, if any, above the residual value. The peak strength observed after the first rest period is the recovered strength for that period. The test was stopped after the strength returned to the residual value and then subjected to another rest period under the applied effective normal stress but no shear stress. At the end of the next rest period the test was restarted and the procedure used after the first rest period was repeated to measure a peak strength. Stark et al. (2005a) used rest periods ranging from 1 day to 230 days at a single effective normal stress of 100 kPa. The ring shear device measured ϕ'_{fs} = 33.6º, and ϕ'_r= 28.6º for Duck Creek shale and ϕ'_{fs} = 19º and ϕ'_r= 5.8º for Otay bentonitic shale at an effective normal stress of 100 kPa. One and 230 days healing test results of Duck Creek shale are shown in Figure 2.11 and of Otay bentonitic shale are shown in Figure 2.12.

Stark et al. (2005a) conclude that a failure surface which has achieved a drained residual strength condition may undergo a strength recovery/healing and exhibit a shear strength that is greater than the residual value upon re-shearing at an effective normal stress of 100 kPa (see Figure 2.13). It was also observed that the magnitude of recovered shear strength increases with increasing soil plasticity but the recovered strength is lost with small shear displacement after the rest period as shown in Figures 2.11 and 2.12. Stark et al. (2005a) suggest that the mechanisms of strength gain/recovery may include van der Waals attraction and thixotropy.

Stark et al. (2005a) used overconsolidated specimens with an OCR of seven which prevented noticeable vertical settlement during the rest period. Furthermore, these are the first strength recovery tests which were performed for a duration of up to 230 days and on specimens passing Number 200 sieve. However, Stark et al. (2005a) did not apply any shear stress to the specimens during the rest period whereas in the field the sliding mass after coming to rest will still apply shear stress to the slip surface at the effective normal stress equal to the overburden pressure. The field shear stress will be equal to or near the residual strength because of the movement. Thus specimens should be subjected to the applied effective normal and shear

stresses, i.e., the residual strength of the soil, to better simulate field conditions in laboratory strength recovery tests.

2.3.3.3 Carrubba and Del Fabbro (2008) Study

Carrubba and Del Fabbro (2008) performed laboratory tests to investigate the possibility of strength recovery in two Flysch soils using an unmodified Bromhead ring shear tests. Ring shear tests used soil specimens obtained from the shallow weathered crust of the Cormons flysch formation from Montona and Rosazzo areas from northeastern Italy, where two landslides occurred in the past. Both the flyschs are medium plasticity soils with the Montona specimen has LL = 51%, PL = 24%, and CF = 40%, whereas, the Rosazzo specimen has LL = 45%, PL = 22%, and CF = 25%. Strength recovery tests were performed on soil specimens passing Number 40 sieve whereas some tests on Montona flysch were also performed on specimen passing Number 200 sieve at σ'_n = 25 kPa.

The reconstituted specimens were prepared at an initial water content about 1.5 times the liquid limit (1.5xLL) of the soil, hydrated, and consolidated in the ring shear apparatus to the required effective normal stress. The normally consolidated specimens were first pre-sheared at a fast rate to form a shear surface and subsequently sheared at a slower rate of 0.09 mm/min which is still five times faster than the rate suggested by ASTM D6467. After establishing the residual strength conditions the specimens were subjected to the rest period under the applied effective normal and shear stresses. The rest periods used by the researchers range from 15 minutes to 30 days at effective normal stresses of 25, 50, and 100 kPa. After the rest period, shearing was restarted using the same shear rate (0.09 mm/min) and strength recovery, if any, was observed. Each specimen was sheared until it returned to the initial residual strength and then stopped for another rest period, if required.

Drained residual friction angles measured for the specimens processed through Number 40 sieve for both of the soils are 3 to 5 degrees higher than the values obtained from empirical correlation by Stark et al. (2005a) and that shown in Figure 6.24 at corresponding effective normal stresses. Carrubba and Del Fabbro (2008) also report residual friction angles measured on specimens processed through Number 200 sieve and these values are also greater than the values obtained from the empirical correlations. Furthermore, the specimens processed through Number

200 sieve yielded higher values of drained residual friction angles than the specimens processed through Number 40 sieve at effective normal stresses less than 100 kPa as shown in Figure 4, 5, and 18 of Carrubba and Del Fabbro (2008). The higher measured values of drained residual friction angles may be caused by a higher shear displacement rate being used by Carrubba and Del Fabbro (2008) in their testing than Stark et al. (2005a) used to establish their empirical correlation. The difference also may be caused by specimen preparation and testing procedures that differ from ASTM D6467 (2008c). Carrubba and Del Fabbro (2008) use specimens prepared from material processed through Number 40 sieve to investigate the strength recovery in both flyschs. Only one specimen processed through Number 200 sieve of Montona flysch has been used for strength recovery at an effective normal stress of 25 kPa.

Carrubba and Del Fabbro (2008) subjected the specimens to a rest period under an applied effective normal stress and a shear stress less than or equal to the residual strength of the soil and termed this condition the "acting shear stress" (A.S.) condition. The researchers consider that A.S. condition to be a good representation of field conditions along the sliding surface of a reactivated landslide and used this condition during the rest periods.

Although both Montona and Rosazzo flyschs have medium plasticity, the Motona flysch has a higher clay content and also contains some montmorillonite. Carrubba and Del Fabbro (2008) report a high strength gain in Montona flysch as compared to Rosazzo flysh. Both of the flyschs show a higher strength gain at an effective normal stress of 25 kPa compared to the other effective normal stresses of 50 and 100 kPa (see Figure 2.14). The researchers also show that the strength gains are greater for the Montona specimens with same mineralogy but greater particle size, i.e., soil size distribution passing Number 40 sieve, as compared to finer material, i.e., passing Number 200 sieve, at an effective normal stress of 25 kPa (see Figure 2.14).

Carrubba and Del Fabbro (2008) used normally consolidated specimens to observe the strength recovery which may have produced some settlement and other changes along the shear surface and contributed to the observed recovered shear strength. The measured residual friction angles are higher than those estimated from the updated empirical correlation shown in Figure 6.24 which may be due to the higher shear rate used by Carrubba and Del Fabbro (2008) than suggested by ASTM D6467 (2008c). The higher shear rate of 0.09 mm/min was used for

shearing after the rest period and may have resulted in some strength gain and/or generation of a small amount of pore pressure. Thus, the recovered strength measured may not only represent the recovered strength above the residual value which is the property of a soil but may also be affected by some other factors. Furthermore, the predicted increase in friction angle above the initial residual values shown in Table 5 of Carrubba and Del Fabbro (2008) range from 5.5 to 14.5 degrees at different effective normal stresses for a period of 100 years to simulate field conditions. This large increase seems unrealistic because the magnitude of the predicted friction angles (5.5 to 14.5 degrees) approaches the fully softened friction angle of the soil. Fully softened strength is the upper bound strength for the recovered strength which is not expected to be reached because of the presence of a shear surface in the soil. Therefore, the recovered strengths predicted by Carrubba and Del Fabbro (2008) seem too high. Use of overconsolidated specimens prepared from the material passing Number 200 sieve and a slower displacement rate may have yielded better results for strength recovery prediction.

2.4 Review and Summary of Strength Recovery Tests and Procedures

Although all of the researchers described above have observed that shear surfaces after obtaining the residual strength conditions show a strength greater than the residual value when subjected to a rest period, most of the recovered strength is lost with a small shear displacement upon reactivation/renewal of the movement. Therefore all of the researchers who measured a strength greater than the residual value in the laboratory along preexisting shear surfaces did not recommend relying on the recovered strength for the design of remedial measures. The research discussed in this chapter have used different test devices, test procedures, and soils so there is variability in the reported test results. Summary of residual and fully softened friction angles measured in strength recovery tests by different researchers and estimated from updated empirical correlations shown in Figures 6.24 and 6.36 is shown in Table 2.2.

Figure 2.15 summarizes the test results presented by these prior researchers in terms of a "strength ratio" which is the ratio between the recovered shear strength (τ_{Rec}) and residual strength (τ_r) as a function of rest time at effective normal stresses equal to or close to 100 kPa. Even though these researchers used different devices, test procedures, and soils all of the soils

tested show a strength gain above the residual strength at effective normal stresses of less than or equal to 100 kPa which corresponds to shallow depths of landslides.

Based on the test results discussed in this chapter and shown in Figure 2.15 the following statements can be made:

- All of the researchers used material passing Number 40 sieve for the strength recovery tests except Stark et al. (2005a) which used material passing Number 200 sieve. If the specimen is prepared from material passing Number 40 sieve, silt size particles may be present near or along the shear surface after establishing the residual strength conditions and before subjecting the specimen to a rest period. The silt size particle(s) present along and around the shear surface during the rest period may move into the shear surface causing an increase in shear stress when shearing is restarted after the rest period. High fines content material along the shear surface is more suited to establishing a sliding residual strength condition and development of a residual strength condition as suggested by Skempton (1985). Therefore using finer material, e.g., passing Number 200 sieve, for strength recovery testing may be more realistic and closer to field conditions. Although Carrubba and Del Fabbro (2008) present a comparison between the recovered strength observed for specimens prepared from material passing the Number 200 and Number 40 sieves at an effective normal stress of 25 kPa, the initial residual strength measured on a specimen prepared from material passing Number 200 sieve is greater than for a specimen prepared from material passing Number 40 sieve. This contradicts other data, e.g., Stark et al. (2005a) that show finer grained material exhibits a lower residual friction angle. Stark et al. (2005a) present a laboratory study using material passing Number 200 sieve (< 200μ) which may simulate better field conditions.
- All of the researchers described above used normally consolidated specimens except Stark et al. (2005a) which used overconsolidated specimens to an overconsolidation ratio (OCR) of seven. A normally consolidated specimen is likely to undergo more vertical settlement due to soil extrusion and secondary compression compared to an overconsolidated specimen. The effect of secondary

compression may not be that pronounced in a ring shear device but may be considerable in a direct shear device. In a direct shear test during a rest period, excessive settlement of a normally consolidated specimen can cause the shear surface to move within the gap or even below the gap between the top and bottom halves of the shear box. Either case may result in shearing along a new surface when the test is restarted after the rest period which will result in a peak strength greater than the residual value. Landslides are more common in areas having stiff clays and shales which have historically experienced high consolidation stresses and most of these materials exhibit an OCR of at least 4 to 6. Therefore using overconsolidated specimens for strength recovery tests seems more appropriate than normally consolidated specimens. To minimize the impact of secondary compression on the recovered strength after the rest period, an overconsolidated specimen is recommended for performing strength recovery tests in the laboratory.

- To establish the residual strength conditions in a ring shear device, the specimen is sheared in one direction but in the direct shear device the direction of shearing is changed by reversing the direction of the shear box at the end of each cycle. In a direct shear test when the shearing direction is changed, the clay particles reorient along the shear surface to align with the new shear direction of shear. This results in a peak strength on the shear stress-displacement relationship which decreases to a lower value during shearing in the new direction. The strength measured at the end of this traverse of the shear box may or may not be equal to the initial residual value because particles have been reoriented and the amount of shear displacement in each traverse is small. The test is stopped for healing or rest at a point when the peak is reduced to an almost constant value (shear stress-displacement relationship is almost horizontal) after changing the direction of movement of the shear box. Ramiah et al. (1973) and Angeli et al. (1996) do not specify the point at which their tests were stopped for healing. Therefore it is difficult to comment on whether the peak strength observed after the rest period is actually a recovered strength or it is the peak strength caused by changing the direction of movement of the shear box. It is recommended that the direct shear

test be stopped to observe the strength recovery/healing when the peak strength has decreased to near the residual value after changing the direction of shear movement of the shear box or when the shear stress-displacement relationship becomes constant (no change in shear stress with increase in shear displacement).

- The recovered strength observed in the laboratory shear tests is lost after a small shear displacement upon restarting the test after the rest period in all the cases and the strength is eventually reduced to the initial residual value. This behavior has created some doubts on the reliability of the recovered strength for design of remedial and some researchers suggest that the recovered strength should not be relied upon for remedial design.
- All of the researchers except Gibo et al. (2002) and Stark et al. (2005a) used a higher shear displacement rate than that typically used laboratory tests recommended by ASTM D6467 (2008c) . For drained direct shear tests on cohesive soils, the typical rate of shear suggested by Skempton (1985) is 0.005 mm/min and for drained ring shear tests on cohesive soils the typical rate of shear displacement from ASTM D6467 (2008c) is 0.018 mm/min. Skempton (1985) suggests that "variations in the residual strength within the usual range of slow laboratory tests (say 0.002-0.01 mm/min) are negligible." The shear rates used by different researchers during strength tests are:
    - D'Appolonia et al. (1967) (DS) - 0.127 mm/min
    - Ramiah et al. (1973) (DS) - 0.0127 mm/min for 1st forward cycle
0.0254 mm/min for remaining cycles
    - Angeli et al. (1996) (DS) - 0.0609 mm/min
    - Gibo et al. (2002) (RS) - 0.01 mm/min
    - Angeli et al. (2004) (RS) - not reported
    - Stark et al. (2005a) (RS) - 0.018 mm/min
    - Carrubba and Del Fabbro (2008) (RS)- 0.09 mm.min

High residual shear strength parameters reported by most of the researchers may be due to higher shear displacement rates used during the tests. The residual strength is the reference point because strength gain, if any, is the strength above

the residual value. In the absence of a correct reference strength (residual strength), it becomes difficult to develop conclusions about the recovered strength. To establish the initial residual strength conditions it is recommended that the maximum shear displacement rate in the direct shear test be 0.005 mm/min as suggested by Skempton (1985) and in the ring shear test it should be 0.018 mm/min as recommended in ASTM D6467 (2008c).

- Some researchers have used short/small rest periods (2-5 days) for the strength recovery tests which may not be sufficient to confirm the existence of strength recovery along preexisting shear surfaces. Although the test results suggest that strength recovery is possible along preexisting shear surfaces and the recovered strength is a function of time for effective normal stresses of 100 kPa or less, the test durations in some cases are too small, especially in Gibo et al. (2002), Ramiah et al. (1973), and Angeli et al. (1996), to confirm strength recovery. Small rest periods, e.g., Gibo et al. (2002) used only 2 days, might have led to a false conclusion that a high plasticity soil with more fines (CF) exhibits little or no strength gain. If the rest periods used by Gibo et al. (2002) had extended beyond two days, the results might be different. Maximum rest periods used by various researchers discussed above are as follows:
  - Ramiah et al. (1973) - 4 days
  - Angeli et al. (1996) - 5 days
  - Gibo et al. (2002) - 2 days
  - Angeli et al. (2004) - 9 days
  - Stark et al. (2005a) - 230 days
  - Carrubba and Del Fabbro (2008) - 30 days
- The researchers discussed in this chapter have used direct shear, Japanese ring shear (similar to Bishop-type ring shear), and Bromhead ring shear devices and different methods to study the possibility of strength recovery along a preexisting shear surface. In the absence of standard test method and suitable test device for strength recovery tests, it is difficult to compare the test results and evaluate the reliability of the measured recovered strengths.

2.5 Tables and Figures

Table 2.1. Back-analyses results of Stag Hill landslide near Guildford, Surrey

Ground Water Surface (GWS) / Average Pore Pressure Ratio, r_u	Factor of Safety (Spencer (1967) Method)	
	Empirical Correlation (Figure 6.24)	Chandler (1984) Back-Analysis
GWS estimated from Figure 2.3	0.82	0.88
0.4	0.8	0.88
0.3	0.92	1.01
0.25	0.98	1.07
0.23	1.00	1.10
0.22	1.01	1.11
0.20	1.04	1.14

Table 2.2. Summary of type of soils tested by various researchers along with their index properties.

No	Soil/Material	Reference	Shear displ. Rate (mm/min.)	Index Properties	Drained Residual and Fully Softened Friction Angles at shown σ'_n							
					Measured		Updated Correlation (Figure 6.24)		Measured		Updated Correlation (Figure 6.36)	
					ϕ'_r, deg	σ'_n, kPa	ϕ'_r, deg	σ'_n, kPa	ϕ'_{fs}, deg	σ'_n, kPa	ϕ'_{fs}, deg	σ'_n, kPa
1.	Colluvium, West Virginia	D'Appolonia et al. (1967)[@]	0.127	LL =51 % PL = 25% CF = 55% PI = 26%	16º	M-C	19.3º 17.9º 16.0º	50 100 400	-	-	28.3º 25.1º 21.5º	50 100 400
2.	Kaolinite, India (passing No. 40 sieve)	Ramiah et al. (1973) *	0.0127 (first forward cycle) 0.0254 (remaining cycles)	LL = 66% PL = 43% CF = 11% PI = 23%	24.2º	29.4	23.4º 22.7º 21.4º	50 100 400	-	-	31.2º 29.9º 28.2º	50 100 400
3.	Bentonite, India (passing No. 40 sieve)			LL=400% PL = 46% CF = 71% PI =354%	12.7º 9.4º 7.5º	29.4 58.8 98.4	5.2º 4.9º 4.6º	50 100 400	-	-	13.0º 12.0º 10.0º	50 100 400
4.	Alver`a landslide, Italy (passing No. 40 sieve)	Angeli et al. (1996) *	0.0609	LL = 99% PL = 48% CF = 71% PI = 51%	9.0º	100	10.9º 9.6º 7.8º	50 100 400	-	-	24.5º 21.0º 17.6º	50 100 400
4a.	"	Angeli and Silvano (2004)	not given	LL = 69% PL = 40% CF = 56% PI = 30%	15.9º	71	15.4º 14.0º 12.1º	50 100 400			26.8º 23.4º 19.8º	50 100 400
5.	Xuechengzhen, China (passing No. 40 sieve)	Gibo et al. (2002) [$]	0.01	LL = 32% PL = 17% CF = 10% PI = 15%	30º 29º 28º 25º	30 60 100 200	31.1º 30.6º 29.6º	50 100 400	-	-	32.8º 31.9º 31.1º	50 100 400

Table 2.2 (Cont.)

No.	Soil/Material	Reference	Shear displ. Rate (mm/min.)	Index Properties	Drained Residual and Fully Softened Friction Angles at shown σ'_n							
					Measured		Updated Correlation (Figure 6.24)		Measured		Updated Correlation (Figure 6.36)	
					ϕ'_r, deg	σ'_n, kPa	ϕ'_r, deg	σ'_n, kPa	ϕ'_{fs},deg	σ'_n, kPa	ϕ'_{fs}, deg	σ'_n, kPa
6.	Kamenose, Japan (passing No. 40 sieve)	Gibo et al. (2002) $	0.01	LL= 114% PL = 50% CF = 73% PI = 64%	12º 10º 8.5º 7.5º	50 100 200 300	9.7º 8.6º 7.0º	50 100 400	-	-	23.4º 20.1º 16.6º	50 100 400
7.	Tessina clay, Italy (passing No. 40 sieve)	Angeli et al. (2004) #	not given	LL = 39 % PL = 20% CF = 40% PI = 19%	22.8º	100	26.5º 25.2º 22.7º	50 100 400	-	-	32.0º 29.2º 26.3º	50 100 400
8.	Duck Creek shale, IL (passing No. 200 sieve)	Stark et al. (2005a) &	0.018	LL = 37% PL = 25% CF = 19% PI = 12%	28.6º	100	29.9º 29.3º 28.2º	50 100 400	33.6º	100	32.5º 31.6º 30.6º	50 100 400
9.	Otay bentonitic shale, CA (passing No. 200 sieve)		0.018	LL= 112% PL = 53% CF = 73% PI = 59%	5.8º	100	9.9º 8.7º 7.0º	50 100 400	19.0º	100	23.6º 20.2º 16.7º	50 100 400
10.	Montona flysch, Italy (passing No. 40 sieve)	Carrubba and Del Fabbro (2008) #	0.09	LL = 51% PL = 24% CF = 40% PI = 27%	28.4º 27.0º 26.5º	25 50 100	24.1º 22.9º 20.2º	50 100 400	-	-	31.0º 28.2º 25.5º	50 100 400
11.	Rosazzo flysch, Italy (passing No. 40 sieve)		0.09	LL = 45% PL = 22% CF = 25% PI = 23%	27.5º 27º 26.5º	25 50 100	25.5º 24.2º 21.5º	50 100 400	-	-	31.5º 28.7º 25.7º	50 100 400

@Direct shear test on intact/undisturbed specimens containing slickensides
*Direct shear test on remolded normally consolidated specimens
Ring shear test using Bromhead ring shear device and reconstituted normally consolidated specimens
& Ring shear test using Bromhead ring shear device and reconstituted overconsolidated specimens
$Ring shear test using Japanese ring shear device and reconstituted specimens

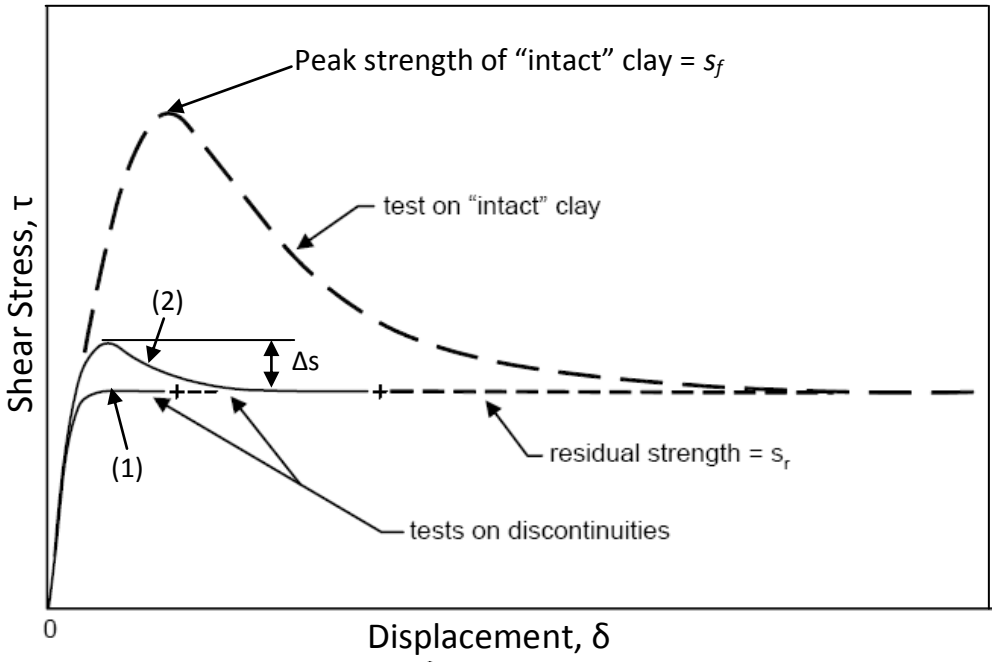

Figure 2.1. Shear stress-displacement relationship in tests on a discontinuity and intact clay (from Skempton and Petley, 1967)

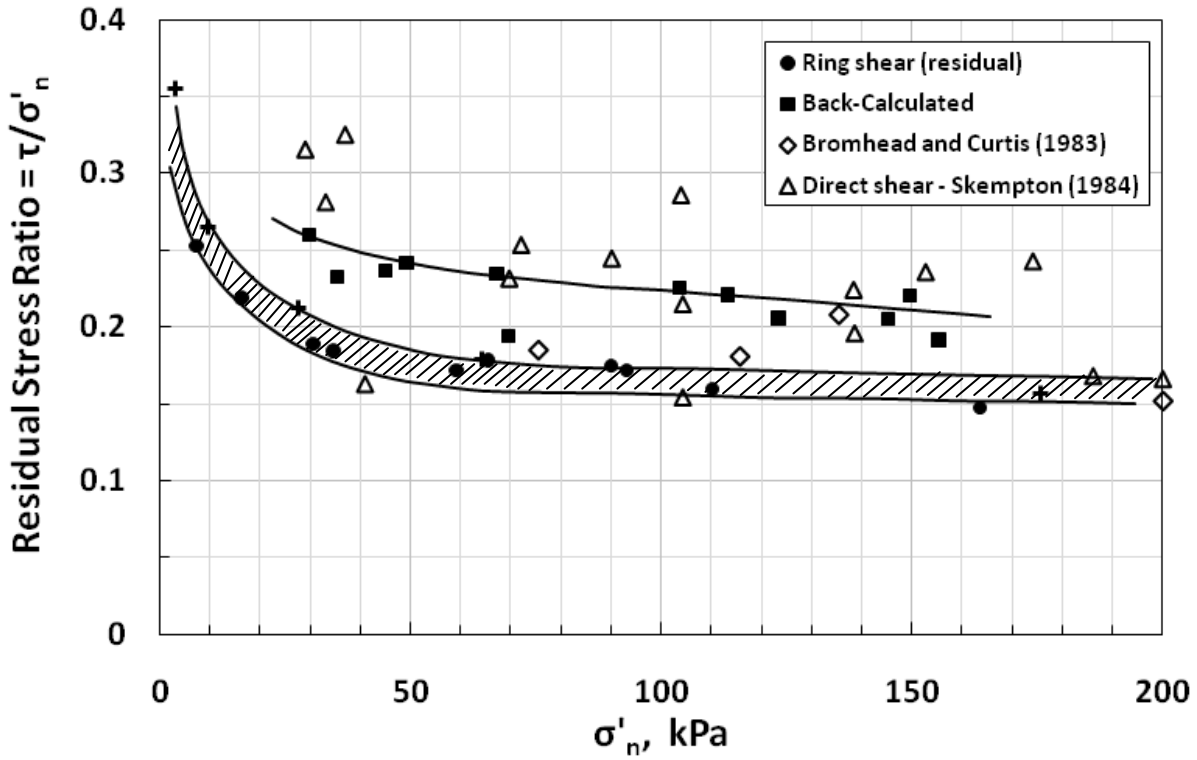

Figure 2.2. Comparison of London clay shear strengths obtained from back-analysis of landslides, direct shear, and ring shear test data of Chandler (1984).

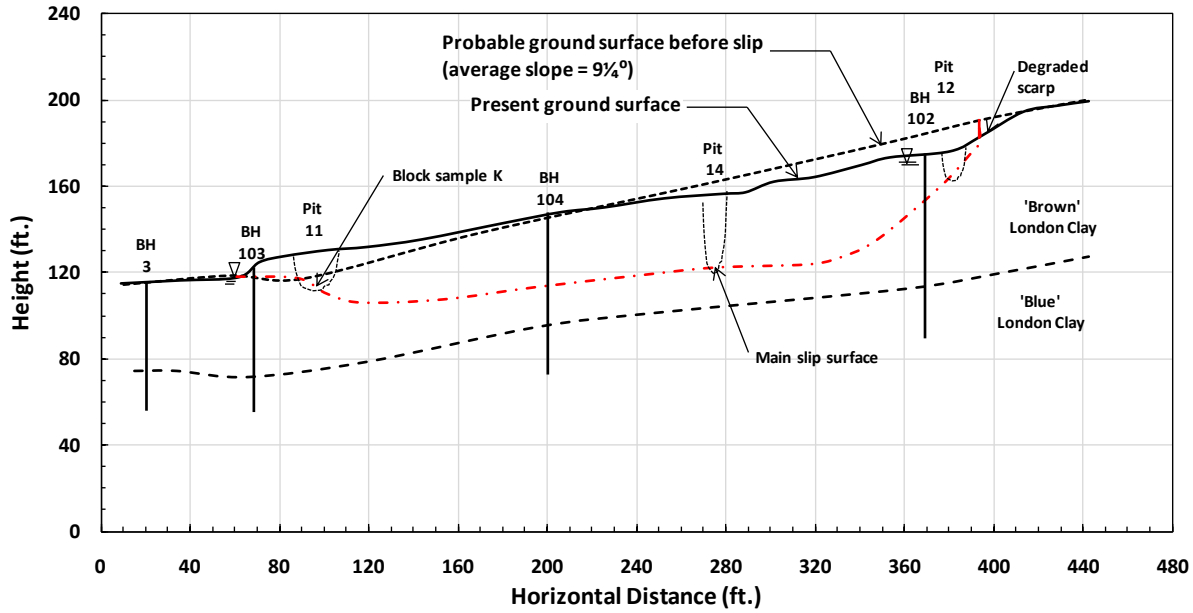

Figure 2.3. Cross-section of Stag Hill landslide, near Guildford, Surrey (from Skempton and Petley, 1967).

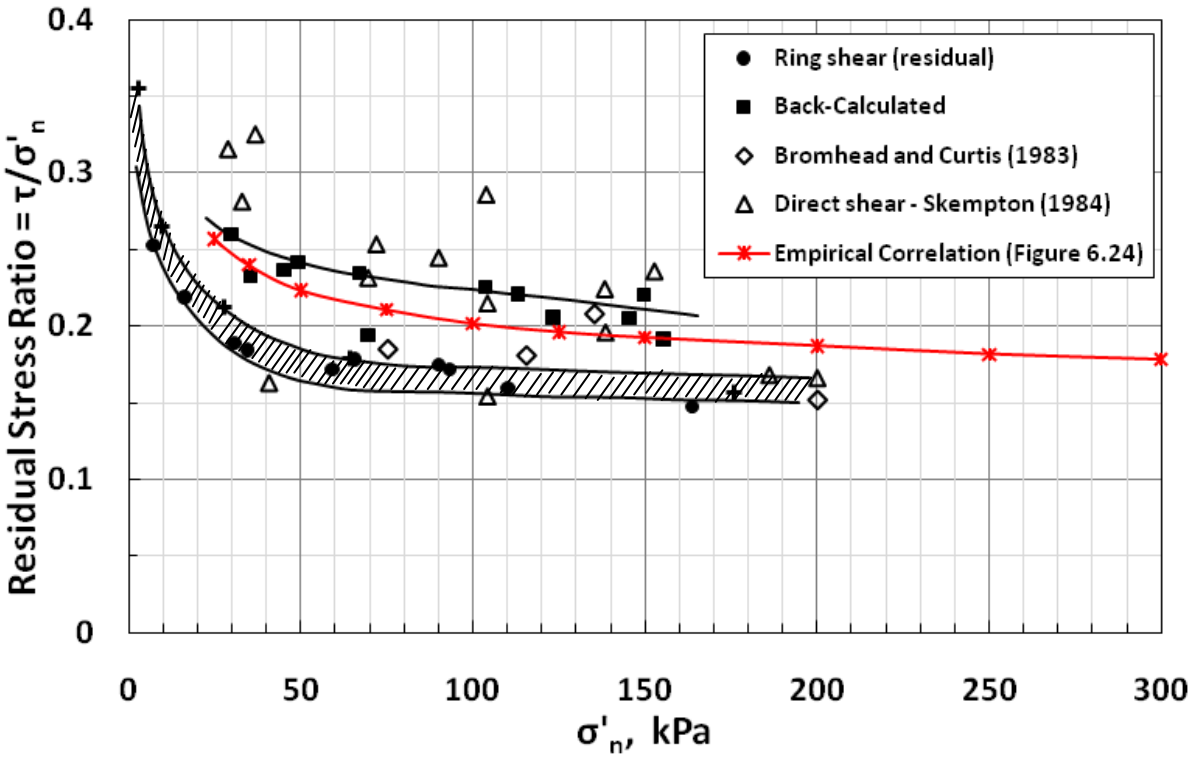

Figure 2.4. Back-calculated residual stress ratio obtained from empirical correlation (Figure 6.24) plotted on Chandler (1984) plot for comparison.

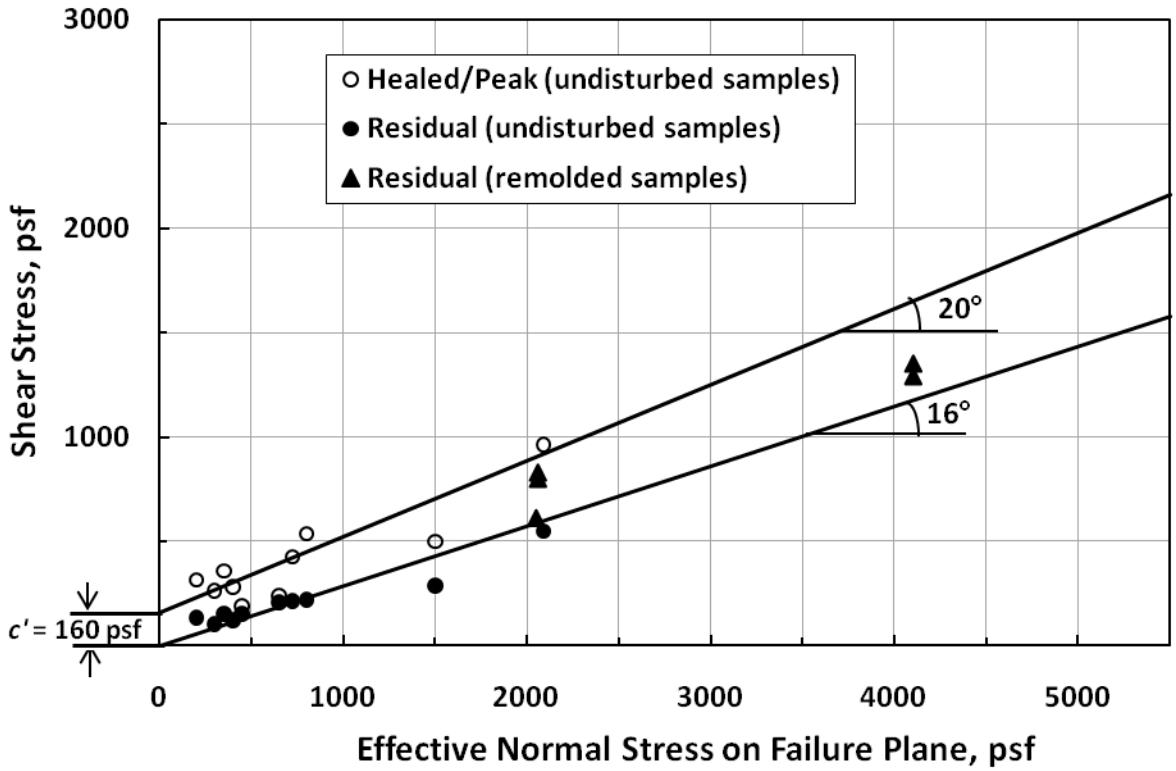

(a)

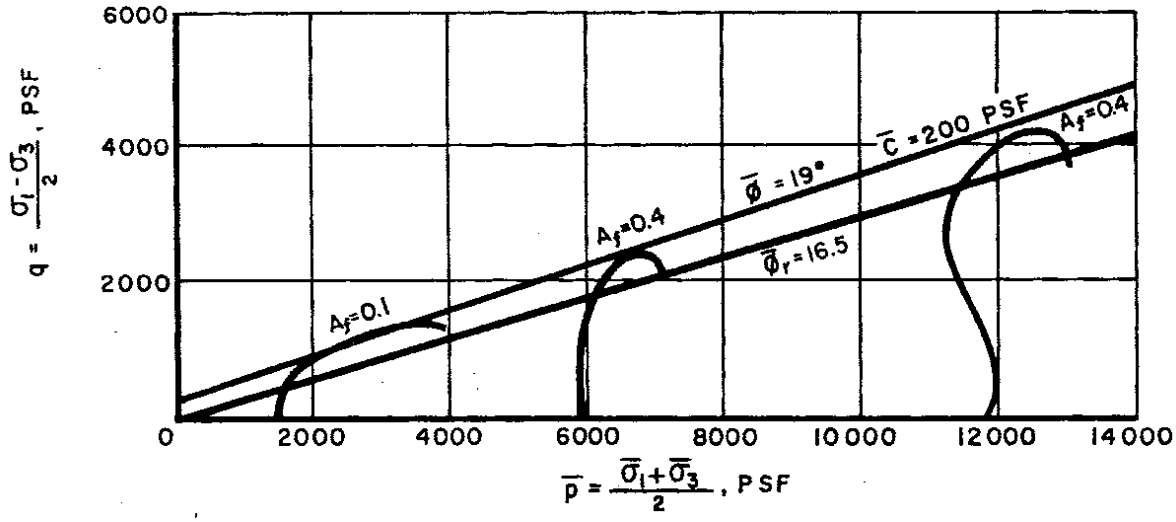

(b)

Figure 2.5. Summary of test results on block samples containing slickensides (a) drained direct shear test results and (b)effective stress paths from undrained triaxial compression tests (from D'Appolonia et al., 1967) .

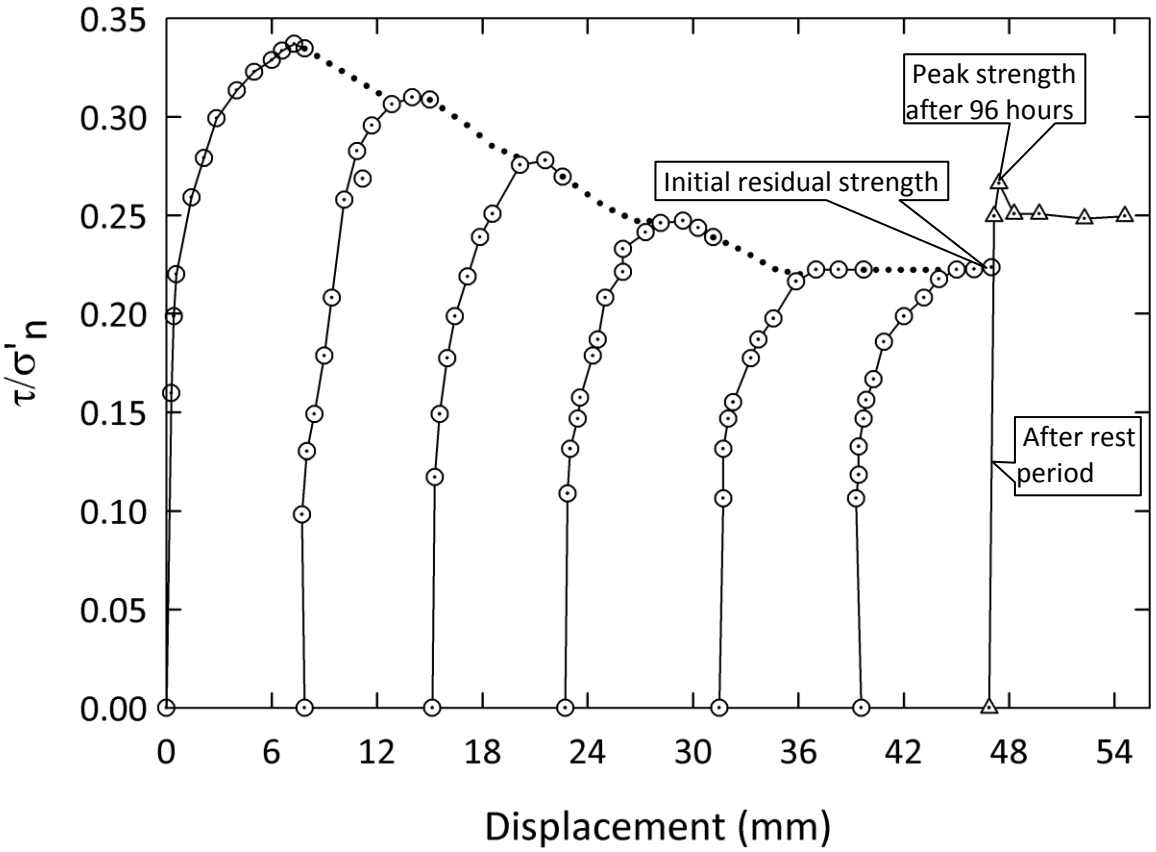

Figure 2.6. Strength-displacement relationships for bentonite at effective normal stress of 29.4 kPa (0.3 kg/cm^2) after a rest period of 96 hours (from Ramiah et al., 1973).

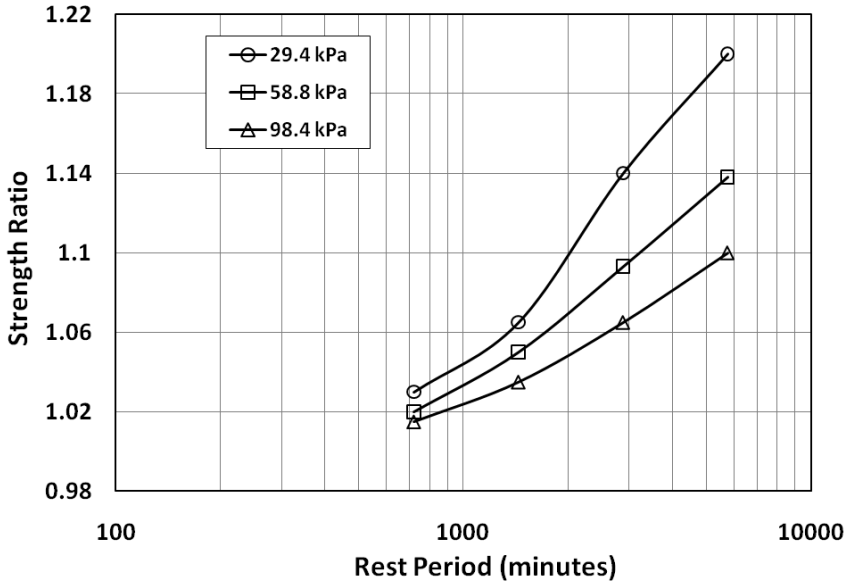

Figure 2.7. Strength ratio for applied normal stresses of 30, 60, and 100 kPa as a function of rest period for Bentonite (data from Ramiah et al., 1973).

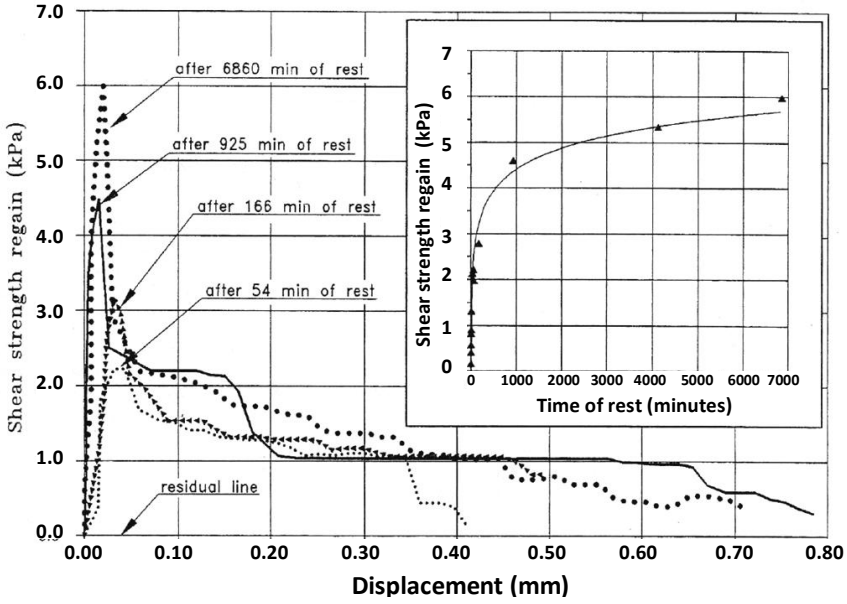

(a)

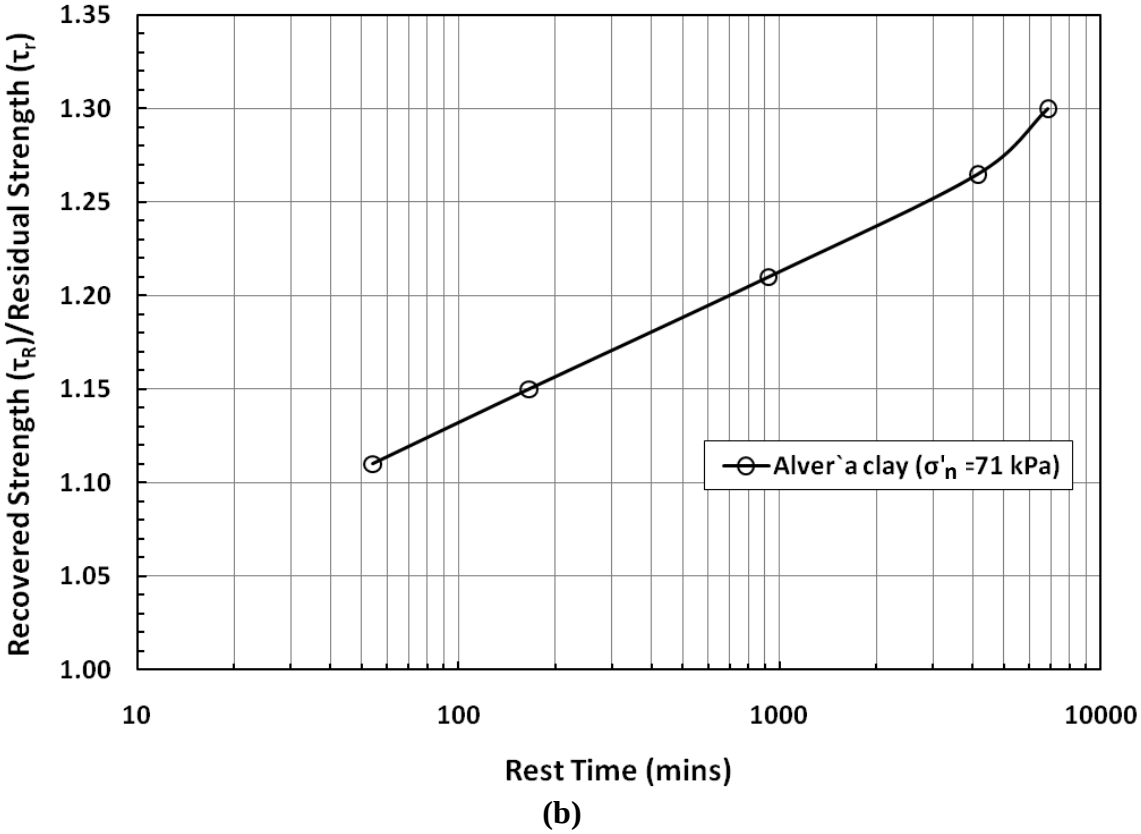

(b)

Figure 2.8. (a) Shear strength regain in direct shear test on slip surface specimen from Alver`a landslide for different rest periods (from Angeli et al., 1996) and (b) Ratios of the recovered strength and residual strength versus log of time (same data as shown in top figure).

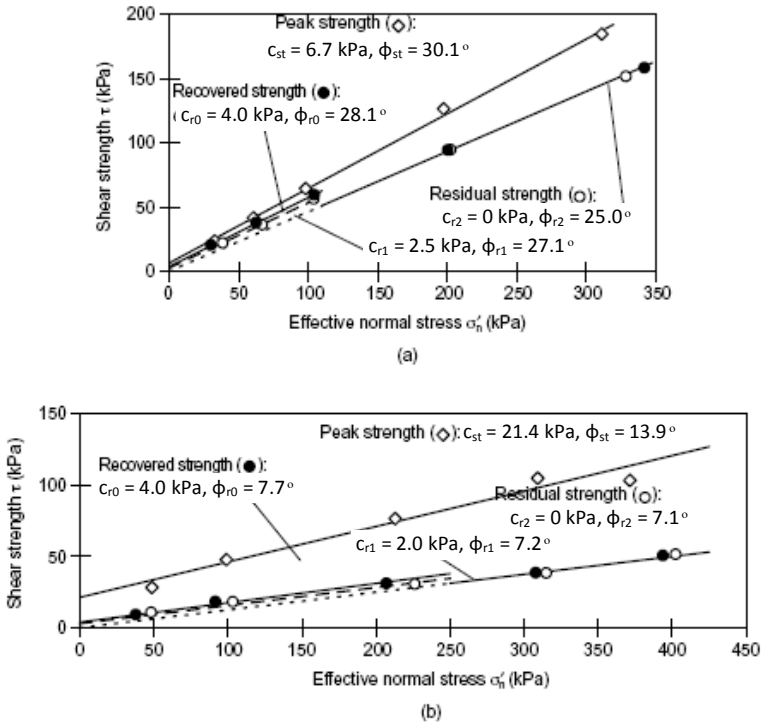

Figure 2.9. Test results and strength envelopes for (a) Xuechengzhen and (b) Kamenose soils (from Gibo et al., 2002).

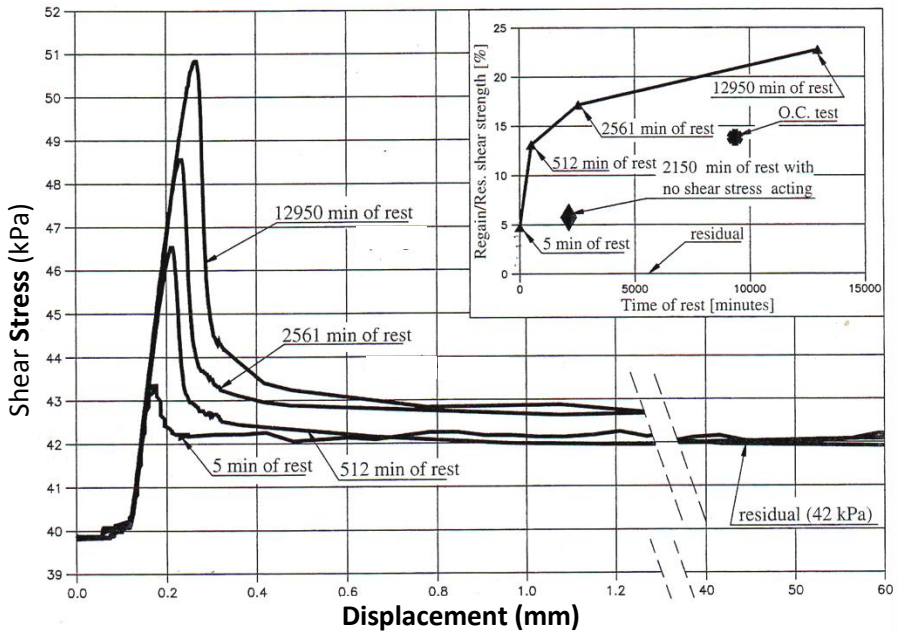

(a)

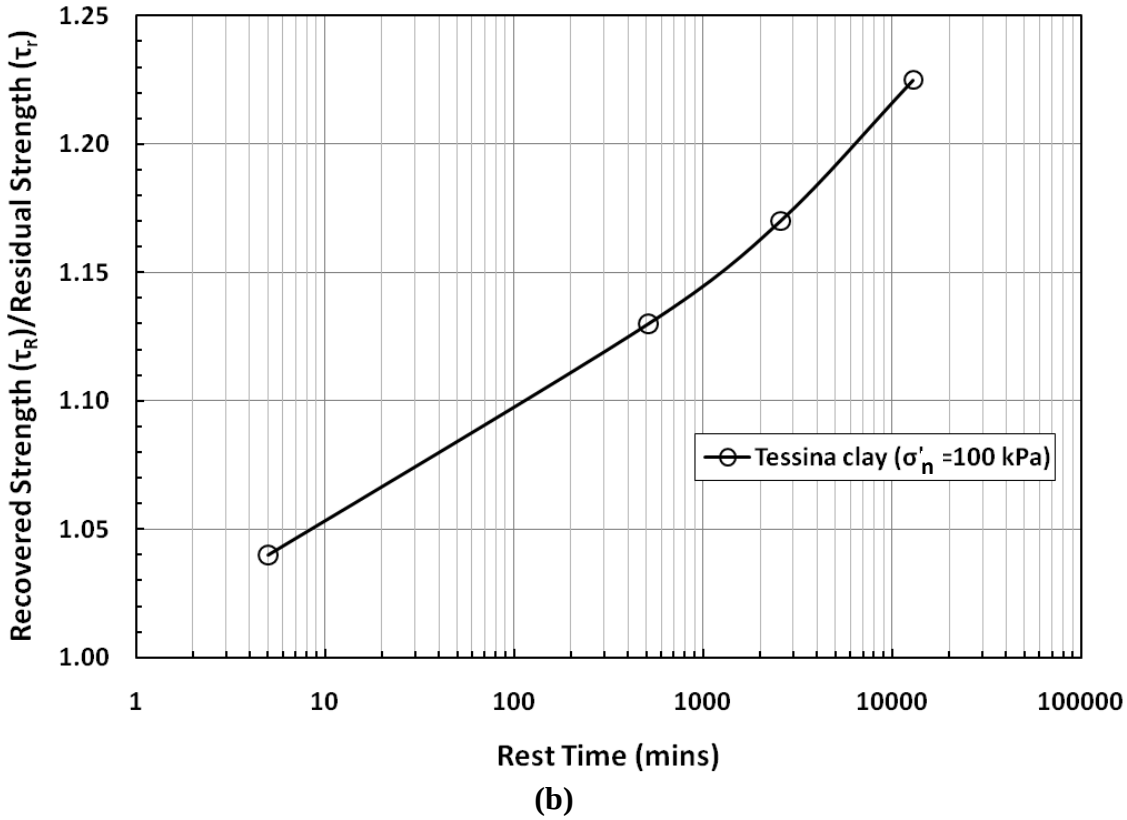

(b)

Figure 2.10. (a) Shear stress-displacement relationships for different rest periods, Tessina clay (from Angeli et al., 2004) and (b) Ratios of recovered strength and residual strength versus log of time (same data as shown in top figure).

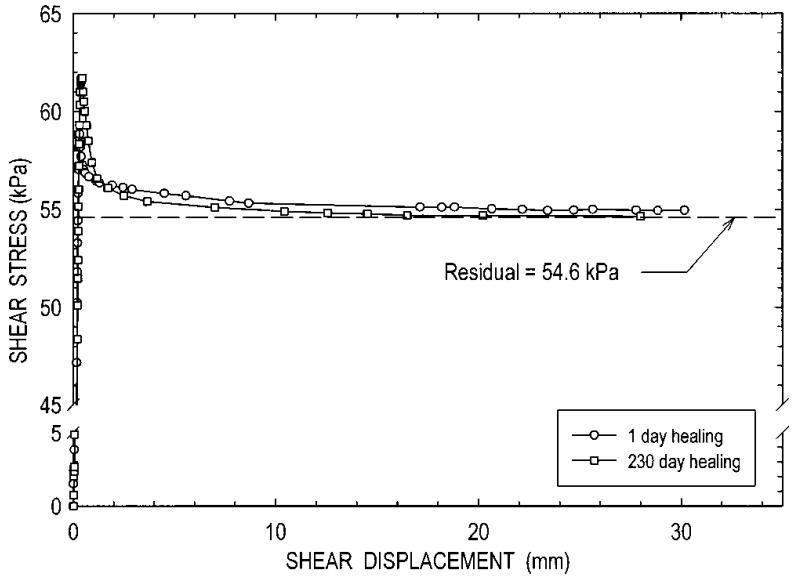

Figure 2.11. Shear stress–shear displacement relationships from healing tests on Duck Creek shale from Stark et al. (2005a).

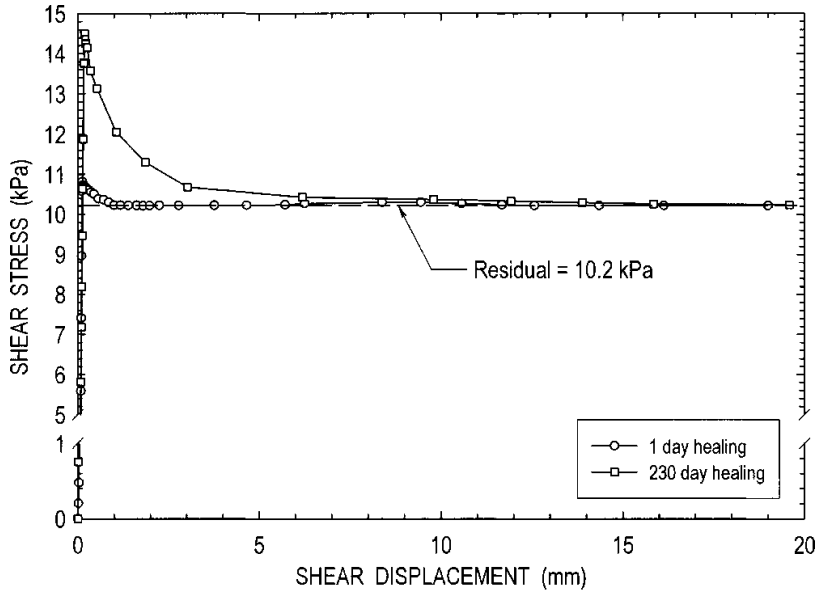

Figure 2.12. Shear stress–shear displacement relationships from healing tests on Otay bentonitic shale from Stark et al. (2005a).

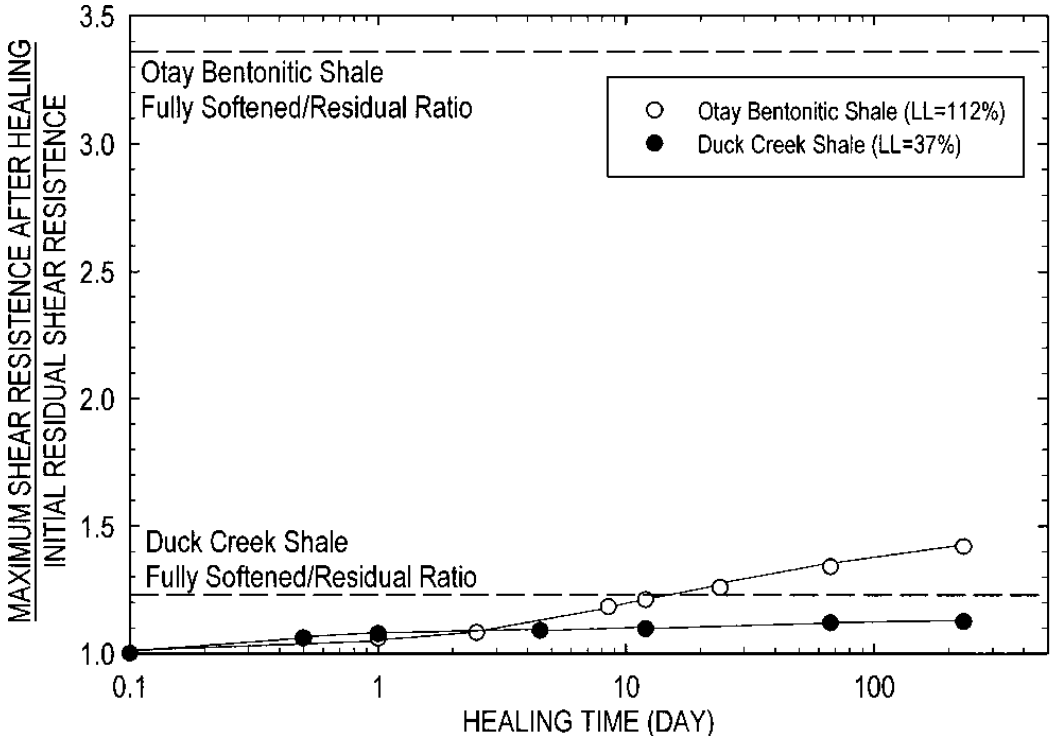

Figure 2.13. Ratio of maximum shear resistance after healing to initial residual shear resistance for Duck Creek shale and Otay bentonitic shale at effective normal stress of 100 kPa (from Stark et al., 2005).

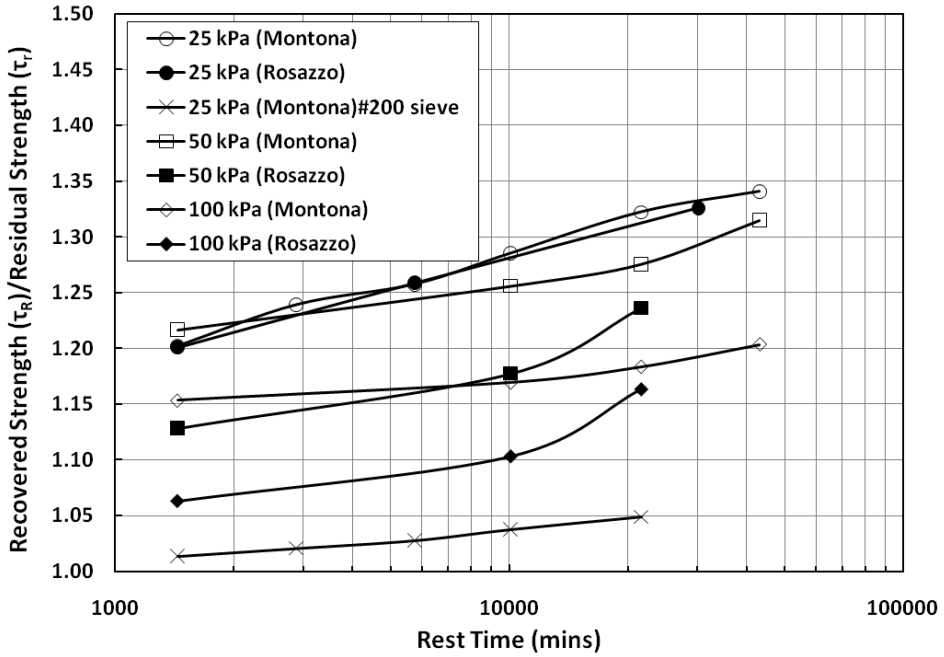

Figure 2.14. Recovered strength ratio versus rest time for Montona and Rosazzo flyschs at effective normal stresses of 25, 50, and 100 kPa (data from Carrubba and Del Fabbro, 2008).

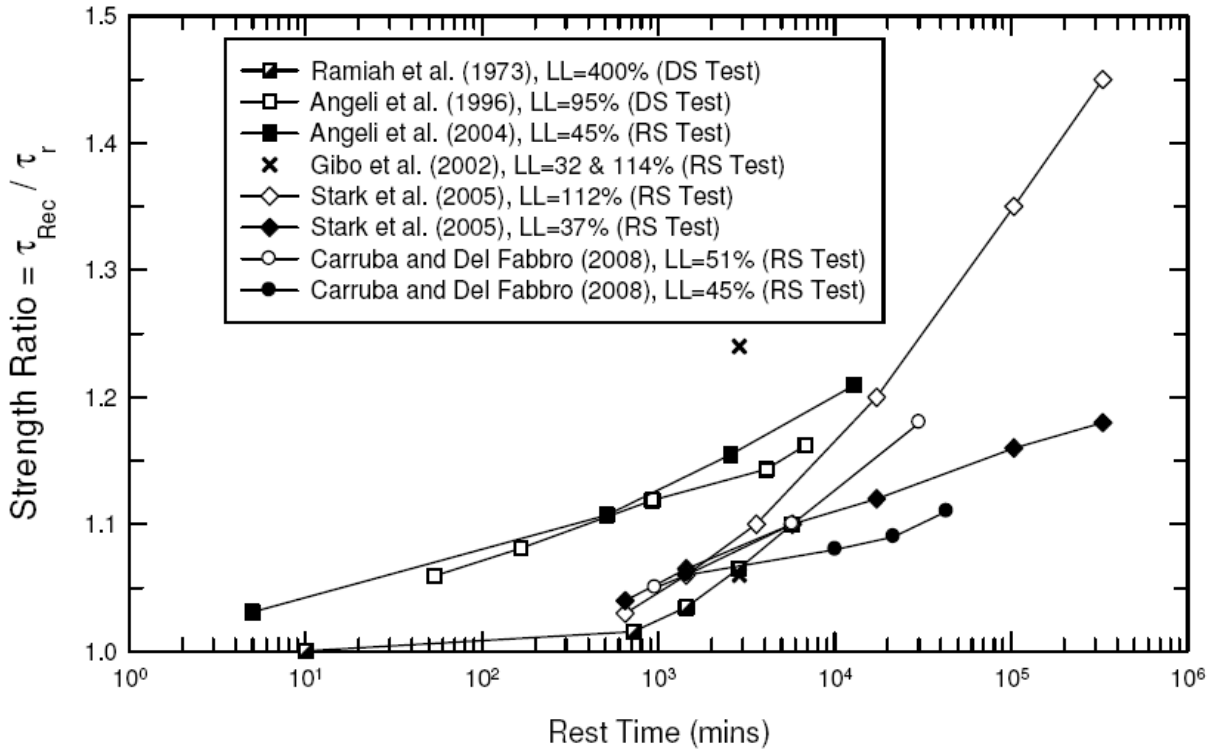

Figure 2.15. Summary of published strength recovery test results for effective normal stress of 100 kPa or less.

CHAPTER 3: STRENGTH RECOVERY TESTING ON PREEXISTING SHEAR SURFACES

3.1 Introduction

D'Appolonia et al. (1967) suggest that shear surfaces in cohesive soil, in particular colluvium, can undergo a "healing" causing the shear strength mobilized along a preexisting failure surface to be greater than the residual value. D'Appolonia et al. (1967) performed drained direct shear tests on intact undisturbed shear surface specimens and measured a peak strength which was greater than the residual strength of the slip surface material. Some researchers such as Ramiah et al. (1973), Angeli et al. (1996 and 2004), Gibo et al. (2002), Stark et al. (2005a) and Carrubba and Del Fabbro (2008), also suggest that preexisting shear surfaces may exhibit a higher shear strength than the drained residual value due to strength recovery during the time the slope remains stable based on laboratory test results. Ramiah et al. (1973) and Angeli et al. (1996) use a direct shear device, whereas, Gibo et al. (2002), Angeli et al. (2004), Stark et al. (2005a), and Carrubba and Del Fabbro (2008) use a torsional ring shear device to measure the strength gain with time above the residual value for different soils.

All of the researchers noted above observed a strength gain above the residual value with time in the laboratory using a different test procedure and various direct shear and ring shear devices. All of the researchers, except Stark et al. (2005a), use normally consolidated specimens in the tests. It is believed that a normally consolidated specimen will undergo more secondary compression and soil extrusion than an overconsolidated specimen when subjected to a rest period under the applied normal stress. Hence, the strength increase above the residual value in a normally consolidated specimen may not be representative of the field recovered shear strength instead it may be influenced by the test procedure.

For low plasticity soils, with a small difference between the fully softened and residual strengths, the importance of strength recovery may not be significant. Whereas high plasticity soils with a large difference between fully softened and residual strengths, the strength recovery could be significant. Therefore, it is important to determine the existence and magnitude of recovered shear strength of preexisting shear surfaces, if any, as a function of time. If a

preexisting shear surface exhibits strength recovery in a short period of time, i.e., prior to remediation, it might be possible to design the remedial measures using a shear strength greater than the drained residual strength for the problematic layer. This higher strength could reduce the cost of the remedial measures. This question was raised in 1991 for a landslide near Seattle, Washington and was the impetus for the strength recovery tests shown in Stark et al. (2005a). The 1990 movement involved less than 0.6 m of lateral movement of the reactivated landslide. A consultant proposed that the cohesive colluvium responsible for the slide had gained strength, i.e., healed, during the inactive or dormant period prior to 1990. As a result, it was concluded that the slide was less stable than before the 1990 movement because the shear strength increase due to healing was removed because of the less than 0.6 m of lateral displacement. The small amount of movement did not significantly change the driving forces but may have resulted in decreasing the resisting forces. In other words, the strength gain that occurred from the time that the ancient landslide occurred until 1990 was not available after the 1990 movement and thus the slope was less stable after 1990 than before 1990 because the slope geometry had not changed significantly. If the slip surface material had exhibited some strength gain it would have resulted the insurance company to install some additional remedial measures to bring the slope back to pre-slide stability/condition.

The study presented herein shows that the recovered shear strength at an effective normal stress of 100 kPa is greater than the drained residual strength of the soil but is essentially negligible at effective normal stresses greater than 100 kPa. Because an effective stress of 100 kPa corresponds to shallow landslides, the strength recovery may only have some impact on the repair of shallow or shallower portions of deep-seated preexisting landslides. Because remediation of deep landslides is more of a concern because of the greater repair costs than shallow landslides, the recovered strength may be applicable to the shallow portion of a deep landslide which is usually small. Thus, the present study suggests that the recovered strength may not significantly impact the analysis or repair of deep landslides. Furthermore, during the laboratory tests it was observed that the recovered strength was lost after small shear displacement which suggests that the recovered strength may not be reliable in remedial designs. The recovered strength may help explain the behavior of shallow landslides, e.g., little or no slope creep and observed period of no movement.

To investigate the possibility of strength gain along preexisting shear surfaces, there is a need to develop a refined test procedure that simulates field conditions. This chapter presents torsional ring and direct shear strength recovery test procedures, the test results, and conclusions about strength recovery in four soils with a range of plasticity.

3.2 Soils Selected for Strength Recovery Tests

Four natural soils obtained from field preexisting shear surfaces were selected for the laboratory strength recovery tests conducted herein. The soils were selected to represent a range of plasticity of soil (LL = 37-112%) which also represents the soils involved in most of the case histories discussed in Chapter 4. The four soils used for the strength recovery tests are Duck Creek shale from Fulton, Illinois with LL = 37%, silty clay from Esperanza Dam, Ecuador with LL = 55%, Madisette clay from Los Angeles, California with LL = 83%, and Otay bentonitic shale from San Diego, California with LL = 112%. Duck Creek shale and Otay bentonitic shale were re-tested herein because a shear stress corresponding to the residual strength condition was not applied during the rest periods in Stark et al. (2005a) testing.

To determine the index properties, remolded specimens were obtained by air drying a representative sample, crushing it with a mortar and pestle, and processing it through the Number 200 sieve. Ball milling was not used for these materials because it would change the texture and gradation of the soil and the soils did not have to be disaggregated. Distilled water was added to the processed soil until a liquidity index of about 1.5 was obtained for Atterberg limit tests. The samples for Atterberg limit tests, hydrometer analysis, and shear testings were allowed to hydrate for at least one week in a moist room. The index properties of the soils (LL, PL, and CF) were determined using the specimens passing the Number 200 sieve and the procedures presented in ASTM D4318 (2008a) and D422 (2008b) (see Table 3.1). The index properties of the specimens were measured using the same sieved soil samples used to create the ring and direct shear test specimen.

Table 3.2 shows the drained fully softened (ϕ'_{fs}) and residual (ϕ'_{r}) friction angles for the four soils measured using torsional ring shear tests. Drained fully softened friction angles were measured using separate ring shear tests on a normally consolidated specimen following the procedure suggested in ASTM WK#18521 (ASTM, 2010a). Drained residual friction angles

were obtained during the first portion of each strength recovery test using the procedure described by Stark and Eid (1993 and 1994) and ASTM D6467 (2008c).

Drained fully softened and residual friction angles for the soils measured during torsional ring shear testing at various effective normal stresses are compared in Table 3.2 to friction angles obtained from new empirical correlations presented in Figures 6.24 and 6.36. Table 3.2 shows good agreement between the measured and estimated drained fully softened and residual friction angles.

During the present study, laboratory ring shear strength recovery tests on all four specimens were performed at an effective normal stress of 100 kPa whereas Madisette clay and silty clay from Esperanza Dam were also tested at effective normal stresses greater than 100 kPa. Madisette clay was tested at effective normal stresses of 200, 300, and 600 kPa and silty clay from Esperanza Dam was tested at effective normal stresses of 300 and 600 kPa. Ring shear strength recovery tests were performed for rest periods of 1, 10, 30, and 90 days for all effective normal stresses whereas for an effective normal stress of 100 kPa, all four specimens were tested for a rest period of 300 days.

To verify the ring shear strength recovery test results, some direct tests were also performed on Madisette clay for effective normal stresses of 100 and 300 kPa. These tests were performed in a different shear device to confirm or reject the ring shear test results. Direct shear strength recovery tests on Madisette clay at an effective normal stress of 100 kPa were performed for rest periods of 1, 10, and 30 days whereas at an effective normal stress of 300 kPa the tests were performed for rest periods of 1 and 10 days. The reasons for selecting shorter rest periods for the direct shear strength recovery tests are discussed in subsequent sections and relate to ensuring the shear surface remained in the gap between the two halves of the direct shear box and because strength recovery was noticeable at effective normal stresses of 100 kPa or less and almost negligible at effective normal stress of 300 kPa.

3.3 Comparison of Laboratory Testing Apparatus for Strength Recovery Tests

Direct shear and torsional ring shear apparatus are commonly used to measure the residual shear strength of cohesive soils. The direct shear test provides an approximate value of residual strength because of limited continuous shear displacement whereas the torsional ring

shear test provides continuous shear displacement and thus a more reliable residual strength of cohesive soil (Stark and Eid, 1991). Skempton (1964) presents a procedure for reversing the direction of movement of the direct shear box to estimate the residual shear strength because of the limited continuous shear displacement.

There are different types of torsional ring shear devices around the world that are being used to measure the residual strength of cohesive soil. As a result, there are a number of different test procedures for these devices. The widely accepted torsional ring shear device is the Bishop-type ring shear apparatus suggested by Bishop et al. (1971) in which the specimen is sheared at a mid depth. A more common device is the Bromhead ring shear apparatus suggested by Bromhead (1979) in which shearing occurs at the top of specimen, i.e., smear type shearing. Because these three types of shear testing devices, i.e., direct shear, Bishop-type ring shear, and Bromhead ring shear, are used for measuring the residual shear strength of cohesive soils, all three apparatus were considered and evaluated for strength recovery tests in the study presented herein. Suitability of each apparatus for strength recovery tests is discussed below:

3.3.1 Direct Shear Apparatus

Direct shear apparatus is a common and popular apparatus used to investigate the shear strength of a soil. The Casagrande shear box with bottom and top halves having dimensions of 60 mm x 60 mm x 25 mm (2.36 in. x 2.36 in. x 1 in.) each is frequently used around the world. Direct shear test can be performed on an intact specimen, remolded specimen consolidated in a shear box by connecting the bottom and top halves together, and a precut specimen consolidated in separate oedometers and then assembling the two halves of the shear box as suggested by Mesri and Cepeda-Diaz (1986).

Skempton (1964) concludes that cohesive soils can obtain a residual strength condition along a shear surface after undergoing a large shear displacement. The direct shear box has several limitations for residual strength testing one of which is a maximum continuous shear displacement of about 6 mm in one direction. Thus, to obtain a residual strength condition the specimen must be sheared in different directions to achieve a large displacement by several times changing the direction of movement of the shear box. This is problematic because shear displacement in one direction is required to orient the clay particles parallel to the direction of

shear. Skempton (1964) proposes a reversal direct shear test in which the specimen is subjected to large shear displacement by changing the direction of movement of the shear box. This results in changing the orientation of previously aligned clay particles upon reversing the shearing direction and results in a peak strength being measured on the shear stress-displacement relationship at the start of each reversal. The peak strength observed on shear stress-displacement relationship is sometimes reduced to the observed minimum value at the end of previous movement after a small shear displacement. Skempton (1964) also identifies the danger of some slurrying the clay on the slip/shear surface in a reversal direct shear test. Residual shear strength, a constant value on shear stress-displacement relationship, typically is obtained after completion of 4 to 6 reversals cycles as suggested by Skempton and Petley (1967). Skempton (1964) acknowledges that direct shear reversal technique is not perfect and ideally the specimen should be sheared in one direction which resulted in Bishop developing a ring shear device.

Because of relative movement of the bottom and top halves of the shear box, cross-sectional area of the shear surface changes so an area correction is required. Due to the relative movement of the two halves of the shear box, the specimen at the opposite end of the two halves goes out of contact, experiences no loading, undergoes swelling, gets damaged (see Figure 3.1) and is not likely to contribute in the shearing resistance as the test continues, all of which adversely impacts the results. The direct shear test measures an approximate residual strength of cohesive soil but practitioners still rely on it because it may be the only test available in nearby soil testing facilities. Direct shear testing of a normally consolidated specimen also results in large amount of soil extrusion which results in a different shear surface developing. This extrusion also occurs with overconsolidated specimens but to a lesser extent.

Total thickness of a direct shear specimen is generally 50 mm or more and is likely to undergo secondary compression if kept loaded in the direct shear box for a long time which is required in strength recovery tests. The amount of secondary compression in a normally consolidated specimen is much greater than an overconsolidated specimen. Because shearing occurs in the gap between bottom and top halves of the shear box , if some vertical settlement occurs during the rest period of a strength recovery test it may result in the preexisting shear surface moving into the bottom half of the shear box. The settlement of the specimen and moving of shear surface below the top of bottom half may result in shearing along a new surface

upon re-shearing after a rest period. This shearing along a new surface will result in a peak strength on shear stress-displacement relationship that exceeds the residual value. The direct shear specimen should only be subjected to a rest period after reduction of the peak strength to the residual value and when the shear stress-displacement relationship becomes constant.

Because a gap is maintained between the bottom and top halves of the shear box to avoid metal to metal contact, the unloaded ends of the displaced specimen will undergo swelling whereas the loaded part of the specimen undergoes secondary compression. This swelling at the opposite ends of bottom and top halves of the shear box during the rest period causes damage at the unloaded ends of both the halves as shown in Figure 3.1. Thus, a residual strength measured after a rest period may be much lower than the actual residual strength of the specimen.

Another limitation of the direct shear test is that the top half can also displace in transverse direction with respect to the bottom half during the course of shearing or a rest period due to some loading defect or improper contact between the two halves or any other similar reason. Ramiah et al. (1973) and Angeli et al. (1996) use the direct shear test to investigate the strength recovery/regain in different soils but they used normally consolidate specimens which may be problematic for strength recovery tests so their data should be evaluated accordingly.

Therefore, direct shear strength recovery tests should be performed using overconsolidated specimens instead of normally consolidated specimens and great caution should be exercised to keep the preexisting shear surface in the gap between the bottom and top halves of the shear box. Because a direct shear test provides only an estimate of the residual strength and the residual strength measured after a rest period may be different than the value measured before stopping the test, there are many uncertainties in using a direct shear box for strength recovery test and the results should be evaluated carefully. Three direct shear strength recovery tests on Madisette clay were performed during this study to compare the ring shear strength recovery test results and to develop recommendations for a direct shear strength recovery test procedure.

3.3.2 Torsional Ring Shear Apparatus

3.3.2.1 Bishop-Type Ring Shear Apparatus

To overcome the limitations of the direct shear test, Bishop et al. (1971) developed a torsional ring shear apparatus, called Bishop-type ring shear apparatus, to measure the residual strength of cohesive soils. The Bishop-type torsional ring shear apparatus uses an annular specimen with 152 mm and 101 mm outer and inner diameters, respectively, and a specimen height of 19 mm. The specimen is sheared near the mid-height and shearing occurs only in one direction. Thus, the specimen can be sheared to an unlimited continuous shear displacement without changing the direction of shear (see Figure 3.2). The specimen is confined radially by upper and lower confining rings and a gap is opened and maintained after consolidation near mid-height where shearing occurs with the aid of a gap control mechanism. The Bishop-type ring shear test apparatus usually results in extensive amount of soil extrusion during testing and it is difficult to control it. The specimen is contained in the two confining rings so it is difficult to observe the shearing directly which makes it difficult to control the extrusion or adjust the gap.

In the Bishop et al. (1971) ring shear apparatus, the cross-sectional area of the specimen is constant so an equal effective normal stress is maintained over the entire specimen during consolidation, shearing, and the rest period. The Bishop-type ring shear apparatus can be used for testing normally and overconsolidated, intact and remolded specimens. Because the entire specimen experiences an equal effective normal stress during all stages of a test, the specimen will experience uniform vertical settlement, if any, due to secondary compression during a rest period of strength recovery test. Thus, the effect of vertical settlement due to secondary compression of the specimen is not as pronounced as it is in the direct shear test because of small specimen thickness and also shearing will occur along the same shear surface upon restarting of test after a rest period assuming the shear surface remains in the gap between the two confining rings.

Various torsional ring shear devices have been developed and are being used both in research and practice with confidence. Basic design and testing procedure for most of the ring shear devices being used is similar to the ring shear device developed by Bishop et al. (1971) in which shearing occurs at mid-height of a specimen except the Bromhead device discussed below.

In a strength recovery test when the test is stopped after establishing the residual strength condition and is allowed to rest for a selected period of time, the clay particles will maintain particle-to-particle contact along the shear surface. Thus, any process(s) or mechanism(s) responsible for strength recovery/healing, discussed in following section of this chapter, occurs at the face of the oriented clay particles aligned along the shear surface. Important processes during particle-to-particle contact during the rest period include cation exchange, van der Waals attraction, and cementation. The Bishop et al. (1971) ring shear device is best suited for investigation of strength recovery/healing in the laboratory because the shear is confined and occurs at a soil-to-soil interface. However, the Bishop et al. (1971) ring shear device is not common and difficult to use.

Gibo et al. (2002) use a Japanese ring shear device that is similar to the Bishop et al. (1971) device because shearing occurs near mid-height of the specimen. Gibo et al. (2002) use this device to measure the recovered shear strength of a soil specimen obtained from the actual shear surface of a landslide. These torsional ring shear apparatus can be used in accordance with ASTM D6467 (2008c) to measure the drained residual shear strength of cohesive soils.

3.3.2.2 Bromhead Ring Shear Apparatus

Bromhead (1979) suggests another type of torsional ring shear device, called a Bromhead ring shear device, which is similar to the Bishop-type ring shear apparatus except that the shearing occurs at the top of the specimen, i.e., a smear type shearing at the soil-to-top bronze porous stone interface. This device uses a thin specimen (5 mm thick) and allows unlimited continuous shear displacement in one direction. Stark and Eid (1994 and 1997) and Stark et al. (2005a) show that the Bromhead ring shear apparatus yields reliable values of residual shear strength of cohesive soils because these results are in agreement with the shear strength parameters obtained from the back-analyses of various case histories of reactivated landslides. Mesri and Shahien (2003) use the ring shear data of Stark and Eid (1994 and 1997) to augment the conclusion of Stark and Eid (1994 and 1997) that the residual strength measured from Bromhead ring shear tests is in agreement with the shear strength obtained from back-analysis of reactivated landslides.

In the Bromhead ring shear device the cross-sectional area is constant so the specimen experiences an equal and constant effective normal stress during all stages of a test. The specimen also experiences uniform vertical settlement, if any, due to secondary compression during a rest period of strength recovery test. Thus, the effect of vertical settlement due to secondary compression of the specimen with thickness less than 5 mm is also not pronounced as it is in the direct shear test with a relatively thick specimen.

The laboratory study conducted herein uses the Bromhead (1979) ring shear apparatus with the modified specimen container suggested by Stark and Eid (1993). The Bromhead ring shear apparatus is manufactured by Wykeham-Farrance Engineering Limited and was used to investigate the drained residual shear strength of claystones, mudstones, and clay shales by Stark and Eid (1994 and 1997) and Stark et al. (2005a). The ring shear specimen is annular with an inside diameter of 70 mm and an outside diameter of 100 mm. Drainage is provided by two bronze porous stones mounted on the top platen and the bottom of the specimen container. The reconstituted specimen is confined radially by the specimen container, which is 5 mm deep. This apparatus can be used according to the procedure in ASTM D6467 (2008c) to measure the drained residual shear strength. The modified Bromhead ring shear apparatus (Stark and Eid, 1993) reduces the effect of wall friction by allowing the specimen to be raised after consolidation and preshearing. Based on back-analysis of case histories and comparisons with other ring shear data, e.g., Bishop et al. (1971), the modified Bromhead device yields representative values of the field drained residual shear strength when used in accordance with ASTM D6467 (2008c).

3.3.2.2.1 Strength Recovery Tests with Modified Bromhead Ring Shear Device

After establishing the drained residual strength condition, the soil specimen can be kept fully submerged in the container under the applied normal stress for any duration. The gears used to rotate the ring shear specimen container remain engaged and prevent any reduction in applied shear force from the proving rings. Furthermore, after reaching the residual condition, a soil specimen under applied shear stress almost equal to the residual strength of the soil will prevent any shear displacement during the rest period.

In a modified Bromhead ring shear apparatus, the shear strength recovery period can occur for any duration without undergoing shear displacement under the applied stresses. Any

change in the vertical dial gauge during the rest period represents vertical settlement of the specimen. The arrangement of the apparatus is such that every time the test is restarted, shearing occurs along the same shear surface developed during the prior shearing, i.e., at or near the top of the specimen. Upon restart of the test after a rest period, the peak strength is recorded and compared to the initially established drained residual shear strength of the specimen. Angeli et al. (2004), Stark et al. (2005a), and Carrubba and Del Fabbro (2008) use the Bromhead ring shear device to investigate the shear strength recovery of cohesive soils.

In Bromhead ring shear device shearing occurs at or near the top of specimen and at the bottom of top bronze porous stone with knurled surface (see Figure 3.3(a)). An investigation was also made to determine the effect of this knurled surface of the top bronze porous stone on strength recovery/healing. The ASTM D6467 (2008c) procedure suggests using a specimen overconsolidated to 700 kPa and unloaded to a lower effective normal stress at which the drained residual strength test is to be performed so the specimen remains overconsolidated to reduce vertical settlement due to secondary compression. The specimen is overconsolidated in the ring shear with a bronze porous stone attached to the top platen so the specimen is forced into the knurled surface of top bronze porous stone. Thus, the soil in the knurled surface and below it is overconsolidated.

During preshearing, shearing, rest period after reaching the residual strength condition, and reshearing, the soil in the knurled surface is likely to exhibit a similar behavior as the soil below the shear surface except a shear surface does not form in the knurled area. The knurled area of the top bronze porous stone is about 25% of the surface area of the top bronze porous stone. Stark and Eid (1993 and 1994) conclude that a soil-to-soil contact is maintained along the shear surface during the shearing process and at no point soil-to-metal (top bronze porous stone) contact is observed. In other words, the shear surface develops just below the knurled surface in soil not at the soil-metal interface.

The bottom of the top bronze porous stone at the end of a residual strength test contains a thin soil layer at the knurled surface and the knurled surface and the knurled area is filled with soil (see Figure 3.3). Stark and Eid (1993) also determine that the top bronze porous stone has 0.1-0.3 mm thick soil attached to it at its end and at no stage the shearing occurs at soil-to-metal interface. Figure 3.3 shows a picture of the top bronze porous stone attached to the top platen

before testing and after a 90- days strength recovery test on Madisette clay at an effective normal stress of 200 kPa. Figure 3.3(b) shows the presence of a thin soil/clay layer at the bottom of top porous bonze which suggests shearing along a soil-to-soil interface not soil-to-metal interface. This is concluded because no portion of the knurled surface is visible. In addition, there are no striations in the soil that indicate shearing in the knurled surface.

The location and geometry of the shear surface is important because any observed strength gain may be caused by movement of the shear surface. For example, if the shearing initially occurred below the knurled surface in the soil, during the rest period the shear surface below the knurled area could move up resulting in undulating shear surface as shown in Figure 3.4. Upon reshearing the undulating shear surface would result in a shear resistance greater than the residual strength value. This does not seem plausible because:

- The greater strength gain occurs at an effective normal stress of 100 kPa or less which is less likely to cause the shear surface to move up in the knurled surface area than at higher normal effective stresses, e.g., 200, 300, and 600 kPa.
- The specimen was overconsolidated to 700 kPa and unloaded to 100 kPa so little, if any, consolidation or secondary compression should occur during the entire duration of the test.
- The wall friction mobilized along the vertical surfaces of knurled surface should also resist upward movement of the shear surface.
- If a new failure surface was created by the prior shear surface moving in the knurled surface, the peak strength measured would require a larger shear displacement to return to the residual strength value than the extremely small shear displacement observed in the tests performed herein.
- Soil extrusion, if any, occurs below the knurled surface so soil loss is not a mechanism for upward movement of the shear surface.

In summary, the strength recovery measured at effective normal stress of 100 kPa or less is not due to the Bromhead ring shear device for the reasons mentioned above and other researchers with different devices measured a similar strength gain.

Figure 3.5 shows the shear displacement required to reach the residual strength condition in intact (not presheared), presheared, and resheared after a rest period of 300 days of Madisette clay. Figure 3.5(a) shows that shearing of a specimen at a drained rate after preshearing may require a shear displacement of 5-10 mm depending on the shear displacement induced during preshearing, to reach the residual strength condition. The specimen without preshearing reached the residual strength condition after undergoing a large shear displacement (approximately 40 mm) as shown in Figure 3.5(b). Figure 3.5(c) shows that the smallest shear displacement (≈ 2 mm) is required to reach the residual strength condition after a rest period of 300 days at an effective normal stress of 100 kPa. Therefore, if shearing was occurring along a new shear surface after the rest period due to shear surface moving into the knurled surface, the shear stress-displacement relationship should have shown a peak strength and a shear displacement greater than 10 mm to reach the residual strength value. Instead, upon restarting the test after the rest period, the peak strength was reduced to the residual value after a small shear displacement (≈ 2 mm) as shown in Figure 3.5(c). This is also in agreement with findings of other researchers, such as Angeli et al. (2004), Stark et al. (2005a), Carruba and Del Fabbro (2008), and Stark and Hussain (2010a). Upon restarting the test after a rest period, no volume change, i.e., vertical displacement, occurs for the initial 4-5 mm of shear displacement during which the peak strength is observed and the strength is reduced to the residual value. The observed volume change usually occurred after reaching the residual strength condition due to some specimen extrusion.

In the Bromhead ring shear device a thin soil/clay layer remains at the bottom of top bronze porous stone ensuring soil-to-soil contact along the shear surface and there is no evidence of the preexisting shear surface moving up into the knurled area causing a new shear surface to develop and a strength greater than the residual value to be measured. Thus, Bromhead ring shear device is equally suitable for strength recovery tests.

3.4 Ring Shear Strength Recovery Tests

3.4.1 Ring Shear Strength Recovery Test Procedure

The shear strength recovery tests performed herein utilize remolded and reconstituted specimens obtained from shear surface samples. Prior to the test, liquid limits (LL) and plastic limits (PL) are determined using ASTM D4318 (2008a) and clay size fraction (CF) (less than

0.002 mm) using ASTM D422 (2008b). The drained residual strength of the soil is determined using the equipment and procedure described in Stark and Eid (1993 and 1994) and ASTM D6467 (2008c). The reconstituted specimen is consolidated in the ring shear device to an effective normal stress of 700 kPa. After consolidation at 700 kPa, the specimen is unloaded to the effective normal stress at which the strength recovery test will be conducted. After unloading to the desired effective normal stress, the specimen is pre-sheared to start formation of a shear surface using the procedure described in ASTM D6467 (2008c). This reduced the shear displacement required to reach the residual strength condition. The presheared specimen is allowed to dissipate excess pore-water pressures for 24 hours after pre-shearing before drained shearing is commenced. This 24 hour period is not a healing period but a pore pressure equilibration period. Afterwards, the pre-sheared specimen is sheared at a drained shear displacement rate of 0.018 mm/min until the drained residual shear strength is obtained. After achieving a drained residual strength, shearing is stopped and the specimen is allowed to rest in the ring shear device.

The specimen is subjected to the applied effective normal stress and the measured residual shear stress for the entire duration of the rest period. Because the sliding mass in the field remains subjected to a shear stress after movement, the shear force applied at the end of residual strength test is maintained on the specimen throughout the rest period to simulate field conditions. The gears used to rotate the ring shear specimen container remain engaged and prevent any reduction in shear force during the rest period. Thus, the specimen remains subjected to the residual shear and normal stresses during the rest period. The rest periods used herein are 1, 10, 30, and 90 days for all applied effective normal stresses except 100 kPa which also used 300 days.

After a rest period of one day, shearing is restarted with the shear and effective normal stress corresponding to the initial drained residual condition. The specimen is sheared at the same rate, i.e., 0.018 mm/min, and the maximum strength after healing is measured, which may or may not be greater than the residual value. Shearing is continued until the initial drained residual strength is achieved again. After the drained residual strength is achieved again with additional shear displacement, shearing is stopped and the specimen is allowed to rest for the next rest period under the imposed shear and effective normal stress.

The recovered shear strengths for the other rest periods, i.e., 10, 30, 90, and 300 days, are measured by repeating the procedure described above for the one day rest period (see Figure 3.6). The drained residual strength at the end of shearing performed after each rest period is at or near the initially determined drained residual strength as shown in Figure 3.6.

3.4.2 Ring Shear Strength Recovery Test Results and Discussion

The recovered shear strength ($\boldsymbol{\tau_{Rec}}$) measured for all of the soils in ring shear tests is greater than the drained residual shear strength at all the effective normal stresses used and for the rest periods considered in the present study. However, the test results show that the increase in shear strength above the residual value in each soil is greater at low effective normal stresses, i.e., $\sigma'_n \leq 100$ kPa, and almost negligible at high normal stresses, i.e., $\sigma'_n > 100$ kPa, and the increase is a function of rest time. Therefore, the ring shear strength recovery test results at an effective normal stress of 100 kPa are discussed in more detail because the recovered strength for $\sigma'_n \leq 100$ kPa do not have any engineering significance .

The fully softened shear strength ($\boldsymbol{\tau_{fs}}$) corresponds to the peak shear strength of a normally consolidated soil with random particle arrangement which is the upper bound strength used for the analysis of slopes that have not undergone previous sliding. Therefore, $\boldsymbol{\tau_{Rec}}$ is not expected to exceed $\boldsymbol{\tau_{fs}}$ in the laboratory or field because of the presence of a preexisting shear surface and alignment of clay particles along the shear surface parallel to the direction of shear. Furthermore, $\boldsymbol{\tau_r}$ is the minimum or lower bound strength which is used in the analysis of ancient and reactivated landslides and is also used as a reference strength for strength recovery because the recovered strength is the increase above the residual value. Thus, $\boldsymbol{\tau_{fs}}$ and $\boldsymbol{\tau_r}$ are considered the upper and lower bound strengths, respectively, for the recovered strength and provide a means for evaluating the significance, if any, of the measured strength gain. Because $\boldsymbol{\tau_{Rec}}$ is not expected to exceed $\boldsymbol{\tau_{fs}}$, a *"recovered strength ratio"* is introduced that incorporates $\boldsymbol{\tau_r}$, $\boldsymbol{\tau_{fs}}$, and $\boldsymbol{\tau_{Rec}}$. The *recovered strength ratio* (RSR) is the difference between $\boldsymbol{\tau_{Rec}}$ and $\boldsymbol{\tau_r}$ divided by the difference between $\boldsymbol{\tau_{fs}}$ and $\boldsymbol{\tau_r}$ as shown in Equation (3.1).

$$\text{Recovered Strength Ratio}\,(\text{RSR}) = \frac{\left(\tau_{\text{Rec}} - \tau_r\right)}{\left(\tau_{fs} - \tau_r\right)} \tag{3.1}$$

If no strength recovery occurs, τ_{Rec} equals τ_r and the *recovered strength ratio* equals zero (RSR = 0). If the soil gains strength to τ_{fs} (which is not likely), τ_{Rec} equals τ_{fs} so the *recovered strength ratio* equals unity (RSR = 1.0). Thus, the range of values of the recovered strength ratio is zero to less than unity.

The data in Table 3.3 are used to calculate the RSR for each soil and rest period at an effective normal stress (σ'_n) of 100 kPa. Table 3.3 also presents the values measured for drained fully softened friction angle (ϕ'_{fs}), drained residual friction angle (ϕ'_r), and difference between drained recovered friction angle (ϕ'_{Rec}) and drained residual friction angles, i.e., $\phi'_{Rec} - \phi'_r$, for the four soils at σ'_n = 100 kPa. Corresponding RSR values calculated using Equation 3.1 are plotted in Figure 3.7. Figure 3.7 also shows an increase in recovered strength ratio with increasing rest period for all four soils tested. However, Figure 3.7 shows that the RSR at an effective stress of 100 kPa is measurably greater than the drained residual strength but is negligible at higher effective normal stresses. Furthermore, RSR increases for all of the soils tested with increasing rest time albeit at different magnitudes (see Figure 3.7). These results are in agreement with prior testing, e.g., Ramiah et al. (1973), Angeli et al., (1996 and 2004), Gibo et al., (2002), Stark et al., (2005a) and Carrubba and Del Fabbro, (2008), that show a strength gain at $\sigma'_n \leq 100$ kPa (see Figure 2.13). The main differences in the current study and other studies is the investigation of strength recovery at $\sigma'_n > 100$ kPa (up to σ'_n = 600 kPa) and rest periods up to 300 days or almost one year. Figure 3.7 shows test results at $\sigma'_n > 100$ kPa are substantially lower than at σ'_n = 100 kPa with values of RSR less than 0.2 for Esperanza Dam sample and less than 0.1 for Madisette clay for rest periods of up to 90 days. At σ'_n = 100 kPa, the value of RSR for Esperanza dam sample is greater than 0.5 and for Madisette clay is greater than 0.2 for rest periods of up to 90 days.

Duck Creek shale with the lowest plasticity (LL=37%) and the smallest difference between τ_{fs} and τ_r exhibits the highest RSR at 100 kPa (see Figure 3.7). Figure 3.7 indicates that the rate of increase in RSR ($\approx$ 0.6) is decreasing at 300 days at σ'_n = 100 kPa so the RSR for Duck Creek shale probably will not reach unity. Otay bentonitic shale with the highest plasticity (LL=112%) and the largest difference between the τ_{fs} and τ_r exhibits the lowest RSR for the rest periods considered. Figure 3.7 also shows that the increase in RSR for Otay bentonitic shale is starting to decrease with time and probably will not exceed an RSR of 0.4. Silty clay from

Esperanza Dam and Madisette clay from Los Angeles exhibit RSRs in between Duck Creek and Otay bentonitic shales which is in agreement with the liquid limit/plasticity of these materials.

Figure 3.8 presents the normalized strength ratio (NSR) given by Equation (3.2) as a function of rest time on a semi-log scale.

$$\text{Normalized Strength Ratio (NSR)} = \frac{\left(\tan\phi'_{Rec} - \tan\phi'_r\right)}{\left(\tan\phi'_r\right)} \tag{3.2}$$

The value of NSR relates the strength gain to the residual value. If NSR equals zero there is no strength recovery and if NSR is greater than zero the value represents the ratio of the recovered strength to the residual value.

Figure 3.8 shows the largest increase in NSR occurs for the highest plasticity soil and increases quicker than for lower plasticity soils at an effective normal stress of 100 kPa. The data in Figure 3.8 may be important for landslides because many slides occur through high plasticity soil but a significant strength gain only occurred at an effective normal stress of 100 kPa.

The NSR in Figure 3.8 can be used to estimate the recovered friction angle (ϕ'_{Rec}) at σ'_n = 100 kPa using the measured or estimated residual friction angle (ϕ'_r). A limitation to using the NSR to estimate ϕ'_{Rec} is having to measure ϕ'_r in the laboratory or estimating it from an empirical correlation, such as Stark et al. (2005a). Given that 300 days usually expires between the occurrence of a landslide and repair, a more meaningful method to estimate the increase in friction angle is using the liquid limit. Figure 3.9 presents a relationship between LL and the difference between ϕ'_{Rec} and ϕ'_r which is referred to as $\Delta\phi'$ at an applied normal stress of 100 kPa. Thus, the increase in the drained friction angle can be estimated directly using Figure 3.9 and the LL measured using ASTM D4318 (2008a).

Figure 3.10 shows the ratio between the recovered shear strength and initial residual shear strength as a function of rest time. The results agree with the results of ring shear tests for strength recovery tests conducted by Gibo et al. (2002), Angeli et al. (2004), Stark et al. (2005a) and Carrubba and Del Fabbro (2008), and also reversal direct shear tests conducted by Ramiah et al. (1973) and Angeli et al. (1996) as shown in Figure 2.13.

The data from the strength recovery tests on Duck Creek shale, Esperanza Dam silty clay, Madisette clay, and Otay Bentonitic shale are plotted in terms of normalized recovered strength (τ/σ'_n) as a function of time in Figure 3.11. Figure 3.11 shows that a linear relationship is obtained for the normalized recovered strength with time at an applied normal stress of 100 kPa. Because the slope of these four plots is approximately constant, the general expression given in Equation (3.3) can be used to represent these four relationships.

$$\left(\frac{\tau_{Rec}}{\sigma'_n}\right)_{t=rest\ period} = \left(\frac{\tau_r}{\sigma'_n}\right) + 0.01*\ln(t) \qquad (3.3a)$$

$$\left(\frac{\tau_{Rec}}{\sigma'_n}\right)_{t=rest\ period} = \left(\frac{\tau_r}{\sigma'_n}\right) + \left(\frac{\ln(t)}{\sigma'_n}\right) \qquad (3.3b)$$

$$\left(\tau_{Rec}\right)_{t=rest\ period} = \tau_r + \ln(t) \qquad (3.3c)$$

where: $(\tau_{Rec}/\sigma'_n)_{t\ =\ rest\ period}$ is the normalized drained recovered strength after a rest period of t days, (τ_r/σ'_n) is the normalized initial drained residual strength, t is the recovery time is *days* ($t \leq$ *1000 days)*, and σ'_n is applied normal stress which is *100 kPa* in this case.

The residual strength ratio (τ_r/σ'_n) differs for each soil but the slope (*0.01*ln (t)*) is almost constant for the four soils considered at an effective normal stress of 100 kPa. Equation (3.3) can be used to estimate the strength recovery during the period of interest after the drained residual is obtained at an effective normal stress of 100 kPa using ASTM D 6467 (2008c). This expression also can be used to determine how much strength recovery could occur in a specified amount of time after a landslide. It is important to note that the recovered strength should be less than the fully softened strength of a soil and Equation (3.3) may only be considered applicable for a rest period of 1000 days or less.

One strength recovery ring shear test (RS-10) on silty clay from Esperanza Dam was also performed at an effective normal stress of 100 kPa and no shear stress being applied during the rest period. The procedures above were used for specimen preparation, consolidation, and shearing except that after establishing the initial residual strength condition, the shear stress exerted by the proving ring force couple was removed by disengaging the gears and removing

the proving rings from the top platen. Therefore, this specimen (RS-10) is referred to as a "relaxed" specimen. Because the test specimen in RS-2 was subjected to the applied effective normal stress and the shear stress that corresponds to the residual strength during the rest period, the test specimen (RS-2) is referred herein as an "engaged" specimen. The strength ratios ($\boldsymbol{\tau}_{Rec}/\boldsymbol{\tau}_r$) for the relaxed specimen (RS-10) and the engaged specimen (RS-2) at an effective normal stress of 100 kPa and for rest periods of 1, 10, 30, and 90 days are shown in Figure 3.12. Figure 3.12 shows that $\boldsymbol{\tau}_{Rec}$ in an engaged specimen (RS-2) is greater than $\boldsymbol{\tau}_{Rec}$ in a relaxed specimen (RS-10) for similar rest periods at effective normal stress of 100 kPa. This may be cause by starting shear of the relaxed specimen (RS-10) after each rest period from the no initial shear stress condition instead from the residual stress. But as discussed earlier, the applied shear stress conditions during the rest period simulate the field conditions therefore the results of ring shear test RS-2 (engaged specimen) are believed to be representative of actual field conditions.

During the ring shear tests, the water content of the specimens could not be determined because the specimens would have to be unloaded and new soil added to repair the specimen to measure water content. Water contents measured at the end of the test for each specimen were close to the plastic limit of the soil and were in the range of 33-39%. Some very small vertical settlements were also observed during each rest period for all four soils even though the applied effective normal stress remained constant during the rest period. Cumulative vertical strains measured during the rest period for all four soils at an effective normal stress of 100 kPa are shown in Figure 3.13. This observed vertical settlement during the rest period is probably due to secondary compression of the specimen and the shear zone material during the rest period.

In summary, the ring shear strength recovery test results discussed above show that the recovered shear strength is more relevant at effective normal stresses of 100 kPa or less which correspond to a shallow depths of landslides. Thus, the recovered strength may have an impact, if any, on the analysis and repair of shallow landslides in high plasticity material and appears to have little, to no, practical impact for deep landslides. Remediation of deep landslides is more of a concern because of the higher repair costs involved than shallow landslides. The recovered strength may be applicable to the shallow portion of a deep landslide which is usually fairly small. Thus, it is anticipated that the recovered strength may not significantly impact the analysis or repair of deep landslides.

In addition, the test results herein show that even at low effective normal stress, most of the strength gain is lost if the specimen undergoes a small shear displacement. This indicates τ_{Rec} reflects a brittle and sensitive soil structure and probably should not be relied upon in remedial design even at effective normal stresses of 100 kPa or less.

3.5 Direct Shear Strength Recovery Tests

3.5.1 General

To verify the ring shear strength recovery test results, direct shear tests were performed on Madisette clay using reconstituted, precut, and overconsolidated specimens and the test procedure proposed by Mesri and Cepeda-Diaz (1986). Because the ring shear strength recovery test results presented above show that the shear strength recovery was pronounced at effective normal stress of 100 kPa and negligible at effective normal stresses greater than 100 kPa, the direct shear strength recovery tests were performed at two effective normal stresses, i.e., 100 and 300 kPa, to verify the findings of the ring shear strength recovery tests.

The direct shear specimens were overconsolidated to reduce the potential of the shear surface moving below the gap between the upper and bottom halves of the shear box, i.e., below the top of bottom half of the shear box, during shearing or a rest period which would result in an increase in strength upon reshearing as discussed previously. Overconsolidation of the specimen also reduced the amount of extrusion during shearing.

Initially one specimen was consolidated to high consolidation pressure of 2700 kPa and unloaded to the desired effective normal stress at which the specimen was sheared at drained rate to calibrate the equipment for the strength recovery tests and streamline the procedures for further testing. A high consolidation pressure of 2700 kPa was used to simulate the formation of a shale or mudstone in the field. After calibration of direct shear device and streamlining the procedures for strength recovery tests, one specimen was tested after consolidating to the same consolidation pressure, i.e., 2700 kPa, afterwards another specimen was tested after consolidating to consolidation pressure of 700 kPa and unloading it to the required effective normal stress for shearing to simulate the ring shear test procedure so the test results from these two devices could be compared. Detailed direct shear procedures for specimen preparation, consolidation, shearing to establish residual strength condition and strength recovery tests are

discussed below. The direct shear strength recovery test procedure and test results for the specimen consolidated to effective normal stresses of 700 and 2700 kPa and tested at two effective normal stresses of 100 and 300 kPa are presented below.

3.5.2 Direct Shear Specimen Preparation and Consolidation

A laboratory study was conducted herein to investigate the strength recovery using a direct shear device and a natural cohesive soil, i.e., Madisette clay from Los Angeles, California, with liquid and plastic limits of 83% and 29%, respectively, and a clay-size fraction, CF, (< 0.002 mm) of 52%. As described before the index properties were determined using ASTM D4318 (2008b) and D422 (2008c). The reconstituted specimen passing Number 200 sieve was prepared at an initial water content higher than the liquid limit, at a liquidity index of about 1.5, and are hydrated for one week under a moisture controlled environment. Direct shear pre-cut specimens were prepared from a rehydrated soil sample with water contents below the liquid limit to reduce the time to end of primary consolidation. The pre-cut specimens were prepared using the procedures described by Mesri and Cepeda-Diaz (1986). The rehydrated soil was transferred to the bottom and top halves of a shear box separately with the shear surface sides supported by Tetko polyester screen (HD-7-6) placed on a smooth and flat Teflon plate. Tetko polyester screen (HD-7-6) is used in place of filter paper because it is resistant to biodegradation. Drainage on the other side of the bottom and top half was provided with porous stones with a Tetko polyester screen in between. Each half was connected to a separate specimen container with the help of screws and each specimen container was then transferred to a separate oedometer for consolidation. The specimens were subjected to consolidation pressures of 700 and 2700 kPa. The specimens were kept submerged in distilled and deionized water for the entire duration of consolidation. The laboratory tests were conducted at constant temperature of 20ºC (70ºF).

Each specimen was consolidated in the oedometer using load increment ratio of one (LIR = 1.0) and ASTM D2435 (2008d). Normal pressures/stresses were calculated using actual loads at each increment and loaded area of direct shear box (60 mm x 60 mm). Each specimen was allowed to complete primary compression under the applied load. After completion of loading to the required normal pressure/stress each specimen was unloaded to 100 kPa in decrements of two and allowed to rebound during unloading. After unloading to 100 kPa, each specimen was

reloaded to 300 kPa, and allowed to recompress. This procedure was used to ensure that the direct shear specimens are in recompression during the entire test duration that can help to reduce the amount of soil extrusion, minimize the secondary compression, and prevent the movement of the shear surface.

Two direct shear specimens were consolidated in separate halves to consolidation pressure of 2700 kPa and the other to 700 kPa and in both cases the specimens were unloaded to 100 kPa, and then reloaded to 300 kPa. The specimens that were consolidated to high consolidation pressures of 2700 kPa are referred herein as specimens DS-1 and DS-2 and the specimen that was consolidated to 700 kPa is referred herein as specimen DS-3. Direct shear test, DS-1 was used to calibrate the equipment and streamline the direct shear strength recovery test procedure whereas the test results of DS-2 and DS-3 are discussed in detail in this chapter. End of primary (EOP) e-log σ'_v relationships for DS-2 and DS-3 are shown in Figures 3.14 and 3.15, respectively.

After consolidating each half of the shear box separately, both bottom and top halves were removed from the oedometer. To create a slickensided surface after consolidation, a surgical blade was used to pre-cut the lower face of the upper half of the shear box and the upper face of the lower half of the shear box. This pre-cutting resulted in the maximum possible orientation and alignment of clay particles along the face of each half of the shear box in the direction of first movement of the shear box. This pre-shearing process reduced the shear displacement required to achieve a residual strength condition because of the limited continuous shear displacement allowed in the direct shear box (see Figures 3.16 and 3.17). This reduced the amount of soil extrusion and the potential for the shear surface to move below the gap between the top and bottom halves of the shear box.

After completion of consolidation and pre-cutting, the two halves of the direct shear box were combined to create a 11.3 mm thick specimen for DS-2 and 12.5 mm thick specimen for DS-3 in the direct shear device. The assembled shear box in each test was then placed in the direct shear apparatus and loaded to an effective normal stress of 300 kPa and allowed to equilibrate for two days before shearing. Special care was taken to ensure that the shear surface remained within the gap between two halves of the shear box.

3.5.3 Shearing and Strength Recovery

Specimens DS-2 and DS-3 were tested using the same shearing and recovery procedure described herein. After observing the compression/swelling behavior of the specimen in the assembled box, the specimen was sheared at a drained rate of 0.0034 mm/min following procedure described in ASTM D3080 (2008e) until the drained residual strength condition was established. The residual strength condition was obtained by reversing the shear box back and forth as shown in Figures 3.16 and 3.17 until a constant minimum strength was obtained.

After obtaining the residual strength condition, the test was continued until shear stress-displacement relationship became constant while the shear box was moving in the forward direction (see third cycle of shear stress-displacement relationships in Figures 3.16 and 3.17) so the proving ring would be in compression and not in tension during the rest periods. When the shear stress-displacement relationship became constant, the test was stopped for a rest period of one day. During the rest period, the shear stress is not likely to drop because the soil is mobilizing a shear strength equal to its residual strength.

After one day of rest, shearing was restarted at a rate of 0.0034 mm/min and the change in shear stress, if any, was noted. Any increase in shear stress above the residual value observed after restarting the test is the recovered strength after a rest period of one day. The specimen was sheared until the strength returned to the residual value and then the test was stopped for another rest period of 10 days. After 10 days, the test was restarted and changes in shear stress were measured. The maximum strength observed after a rest period of 10 days is the recovered strength at 10 days (Figures 3.16(b) and 3.17(b)). The one day test result was confirmed in DS-3 by repeating the test after obtaining the residual strength conditions after 10 days test (see Figure 3.17b). To avoid excessive settlements at an effective normal stress of 300 kPa, the specimen was not subjected to any other rest period.

After observing the peak strength after the previous rest period, each specimen was sheared until it reached the original position by reversing the direction of the shear box so that both halves of the shear box were aligned (Figures 3.16 and 3.17). Both top and bottom halves of the shear box were connected with the locking box screws and the specimen was unloaded to an effective normal stress of 100 kPa. Each specimen was allowed to swell at this effective normal

stress until no change in specimen height was observed. After each specimen completed swelling, the screws connecting the top and bottom halves of the shear box were removed to start shearing.

Each specimen was sheared at the same drained displacement rate, i.e., 0.0034 mm/min, and a residual strength condition at effective normal stress of 100 kPa was established. The test was stopped following the same procedure described for an effective normal stress of 300 kPa and subjected to rest periods of 1, 10, and 30 days (see Figures 3.18 and 3.19). The maximum shear resistance observed after each rest period is the recovered strength for that particular rest period. Shorter rest periods were selected for the direct shear tests to prevent the shear surface from moving below or above the gap between the two halves of the shear box and causing a strength increase. Vertical displacement versus shear displacement behavior during shearing at σ'_n of 300 and 100 kPa for DS-2 and DS-3 tests are shown in Figures 3.20 and 3.21, respectively.

3.5.4 Direct Shear Strength Recovery Test Results and Discussion

Figure 3.22 shows the ratio between the recovered and residual shear strengths ($\boldsymbol{\tau_{Rec}/\tau_r}$) as a function of rest time from direct shear test results of DS-2 and DS-3 at 100 and 300 kPa on Madisette clay. The DS-2 and DS-3 test results at effective normal stresses of 100 and 300 kPa and for similar rest periods are in agreement which indicate that there is no effect of overconsolidation ratio (OCR) on the direct shear strength recovery test results, i.e., consolidation pressures of 2700 kPa versus 700 kPa. Water content at the end of the each test was measured in the range of 35-38% which is close to the plastic limit of Madisette clay which are in agreement with that water content measured for ring shear specimens at the end of the strength recovery tests.

The DS test results of DS-2 and DS-3 shown in Figure 3.22 show that the recovered strength is greater than the drained residual strength at an effective normal stress of 100 kPa and is negligible at an effective normal stress of 300 kPa. As discussed earlier, an effective normal stress of 100 kPa corresponds to shallow landslides which suggest that the strength recovery is possible only in shallow landslides or at shallow depths of deep-seated landslides. These findings are also in agreement with the conclusions presented by D'Appolonia et al. (1967), Ramiah et al. (1973), Angeli et al. (1996 and 2004), Gibo et al. (2002), Stark et al. (2005a), Carrubba and Del

Fabbro (2008), and Stark and Hussain (2010a and 2010 b). It is thought that at shallower depths this gain may be caused by the rebound or unbending of the oriented clay particles along the shear surface at the lower effective normal stress which may not be possible at greater depths due to higher effective normal stresses.

Figure 3.22 also shows that the recovered shear strengths measured from the direct shear strength recovery tests differ from the values of recovered shear strengths obtained from the ring shear tests at both effective normal stresses of 100 and 300 kPa. The ring shear device yielded a higher recovered strength at σ'_n = 100 kPa but the direct shear device gave a higher recovered strength at σ'_n = 300 kPa. This difference between the ring shear and direct shear test results may be due to differences in measured drained residual shear strength in each device, difference in test procedures, and state of applied stresses during the rest periods in both devices. Both the ring shear and direct shear recovered strengths are noticeably greater than the drained residual shear strength at an effective normal stress of 100 kPa and negligible at an effective normal stress of 300 kPa.

The observed recovered strength in the direct shear tests even at an effective normal stress of 100 kPa was lost with a small shear displacement and this strength should not be used in design of landslide remedial measures. As suggested during the discussion on ring shear strength recovery test results, the strength gain at 100 kPa or less may not be economically significant for the repair of shallow landslides or shallower portion of a deep-seated landslide but may be helpful in explaining the behavior of shallow landslides.

3.6 Probable Causes of Strength Recovery

Although prior researchers have recognized a strength gain above the residual value with time (D'Appolonia et al., 1967, Ramiah et al, 1973, Angeli et al., 1996 and 2004, Gibo et al., 2002, Stark et al., 2005a, and Carrubba and Del Fabbro, 2008), the actual mechanism(s) causing the strength gain is not known. Some probable causes of strength recovery considered in this study are described below in no particular order.

3.6.1 Primary and/or Secondary Compression

In the case of a first time slide, randomly aligned clay particles orientate along the shear surface such that interparticle contacts change from edge-to-face to face-to-face orientation. A drained residual strength condition develops when a majority of the clay particles achieve a face-to-face orientation parallel to the direction of shear. When the sliding mass comes to rest and stabilizes, the disturbed soil mass is subjected to the applied normal stress and can undergo primary consolidation if excess pore-pressures were developed during shearing. If the shear surface had previously reached a residual condition, the majority of the clay particles along the shear surface should have been oriented parallel to the direction of shear so there should be little, if any, porewater pressure generation because no additional particle re-orientation should occur (Terzaghi et al., 1996).

Even if no significant primary consolidation occurs, secondary compression will occur under constant applied normal stress (Mesri and Castro, 1987). Secondary compression results in an increase in strength primarily due to a decrease in void ratio (Mesri and Castro, 1987), microinterlocking, and interparticle contacts (Schmertmann, 1991). The strength recovery reported herein occurred under constant shear and effective normal stress and some vertical settlement was observed during each rest period. The thickness of specimens during ring shear tests conducted herein is ranges from 3.0 - 3.5 mm. Figure 3.13 shows cumulative vertical strains that occurred during a particular rest period as a function of rest time for the four soils tested. This suggests that the specimens underwent some secondary compression during each rest period and the amount of secondary compression increased with increasing plasticity and rest time.

At a higher effective normal stresses the amount of secondary compression should be greater than at lower effective normal stresses. Therefore, the strength recovery should have been more pronounced at higher effective normal stresses and less at lower effective normal stresses. Whereas the laboratory test results showed that the strength recovery is noticeable at low effective normal stresses of 100 kPa or less and is almost negligible at effective normal stresses greater than 100 kPa. This suggests that the primary and secondary compression of the slip surface material may not have considerable effect on the strength recovery.

3.6.2 van der Waals Attraction

When two solids or silicate plates approach each other, their atoms can act as instant dipoles and attract each other. This involves long range as well as short range interaction. Czarneck and Dabros (1980) show that the roughness of particle surfaces markedly decreases the van der Waals attraction energy in a particle-semi-infinite medium therefore a smooth shiny slickensided surface is likely to exhibit more van der Waals forces of attraction. It is assumed that oriented clay particles along a shear surface with smooth platy and shiny surfaces are likely to have greater van der Waals attraction than randomly arranged clay particles. Thus, van der Waals attraction may be a mechanism leading to the strength recovery of pre-existing shear surfaces.

3.6.3 Cementation

Many soils contain free carbonates, iron oxides, alumina, and organic matter that may precipitate at interparticle contacts and act as a cementing agent (Mitchell and Soga, 2005). Cementation may not be observed in the laboratory with remolded specimens because of insufficient time for cementation to occur but it may occur in the field when much longer cementation periods are allowed. Thus in an ancient landslide, cementation may be a mechanism that contributes to the strength gain (healing) as suggested by D'Appolonia et al. (1967). This mechanism is not likely to be significant shortly after a landslide because sufficient time has not elapsed for cementation to occur. The bonds formed by cementation tend to be brittle and can be destroyed by small shear displacement. However, the cementation process can restart after each shear displacement event ceases.

3.6.4 Cation Exchange

Under a given set of environmental conditions (temperature, pressure, pH, chemical and biological composition of the water), clay adsorbs cations of specific types and amounts (Mitchell and Soga, 2005). Cations that neutralize the net negative charge on the surface of soil particles in water are readily exchangeable with other cations (Terzaghi et al., 1996). The exchange reaction depends mainly on the relative concentration of cations in the water and also on the electrovalence of the cations. Although the exchange reactions do not ordinarily affect the

structure of the clay particles, it may result in important changes in the physical and physicochemical properties of the soil (Mitchell and Soga, 2005). This cation exchange and/or chemical reaction can result in shear strength gain along the failure surface.

3.6.5 Thixotropic Hardening

Thixotropy is defined as an isothermal, reversible, time-dependent process and occurs under constant composition, stress, and volume. The hardening results in the material becoming stronger and stiffer but is usually removed upon remolding (Mitchell and Soga, 2005). Some of the initial work on thixotropy is reported by Skempton and Northey (1952), Seed and Chan (1957), and Mitchell (1960). These studies suggest that thixotropy may occur in the majority of clay-water systems. Figure 3.23 shows the properties of purely thixotropic material presented by Mitchell and Soga (2005). Thixotropy has been described as a mechanism that balances the forces applied to the deposit (Mitchell, 1960). When a soil is remolded or compacted, a structure is induced that is compatible with the externally applied shear and normal stresses. If a thixotropic soil is then subjected to deformation, the structure is disturbed to resist the applied stress (see Figure 3.24). If the applied shear stress is subsequently removed, the soil is now unbalanced and starts to relax. As the soil relaxes, attraction forces can develop between the soil particles. This attraction may result in the formation of a flocculated structure (Mitchell, 1960). In addition, the adsorbed water and cations will adjust to the reduced shear stress. This equilibration process is time dependent and in general the greater the time the greater the strength gain. However, this mechanism to date has been used to explain increases in peak strength, not residual strength, with time. More specifically, this mechanism has not been evaluated for a preexisting shear surface.

3.7 Summary and Design Recommendations

During the present study, a strength greater than the residual value was measured in ring shear strength recovery tests on the four soils tested and also in direct shear strength recovery tests on one soil. The ring shear strength recovery test results show that high plasticity soils exhibit higher than low plasticity soils for the same rest period. Both ring shear and direct shear test results also show that the recovered strength is significant at low effective normal stress of 100 kPa and is negligible at effective normal stresses of more than 100 kPa.

An effective normal stress of 100 kPa corresponds to shallow landslides which suggest that the strength recovery is relevant to shallow landslides or at shallow depths of deep-seated landslides. These findings are in agreement with the conclusions presented by D'Appolonia et al. (1967), Ramiah et al. (1973), Angeli et al. (1996 and 2004), Gibo et al. (2002), Stark et al. (2005a), and Carrubba and Del Fabbro (2008). At shallower depths this gain may be caused by the rebound or unbending of the oriented clay particles along the shear surface at the lower effective normal stress which may not be possible at greater depths due to higher effective normal stresses. It is also observed during ring and direct shear tests that the recovered strength is lost after a small shear displacement so the recovered strength may not be useful for practice. Furthermore, the strength gain at 100 kPa or less may not be economically significant for the repair of shallow landslides or shallower portion of a deep-seated landslide. Instead this strength gain may only be useful for explaining the behavior of shallow landslides investigated by researchers, such as D'Appolonia et al. (1967), Angeli et al. (1996 and 2004) and Gibo et al. (2002). Back-analysis of these landslides are discussed in Chapter 4.

If strength recovery tests are performed, they should be conducted using an overconsolidated specimen to reduce the magnitude of secondary compression during the rest period especially for direct shear tests. The specimen should be subjected to the normal and shear stresses that correspond to the residual strength of the soil to simulate field conditions. A torsional ring shear apparatus is a better device for performing strength recovery tests than the direct shear device because shearing occurs in one direction, the effective normal stress is uniformly applied to the entire specimen, and secondary compression results in a uniform vertical movement of the entire shear surface.

In direct shear strength recovery test, the test should be stopped for a rest period after a constant, minimum strength is achieved. Furthermore, the direct shear test period should be stopped for a rest when the direct shear box is moving in the forward direction so the proving ring is under compression not in tension. This is recommended because the proving ring is usually calibrated in compression and performs well in compression as compared to tension. Caution should be exercised when setting up the direct shear test, during shear and during the rest periods so that the shear surface remains between the gap between the two halves of the shear box in particular above the top of bottom half.

The drained residual strengths measured in DS-2 and DS-3 tests at similar effective normal stresses are in agreement and confirm that the residual shear strength is independent of the OCR or loading history. However, the values of drained residual friction angle obtained from DS-2 and DS-3 are lower than the values obtained from the ring shear tests at similar effective normal stresses and also than the values obtained from the empirical correlation presented by the present study as shown in Figure 6.24. This difference between the values of drained residual friction angle measured in the direct shear and ring shear tests at similar effective normal stresses is greater than 3.5° which reinforces that the direct shear device is not best suited for measuring the drained residual strength of cohesive soils.

During the laboratory study it was determined that the direct shear strength recovery test results were different from the ring shear strength recovery test results for Madisette clay at effective normal stresses of 100 and 300 kPa. The difference between the ring shear and direct shear test results may be due to differences in measured drained residual shear strength in each device, difference in test procedures, and state of applied stresses during the rest periods in both devices.

The mechanism(s) involved in strength recovery/healing may be secondary compression of shear surface material, van der Waals attractions, cation exchange, thixotropic hardening and/or particle reorientation as result of unbending especially at low effective normal stresses. The ring shear specimens tested herein were submerged in distilled and deionized water, and the tests were conducted at a constant temperature of 70ºF so desiccation, water chemistry, and temperature probably did not play a major role in the observed strength increase.

The present study and its results differ from the previous studies in following ways:

1) The present study used four natural soils with range of plasticity with LL from 37% to 112%.

2) Particle size of the material tested during the present study passed Number 200 sieve, i.e., <0.002 mm. All prior researchers, except Stark et al. (2005a), used material passing Number 40 sieve (0.425 mm) which may have included some silt and fine sand that may not be representative of field conditions along the shear surface.

3) Tests were performed at a range of effective normal stresses from 100 to 600 kPa, whereas, previous researchers performed tests at effective normal stresses of 100 kPa or less. Only Gibo et al. (2002) performed tests at $\sigma'_n > 100$ kPa.

4) Stress conditions during the rest period include an effective normal stress and a shear stress that correspond to the residual strength of the soil to simulate field conditions.

5) During the present study strength recovery tests were performed for rest period up to 300 days. Gibo et al. (2002) use a maximum rest period of only two days, Ramiah et al. (1973) use up to 4 days, Angeli et al. (1996 and 2004) use up to 5 and 9 days, respectively, and Carrubba and Del Fabbro (2008) use up to 31 days. Although Stark et al. (2005a) used longer rest periods i.e., up to 230 days, no shear stress was applied to the specimen during the rest period which is not representative of field conditions.

6) Gibo et al. (2002) conclude that strength recovery is possible in silty and sandy clays whereas this study shows the largest strength recovery occurs in high plasticity soil.

3.8 Tables and Figures

Table 3.1. Index properties of soils selected for strength recovery tests.

Soil Type	Soil Locations	Liquid Limit (%)	Plastic Limit (%)	Clay size fraction (CF) (<0.002mm, %)	Plasticity Index (PI)	Activity (A_c)
Duck Creek Shale	Fulton, IL	37	25	19	12	0.63
Silty Clay	Esperanza Dam, Ecuador	55	40	28	15	0.54
Madisette Clay	Los Angeles, CA	83	29	52	54	1.04
Otay Bentonitic Shale	San Diego, CA	112	53	73	59	0.81

Table 3.2. Comparison of measured and estimated drained fully softened and residual friction angles for soils used for strength recovery tests at various effective normal stresses.

Soil Type	Effective Normal Stress, σ'_n	Drained Fully Softened Friction Angles, ϕ'_{fs}		Drained Residual Friction Angles, ϕ'_r	
		Measured	Updated Correlation (Figure 6.36)	Measured	Updated Correlation (Figure 6.24)
	kPa	deg	deg	deg	deg
Duck Creek Shale	100	33.6	32.5	28.6	29.9
Esperanza Dam	100	30.1	28.5	22.6	23.2
	300	27.6	-	20.5	-
	400	-	24.8	-	19.3
	600	24.2	-	18.2	-
Madisette Clay	100	22.8	22.2	10.8	11.6
	200	21.8	-	10.0	-
	300	21.0	-	9.8	-
	400	-	18.7	-	9.7
	600	19.0	-	8.0	-
Otay Bentonitic Shale	100	19.0	20.2	5.8	8.7

Note: Updated empirical correlations show values of ϕ'_{fs} at σ'_n = 50, 100, and 400 kPa and ϕ'_r at σ'_n = 50, 100, 400, and 700 kPa based on LL and CF of the soil.

Table 3.3. Increase in friction angles measured during strength recovery tests at effective normal stress of 100 kPa.

Soil Type	Secant Friction Angles		Increase in Friction Angles ($\Delta\phi' = \phi'_{Rec} - \phi'_r$)				
	(ϕ'_{fs}, deg)	(ϕ'_r, deg)	1 day	10 day	30 day	90 day	300 day
Duck Creek	33.6	28.6	1.00	2.40	3.05	3.53	3.86
Silty Clay	30.1	22.6	1.02	3.03	3.79	4.47	5.01
Madisette Clay	22.8	10.8	0.63	2.14	2.9	3.72	4.92
Otay Bentonitic Shale	19.0	5.8	0.45	1.97	2.71	3.57	4.32

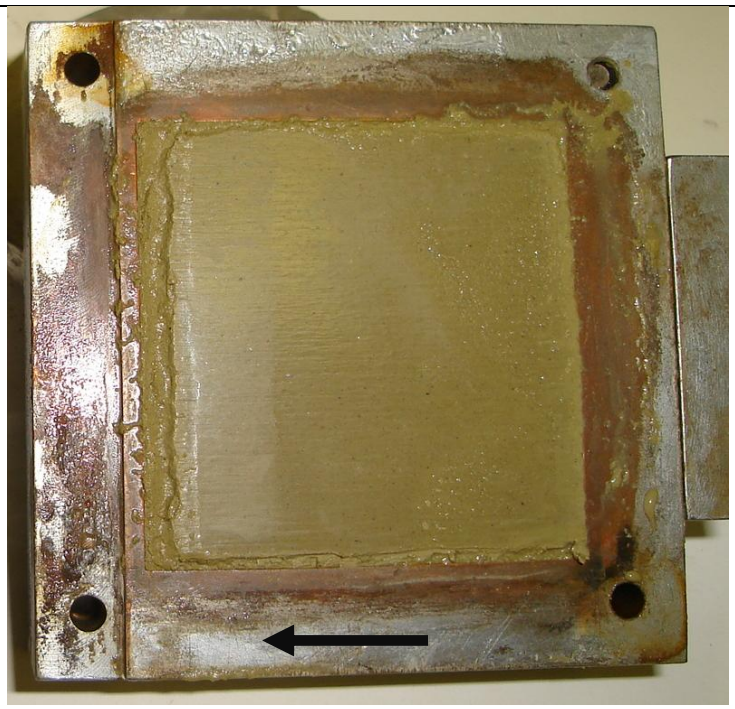

(a) Top half

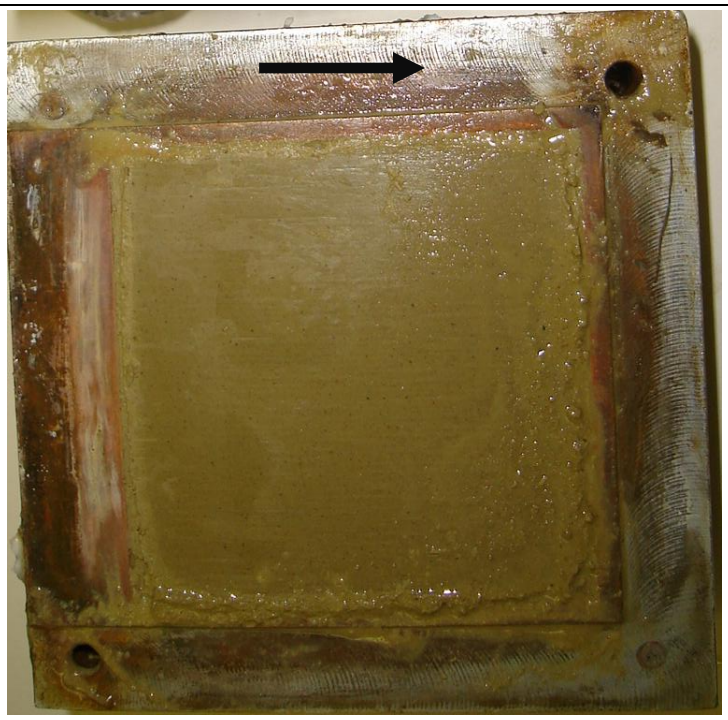

(b) Bottom half

Figure 3.1. Direct shear specimen showing the damaged part on the two opposite ends of the bottom and top halves.

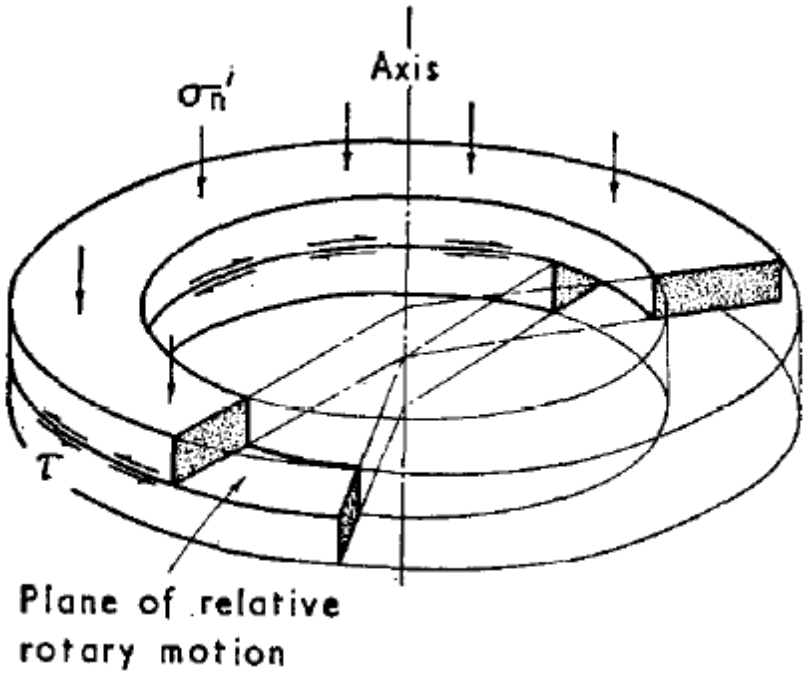

Figure 3.2. Ring shear test specimen (from Bishop et al., 1971).

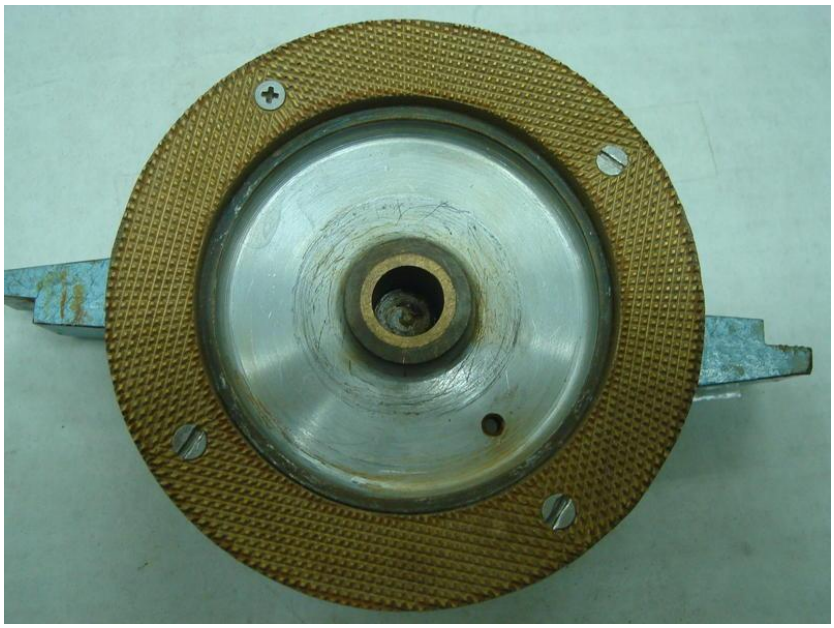

(a)

(b)

Figure 3.3. Top bronze porous stone attached to the top platen of Bromhead ring shear device (a) before starting the test (b) removed after completion of a strength recovery test for a period of 300 days at an effective normal stress of 100 kPa.

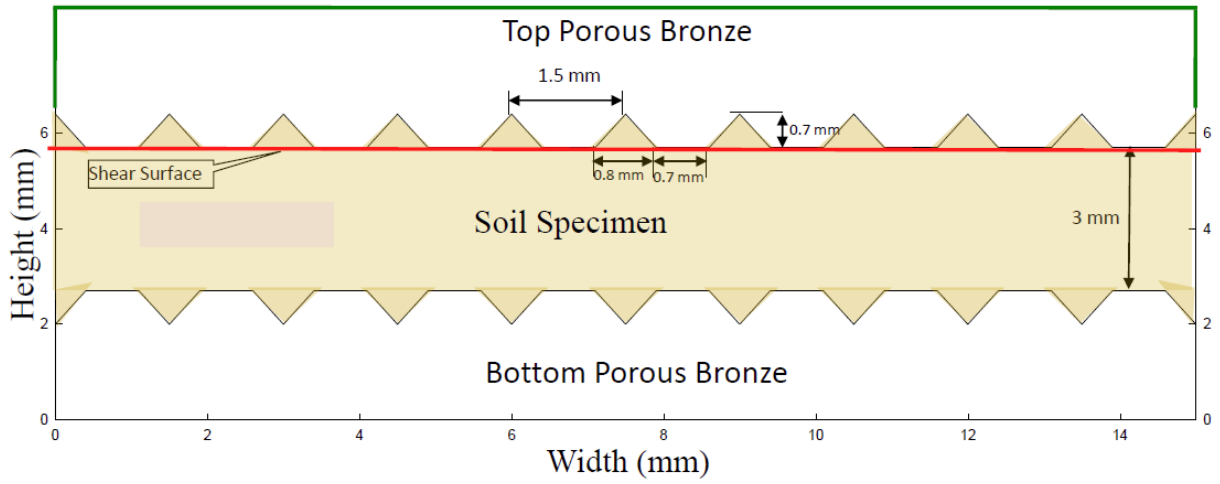

(a)

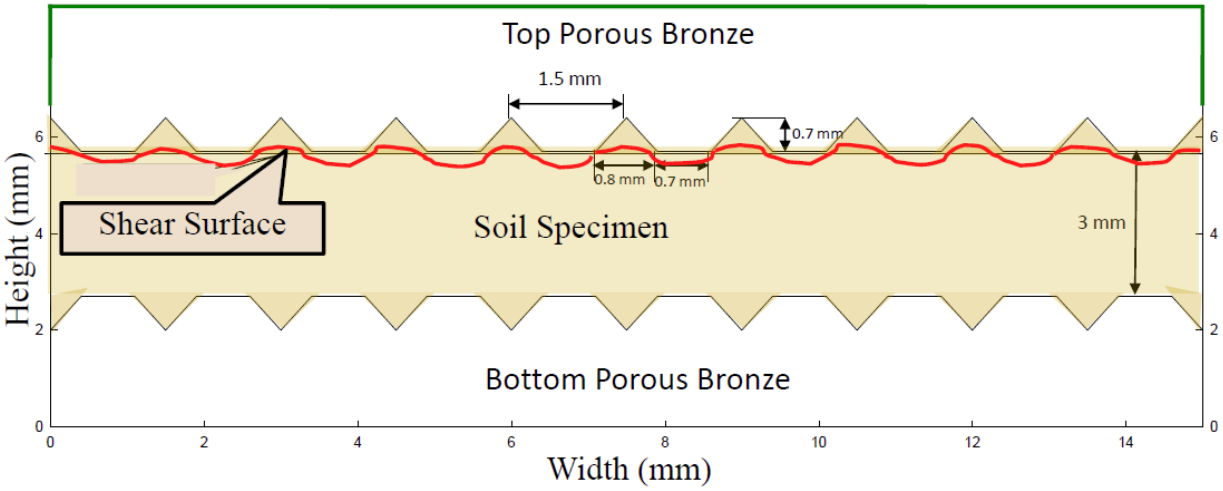

(b)

Figure 3.4. Cross-section of Bromhead ring shear specimen showing (a) horizontal shear surface at the bottom of knurled surface (b) undulating shear surface going into the knurled surface.

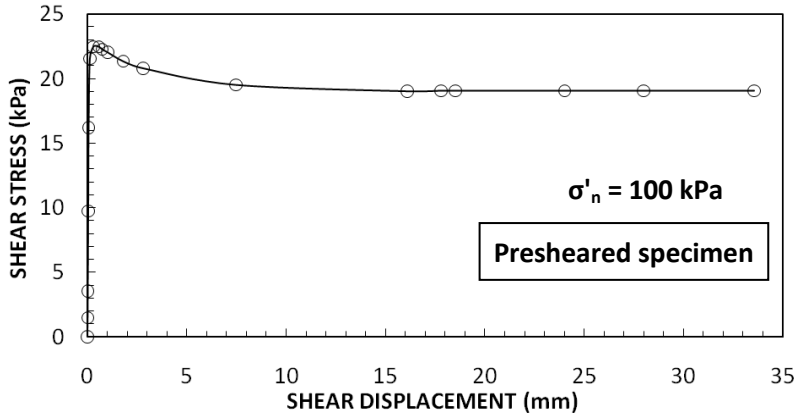

(a)

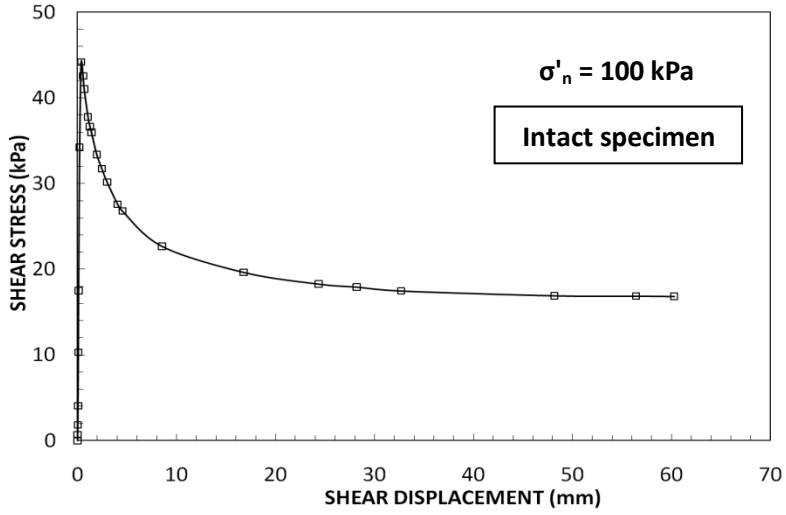

(b)

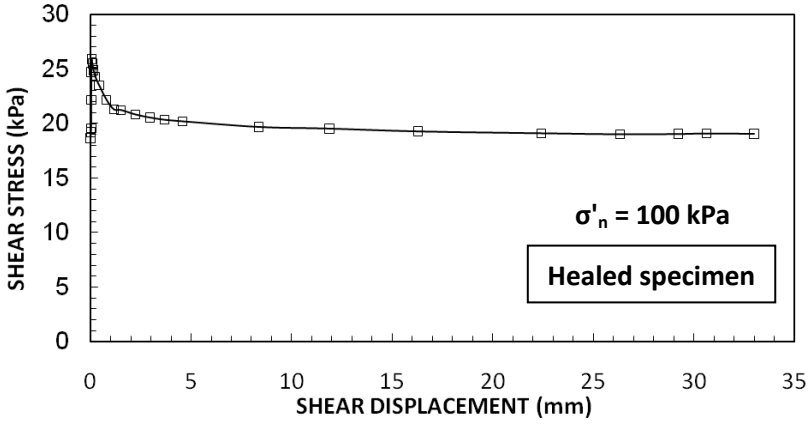

(c)

Figure 3.5. Shear stress-displacement relationships for Madisette clay at an effective normal stress of 100 kPa to illustrate shear displacement to residual condition (a) presheared specimen (RS-3) (b) intact (not presheared) specimen (RS-20) (c) specimen sheared after a rest period of 300 days (RS-3).

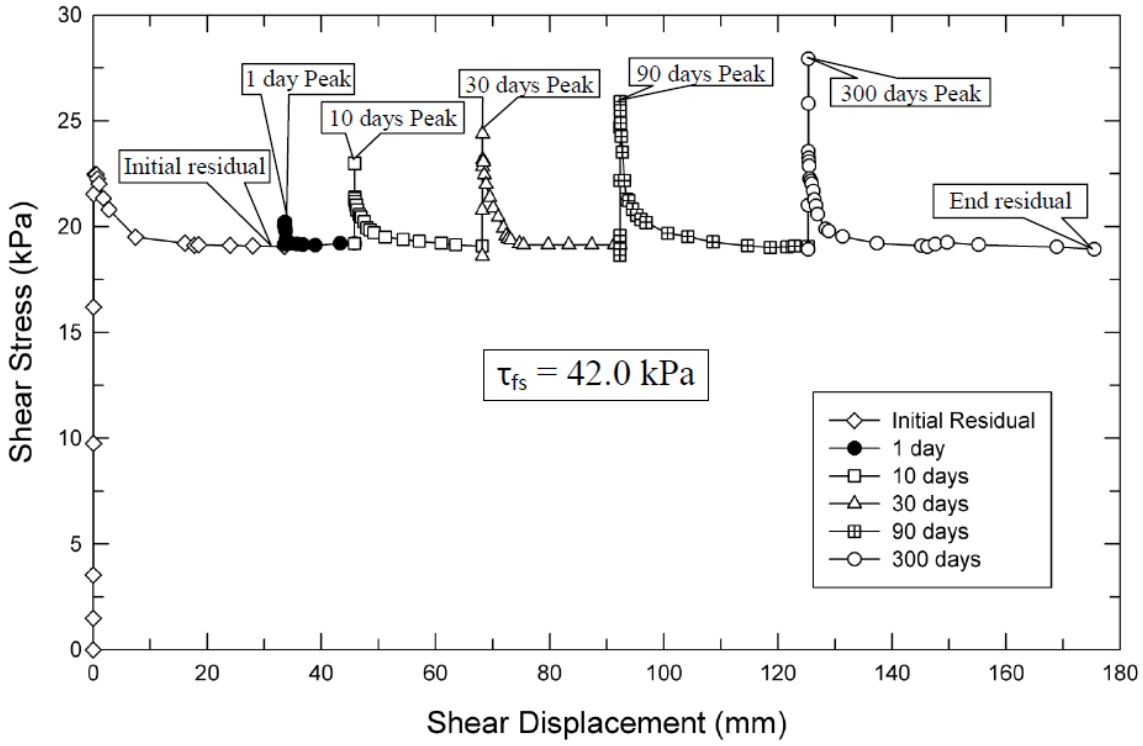

Figure 3.6. Schematic diagram showing results of a strength recovery test on Madisette clay under an effective normal stress of 100 kPa (RS-3 test).

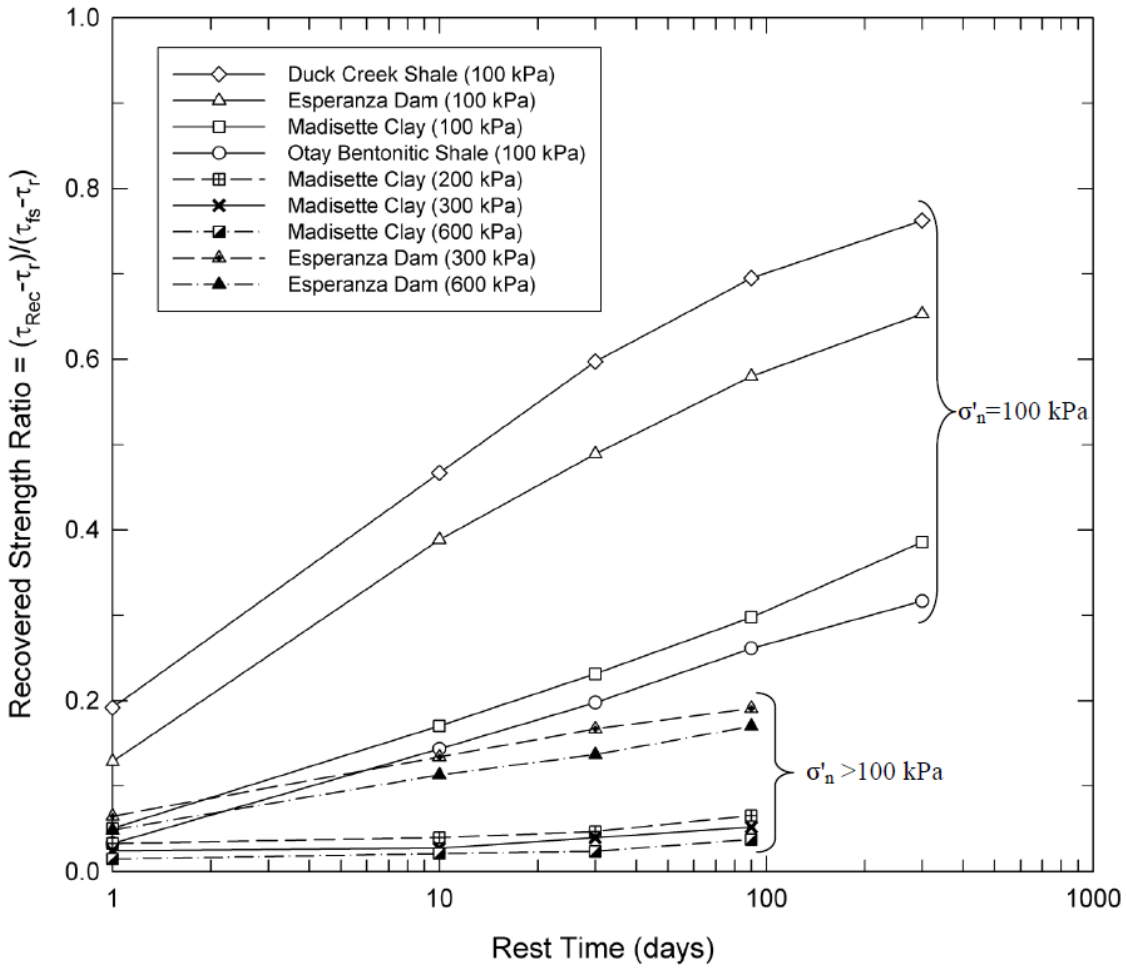

Figure 3.7. Relationships between recovered strength ratio and rest time for the four soils tested at different effective normal stresses.

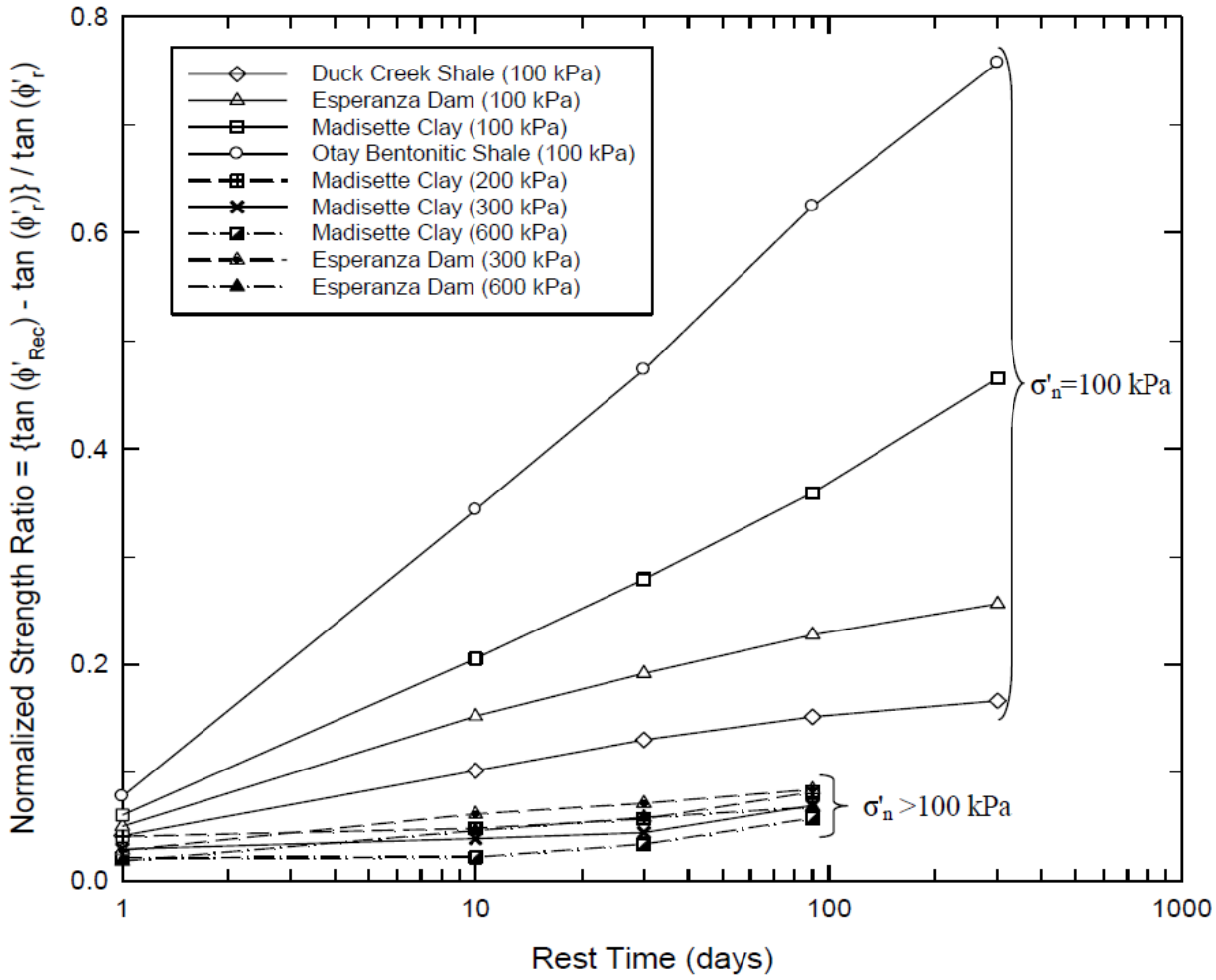

Figure 3.8. Normalized strength ratio (NSR) versus rest time for the four soils tested at different effective normal stresses.

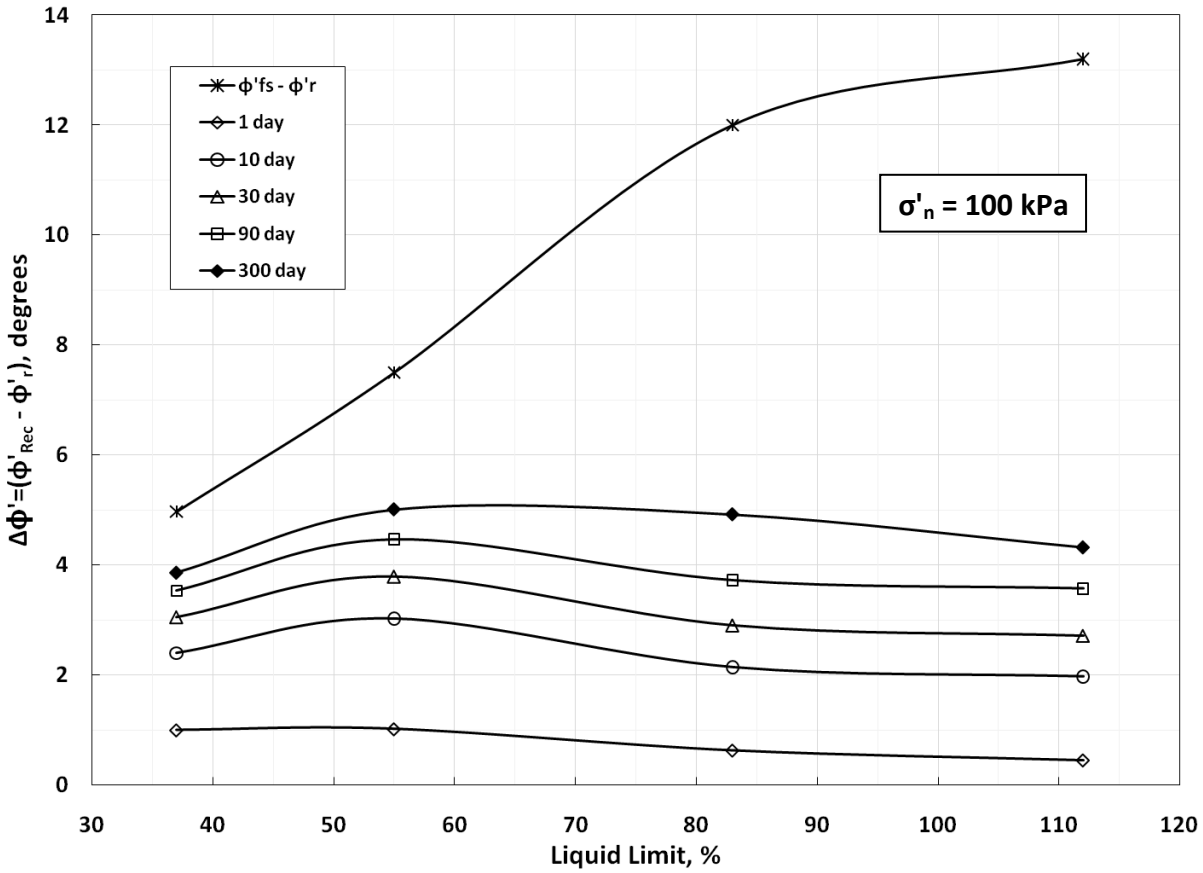

Figure 3.9. Difference between fully softened and residual friction angles and Δϕ' as a function of LL for the ring shear tests at an effective normal stress of 100 kPa.

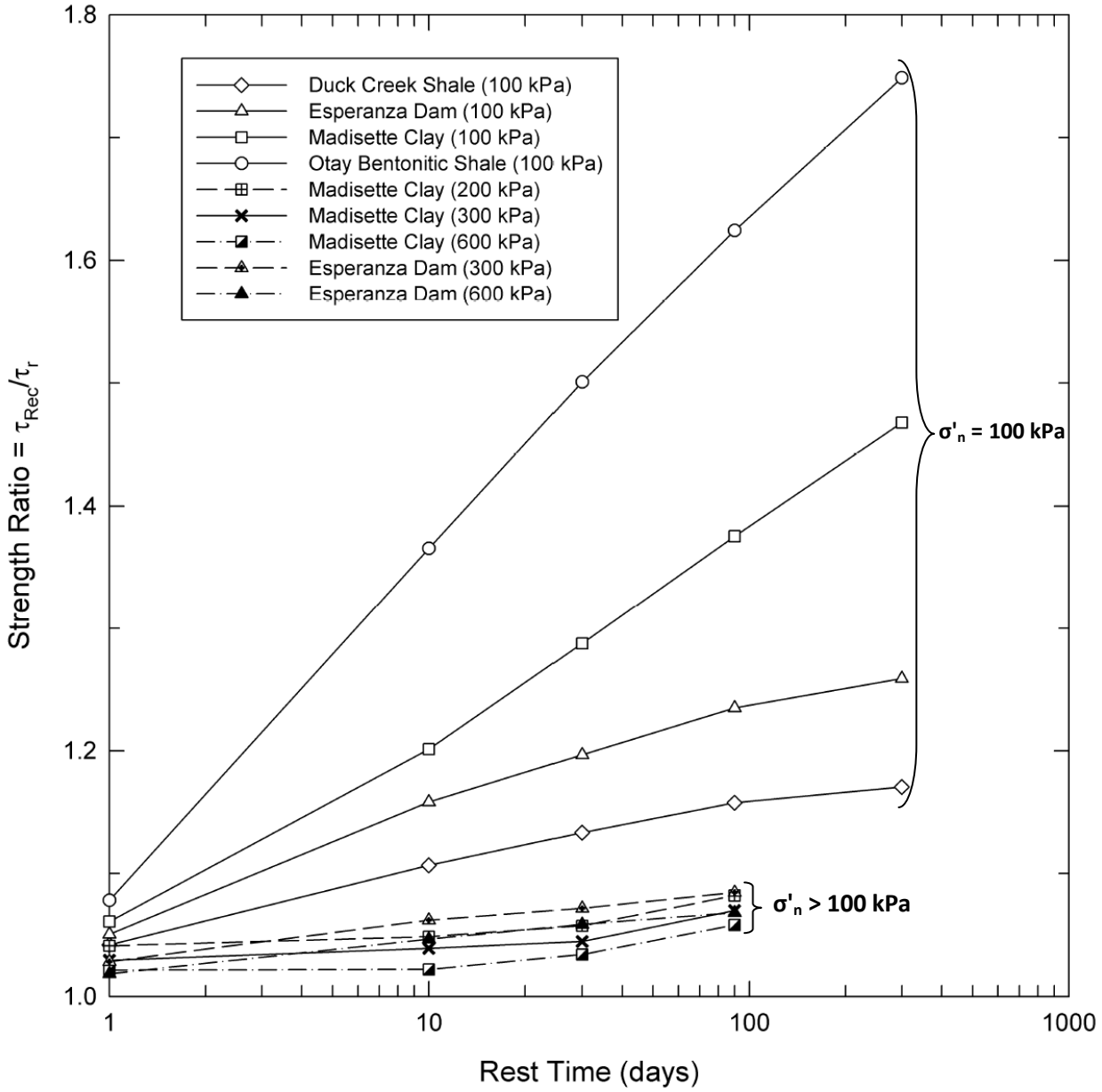

Figure 3.10. Recovered shear strength and rest time for the soils under shear strength recovery tests.

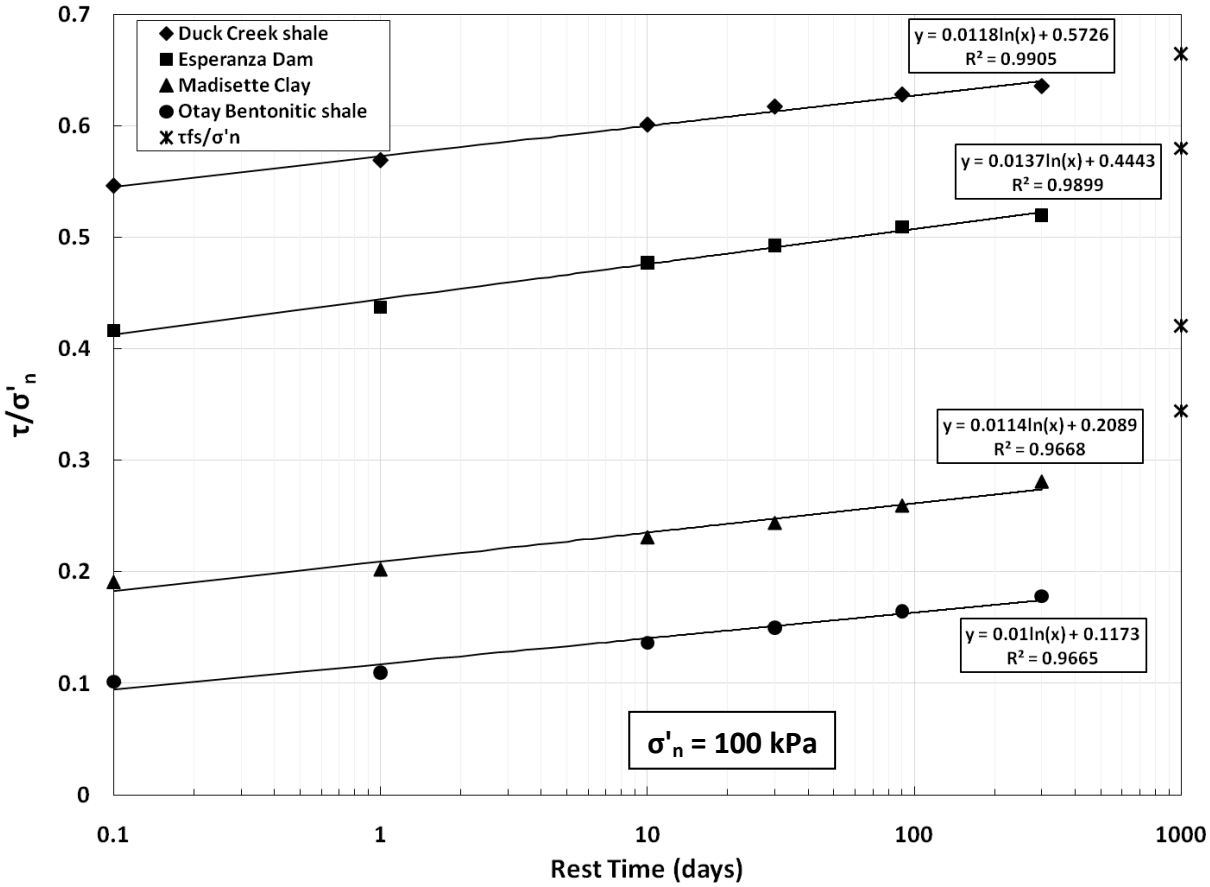

Figure 3.11. Normalized recovered shear stress versus rest time for ring shear strength recovery tests at an effective normal stress of 100 kPa.

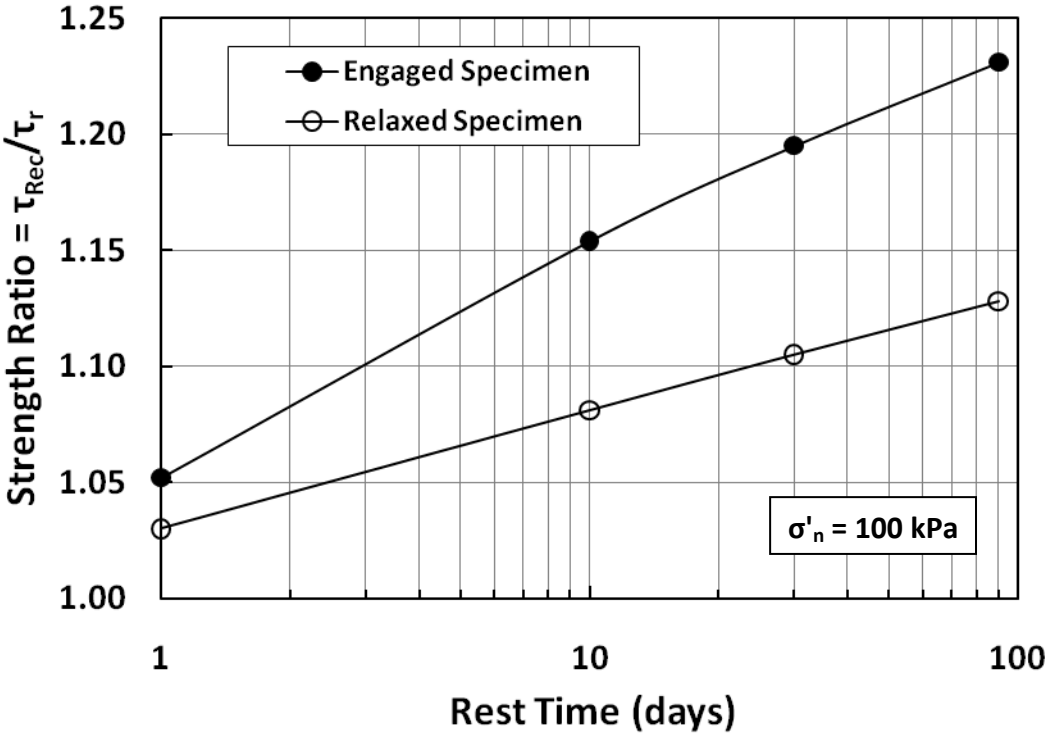

Figure 3.12. Strength ratio (τ_{Rec}/τ_r) versus rest time for ring shear strength recovery tests RS-2 (engaged) and RS-10 (relaxed) at an effective normal stress of 100 kPa.

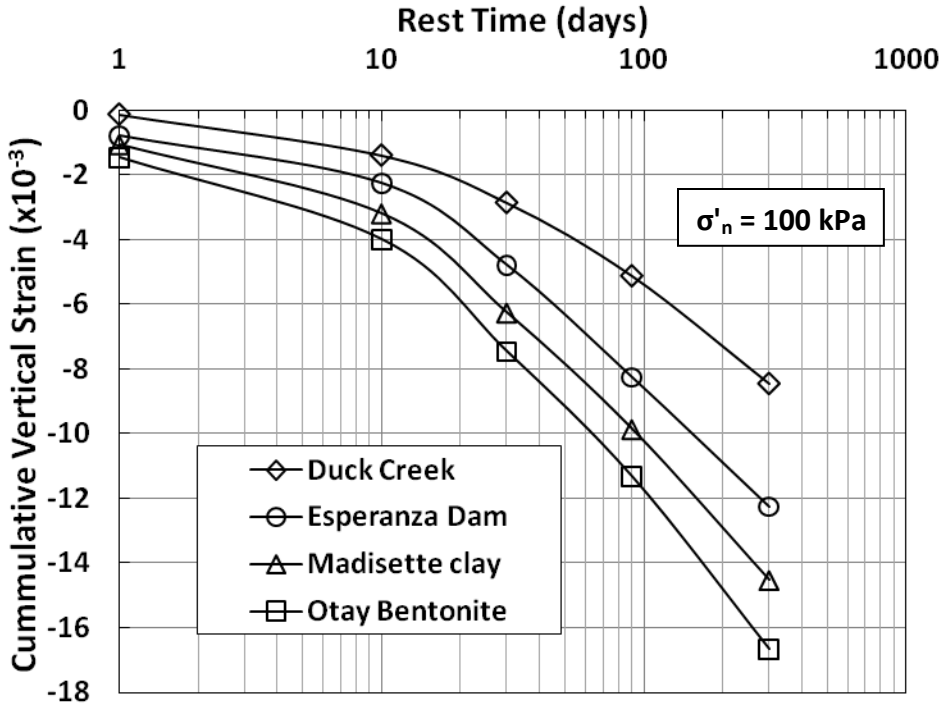

Figure 3.13. Cumulative vertical strain during the rest period as a function of rest time for ring shear tests at effective normal stress of 100 kPa

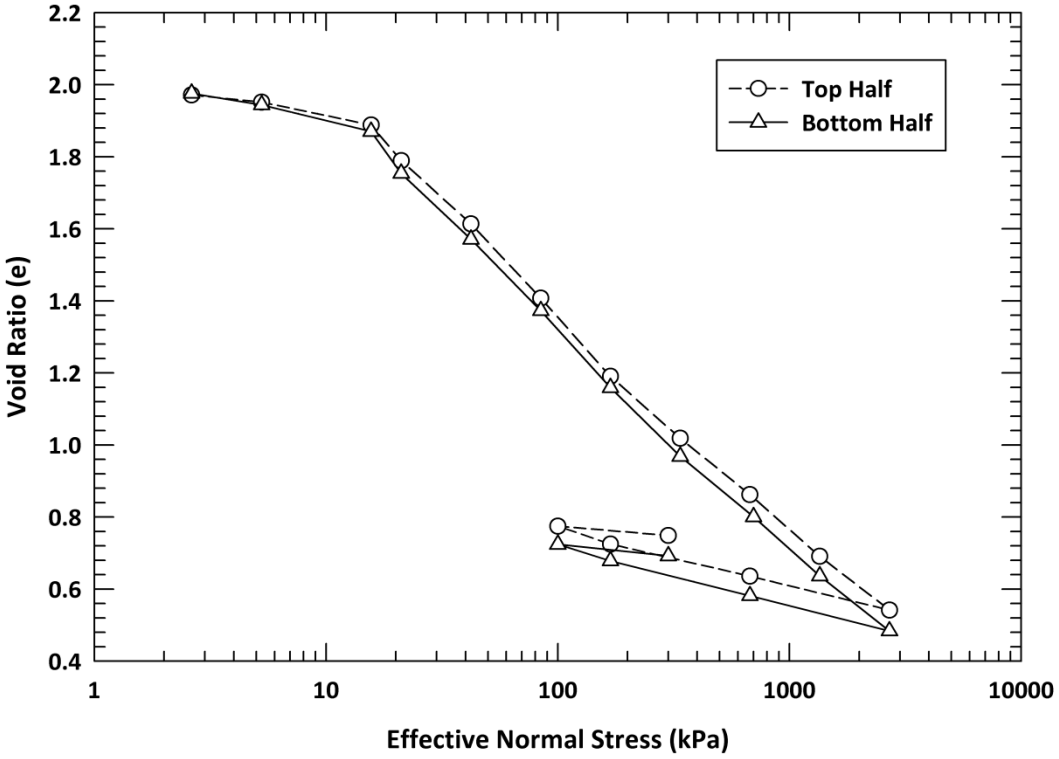

Figure 3.14. End of Primary e-log (σ'_v) relationship of Madisette clay consolidated to 2700 kPa, unloaded to 100 kPa and then reloaded to 300 kPa (DS-2 specimen).

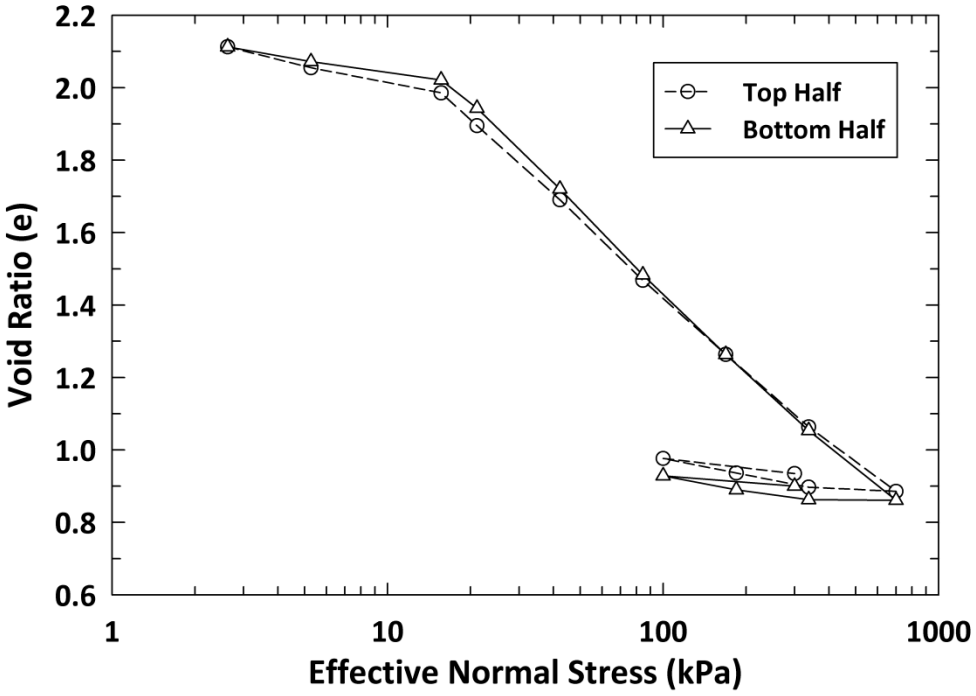

Figure 3.15. End of Primary e-log (σ'_v) relationship of Madisette clay consolidated to 700 kPa, unloaded to 100 kPa and then reloaded to 300 kPa (DS-3 specimen).

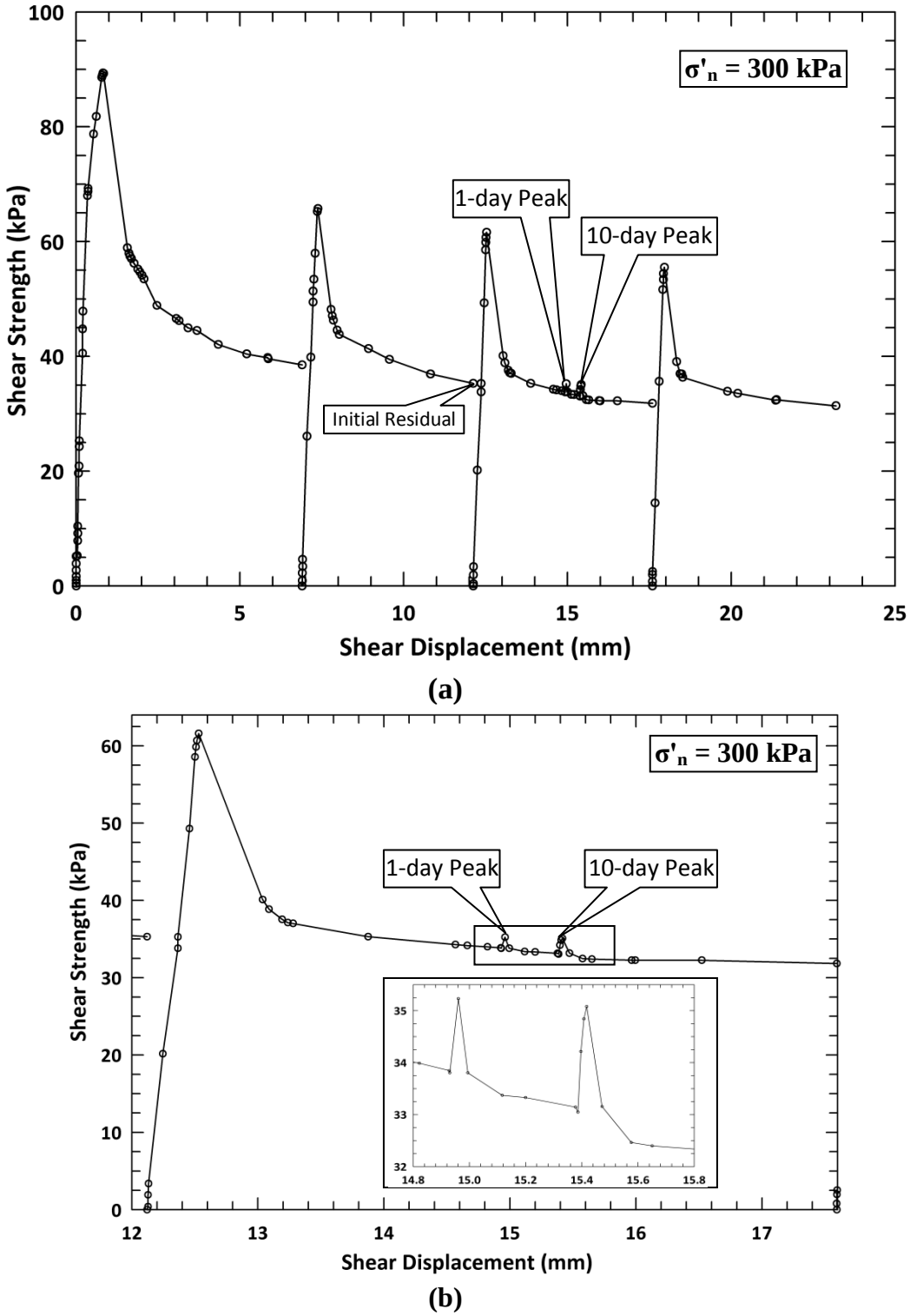

Figure 3.16. (a) Complete test result of reversal direct shear strength recovery test at an effective normal stress of 300 kPa for DS-2 (specimen consolidated to 2700 kPa) and (b) only third cycle of test (see above figure) during which specimen subjected to various rest periods.

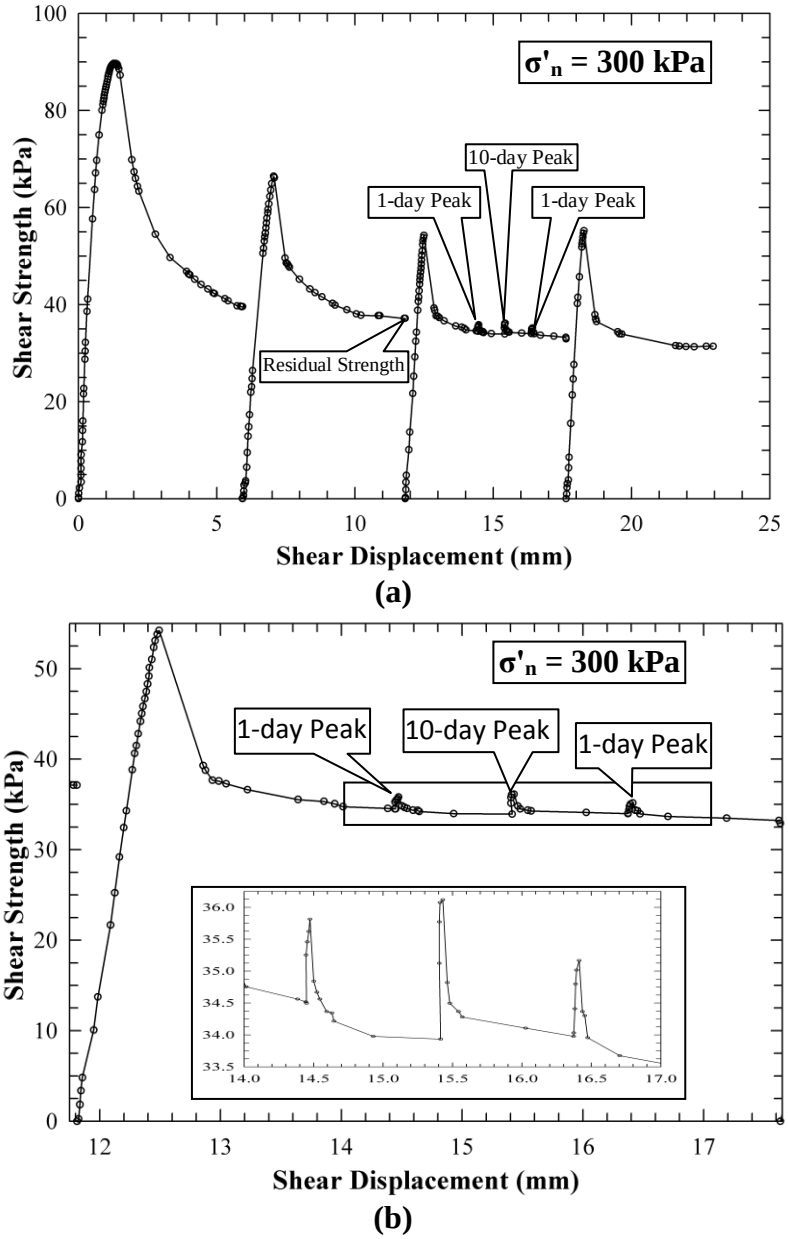

Figure 3.17. (a) Complete test result of reversal direct shear strength recovery test at an effective normal stress of 300 kPa for DS-3 (specimen consolidated to 700 kPa) and (b) only third cycle of test (see above figure) during which specimen subjected to various rest periods in DS-3.

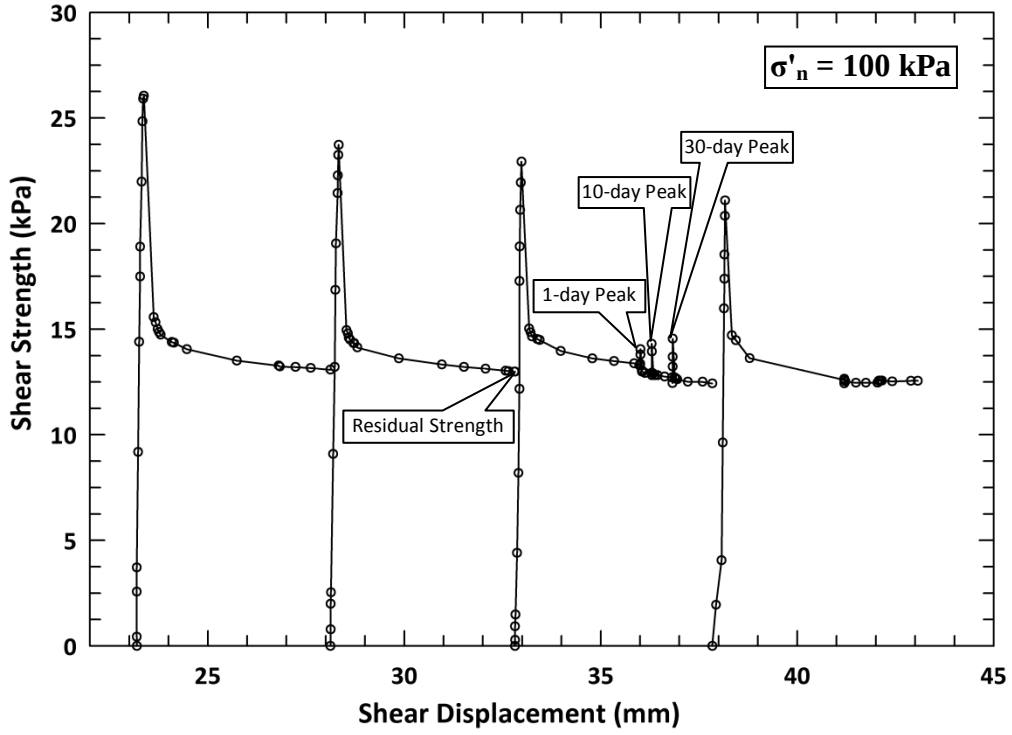

(a)

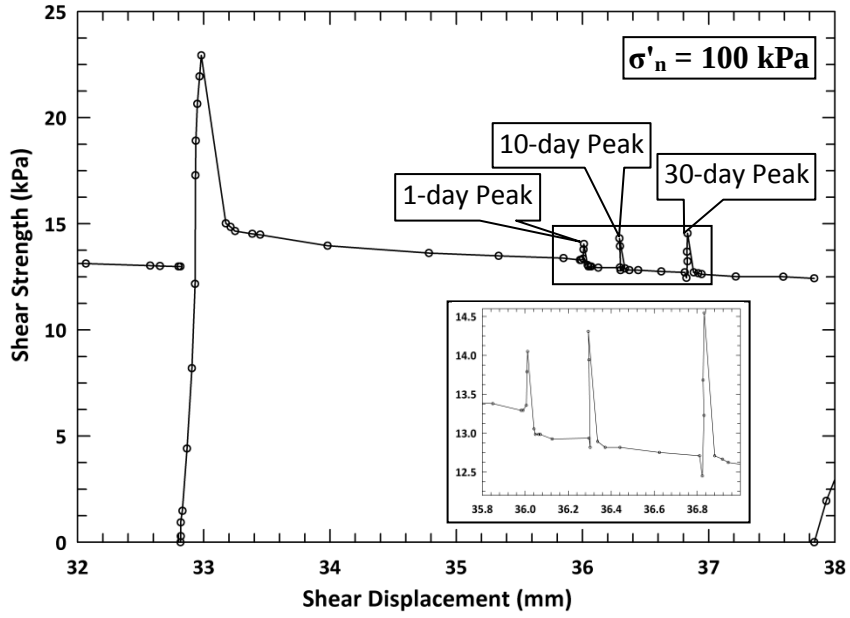

(b)

Figure 3.18. (a) Complete test results for direct shear strength recovery test at an effective normal stress of 100 kPa after σ'_n = 300 kPa for DS-2 (specimen consolidated to 2700 kPa) and (b) third cycle of test (see above figure) during which specimen subjected to various rest periods in DS-2.

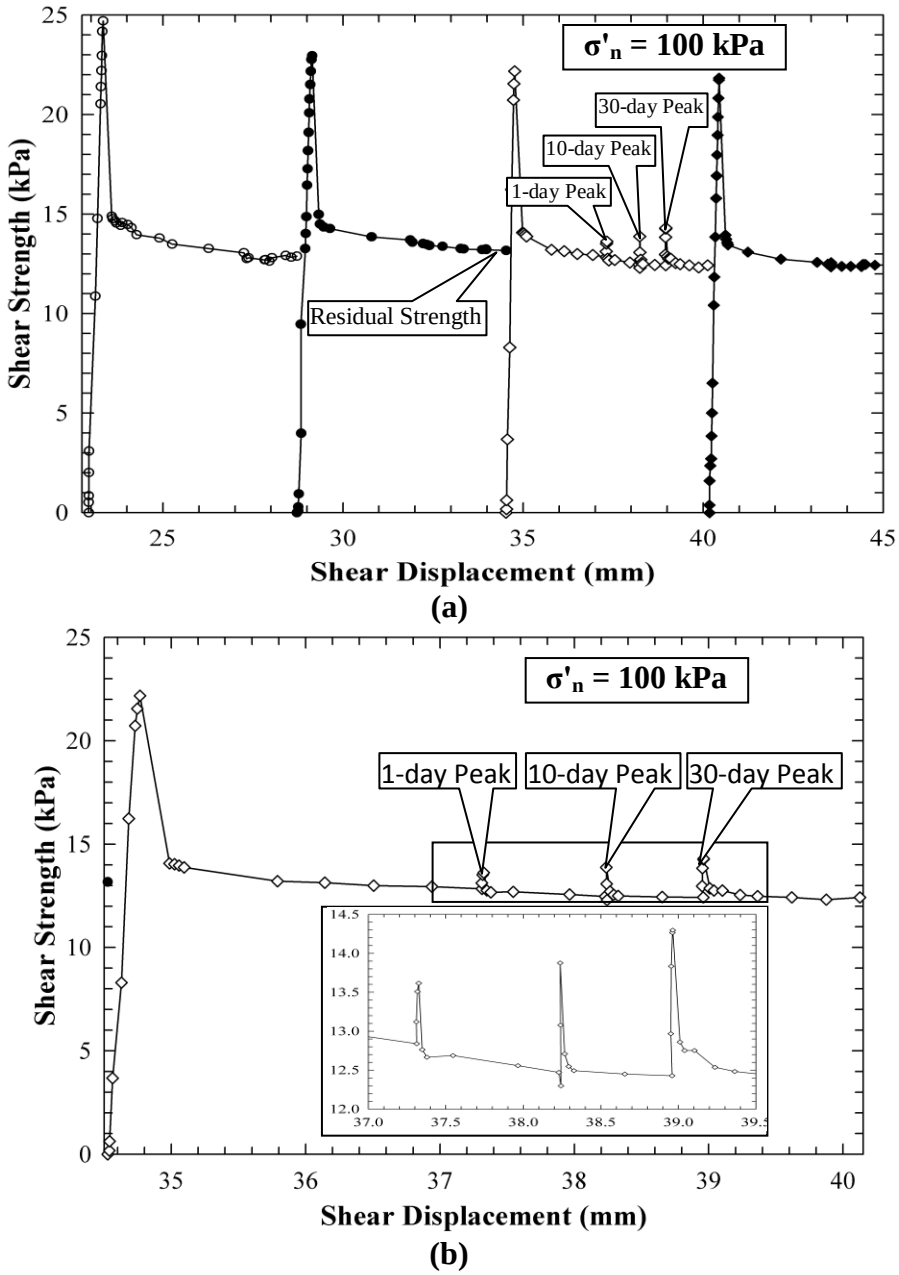

Figure 3.19. (a) Complete test results for direct shear strength recovery test at an effective normal stress of 100 kPa after σ'_n = 300 kPa for DS-3 (specimen consolidated to 700 kPa) and (b) third cycle of test (see above figure) during which specimen subjected to various rest periods in DS-3.

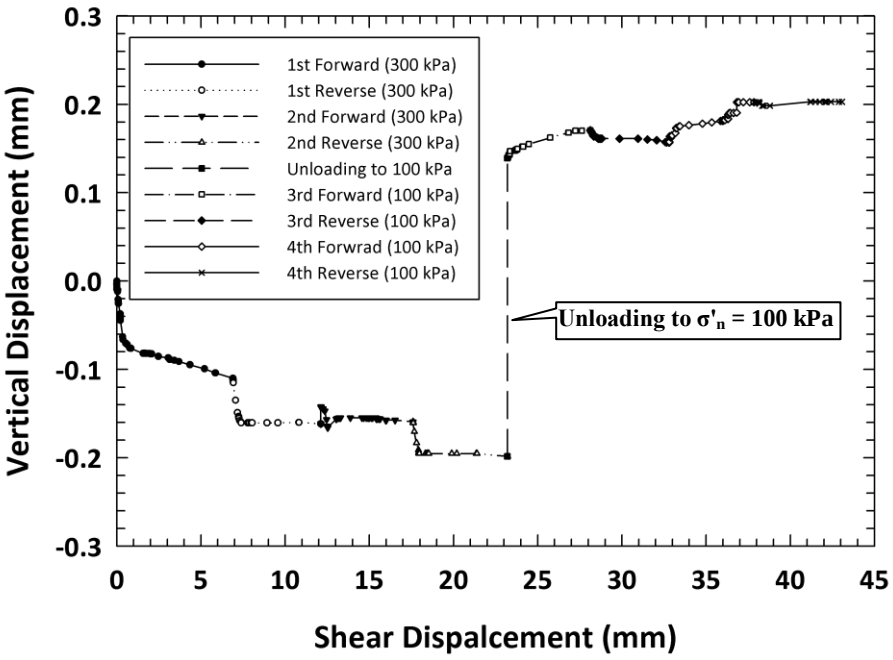

Figure 3.20. Vertical displacement versus shear displacement during reversal direct shear strength recovery test at effective normal stresses of 300 and 100 kPa in DS-2 (specimen consolidated to 2700 kPa).

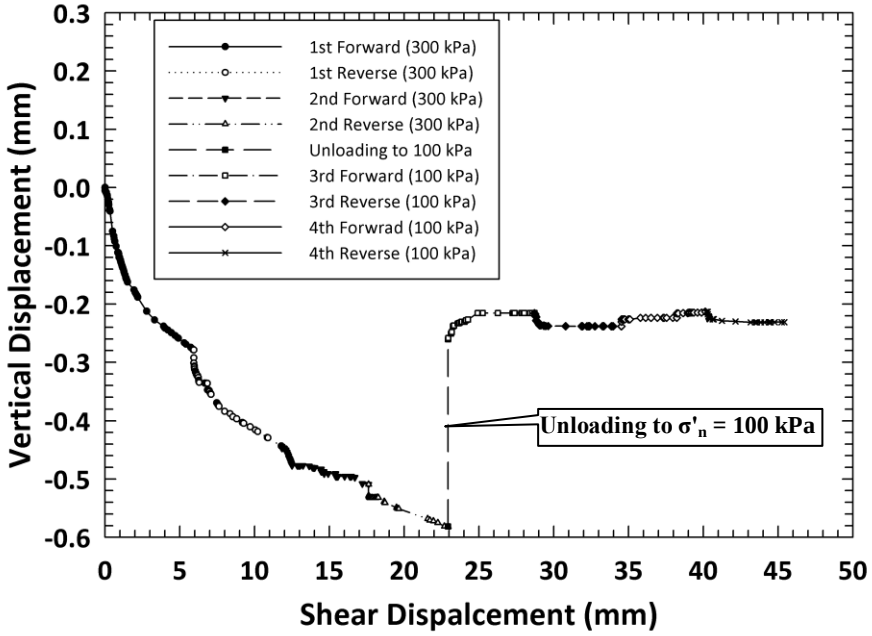

Figure 3.21. Vertical displacement versus shear displacement during reversal direct shear strength recovery test at effective normal stresses of 300 and 100 kPa in DS-3 (specimen consolidated to 700 kPa).

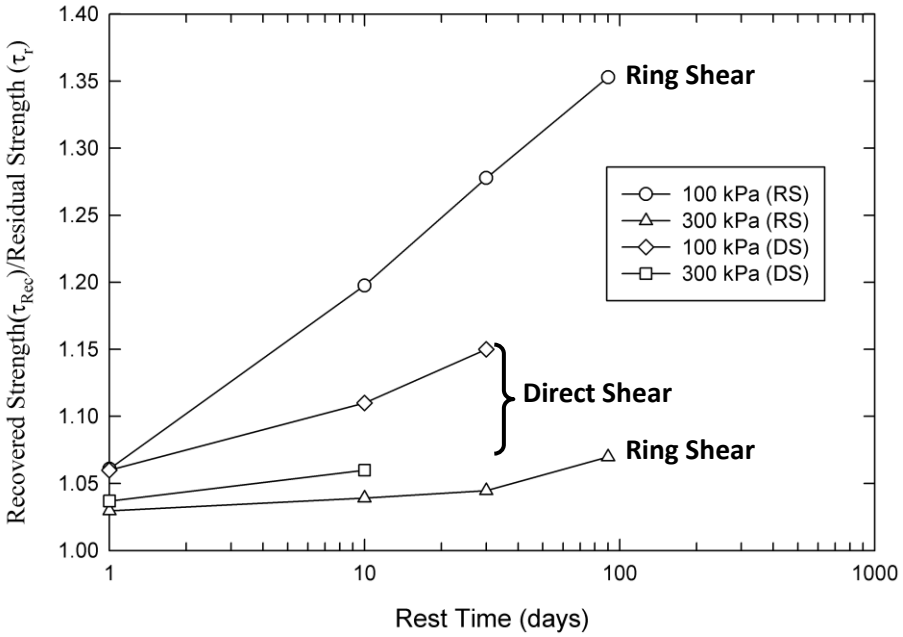

Figure 3.22. Ratio between recovered and residual strength as function of time observed during ring shear (RS) and direct shear (DS) tests at effective normal stresses of 100 and 300 kPa.

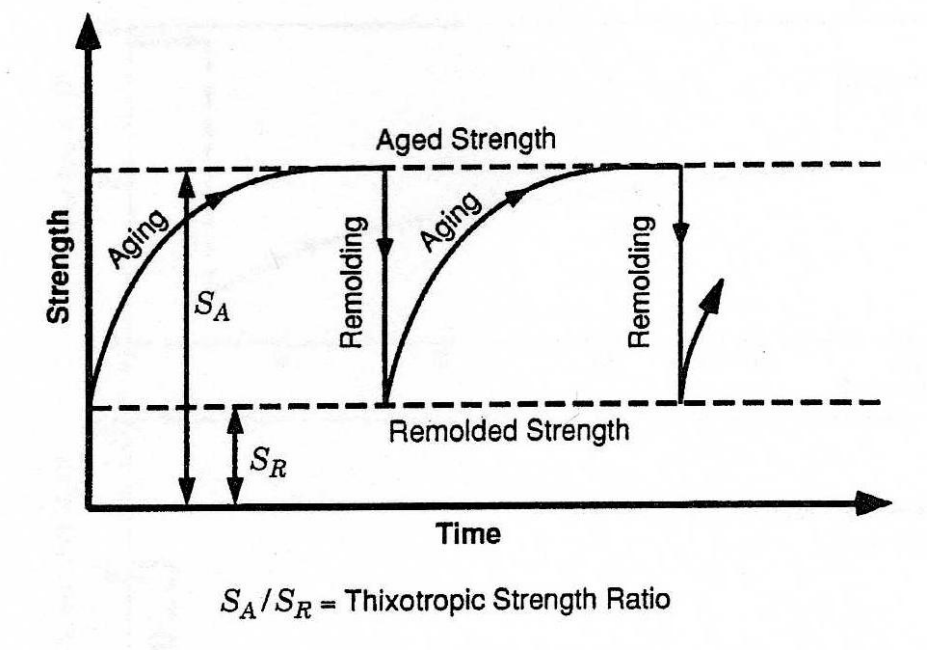

Figure 3.23. Properties of a purely thixotropic material (from Mitchell and Soga, 2005).

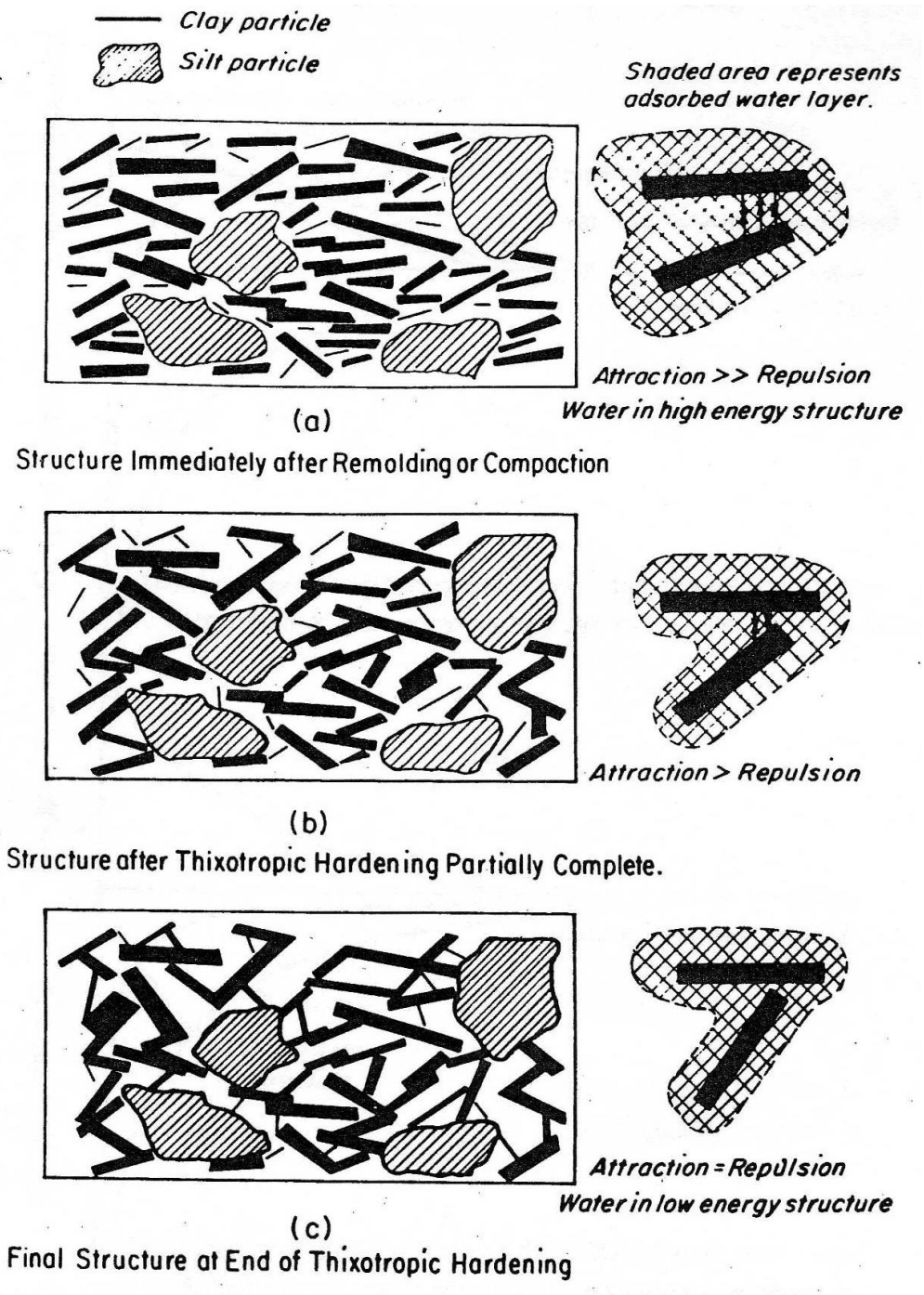

Figure 3.24. Schematic diagram of thixotropic structure change in a fine grained soil (from Mitchell, 1960).

CHAPTER 4:BACK-ANALYSIS OF STRENGTH RECOVERY CASE HISTORIES

4.1 Introduction

Drained residual strength of soil present along the shear surface is considered applicable for the analysis of reactivated landslides (Skempton, 1964). After introduction of the residual strength by Skempton (1964), a linear Mohr-Coulomb stress envelope for the residual strength, with an effective stress cohesion (c') and residual friction angle (ϕ'_r), was considered appropriate in the analysis of natural and manmade slopes. Subsequently Chandler (1977) and Bromhead (1978) used the back-analyses of landslides involving Lias and London clays, respectively, to conclude that the residual shear strength mobilized decreases with increasing effective normal stress. Stark and Eid (1994) recommend that a stress dependent or nonlinear failure envelope should be used in stability analyses to model the effective stress dependent behavior of the residual strength. Thus, using a stress dependent residual strength failure envelope in the back-analysis and design of slopes is becoming more acceptable to the practitioners.

D'Appolonia et al. (1967), Angeli et al. (1996), Gibo et al. (1997), and others used case histories and laboratory test results to suggest that the strength along a preexisting shear surface in an old landslide can be greater than the residual strength because of some strength recovery. Although no well documented case history supporting the concept of strength recovery is currently available in the literature. Stark et al. (2005a) report a consulting project to stabilize a landslide near Seattle, Washington. The landslide was reactivated in 1990 and a consultant contacted Professor Stark in 1991 about the possibility of strength gain in the cohesive colluvium responsible for the slide during the inactive period prior to 1990. If strength gain had occurred, the slide would be less stable now than before the 1990 movement because the shear strength increase due to healing was removed by the recent movement. This case was the impetus for the strength recovery testing started in year 2000 and published by Stark et al. (2005a). The Weirton landslide in West Virginia (D'Appolonia et al., 1967) and the Alver`a landslide from northeastern Italy (Angeli et al., 1996) are also relevant to the issue of strength recovery and analyzed herein.

D'Appolonia et al. (1967) use a linear strength envelope developed from direct shear testing of intact slip surface specimens from the Weirton landslide to perform this back-analysis. The back-analysis was performed by D'Appolonia et al. (1967) using the peak strength measured from direct shear tests on intact specimens and yielded a FS of 1.4. They also performed a back-analysis using the residual strength which gave a FS of 1.03. Because the slope was stable and no evidences of recent movement could be found at that time, D'Appolonia et al. (1967) concluded that some healing may have occurred along preexisting shear surface which was keeping the slope stable with an increased FS of 1.4.

On the basis of measured piezometric levels required to start and stop movement of the Alver`a landslide, Angeli et al. (1996) suggest the preexisting shear surface may have undergone some strength recovery because of the piezometric threshold to restart the movement was higher than the piezometric level required to stop the movement. Gibo et al. (1997) based on ring shear test results that are published in Gibo et al. (2002), present a model slope that suggests the recovered strength can be used at shallower depths of a landslide, i.e., at the top and/or toe, and the residual strength can be used at greater depths (see Figure 4.1).

Some laboratory studies, such as Ramiah et al. (1973), Angeli et al. (1996 and 2004), Gibo et al. (2002), Stark et al. (2005a), and Carrubba and Del Fabbro (2008) discussed in Chapter 2, suggest that preexisting shear surfaces may gain strength during the period of no movement and exhibit a strength greater than the residual value upon restarting the movement. A laboratory study presented in Chapter 3 also suggests that preexisting shear surfaces can undergo strength recovery/healing during a rest period. The recovered strength increases with rest time and is noticeable at effective normal stresses of 100 kPa or less which corresponds to shallow landslides (5 m or less) and is negligible at effective normal stresses greater than 100 kPa. The strength recovery may also be applicable at shallow depths of a deeper landslide, e.g., top and/or toe, as suggested by Gibo et al. (1997). It is also determined during the study that the strength recovery is more pronounced in high plasticity soils as compared to the low plasticity soils.

Existing literature on the start and stop of slope creep movement suggest that creep movement starts when FS reaches a value at or near unity and stops when FS becomes greater than unity. Patton (1984) concludes from the study of the Downie landslide in British Columbia, Canada that when FS decreases due to a rise in groundwater level, slope creep will begin when

FS ≈ 1.03 (see Figure 4.2). Hutchinson (1988) uses two landslides, Sandnes in Norway and Sandgate in England, to conclude that movements due to slope creep became negligible when a FS reached 1.05. Also Bertini et al. (1984) studied the slow moving San Martino landslide in central Italy and conclude that slide movements became negligible when the computed FS became larger than 1.05. Observation by Bertini et al. (1984), Patton (1984), and Hutchinson (1988) can be used to conclude that FS ≈ 1.10 is sufficient to prevent a slide movement or slope creep in natural slopes and landslides. Conversely, these cases may be used to conclude that slope creep movement can start when FS < 1.05.

The following paragraphs present back-analyses of two case histories that suggest strength recovery occurred. The back-analyses were performed using stress dependent strength envelopes developed for the residual strength of the soil and for the healed/recovered strength estimated from the test results presented in Chapter 3. These back-analyses indicated that if strength recovery occurred, it affected the creep behavior of the landslide and did not contribute significantly to its stability. Therefore, the recovered strength may not be applicable to design.

4.2 Colluvium Slope in West Virginia (D'Appolonia et al., 1967)

4.2.1 Description of Landslide and Mobilized Strength in Landslide

The concept of "healing" of shear surfaces is described by D'Appolonia et al. (1967) in relation to a colluvial slope failure in Weirton, West Virginia. The landslide occurred in an area which has typical topography of the upper Ohio River Valley region. The slide occurred due to excavation of the toe of an ancient landslide for a steel plant expansion. The excavation varied in height from 6.1 to 18.3 m over a length of 762 m. The ancient landslide is 1,524 m in length, rises over 61 m in elevation, and has a slope length of approximately 304.8 m. The inclination of the slope is 3H:1V. The rock strata at the site have nearly horizontal bedding and consist predominantly of medium to hard shales, siltstones, and sandstones of Pennsylvanian age. At the time of toe excavation, the rock was weathered and highly jointed to a depth of about 12.2 m below the rock surface. To prevent a recurrence of movement of the ancient landslide during and after excavation at the slope toe, a sheet pile wall anchored with steel H-piles tensioned prior to making the excavation, sand drains along the toe of the slope, and two galleries and a cut-off trench to intercept ground water seepage near the upper portion of the slope were installed.

The soils at the site were classified into three major types; sand and gravel, alluvium, and colluvium (see Figure 4.3). The sand and gravel overlies bedrock in the valley bottom and was deposited as outwash from melting Pleistocene glaciers. D'Appolonia et al. (1967) established that the alluvium near the construction area consists of clayey silt and silty clay and was deposited primarily during flood stage activity of the present Ohio River. The colluvium that blankets the slope extends into the construction area along the entire length of the site.

At the time of the toe excavation, carbon dating of the toe material suggested the minimum age of the slip surface was at least 40,000 years ago. Also the slope was stable with no discernable landslide movement occurring during the last several decades because no evidence of tension cracks, curved tree trunks, or displaced retaining walls, roadways, foundations or utility lines were observed.

The geometry of the old slide surface, which was also the critical failure surface after the excavation was made, is located at the colluvium-alluvium interface below elevation of 243.8 m and at observed slickensides near the colluvium-rock interface above elevation 243.8 m as shown in Figure 4.3. The natural water content and the index properties show a marked increase near the colluvium-alluvium interface as shown Figure 4.4. Based on the difference in index properties of the slip surface material, it was concluded that the soil comprising the old failure plane was of different composition than the surrounding colluvium and may be composed of soil derived from the underlying claystones. The material present along the slip surface has LL = 51%, PL = 25%, CF = 55%, and natural water content of 26%. Because the natural water content along the shear surface was near the plastic limit, D'Appolonia et al. (1967) postulated that the colluvium was overconsolidated.

Sixty nine (69) piezometers were installed along the slope in the slide area before the toe excavation. The groundwater condition shown in Figure 4.3 was established using data obtained from 29 of the 69 piezometers that were along the cross-section shown in Figure 4.3. Thus, the phreatic surface at the time of sliding is well established based on data from 69 piezometers. This is important because the subsequent back-analysis is sensitive to the location of the phreatic surface. The piezometer data indicates that the flow of groundwater is predominantly parallel to the potential failure surface, i.e., the colluvium-rock interface. This was determined from

piezometer groups having their porous stones at various elevations above the slip surface and showing nearly the same piezometric head (D'Appolonia et al., 1967). All piezometers below the assumed potential failure surface in either the colluvium or the alluvium show zero piezometric head. Thus, water was building up on the colluvium-rock interface due to infiltration and facilitating movement.

The drained strength parameters were established using consolidated drained direct shear tests and consolidated undrained triaxial compression tests with pore pressure measurements on undisturbed and remolded block samples obtained from exposed slickensided surfaces. Peak strength parameters determined from drained direct shear tests on intact/undisturbed slickensided specimens with a best fit linear relationship between shear and effective normal stresses yielded $c' = 7.66$ kPa and $\phi' = 20^o$ and residual strength parameters of $c' = 0$ and $\phi'_r = 16^o$ as shown in Figure 2.3. Direct shear tests using undisturbed specimens were performed at effective normal stress of 100 kPa or less to determine both peak or current strength and residual strength parameters. Whereas, direct shear tests with remolded specimens were used to determine the residual strength parameters at effective normal stresses of 100 and 200 kPa. The measured peak strength parameters $c' = 7.66$ kPa and $\phi' = 20^o$, fall below the fully softened shear strength parameters for a LL = 51% and CF = 55% estimated from the empirical correlation shown in Figure 6.36 which are $\phi'_{fs} = 28.3^o$ and 25.1^o at effective normal stress of 50 and 100 kPa, respectively. This shows that large shear displacement had occurred in the field and a shear surface had been established in the past because the peak or current strength is well below the fully softened value. This is confirmed because the current strength is close to the measured residual friction angle, 16°, which is also in agreement with the empirical correlation presented in Figure 6.24 for $\sigma'_n = 100$ kPa.

In summary, the peak strength of the undisturbed slickensided material is less than the fully softened value and the residual strength from direct shear tests is in agreement with the torsional ring shear tests performed by Stark and Eid (1994 and 1997) and Stark et al. (2005a). Furthermore, the peak strength measured in direct shear tests is in agreement with the recovered/healed strength measured during ring shear strength recovery tests on silty clay from Esperanza Dam, Ecuador with a similar plasticity. Ring shear strength recovery test results of silty clay from Esperanza Dam are discussed in Chapter 3. The ring and direct shear strength

recovery tests discussed in Chapter 3 show that a small shear displacement is required to remove the recovered/healed strength and re-establish the residual strength condition. D'Appolonia et al. (1967) do not provide an explanation for the undisturbed slickensided specimens exhibiting a strength greater than the residual value measured in direct shear tests.

4.2.2 Back-Analysis by D'Appolonia et al. (1967)

D'Appolonia et al. (1967) performed stability analyses using four cross-sections including the one shown in Figure 4.3, the drained peak and residual strength parameters dicussed above (linear Mohr-Coulomb envelope), measured pore-water pressures from 29 piezometers, and two stability methods, Morgenstern and Price (M&P) (Morgenstern and Price , 1965), and Ordinary Method of Slices (OMS) (Taylor, 1948). The results of the stability analyses performed by D'Appolonia et al. (1967) using the cross-section shown in Figure 4.3 are shown in Table 4.1. D'Appolonia et al. (1967) show that the insitu factor of safety using the residual friction angle of 16° varies from 0.95 to 1.03 for the four cross-sections analyzed using OMS and M&P stability methods, respectively. The factor of safety with measured peak shear strength parameters of c' = 7.66 kPa and ϕ' = 20° varies from 1.4 at the south end (with excavation depth of 6.1 m) to 1.6 at the north end (with excavation depth of 18.3 m) of the site. D'Appolonia et al. (1967) also show that varying the slip surface within the range of uncertainty with which it was established did not significantly affect the factor of safety. However, the factor of safety was found to be sensitive to the assumed pore pressures on the failure surface, as shown in Figure 4.5. For example, raising or lowering the phreatic surface by 1.52 m resulted in about a 10% change in the factor of safety. D'Appolonia et al. (1967) postulate that if the residual strength was being mobilized on the slip surface and a healed strength did not exist, a rise in the ground water table by about 1.52 m would have reduced the average factor of safety to approximately 0.95 and had resulted in the slope movement(s).

Because the shear surface was formed by shear movements in the geologic past and was stable at the time of excavation, it was thought by D'Appolonia et al. (1967) that the factor of safety must have been greater than unity. D'Appolonia et al. (1967) suggest that if the residual strength was the maximum strength that could have mobilized at the time of toe excavation, the slope should have shown evidence of at least slope creep and a rise in groundwater in the past then caused the major slide movement. In the upper Ohio River Valley region, colluvial slope

movement occurs in the spring after a wet winter because a rise in groundwater can adversely impact marginally stable slopes. Based on the observed stable slope and the laboratory strength data, D'Appolonia et al. (1967) conclude that the strength on the potential failure surface at the time of toe excavation was greater than the residual strength due to healing of the shear surface by desiccation and/or natural cementation. Given that the phreatic surface was well-established by 29 piezometers along the cross-section in Figure 4.3, the direct shear test results are in agreement with a small strength gain at low values of σ'_n.

4.2.3 Current Back-Analyses Results and Discussion

Because Weirton landslide is a well-instrumented and well-documented landslide that indicates healing of a preexisting shear surface, a detailed analysis of the case was performed during this study. D'Appolonia et al. (1967) use a linear residual shear strength failure envelope to perform the stability analyses even though the measured failure envelope is streess dependent (see Figure 6.24). The present study uses a stress dependent residual shear strength failure envelope for the stability analyses as suggested by Stark and Eid (1994) because of the variable depth of the landslide. The cross-section shown in Figure 4.3 was used for the analyses and input to the slope stability software XSTABL (Sharma, 1995). A specified noncircular failure surface and phreatic surface established from the 29 piezometric levels shown in Figure 4.3 were used for the stability analyses. The analysis was performed using Generalized Limit Equilibrium (GLE) method as coded in the stability software. The GLE method is an extension of Spencer's (1973) method, generalized by Chugh (1986), and emulates a discrete version of the Morgenstern and Price (1965) solution by considering different interslice force angles and satisfying both force and moment equilibrium conditions. Because D'Appolonia et al. (1967) use the Morgenstern and Price (1965) method and XSTABL (1995) does not have this method, the GLE method which emulates Morgenstern and Price (1965) method was used for performing the back-analysis so the results could be compared.

Initially shear strength parameters used by D'Appolonia et al. (1967) were selected to establish that slope geometry and other input parameters are in agreement. The slip surface shown in Figure 4.3 was identified by D'Appolonia et al. (1967) from the observed slickensides and slip surface material with different index properties from the material above and below as shown in Figure 4.4. The observed slip surface was modeled as an interface having a thickness of

about 0.3 m with properties different from the material above and below the slip surface (see Table 4.2). A noncircular slip surface passing along the middle of the interface layer was specified for the stability analysis. Stability analyses were performed using the following slip surface locations:

1) **Case I: D'Appolonia et al. (1967) Slip Surface and Actual Slope Geometry**
   The stability analysis was performed using the slope geometry, slip surface, phreatic surface shown in Figure 4.3, and the residual strength parameters shown in Table 4.2. This analysis yielded a FS = 1.03 which is the same FS reported by D'Appolonia et al. (1967). Thus, the slope geometry, slip surface, phreatic surface, and shear strength parameters are in agreement with those used by D'Appolonia et al. (1967) and the stability model developed herein was assumed to be calibrated.
2) **Case II: Slip Surface at Alluvium-Colluvium Interface**
   D'Appolonia et al. (1967) mention that the slickensides were observed at alluvium-colluvium interface at the bottom of slope. However, the slip surface shown in Figure 4.3 only passes through alluvium. It is likely that the slip surface is located at the interface between a weak (colluvium) and strong (alluvium) material. Therefore, a stability analysis was also performed to investigate the effect of locating the failure surface along the alluvium-colluvium interface instead of the location proposed by D'Appolonia et al. (1967) near the slope toe. Using the failure surface along the alluvium-colluvium interface and the same input parameters used by D'Appolonia et al. (1967), see Case I above, yielded a FS of 1.19. Because all of the input parameters are the same except the failure surface location the alluvium-colluvium interface resulted in a higher value of FS than that calculated for the D'Appolonia et al. (1967) slip surface. Therefore, the slip surface shown in Figure 4.3 is the critical failure surface.
3) **Case III: Alluvium-Colluvium Interface at the Observed Slip Surface**
   A stability analysis was also performed by lowering down the alluvium-colluvium boundary so it coincides with the slip surface reported by D'Appolonia et al. (1967). This analysis used the new layer boundary and the other input parameters from Case I above. The interface was lowered so the failure surface did not have to pass through the stronger alluvium. However, moving the alluvium-colluvium interface to coincide

with the slip surface did not change the FS. Because the slip surface material was modeled as an interface, this stability analysis yielded the same FS as calculated in Case I above, i.e., 1.03. Thus, lowering the alluvium-colluvium interface to coincide with the slip surface did not impact the stability analysis.

The stability analysis for Case I, i.e., slope geometry, slip surface, phreatic surface shown in Figure 4.3, and residual strength parameters for the slip surface of $c' = 0$ and $\phi'_r = 16°$, yielded a FS = 1.03 which is in agreement with that calculated by D'Appolonia et al. (1967). Thus, subsequent stability analyses were performed using the verified slope geometry, phreatic surface, slip surface, and linear failure envelope. Because D'Appolonia et al. (1967) concluded that raising the phreatic surface by 1.52 m, which is likely after wet winters, results in a 10% decrease in FS (see Figure 4.5). Therefore, stability analyses were performed by raising the phreatic surface 1.52 m from the location shown in Figure 4.3 to investigate the effect on FS and are described below:

1) **Case I: Linear Residual and Peak Failure Envelopes**

   Stability analysis using the measured drained residual strength parameters ($c' = 0$ and $\phi'_r = 16°$) and slope geometry, slip surface, and phreatic surface shown in Figure 4.3 yielded a FS = 1.03 which is in agreement with stability analysis results of D'Appolonia et al. (1967). Stability analyses performed after raising the phreatic surface by 1.52 m and using the same input parameters yielded a FS = 0.95 (see Table 4.3). The rise in phreatic surface by 1.52 m resulted in about a 9% decrease in FS. Thus, the stability analysis is sensitive to a rise in phreatic surface by 1.52 m or more. A rise in the phreatic surface by 1.52 m with the soil strength equal to the residual value, should have resulted in major slide movement but there is no evidence of slide movement in the recent past (D'Appolonia et al., 1967).

   Stability analysis using actual slope geometry, phreatic surface, and the peak strength parameters measured by D'Appolonia et al. (1967), i.e., c' = 7.66 kPa and $\phi'_r = 20°$, yielded a FS of 1.50. The same analysis with the phreatic surface raised by 1.52 m yielded a FS of 1.39. Because the measured peak strength parameters with a raised surface by 1.52 m yielded a FS = 1.39, no slope creep or slide movement should have occurred which was observed by D'Appolonia et al. (1967).

2) **Case II: Stress Dependent Residual Strength Relationship**

Stark and Eid (1994 and 1997) and Stark et al. (2005a) recommend using a stress dependent residual strength failure envelope in stability analyses. Therefore, a stress dependent relationship between the residual shear strength of the material present along the shear surface and effective normal stress was developed using the empirical correlation shown in Figure 6.36 for LL =51% and CF = 55% for the slip surface material as discussed in Case I above (see Figure 4.6). Because the drained residual friction angle measured in direct shear tests is in close agreement with that obtained from the empirical correlation, the stress dependent residual strength failure envelope encompasses the direct shear data.

Stability analyses performed using a stress dependent residual strength failure envelope and the verified slope geometry, phreatic surface, and slip surface, yielded a factor of safety of 1.03 which equals that computed by D'Appolonia et al. (1967) (see Table 4.3). A stability analysis was also performed using the stress dependent residual strength failure envelope shown in Figure 4.6, the verified slope geometry and slip surface shown in Figure 4.3, and the phreatic surface raised by 1.52 m and yielded a FS = 0.95. The decrease in FS due to rise in phreatic surface by 1.52 m should have resulted in a major slide but D'Appolonia et al. (1967) found no evidence of slide movement in the recent past.

3) **Case III: Stress Dependent Recovered/Healed Strength Relationship**

D'Appolonia et al. (1967) measured peak strengths on undisturbed slickensided specimens in direct shear tests but reported linear peak strength parameters as discussed in Case I above. The drained peak shear stresses measured on undisturbed slickensided specimens do not show linear relationship but are actually stress dependent with $c' = 0$ (see Figure 2.3). Furthermore, the undisturbed slickensided specimens were tested only at effective normal stresses of 100 kPa or less. Thus, a nonlinear peak failure envelope was developed using direct shear test results from D'Appolonia et al. (1967) shown in Figure 2.3 and new failure envelope is shown in Figure 4.6. This stress dependent peak strength failure envelope is referred herein as the stress dependent recovered/ healed strength failure envelope from D'Appolonia et al. (1967). Stability analyses performed using the stress dependent recovered/healed

strength failure envelope, the verified slope geometry, phreatic surface, and slip surface, yielded a FS = 1.19 (see Table 4.3). Another stability analysis using the same stress dependent recovered/healed strength failure envelope shown in Figure 4.6, the verified slope geometry and slip surface shown in Figure 4.3, and raising the phreatic surface by 1.52 m yielded a FS of 1.12.

A stress dependent recovered/healed strength envelope was also developed using the ring shear strength recovery test results presented by Stark and Hussain (2010) on silty clay from Esperanza Dam, Ecuador, with a similar LL, i.e., 55% (see Figure 4.6). Ring shear strength recovery tests and results are also discussed in Chapter 3. Thus, the stress dependent recovered/healed strength envelope developed from the ring shear strength recovery test results of silty clay from Esperanza Dam was used in the stability analysis along with verified slope geometry, phreatic surface, and slip surface shown in Figure 4.3 and yielded a FS = 1.19 (see Table 4.3). Stability analysis using the same stress dependent recovered/healed strength failure envelope shown in Figure 4.6, verified slope geometry, and slip surface shown in Figure 4.3, and raising the phreatic surface by 1.52 m, yielded a FS of 1.12.

Thus, the FS calculated using the D'Appolonia et al. (1967) stress dependent peak (recovered/healed) strength failure envelope and stress dependent recovered/healed strength failure envelope developed from the ring shear strength recovery test results are in agreement for the observed phreatic surface and also when the phreatic surface is raised by 1.52 m. This close agreement confirm the reliability of the ring shear strength recovery test results presented by Stark and Hussain (2010a) and discussed in Chapter 3.

The values of FS using stress dependent recovered/healed strength failure envelopes developed from D'Appolonia et al. (1967) direct shear tests and ring shear strength recovery test results by Stark and Hussain (2010a) are higher than the corresponding FS values calculated using a stress dependent residual strength failure envelope for the measured phreatic surface and a rise in the phreatic surface of 1.52 m (see Table 4.3). The value of FS yielded by the peak and recovered/healed shear strengths even with a rise in the phreatic surface of 1.2 to 1.19, respectively, 1.52 m is probably

sufficient enough to prevent any slope creep or slide movement which D'Appolonia et al. (1967) observed.

Results of slope stability analyses presented in Table 4.3 suggest that the critical failure surface was correctly identified by D'Appolonia et al. (1967) and shown in Figure 4.3. Slip surface material was different from the soil above and below the failure surface which was also identified by D'Appolonia et al. (1967) based on the index properties and it consists of the material/soil derived from bedrock/claystone. The soil/material along the failure surface must be at residual strength conditions because major movement occurred previously as evidenced by the presence of slickensides. The results of slope stability analyses using a stress dependent residual failure envelope suggest that the slope should have been marginally stable at the time of toe excavation because the calculated FS was near unity (FS = 1.03) the same value computed by D'Appolonia et al. (1967) by using a linear strength relationship. Patton (1984) concludes that slope creep starts at FS of about 1.03. Thus, the landslide with slip surface material at residual conditions even at a FS =1.03 should have experienced some slope creep in the recent past. Furthermore, a rise in the phreatic surface by 1.52 m with the slip surface material at residual strength conditions yielded a FS = 0.95 which should have resulted in slope movement or creep but it did not.

Slope stability analyses using stress dependent recovered/healed strength failure envelopes established from direct shear tests by D'Appolonia et al. (1967) and ring shear strength recovery test results by Stark and Hussain (2010), yielded FS = 1.19 with the phreatic surface shown in Figure 4.3 and FS = 1.12 with a rise in phreatic surface by 1.52 m. Because stability analyses using recovered/healed strength even with a rise in phreatic surface by 1.52 m yielded a FS = 1.12 was sufficient to prevent a creep movement. Therefore, D'Appolonia et al. (1967) conclusion that the strength along the failure surface was somewhat greater than the residual strength because of healing of shear surface is supported by these values of FS. Because the healed/recovered strength is removed after a small shear displacement and reduces to the residual value with shear displacement, it is concluded that the healed/recovered strength may be useful in explaining slope creep behavior or slope stability prior to reactivation but it has little or no effect on the stability of the slope after the restart of movement.

4.3 Alvera Landslide in Northeastern Italy

4.3.1 Description of Landslide

Angeli et al. (1996, 1999, and 2004) describe the Alver`a landslide in the area of Cortina d'Ampezzo located in northeastern Italy. Cortina d'Ampezzo is situated at the bottom of a large valley which is part of the eastern Dolomites in northeastern Italy (Angeli et al., 1999). The slope consists of clayey material resulting from the weathering of San Cassiano Formation, which mainly consists of alternating beds of sandstone, marl, and clay that outcrop in the hillside above the landslide (Angeli et al., 1996). The climate of the Cortina d'Ampezzo area may be defined as Alpine-type ranging from cold to temperate, with variably cold winters and mild summers. Late springtime and summer are the most rainy periods, with a peak in July.

Because the landslide has a frequent reactivation history, several episodes of repeated movements are available since 1879. The most recent and dangerous reactivation occurred in 1945 (Angeli and Sivano, 2004). Subsequent reactivation occurred in 1966 as a result of flooding that affected northeastern Italy. In 1989 a sophisticated monitoring system was installed (Angeli et al., 1996, 1999, 2004 and Angeli and Sivano, 2004) on the slope. The monitoring system was improved in 1994 and consists of inclinometers, piezometers (equipped with electric transducers for the measurement of the hydraulic head in the slope), and steel wire extensometers to measure the continuous measurement of the landslide displacements.

The main landslide is active and moving at a rate of several centimeters per year (Angeli et al., 1996 and 1999). The landslide is about 1 km long and 50 to 200 m wide. The main slip surface identified by inclinometers is 18-25 m deep (see Figure 4.8). In the lower part of the landslide a secondary surficial slide with a depth of 5 m was also identified by inclinometers (shaded in black in Figure 4.8) which is more active (Angeli et al., 1996, 1999, 2004, and Bonomi and Cavallin, 1999) than the main slide. This slide is independent of the main slide (see Figure 4.8) and is not relevant to the strength gain study. Boreholes were also drilled to depths ranging from 9 to 30 m along the longitudinal profile of the landslide to detect the slip surface at different locations along the landslide body.

Geotechnical laboratory tests show significant differences between samples collected at different depths in the slope and those obtained from the main failure surface in a trial pit

excavated in the lower part of the Alver`a landslide (Angeli et al., 1996, 1999, and Angeli and Silvano 2004). Mineralogical analyses performed on samples collected from the main failure surface have shown that the material essentially consists of montmorillonitic clay. Index properties measured by Angeli et al. (1996) from two main failure surface samples are LL = 91.5, 99.1%, PI = 44.5, 51.1%, CF = 68, 71%, and a drained residual friction angle, ϕ'_r = 15.9º, measured in ring shear tests. The index properties measured by Angeli and Silvano (2004) using four main failure surface samples are LL = 69.3-99.1%, PI = 29.6-51.1%, CF = 56-71%, and drained residual friction angle, ϕ'_r = 9º -15.9º from ring shear testing. Angeli and his coworkers do not report the effective stress at which these ring shear tests were performed but Deganutti and Gasparetto (1992) report ϕ'_r = 15.9º measured in ring shear test at an effective normal stress of 100 kPa.

The installed piezometers (see locations in Figure 4.8) indicate that the groundwater surface is near the ground surface (typically 0.8 m) and subject to rapid fluctuations ranging from 0.4 to 1.5 m below the ground surface (see Figures 4.9 and 4.10). Angeli et al. (1999) report that the groundwater surface responded to rainfall and snow melt during 1994-1996 as recorded by piezometers.

4.3.2 Angeli et al. (1996) Conclusions regarding Strength Regain in Alver`a Landslide

Angeli et al. (1996, 1999, and 2004) do not provide any back-analysis results to reinforce their conclusions of strength gain in the main slide or at the toe. Instead they utilize the upper (u.t.) and lower (l.t.) piezometric thresholds required to start and stop the main landslide, respectively. The upper and lower piezometric thresholds required to start and stop the slide movement were established by Angeli et al. (1996) and are 0.4 and 1.3 m, respectively (see Figures 4.9 and 4.10). Angeli et al. (2004) state "the lower threshold to stop the movement is compatible with the measured residual shear strength in conventional tests." But to restart the movement a higher piezometric level was required which assumes no other change to the slope except shear strength and piezometric level. Angeli et al. (1996 and 2004) conclude that the longer the stationary period, the higher the piezometric level required to restart the slide movement. These upper and lower piezometric thresholds to start and stop the landslide movement, respectively, were used to conclude that the strength regain occurred on preexisting

slip surfaces containing montmorillonitic clays (Angeli et al., 1996 and 2004). Because most of the clays tested are rich in calcite and other soluble minerals, Angeli et al. (2004) postulate that some regrowth in mineral structures and bridging of the slip surface might have occurred during stationary periods. Angeli et al. (2004) postulate that the residual strength could be modified through weathering reactions, clay mineral alterations, and fluctuations in groundwater chemistry due to a change in porewater chemistry during the dry and stationary periods. Strength recovery observed during laboratory direct and ring shear tests by Angeli et al. (1996 and 2004) is additional evidence of strength recovery and helps explain the landslide behavior. However, Angeli et al. (2004) suggest that the application of the recovered strength to stabilization measures should be approached with great caution because the recovered/regained strength is removed with a small shear displacement in laboratory testing and the strength reduced to the residual value.

Deganutti and Gasparetto (1992) performed a back-analysis of the Alver`a landslide and back-calculated a drained residual friction angle of $\phi'_{bc} = 15.2^{o}$ assuming the groundwater at the ground surface and FS = 1.0. Unfortunately these researchers do not include the cross-section analyzed in this paper. The drained residual friction angle measured in the ring shear tests by Deganutti and Gasparetto (1992) is $\phi'_{r} = 15.9^{o}$ at an effective normal stress of 100 kPa which is in agreement with the ϕ'_{bc} of 15.2°. Angeli and Silvano (2004) report a range of drained residual friction angle measured on four slip surface samples of $\phi'_{r} = 9.0^{o}$-15.9^{o} for a range of LL of 69.3-99.1%. Unfortunately, the effective normal stresses used in these ring shear tests are not reported by Angeli and his co-workers so it is difficult to compare these values.

4.3.3 Current Back-Analyses Results and Discussion

Back-analyses were performed during this study using the Alver`a landslide cross-section given in Angeli et al. (1999) and Angeli and Silvano (2004) (see Figure 4.8). The well defined main failure surface in the lower portion of the landslide (see “main failure surface” in Figure 4.8) is considered the critical failure surface and is used for the back-analysis performed herein. The critical failure surface has a well defined geometry that separates it from the entire slide and movement along this surface is independent of the slide movement located at the toe (see Figure 4.8). Furthermore, any movement along this critical failure surface results in movement of the

entire slide. Slope stability software XSTABL (Sharma, 1995) and Spencer's (1967) stability method were used to back-calculate the drained friction angle for a factor of safety of unity (FS = 1.0). A noncircular failure surface was specified to match the critical failure surface shown in Figure 4.8. The slope material unit weight determined by Angeli and his coworkers, i.e., γ_{sat} =18.73 kN/m^3, was used for the back-analysis. Angeli et al. (1996 and 2004) report that the average depth of the groundwater surface (GWS) is about 0.8 m whereas the upper and lower thresholds to start and stop the landslide are 0.4 and 1.3 m, respectively.

Deganutti and Gasparetto (1992) performed a back-analysis with the GWS at the ground surface and back-calculated friction angle, ϕ'_{bc}, of 15.2°. Back-analysis was performed in the present study on the cross-section shown in Figure 4.8 using Spencer's (1967) stability method coded in XSTABL (Sharma, 1995) for a FS = 1.0, and GWS at the ground surface and yielded ϕ'_{bc} of 14.4º. Because Deganutti and Gasparetto (1992) do not show the cross-section analyzed, it is difficult to compare the slope geometry, critical failure surface, and back-calculated friction angle.

Stability analyses were performed in the present study for the following five GWS conditions; phreatic surface at the ground surface and depths of 0.4, 0.8, 1.3, and 1.5 m to investigate the sensitivity of the stability analyses to changes in GWS. Three types of stress dependent failure envelopes were used in the back-analysis for each GWS condition, i.e., linear residual strength relationship, stress dependent relationship for residual strength as suggested by Stark and Eid (1994 and 1997) and Stark et al. (2005a), and stress dependent relationship for recovered/healed strength as suggested by Stark and Hussain (2010) as discussed below:

1) **Case I: Linear Residual Strength Relationship**

   Angeli and Silvano (2004) report a range of liquid limit (LL = 69.3-99.1%) and drained residual friction angle measured in ring shear tests (ϕ'_r = 9.0º -15.9º) on four main slip surface samples. As discussed earlier, Angeli and his coworkers do not report the effective normal stress at which these ring shear tests were performed but Deganutti and Gasparetto (1992) report the same value of drained residual friction angle, i.e., ϕ'_r = 15.9º, measured in ring shear tests at an effective normal stress of 100 kPa. Therefore, a linear relationship between the shear strength and effective normal

stress is assumed to determine the average shear strength parameters available along the critical failure surface which result in FS = 1.0 to compare the ϕ'_{bc}. Considering the marginally stable landslide at an average GWS condition, i.e., GWS 0.8 m below ground surface, an average drained friction angle of 13.6º is back-calculated (see Table 4.4).

Using the friction angle of 13.6º, stability analyses were performed for the four other GWS conditions. Table 4.4 shows the results of the slope stability analyses for the five GWS conditions using ϕ'_{bc} = 13.6º. The stability analysis shows that there is little effect of change in GWS on factor of safety because FS = 0.94 when GWS is at ground surface and FS = 1.06 when GWS is 1.5 m below the ground surface. Thus, the factor of safety does not appear sensitive to changes in GWS within the measured/reported upper and lower piezometer limits (see Table 4.4).

The average value of LL of the slip surface material at the soil-rock interface along the critical slip surface should be about 83% which is in agreement with the average LL being 69.3-99.1% (Angeli et al., 1999, Angeli and Sivano, 2004). The back-calculated friction angle of 13.6°, which is an average friction angle of the main slip surface material, is in agreement with that obtained from the residual strength empirical correlation shown in Figure 6.24, i.e., ϕ'_r = 12º at an effective normal stress of 100 kPa for LL = 83% and CF > 50%.

2) **Case II: Stress Dependent Residual Strength Relationship**

Stark and Eid (1994 and 1997) and Stark et al. (2005a) recommend using a stress dependent residual strength failure envelope in stability analyses. Therefore a stress dependent residual strength failure envelope was developed using new empirical correlation for residual friction angle shown in Figure 6.24 and LL = 83%. The stress dependent residual strength failure envelope shown in Figure 4.11 results in FS = 1.0 for the average GWS condition of 0.8 m below ground surface and the other input parameters used in Case I above. The stress dependent residual strength failure envelope shown in Figure 4.11 was also used for the other four GWS conditions to calculate FS (see results in Table 4.4). These stability analyses show that there is a little effect of changes in GWS within the upper and lower thresholds on factor of safety as FS = 0.94 when GWS is at ground surface and FS = 1.05 when GWS is

1.5 m below the ground surface which are in agreement with the results of Case I computed using a linear residual failure envelope. Thus, the use of a stress dependent residual strength failure envelope also does not seem to be sensitive to changes in GWS within the measured/reported upper and lower piezometer limits.

3) **Case III: Stress Dependent Recovered/Healed Strength Relationship**
The Alver`a landslide is characterized as start-stop slide by Angeli and his coworkers which starts moving with a rise in GWS due to rainfall or snowmelt and stops movement when the GWS is lowered after a rainfall (see Figure 4.9). Because the average value of liquid limit for the Alver`a landslide slip surface material is about 83% with CF > 50% and it contains montmorillonite, the Alver`a landslide main slip surface material can be compared with Madisette clay which was tested herein (see Chapter 3). Considering a stationary/rest period less than 30 days as evidenced from Figures 4.9 and 4.10 and ring shear strength recovery test results for Madisette clay by Stark and Hussain (2010) a stress dependent relationship between recovered/healed strength and effective normal stress was developed and is shown in Figures 4.11 and 4.12. This stress dependent recovered/healed strength failure envelope was used in the back-analyses of all five GWS conditions. The results of the back-analyses using a stress dependent recovered/healed strength failure envelope are shown in Table 4.4. Table 4.4 shows an increase in FS for each GWS condition using a stress dependent recovered/healed strength failure envelope. Table 4.4 shows that for the GWS 0.8 m below ground surface FS = 1.07, for GWS 0.4 m below ground surface FS = 1.04, and for GWS at the ground surface FS = 1.01. This increase in FS as a result of strength recovery/healing during the rest/stationary period may be a reason for a higher piezometric level being required to start movement.

Results of the slope stability analysis presented in Table 4.4 suggest that the FS is not sensitive to change in GWS or piezometric thresholds i.e., GWS 0.4-1.5 m below ground surface. Although Angeli et al. (1996 and 2004) conclude that strength recovery was occurring along the shear surface, but they could not identify the mechanism responsible for the strength gain. Table 4.4 shows that the landslide stops movement at the lower piezometric level, i.e., GWS 1.5 m below ground surface, and FS = 1.05 computed using the stress dependent residual strength failure envelope. As discussed earlier, Hutchinson (1988) and Bertini et al. (1984) report that

movement due to slope creep became negligible when the computed FS $\geq$ 1.05. Thus, a computed FS of 1.05 using the GWS at 1.5 m below ground surface and a stress dependent residual strength failure envelope may explain the stop in slide movement or slope creep as suggested by Hutchinson (1988) and Bertini et al. (1984).

Table 4.4 shows that FS = 1.04 with GWS 0.4 m below ground surface which corresponds to the upper piezometric level which is required to restart the slide movement using a stress dependent recovered/healed strength failure envelope. Patton (1984) shows that slide movement starts due to slope creep when the FS decreases to a rise in GWS and reaches at a value of 1.03. A maximum rest period of less than 30 days was obtained from observed movements shown in Figure 4.10. Otherwise the landslide only remained stationary for short periods during the monitoring period. Thus, using the actual rest/stationary period to develop the recovered/healed strength failure envelope results in a lower FS because less healing occur This may result in slide movement or slope creep restarting at an upper piezometric level, i.e., GWS at 0.4 m from ground surface. Because an increase in shear strength, if any, is reduced after each renewal of movement, the recovered strength cannot be relied upon in landslide remedial design which is also suggested by Angeli et al. (2004).

4.4 Summary and Discussion

Back-analysis of two case histories that suggest strength gain on a preexisting shear surface suggests strength recovery can occur along preexisting shear surfaces. Although no well documented case history is available in the literature to rigorously investigate strength recovery, the Weirton and Alver`a landslides contain sufficient information to investigate the possibility of strength recovery along preexisting shear surfaces.

Because the soil along preexisting shear surface must be at residual condition, marginally stable slopes should experience some evidence of movement due to some recent changes in groundwater conditions or such other reasons. A stable slope with a raised phreatic surface, residual shear strength condition, and FS $\leq$ 1.0, suggests strength gain above the residual value because no movement is occurring with a raised phreatic surface.

Back-analysis of a start-stop landslide, i.e., Alver`a landslide, suggests that FS to start movement after a rest period is always greater than FS at which movement stopped using upper

and lower piezometric level thresholds, respectively. The difference in the value of FS to start and stop the slide movement has been cited as an indication that strength recovery occurred during the rest period required a higher piezometric level after a rest period to restart movement.

In the Weirton landslide, a rise in groundwater level from the reported by D'Appolonia et al. (1967), which is an observed fact in the Ohio River valley, and the residual strength condition should have resulted in some major slide movement. The absence of any slide movement at the time of toe excavation, the direct shear test results of intact slip surface specimens, and the back-analysis results using a higher phreatic surface and observed peak strength suggest that the preexisting shear surface material may have undergone some healing according to D'Appolonia et al. (1967). The stress dependent recovered strength failure envelope developed from the strength recovery test results of a similar soil is in agreement with the peak strength failure envelope from the direct shear test results of intact slip surface specimens. Thus, the strength recovery test results presented in Chapter 3 are in agreement with the measured peak strength of intact slip surface specimens.

The results of slope stability analyses using stress dependent residual strength failure envelope in both case histories suggest that the slopes should have been marginally stable with the average groundwater condition.

Although Angeli and his coworkers conclude that landslide movement stops a lower piezometric level than it restarts which suggests some changes occurred during the period of no movement. The back-analyses performed during the present study using these lower and upper piezometric thresholds and stress dependent residual and recovered strength failure envelopes also suggest some strength gain occurred during the period of no movement. However, the strength gained is lost upon renewal of slide movement and the residual strength conditions are reached shortly after the start of each movement. Thus, the residual strength of slip surface material in a stop-start landslide governs its stability and the recovered strength may inference the slope creep behavior.

Because the healed/recovered strength is removed after a small shear displacement and reduces to the residual value as discussed in Chapter 3, it may be useful in explaining slope creep behavior or slope stability prior to reactivation but it has little impact on slope stability after

restart of movement. Therefore the recovered strength should not be relied upon in remedial design and in the design of slopes.

4.5 Tables and Figures

Table 4.1. Factor of safety of natural slope against drained failure for various soil parameters and cross-section in Figure 4.3 (from D'Appolonia et a., 1967)

ϕ', degrees	***c'*, kPa**	**Factor of Safety**	
		Morgenstern and Price (1965)	**Ordinary Method of Slices (neglecting side forces)**
14	0	0.90	0.83
16	0	1.03	0.95
18	0	1.17	1.08
20	7.66	1.51	1.39

Table 4.2. Material properties and strength parameters used for the back-analysis of Weirton landslide in colluvium slope

Material	**γ_{sat} KN/m^3 (lb/ft^3)**	***c'* kPa**	**ϕ' degrees**
Colluvium	18.86 (120)	0	25
Slip surface material	18.86 (120)	0	16
Alluvium	19.64 (125)	0	30
Bedrock	18.86 (120)	0	35
Sand and gravel	19.64 (125)	0	40

Table 4.3. Summary of stability analysis results for Weirton landslide in colluvium slope.

Stress Parameters/Envelope	FS*	ΔFS
Slip Surface Material Modeled as an Interface with Linear Strength Relationship		
Case I: Observed Slip Surface and Actual Slope Geometry	1.03	
Case II: Slip Surface at Alluvium-Colluvium Interface	1.19	+0.19
Case III: Alluvium-Colluvium Interface at the Observed Slip Surface	1.03	
Linear and Stress Dependent Strength Envelopes		
Case I: Linear Residual/Peak Strength Relationship		
(1) Residual Strength:		
Observed phreatic surface	1.03	
Raising phreatic surface by 1.52 m	0.95	-0.05
(2) Peak Strength:		
Observed phreatic surface	1.50	+0.50
Raising phreatic surface by 1.52 m	1.39	+0.39
Case II: Stress Dependent Residual Strength Failure Envelope		
Observed phreatic surface	1.12	+0.12
Raising phreatic surface by 1.52 m	1.03	
Case III: Stress Dependent Peak/Recovered/Healed Strength Failure Envelope		
(1) Measured Peak/Healed Strength:		
Observed phreatic surface	1.22	+0.22
Raising phreatic surface by 1.52 m	1.15	+0.15
(2) **Recovered/Healed Strength (Ring Shear Strength Recovery Test Results):**		
Observed phreatic surface	1.20	+0.20
Raising phreatic surface by 1.52 m	1.12	+0.12

* FS calculated using GLE method by Chung (1986) and coded in XSTABL (Sharma, 1995)

Table 4.4. Summary of stability analysis results for Alver`a landslide, northeastern Italy.

Stress Parameters/Envelope	ϕ'	FS*	ΔFS
Case I: Linear Residual Strength Relationship			
GWS 0.8 m below the ground surface	13.6º	1.00	
GWS 1.5 m below the ground surface	13.6º	1.06	+0.06
GWS 1.3 m below the ground surface	13.6º	1.05	+0.05
GWS 0.4 m below the ground surface	13.6º	0.98	-0.02
GWS at the ground surface	13.6º	0.94	-0.06
GWS at the ground surface	14.4º	1.00	
Case II: Stress Dependent Residual Strength Relationship $			
GWS 0.8 m below the ground surface	Stress dependent relationship	1.00	
GWS 1.5 m below the ground surface	"	1.05	+0.05
GWS 1.3 m below the ground surface	"	1.03	+0.03
GWS 0.4 m below the ground surface	"	0.98	-0.02
GWS at the ground surface	"	0.94	-0.06
Case III: Stress Dependent Recovered/Healed Strength Relationship@			
GWS 0.8 m below the ground surface	Stress dependent relationship	1.07	+0.07
GWS 1.5 m below the ground surface	"	1.12	+0.12
GWS 1.3 m below the ground surface	"	1.10	+0.10
GWS 0.4 m below the ground surface	"	1.04	+0.04
GWS at the ground surface	"	1.01	+0.01

* FS calculated using Spencer (1967) method.

$ Stress dependent relationship between residual and effective normal stresses determined from new empirical correlations for residual friction angles shown in Figure 6.24.

@ Stress dependent relationship between recovered/healed shear strength and effective normal stress developed from ring shear strength recovery test results by Stark and Hussain (2010).

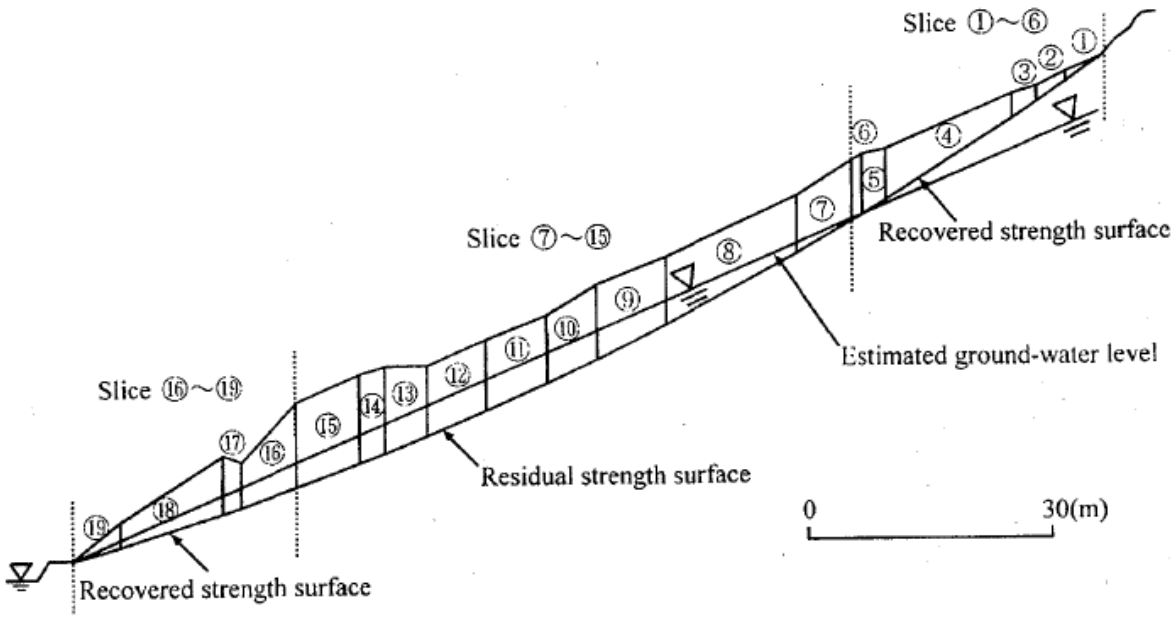

Figure 4.1. Cross-sectional diagram for stability analysis of a model slope (from Gibo et al., 1997).

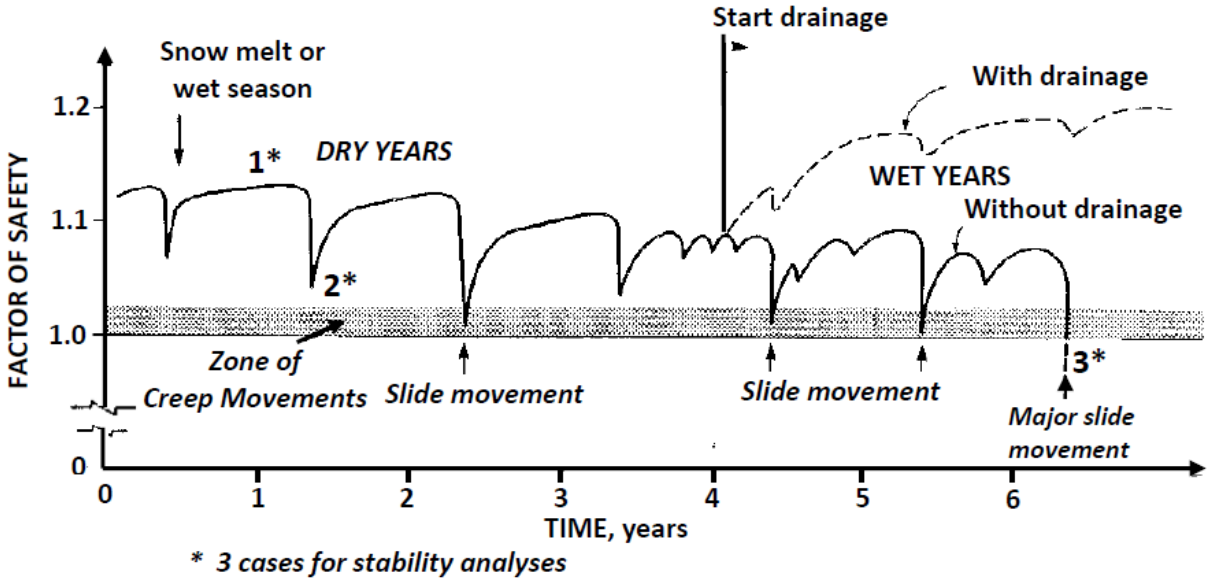

Figure 4.2. Variations in Factor of Safety with Time, with and without Drainage (from Patton, 1984).

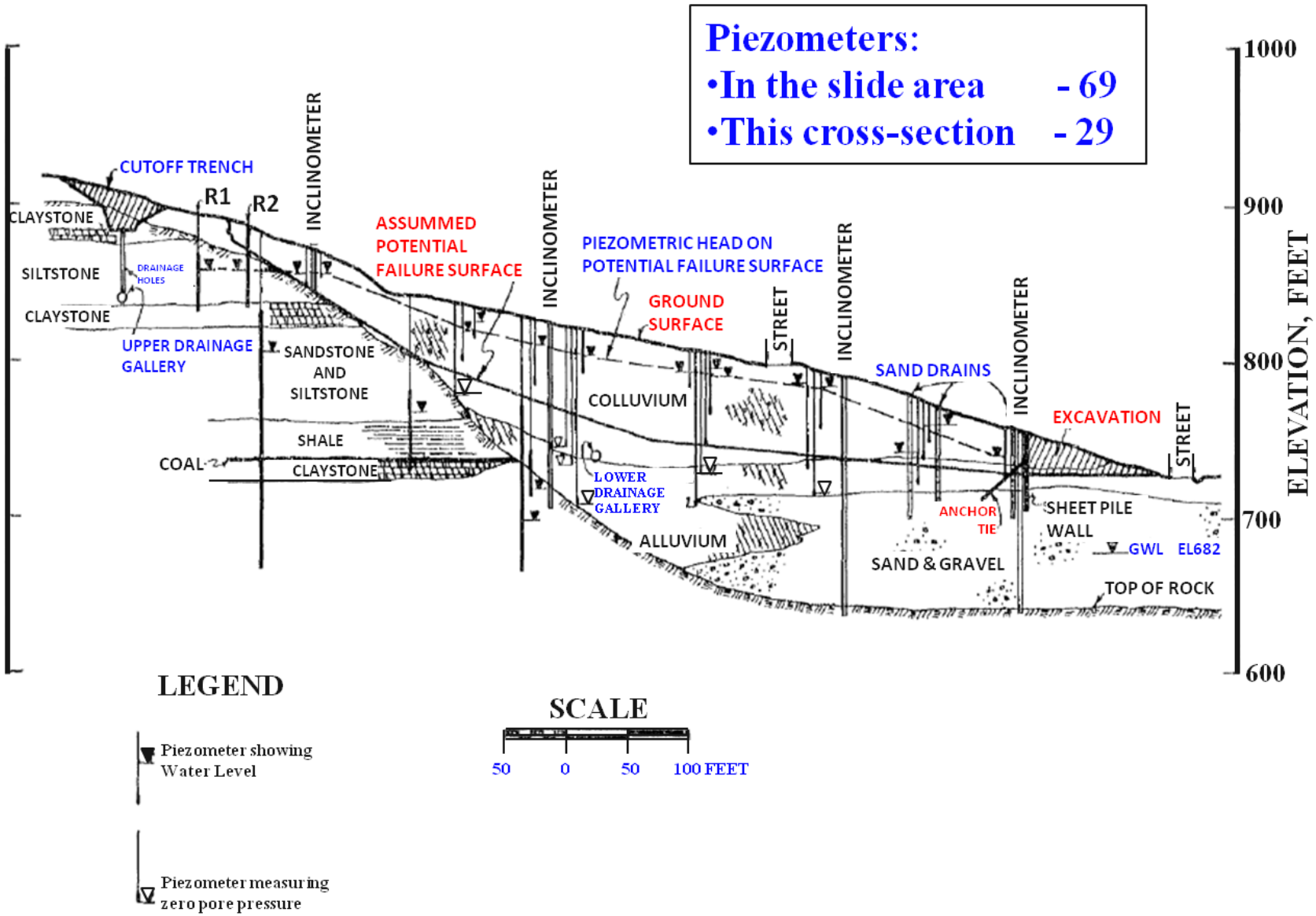

Figure 4.3. Cross section of slope showing instrumentation, excavation and potential failure surface (from D'Appolonia et al. 1967).

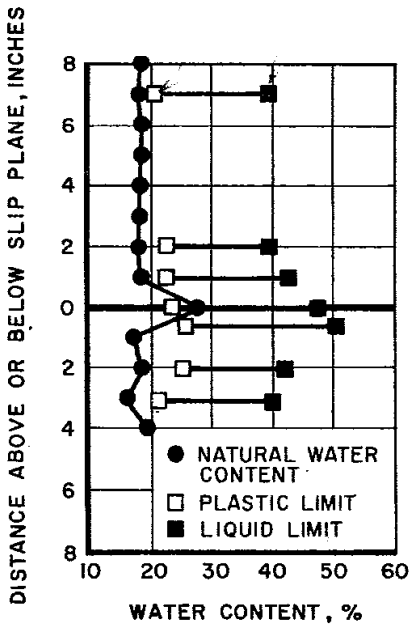

Figure 4.4. Distribution of water content and Atterberg limits near slip plane (from D'Appolonia et al. 1967).

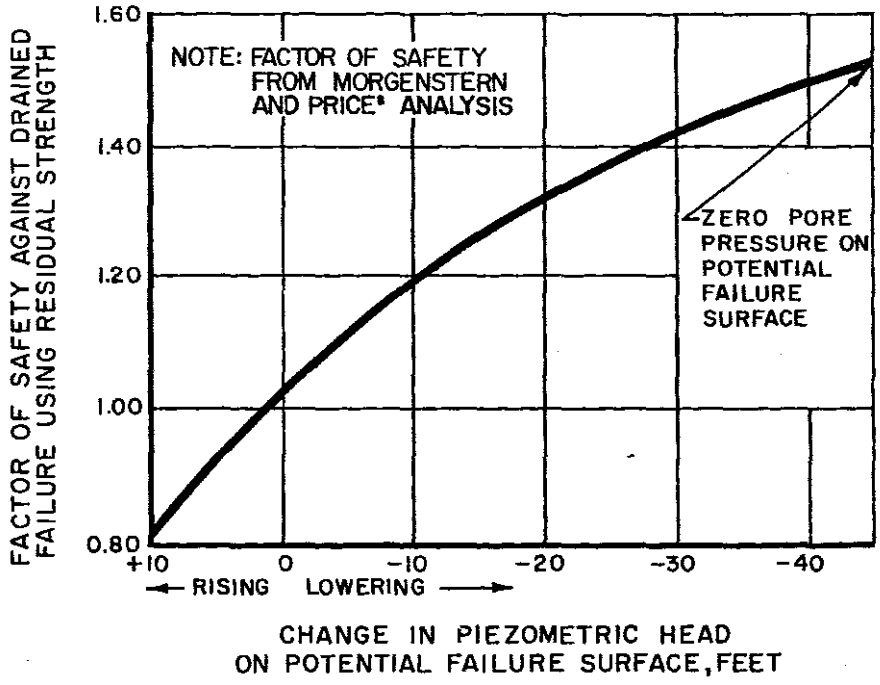

Figure 4.5. Factor of safety against drained failure using the residual strength parameters as a function of ground water level prior to excavation (from D'Appolonia et al. 1967).

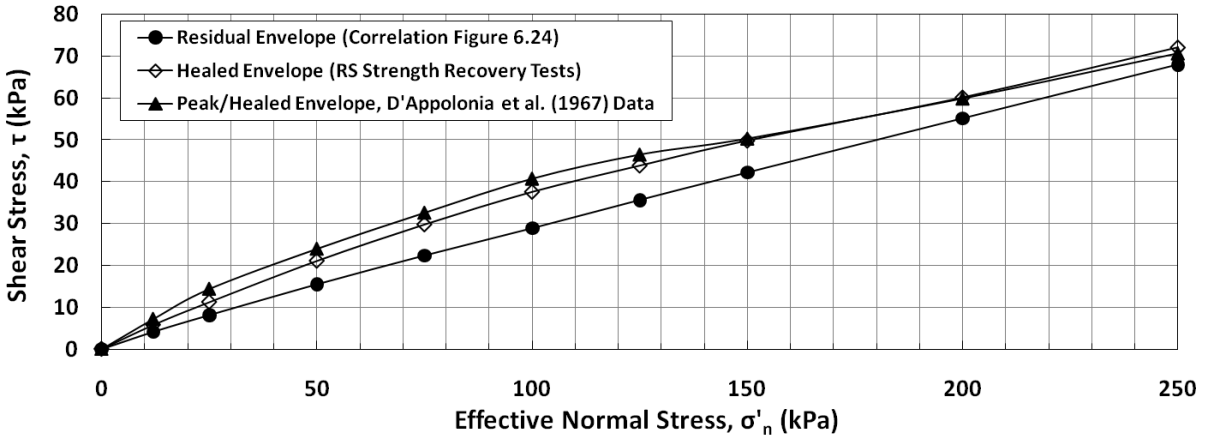

Figure 4.6. Stress dependent residual, peak, recovered/healed strength failure envelopes for slip surface material of Weirton landslide, WV.

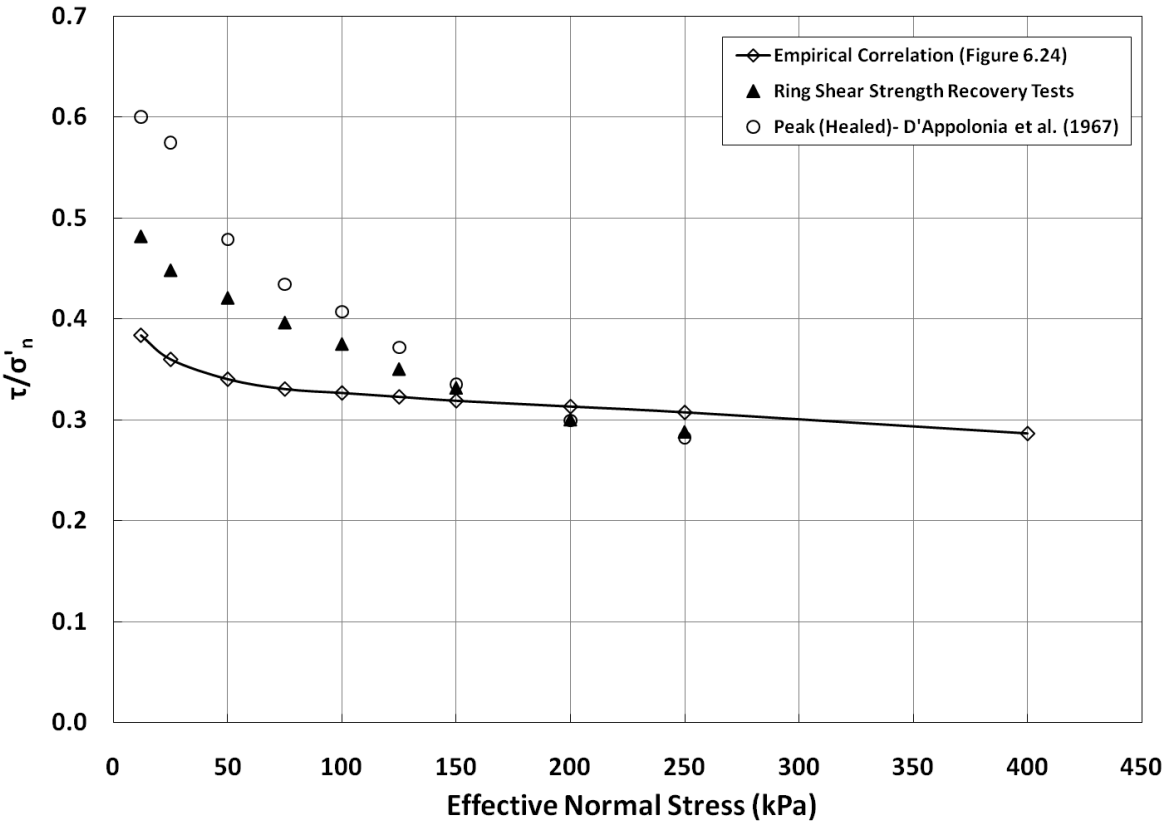

Figure 4.7. Comparison of stress dependent residual and peak/recovered/healed strength failure envelopes.

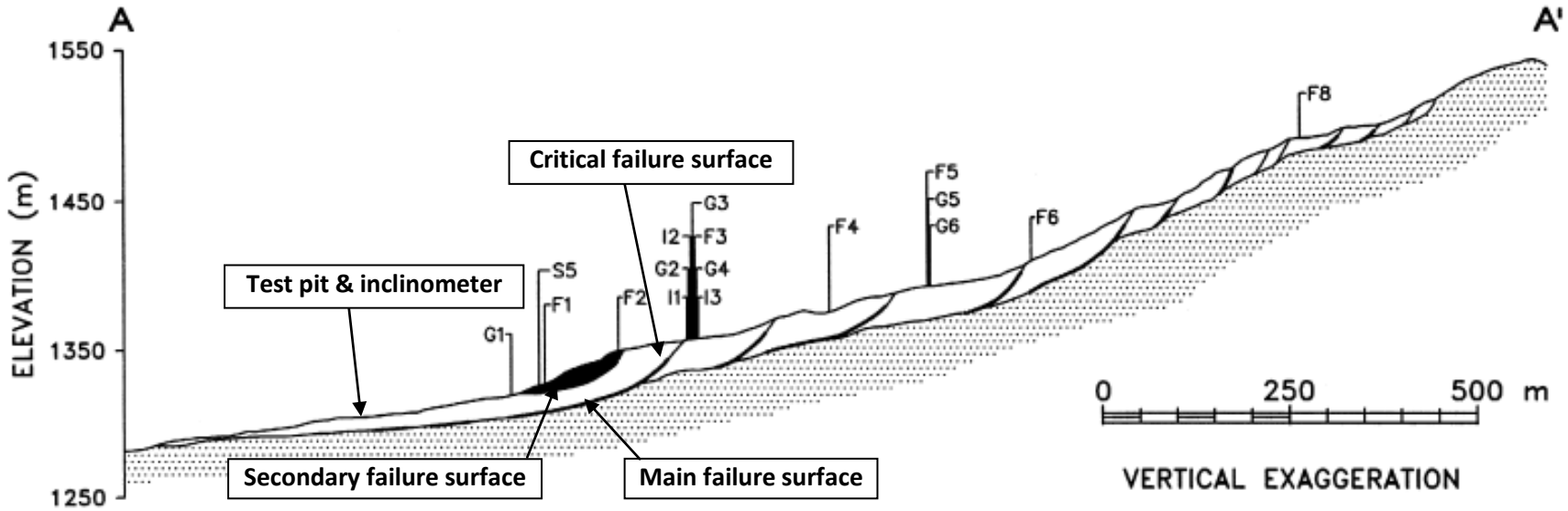

Figure 4.8. Cross-section of Alver`a landslide, Cortina d'Ampezzo, Italy (from Angeli et al. 1999).

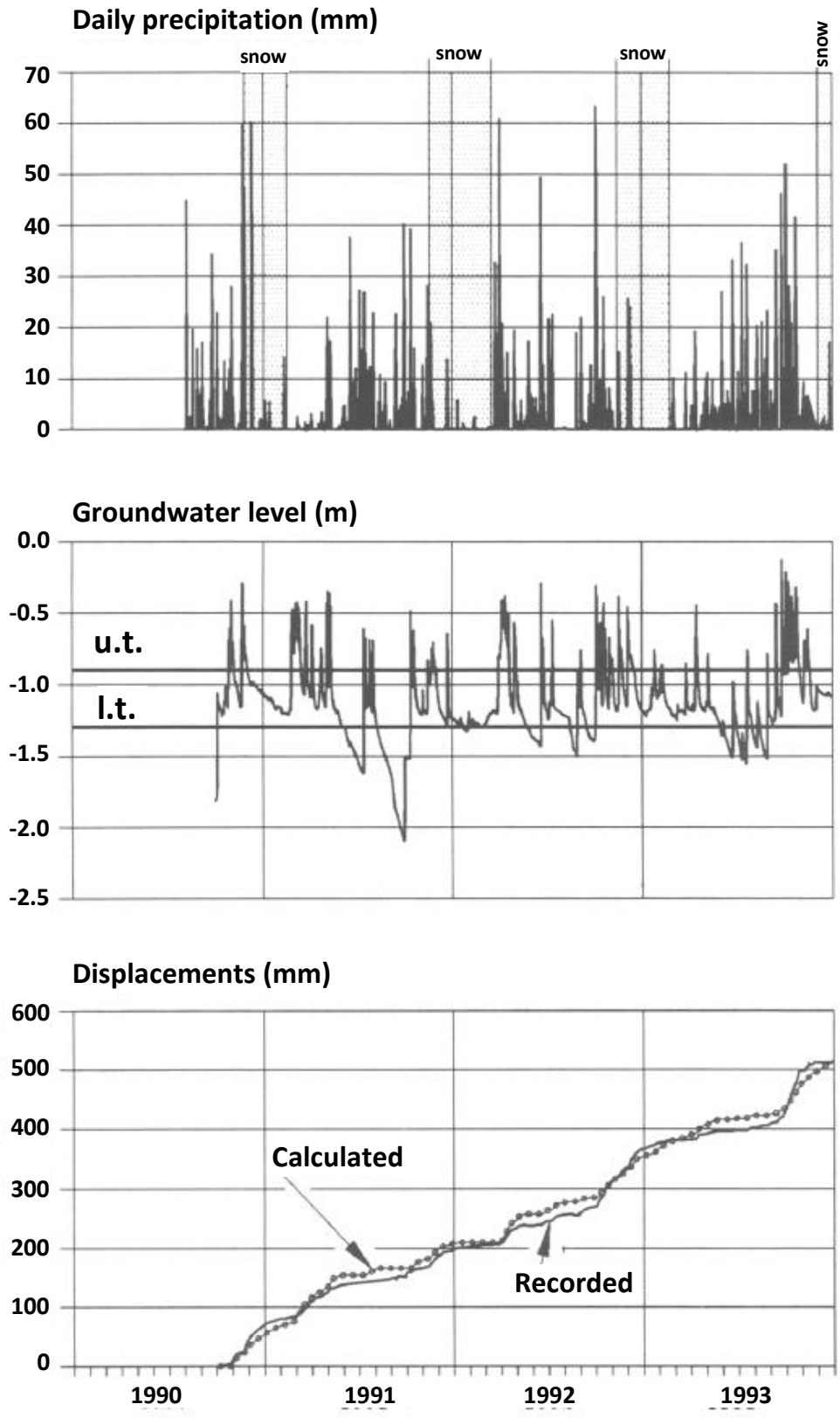

Figure 4.9. Precipitation depth, groundwater level, recorded and calculated displacement, Alver`a landslide, Italy (from Angeli et al. 1996).

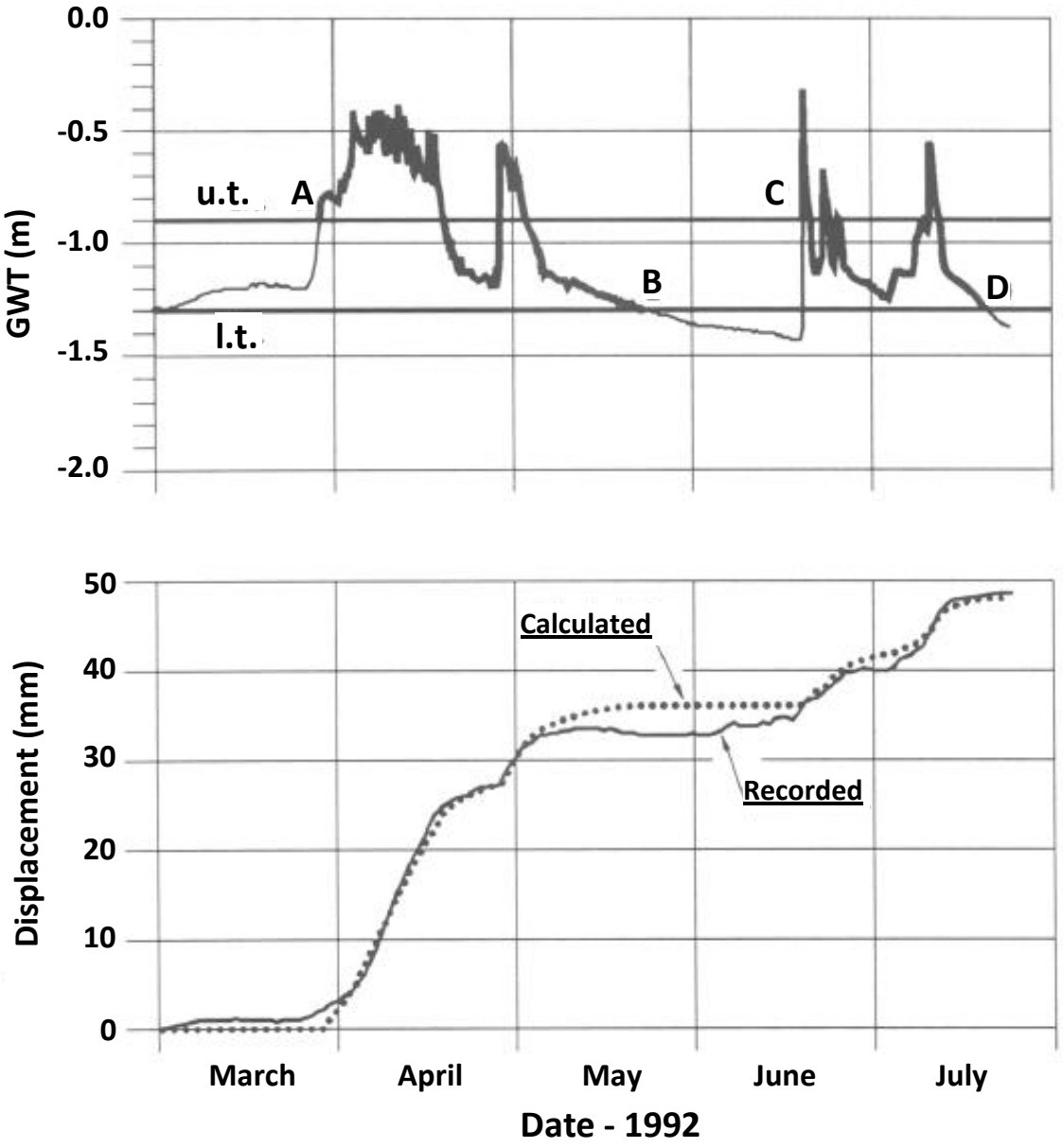

Figure 4.10. A critical situation for stability: groundwater level, upper (u.t.) and lower (l.t.) piezometric thresholds, recorded and calculated displacement, Alver`a landslide, Italy (from Angeli et al. 1996).

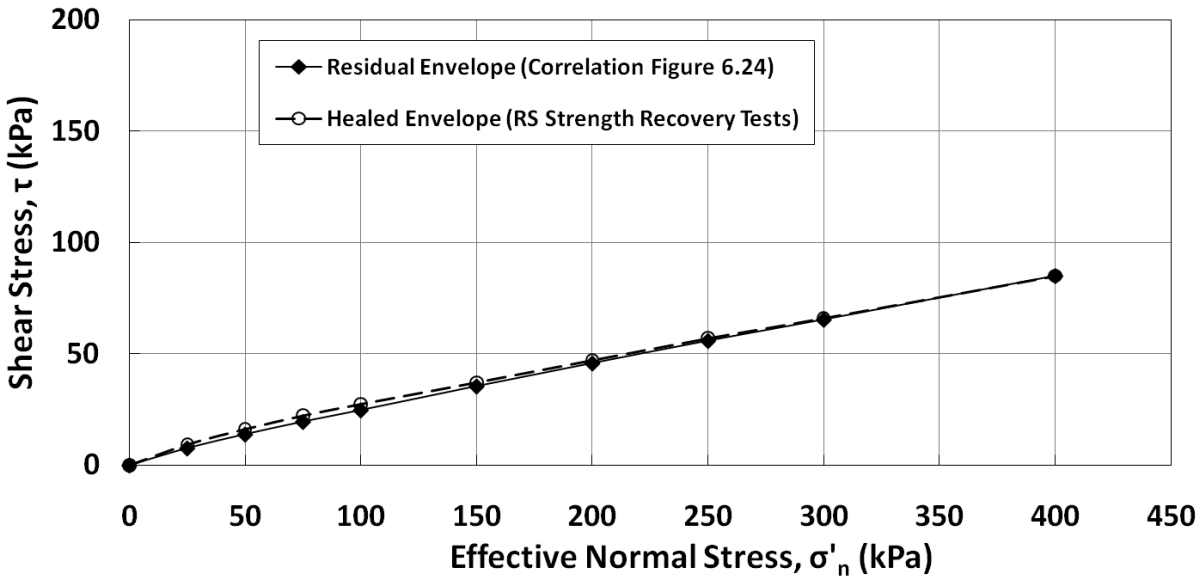

Figure 4.11. Stress dependent residual and recovered/healed strength failure envelopes for main slip surface material of Alver`a landslide, northeastern Italy.

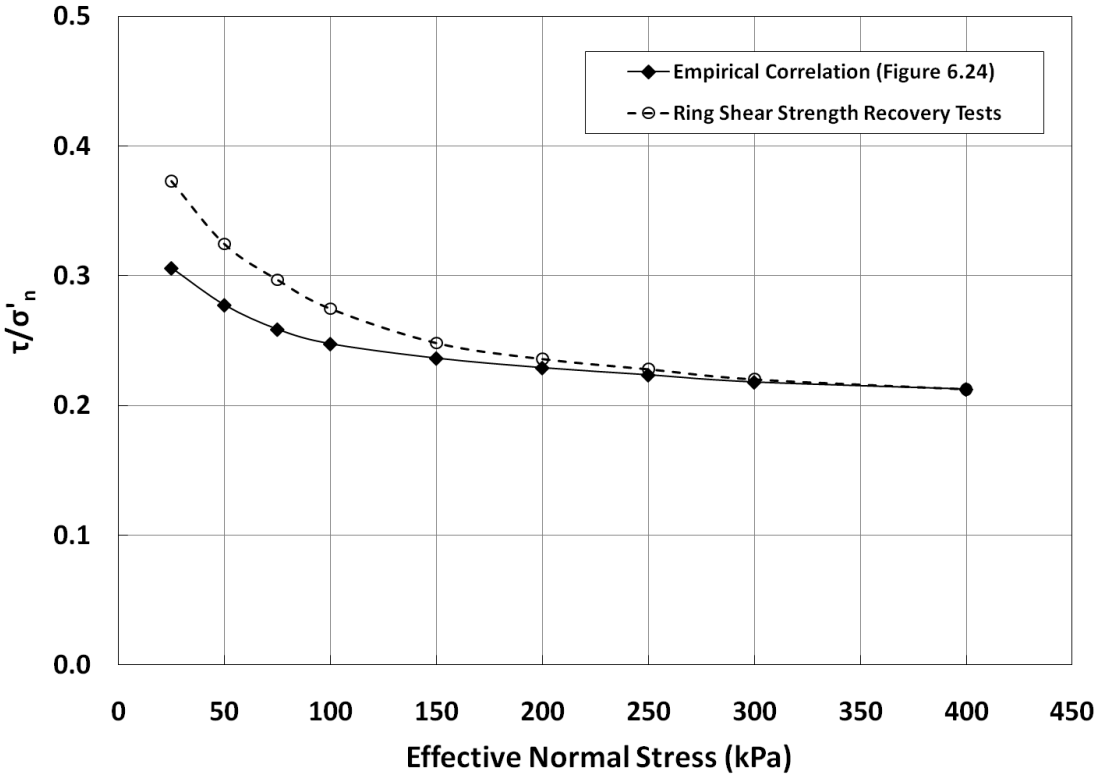

Figure 4.12. Comparison of residual strength stress dependent residual and recovered/healed strength failure envelopes for the main slip surface material of Alver`a landslide, northeastern Italy.

CHAPTER 5:BACK-ANALYSIS OF LANDSLIDES

5.1 Introduction

The back-analysis of a landslide is performed to investigate the mobilized shear strength of the weak layer for use in causation studies and remedial design. Because some of the conditions at the time of failure are unknown, some assumptions are usually required for the back-analysis. In the back analysis of landslides, the factor of safety at the time of failure is considered to be unity (FS = 1.0) and the shear strength parameters available along the failure surface are estimated by measuring or assuming the other input parameters.

Skempton (1964 and 1970) suggests that if the sliding mass undergoes a large shear displacement, e.g., several feet, then the shear strength of the material present along the slip surface will exhibit the residual value. Skempton (1964) also concludes "if failure has already occurred, any subsequent movement on the existing slip surface will be controlled by the residual strength, no matter what type of clay is involved." Also Skempton (1970) concludes that a fully softened strength is mobilized in a first-time slide in slopes in non-fissured clays whereas the residual strength is mobilized along the shear surface in preexisting landslide. Although in the back-analysis of a first-time slide, the fully softened shear strength is mobilized at the time of sliding. However, this strength can be reduced to the residual value if large displacement occurs during the slide so only the residual strength would be available for remedial design.

Some researchers, such as D'Appolonia et al. (1967), Ramiah et al. (1973), Angeli et al. (1996 and 2004), Gibo et al. (2002), Stark et al. (2005a), Carrubba and Del Fabbro (2008), and Stark and Hussain (2010a and 2010b), suggest some strength recovery or healing of a preexisting shear surface may occur as discussed in Chapter 2. This may result in the back-calculated strength not being in agreement with the residual strength value. The back-analyses presented in Chapter 4 also suggest that the observed strength recovery may be useful in explaining the behavior of shallow landslides, such as explaining the amount and rate of slope creep or slope stability prior to reactivation. The testing conducted herein suggests that the recovered strength

may not be relied upon in landslide remedial designs so the residual shear strength should be used for remedial design (Stark and Hussain, 2010a).

This chapter focuses on the mechanics of back-analysis of landslides for estimating the mobilized strength of the weak layer, causation studies, and planning the remedial measures.

When a landslide occurs, the shear strength of each soil layer along the entire length of the slip surface is mobilized. Laboratory and in-situ testing of the problematic layer usually may not yield a reliable estimate of the shear strength because of problems associated with obtaining a representative sample that has been sheared by the slide movement, limitations of existing laboratory tests, and sample disturbance. Some of the factors that are difficult to capture in laboratory tests are the structural fabric of the soil, influence of fissures on the strength of the soil, and the effects of preexisting shear planes within the soil mass (Duncan and Stark, 1992). The representative failure plane has an area many times larger than the failure surface in a laboratory or in-situ test. Furthermore, the actual failure involves a much longer time to occur than laboratory or insitu tests. Therefore, back-analysis is usually a more effective method of estimating the shear strength of the problematic layer than laboratory testing or at a minimum a verification of the laboratory measured strength. Even though back-analysis usually yields a better shear strength estimate than laboratory tests, there are uncertainties in a back-analysis. Some of these uncertainties have been discussed by authors, e.g. Leroueil and Tevenas (1981), Duncan and Stark (1992), Stark and Eid (1998), Gilbert et al (1998), Tang et al (1999), and Deschamps and Yankey (2006). Some of the uncertainties that influence the back-calculated shear strength are engineering properties for the other materials in the cross-section, slope geometry at the time of failure, phreatic surface and porewater pressures present at the time of failure, effect of rainfall, location of failure surface, and existence of tension cracks.

Because monitoring and instrumentation of natural slopes is not common prior to a landslide, frequently the location of phreatic surface along the slope at the time of failure is assumed in a back-analysis. Even if a natural slope is instrumented, the piezometric levels at the time of failure may not be accurately reflected because of faulty installation of piezometer, the piezometer not located in the zones of influence, or many other reasons.

Peck (1980) says "Judgment is required to set up lines of scientific investigation, to select the appropriate parameters for calculations and to verify the reasonableness of the results." Peck (1980) also says "What we can calculate enhances our judgment, allows us to make better judgments, and permits us to arrive at better engineering solutions." Thus experience and judgment should be used in selecting the input parameters and assumptions for the other materials. However, even experienced engineers sometimes make incorrect assumptions for the back-analysis which impacts the results. This chapter investigates the importance of the various input factors involved in a back-analysis using case histories and uses the results to develop guidelines for conducting a landslide back-analysis.

5.2 Uncertainties in Back-Analysis

As discussed earlier, a landslide back-analysis is performed by making some assumptions on the failure conditions present along the slide/slope at the time of failure and assuming input parameters which yield a factor of safety of unity (FS = 1.0). A major difference between a design analysis and a back-analysis is that conservative assumptions in a design analysis are unconservative in a back-analysis. For example, assuming a higher phreatic surface is conservative in a design analysis but it is unconservative in a back-analysis because it results in a larger back-calculated shear strength which may over predict mobilized shear strength along shear surface. Therefore, making reasonable assumptions on the conditions present along the shear surface at the time of sliding is important. Some of the uncertainties in a back-analysis are discussed in detail below and include slope geometry, material properties, phreatic surface and porewater pressures present at the time of failure, effect of rainfall, location of failure surface, and existence of tension cracks.

5.2.1 Slope Geometry at the Time of Failure

To perform a back-analysis, it is necessary to know the slope geometry at the time of the landslide to estimate the driving forces. The slope geometry can be obtained from prior topographic surveys or aerial photographs. Satellite images before and after the slide can also be used to determine slope geometry prior to failure. Measuring the slope geometry after the landslide also may be beneficial to correlate it with surrounding stable slopes to determine the pre-failure geometry, the possibility of additional movement, and confirm the back-analysis. The

slope angles of surrounding slopes provide an insight to the range of the mobilized friction angle because these slopes have remained stable. For example, if the surrounding slopes have a slope angle of 20° to 25°, it can be inferred that the weakest layer in the slope must exhibit a friction angle in the range of 20° to 25°.

5.2.2 Material Properties

The site stratigraphy, i.e. material types and thicknesses, can be obtained from borings and/or insitu tests. Large diameter borings, e.g., 0.6 to 1.0 meter in diameter, can be used to obtain more representative soil samples than conventional borings, better determine soil stratigraphy, estimate of bedding strike and dip, and locate the failure surface by lowering professionals in the borings.

The unit weight (γ) of the various layers can be measured in the laboratory using samples obtained from borings. Unit weights for each type of material should be measured or carefully estimated because this parameter affects the driving and resisting forces imposed on the problematic layer which influences the magnitude of back-calculated strength. For example, overestimating the unit weight of the overlying materials will result in an over estimate (unconservative value) of back-calculated shear strength by overestimating the driving and resisting forces.

5.2.3 Applicable Shear Strength

Another important point in a back-analysis is a conservative design assumption can result in an unconservative back-calculated strength. For example, the shear strength of the other materials is important because underestimating the shear strength parameters of the other materials is conservative for design but will result in a higher back-calculated shear strength which may over predict the mobilized shear strength.

The shear strength is defined as the maximum value of shear stress that the soil can withstand. The time and conditions under which water is able to flow into or out of a soil mass determines whether a drained or undrained analysis should be performed (Duncan and Wright, 2005). Drained strength is the applicable soil strength when the soil is loaded slowly enough so excess pore pressures, i.e. pore pressures that exceed the hydrostatic value, are not induced by

the applied loads. In the field, drained conditions result when loads are applied slowly to a mass of soil, or where they persist for a long enough time that the soil can drain the excess porewater pressure (Duncan and Wright, 2005). One point of confusion in practice is that raising of the groundwater surface by rainfall does not correspond to an undrained condition. This raising of the groundwater surface by rainfall results in a greater hydrostatic pressure but not an undrained condition. Therefore, the back-analysis of such case histories which involve changes in groundwater surface due to rainfall or climatic conditions should utilize a drained analysis.

Drained or undrained shear strength may be applicable for the materials that intersect the failure surface depending on the hydraulic conductivity of the materials and rate of loading involved (Stark et al. 2005a). Because landslides are a common phenomena in cohesive soils subjected to rainfall, drained strength analyses are discussed in detail. The two drained strengths considered are the residual and fully softened shear strengths which are discussed below.

5.2.3.1 Drained Residual Shear Strength

The drained residual shear strength of cohesive soils is applicable to new and existing slopes that contain a preexisting shear surface (Stark et al. 2005a). Therefore a preexisting shear surface, and a residual shear strength condition is present in old landslides, bedding shears in folded strata, in shear joints or faults, and after an embankment failure (Skempton 1985). Shear stresses and displacements induced in a slope by blasting also can result in mobilization of strength at or near the residual shear strength (Stark et al. 2000). Petley (1995) concludes that the mobilized residual shear strength can be obtained by appropriate back-analysis of case histories provided that reliable data on the geometry of the moving mass and the relevant porewater pressures are know. Excess pore pressures usually are not generated along a preexisting shear surface and thus a drained stability analysis should be used. Excess porewater pressures usually do not develop along a preexisting shear surface because the clay particles have already been oriented parallel to the direction of shear so little, if any, volume change occurs during reactivation. Therefore, a drained or an effective stress stability analysis is usually applicable for a residual strength condition. The results of torsional ring shear tests on 66 naturally occurring clays, mudstones, claystones and shale samples were used to develop an empirical correlation for drained residual friction angle (Stark et al. 2005a) which have been extended during the present study by adding the ring shear test results of 5 more soils and adding data and trend lines for σ'_n

= 50 kPa. The shear data and empirical correlation (Figure 6.24) show the residual friction angle is stress dependent which is in agreement with conclusions of Chandler (1977), Bromhead (1978) and Stark and Eid (1994 and 1997). Stark et al. (2005a) recommend using c' is zero in a back-analysis because it provides agreement with laboratory measured residual shear strength and the residual strength is defined. Tiwari et al. (2005) also confirm that the back-calculated residual friction angle with $c' = 0$, agreed well with the experimental results.

Although various researchers since Skempton (1964) conclude that back-calculated shear strength of reactivated landslides is in agreement with the drained residual shear strength of the slip surface material, most of the researchers use a linear relationship between the shear strength and effective normal stress, i.e., a residual friction angle. Petley (1995) concludes from the study of two case histories that the measured shear strength along the preexisting shear surfaces is in agreement with results obtained form back-analysis. Stark and Eid (1994) use two case histories of reactivated landslides, i.e., Portuguese Bend landslide near Los Angeles, CA and Gardiner Dam slide on the South Saskatchewan River in western Canada, to conclude that the back-calculated shear strength of reactivated landslide is in agreement with the drained residual shear strength obtained from torsional ring shear testing using stress dependent strength failure envelope. Stark et al. (2005b) and Stark et al. (2010) also use stress dependent strength failure envelope for drained residual shear strength to investigate two case histories of West Virginia and Ohio. Mesri and Shahien (2003) extend the Stark and Eid (1994 and 1997) study and use 43 reactivated landslides to support the recommendation of using a stress dependent strength failure envelope for drained residual shear strength in the back-analyses of reactivated landslides presented by Stark and Eid (1994).

Two case histories of reactivated/preexisting landslides were also back-analyzed during the present study, i.e., Weirton landslide in West Virginia, and Alver`a landslide in Italy (discussed in Chapter 4) to establish that the drained residual shear strength is relevant for remedial design. Back-analyses of all two case histories suggest that the shear strength available for the remedial design equals the residual value measured from laboratory ring shear tests. Although some evidences of strength recovery/healing along preexisting shear surfaces have been reported, Stark and Husain (2010a) conclude that the drained residual strength is still relevant to the preexisting landslides and the recovered/healed strength may be useful in

explaining the behavior of shallow landslides, such as explaining the slope creep behavior or slope stability prior to reactivation and it may not be considered in the remedial designs.

Thus, the drained residual shear strength should be considered for the back-analysis of reactivated landslides as suggested by Skempton (1964 and 1985) but a stress dependent strength failure envelope developed from the ring shear testing or new empirical correlation shown in Figure 6.24 should be used in the back-analysis instead of using a linear relationship, i.e., a single value of friction angle.

5.2.3.2 Fully Softened Strength

The drained fully softened shear strength of cohesive soils is also an important parameter in evaluating the stability of slopes that have not undergone previous sliding. In case of a first-time slide, the fully softened strength governs the failure not the residual strength (Skempton, 1970). However, Stark and Eid (1997) show that the strength mobilized in first-time slides can be less than the fully softened strength if a part of shear surface contains some slickensides or preexisting shear surface. Mesri and Shahein (2003) extended the Stark and Eid (1997) study and show that slopes in nonhomogeneous stiff clays and clay shales can exhibit a residual strength along at least a portion of the slip surface of first-time slide due to progressive failure. A fully softened condition corresponds to the condition after which the overconsolidated clay has absorbed as much water as it can and has reached equilibrium at a particular site. The results of torsional ring shear test on 39 naturally occurring clays, mudstones, claystones, and shale samples were used to develop a fully softened strength empirical correlation by extending the work of Stark et al., (2005a) and it shows that the drained fully softened failure envelope is also stress dependent (Figure 6.36). Stark et al., (2005a) present the difference between secant fully softened and residual friction angles as function of liquid limit (Figure 5.1) which can also be used to estimate the shear strength parameters and illustrating the importance of determining whether a preexisting shear surface is present or not. Stark et al. (2005a) recommend that c' equals zero be used for back-analysis of first-time landslides unless a first-slide occurred in overconsolidated material so c' can be greater than zero.

Skempton (1964) back-calculated the average strength parameters of $c' = 6.7$ kPa (140 psf) and $\phi_r' = 18°$ for the problematic portion of both the Brown and Blue London clays using a

factor of safety of unity, a circular slip surface, and Bishop's (1954) stability method (Figure 5.2) for the Northolt landslide.

Duncan and Stark (1992) back-analyzed the same landslide using a noncircular slip surface obtained by joining known points along the failure surface (Slip Surface 'E' in Figure 5.3) and using Spencer's (1967) stability method which resulted in a back-calculated linear shear strength parameters of c' = 0.72 kPa (15 psf) and ϕ'= 25°.

Because the Northolt landslide involves a first-time slide the fully softened strength should have governed the failure instead of the residual strength (Skempton, 1970). Thus the back-calculated strength parameters in this case should be closer to the fully softened empirical correlation suggested by the present study than the residual correlation. Using new correlations given in Figures 6.24 and 6.36, for a liquid limit (LL) of 79%, plastic limit (PL) of 28% and clay size fraction (CF) of 55% for the London clay (Skempton, 1964), the drained fully softened and residual friction angles are ϕ_{fs}'=26° and $\phi_r' \approx$13.5° for an effective normal stress of 50 kPa (1044 psf). The residual shearing resistance for the London clay reported by Skempton (1964) is c' = 10.3 kPa (215 psf) and ϕ_r'=16° at an effective normal stress of 35.9 kPa (750 psf), which was measured using a reversal direct shear device on intact specimen obtained from the failure surface. The c' and ϕ' values for the London clay discussed above are shown in Table 5.1.

In the current back-analysis of Northolt landslide in London clay, a noncircular failure surface, 'E' as shown in Figure 5.3, and Spencer's (1967) stability method were used. The Northolt landslide was selected for back-analysis herein because it is a well documented case history and was used by Skempton (1964) using a linear relationship between shear and effective normal stresses. In the back-analysis presented herein, initially the value of c' was taken to be zero for the Brown London clay because it is weathered clay and has fissures and joints as reported by Skempton (1964). A value of c' = 0.72 kPa (10 psf) was assumed for the unweathered overconsolidated Blue London clay to perform the back-analysis. A friction angle of 24.4° for both the Brown and Blue London clays was initially assumed which is lower than the fully softened strength estimated from fully softened strength empirical correlation shown in Figure 6.36.

Stark and Eid (1994) recommend using a stress dependent shear strength envelope for stability and back-analyses. Thus, a stress dependent fully softened strength failure envelope was developed using new empirical correlation presented in Figure 6.36 for LL = 79% and CF = 55% of the London clay which is shown Figure 5.4. The stress dependent fully softened strength failure envelope shown in Figure 5.4 was used to perform the back-analysis of the Northolt landslide as suggested by Stark et al. (2005a).

Back-calculated shear strength parameters for the Northolt landslide using the linear fully softened strength failure envelope from Skempton (1964), Duncan and Stark (1992), and $c' = 0$ and $\phi'=24.4°$ from the present study which yielded FS = 1.0 are shown in Table 5.1. The stress dependent fully softened strength failure envelope shown in Figure 5.4 and developed herein also yielded FS = 1.0.

Thus, the drained fully softened shear strength should be considered for the back-analysis of first-time landslides as suggested by Skempton (1970 and 1985) but a stress dependent strength failure envelope developed from the ring shear testing or the empirical correlation presented in Figure 6.36 should be used in the back-analysis instead of using a linear envelope because the field fully softened strength is stress dependent.

5.2.4 Phreatic Surface and Pore Pressures

Determination of the phreatic surface at the time of the landslide is important because the porewater pressures affect the effective stress acting on the failure plane. The effective stress in turn affects the back-calculated shear strength of the problematic layer. Increases in porewater pressure result in decreases in effective stress and thus a higher back-calculated strength is required to achieve a factor of safety of unity. The back-calculated shear strength is influenced by the porewater pressure or effective stress measured/assumed at the time of the landslide. Reliable values of effective stress cohesion (c') and/or friction angle (ϕ') can be determined through back-analysis if the phreatic surface or shear induced porewater pressure reflects the conditions at the time of failure (Saito, 1980). Leroueil and Tevenas (1981) show that in one case assuming the phreatic surface 0.91 meter (3 feet) higher than it actually had been at the time of the landslide resulted in almost a 50% increase in the c' value back-calculated for a 7.6 m (25 feet) high slope failure. Sauer (1984) performed a back-analysis of a landslide in clay shale in the

North Saskatchewan River Valley of Canada to show the effect of varying the groundwater surface on the back-calculated shear strength of the soil. Sauer (1984) shows that by varying the groundwater surface conditions to the two extreme positions, e.g., considering water surface at the ground surface and at the observed failure surface, the maximum range in ϕ' is 4.8 ° to 11.6 ° while using c' equal to zero as shown in Figure 5.5. The effects of varying the groundwater surface become less as the cohesion increases because the cohesion is not influenced by the effective stress whereas the shear resistance derived from ϕ' is controlled by the effective stress.

During the present study, it was determined that a variation in phreatic surface by 1.52 m (5 ft) results in an 8-10% change in factor of safety (FS) for Weirton landslide in West Virginia and Alver`a landslide in Italy. Thus, assuming a higher phreatic surface than occurred in the field will result in a higher back-calculated shear strength parameters for FS = 1.0. Duncan and Stark (1992) also establish that assuming the porewater pressures higher than at failure is unconservative because it results in back-calculated strengths that are too high. This is contrary to design analyses where a higher level of porewater pressure or phreatic surface is usually conservative. The magnitude of porewater pressure is site- and time-specific and thus it is difficult to determine porewater conditions at the time of failure for use in the back-analysis if piezometers are not installed at the time of the slide.

In summary, the porewater pressure should be measured when possible rather than making assumptions regarding porewater pressure or phreatic surface conditions. Piezometric measurements can be made shortly after the slide in or adjacent to the slide mass to provide an indication of the porewater pressure level at the time of sliding. Thus, it is important to install piezometers as soon as possible after a landslide.

If there is large uncertainty in the phreatic surface or porewater pressure condition, it may be easier and more reliable to back-calculate the phreatic surface rather than shear strength. This can be accomplished by measuring and/or estimating the shear strength of the problematic layer and back-calculating the phreatic surface that yields a FS = 1.0. This can be facilitated by using large diameter borings to inspect the slide mass and obtain representative samples of the shear surface material.

5.2.5 Effect of Rainfall and Pore Pressures in Back-Analysis

The hydrostatic water pressures are positive in a saturated soil and negative in an unsaturated soil. Positive hydrostatic pressures are governed by the location of groundwater surface and the magnitude and direction of any seepage. Negative porewater pressures are associated with pore suction and are governed primarily by grain size and degree of saturation (Fannin and Jaakola, 1999). Porewater pressures are important in stability analyses because they influence the effective stress acting on the failure plane which affects the back-calculated shear strength of the problematic layer.

Rainfall contributes to the triggering of landslides by infiltrating the slope cover, which causes a rise in the groundwater surface and an increase in the hydrostatic porewater pressures along the failure surface, and a decrease in the thickness of unsaturated soil. Rainfall is a common cause of landslides and in particular shallow landslides (Wieczorek, 1996). Rainfall has a large effect on shallow landslides because of the low effective stress acting on the failure surface. Thus, a small increase in the groundwater surface can result in a large percent reduction in effective stress which can result in a large strength reduction. Rainfall can also cause a decrease in shear strength due to increased moisture contents of the soils. Porewater pressure increases may be related directly to rainfall infiltration and percolation (saturation from above) or may be the result of the build-up of a perched water surface on a low permeable layer like a preexisting shear surface (Terllen, 1998).

Because clayey soils have a lower permeability, infiltration/percolation of precipitation takes time to change the porewater conditions for deep seated landslides. However, the secondary permeability of clay and shales in the form of fissures, cracks and also tension cracks can lead to rapid changes in porewater pressures at shallow depths with intense and heavy rainfall. Wieczorek (1996) establishes that the infiltration of rainfall causing soil saturation and a temporary rise in porewater pressures results in triggering shallow landslides.

Stark et al. (2005b) studied the effect of rainfall in triggering a deep-seated landslide along a highway cutslope in the San Francisco Bay area that resulted in distress to a single family residence. The movements observed in or near the two homes that occupied the site and at the cutslope toe indicated a deep-seated translational failure surface. It was determined that movement of the large slide mass usually occurred near the end of a heavy rainy season, because

time was required for the groundwater surface to rise in response to the increased rainfall. Review of the rainfall record revealed that at least 890 mm (35 inches) of rainfall had to occur to re-initiate movement. A drained shear strength is the applicable strength for this deep-seated slide because no load was applied to the slope and the rainfall did not induce excess porewater pressures. Thus, the change in existing hydrostatic porewater pressures can be incorporated in stability analyses by raising the groundwater surface which adjusts the effective stress along the failure surface. The reduced effective stress will result in a lower shear resistance and decreased stability. In summary, in rainfall triggered landslides a drained strength analysis should be used for the back-analysis with a good estimate of the groundwater surface.

Shallow landslides in soils and weathered rock are often generated in steep slopes during intense parts of a storm, i.e., a combined rainfall intensity and duration (Wieczorek, 1996). In the case of deep-seated landslides, movement usually occurs when a cumulative rainfall threshold is reached. Stark et al. (2005b) in their study of a highway cutslope determined that the movement observed in the residence occurred when the cumulative rainfall of 890 mm/year (35in/year) was exceeded. If the cumulative rainfall was less than 890 mm/year (35 in/year), no distress was observed in the residence. Rainfall thresholds for landslide initiation are regional, depending on local geologic, geomorphic, and climatologic conditions (Wieczorek, 1996). Therefore two separate thresholds for each area need to be established:

a) Intense rainfall thresholds resulting in shallow landslides triggering, and
b) Progressive/cumulative rainfall thresholds resulting in deep-seated landslides.

Because rainfall results in a decrease in effective stress and shear strength, the level of the groundwater surface at the time or just before the occurrence of landslide needs to be accurately assessed to back-calculate realistic shear strength parameters. It should be remembered that the effect of the groundwater surface in design is opposite than in a back-analysis. For example, assuming high hydrostatic porewater pressures in design is conservative but in a back-analysis it will yield higher back-calculated shear strength to achieve a FS of unity. Thus, a correct estimate of hydrostatic porewater pressures at the time of occurrence of landslide is required for a meaningful back-analysis.

5.2.6 Locating the Actual Failure Surface for Back-Analysis

Determining the location of the failure surface along which failure occurred is important for defining the size of the slide mass, causation, and back-calculation of the mobilized shear strength parameters in the problematic layer. Slope inclinometers are important in determining the actual failure surface location however they are frequently installed after the slide. The location of the actual failure surface has a large influence on the back-calculated strength parameters because the size of the slide mass and thus the required resisting force is a function of the failure surface location. In practice, a search is frequently conducted to locate the actual failure surface in a back-analysis of a landslide using slope stability software. Searching for the critical failure surface is appropriate for slope design and not for a back-analysis. A back-analysis should only utilize the failure surface along which failure occurred in the field because the shear strength parameters mobilized along that surface are the parameters being sought as the failure surface changes, the shear strength parameters required for equilibrium change. The only objective of a back-analysis is to estimate the shear strength parameters mobilized along the failure surface involved in slide. It may be possible to locate a failure surface during the search process that yields higher back-calculated strength parameters than the observed surface, i.e. it is less stable but because failure did not occur along this surface the analysis is incorrect. Using the higher back-calculated strength parameters would also lead to unconservative remedial measures resulting in an uneconomical design.

Most slope stability software has an option to define a specified circular or non-circular slip surface for computing a factor of safety. Thus, the actual failure surface can be specified and a back-analysis performed using that surface. The shear strength parameters are varied until a factor of safety of unity is achieved. During the process a search for the critical failure surface should not be performed.

If inclinometer data is available, this data along with surface observations can be used to make a best estimate of the actual failure surface. Installing inclinometers quickly after a landslide frequently provides useful information on the location of the actual failure surface as the slide mass is moved to its final geometry. Otherwise the best procedure for locating the actual failure surface involves field observation of the scarp and toe of the slide and a subsurface exploration to identify the weak materials in the slope. Morgenstern and Tchalenko (1967) show

that a shear zone can be several millimeters thick and the structure induced by the shear movement depending upon the composition of the material, its consistency and the magnitude of the displacement involved, can be used to identify the shear surface. Hutchinson (1983) suggests that a slip surface is often "paper-thin," many shear zones are only centimeters in thickness, and there may exist multiple slip surfaces in a cross-section. Therefore, the slip surface should be located using a variety of methods. Hutchinson (1983) explains various methods for locating the failure surface in moving and stationary landslides. Some of the important surface and subsurface exploration methods suggested by Hutchinson (1983) are; inference from earlier ground surface movements, direct observation of slip surface in excavations and large diameter boreholes, porewater pressures record, contrast in material properties above and below the slip surface, and inclinometer data. Thus, some uncertainties are involved in locating the actual failure surface because of the exploration technique employed and personal judgment of the observers in locating the failure surface. This section uses three case histories to illustrate some techniques for locating the actual failure surface.

1) In the back-analysis of the Northolt landslide in London Clay, inclinometer data was reported by Skempton (1964). Connecting the shear surface identified in each inclinometer resulted in a reasonable estimate of the actual failure surface (see Figure 5.2). In the back-analysis, a circular slip surface which passes through or close to the inclinometer data was used by Skempton (1964) to model the actual failure surface. Skempton (1964) may have used a circular slip surface because no standard method for a noncircular slip surface was available at that time. Duncan and Stark (1992) in a back-analysis of the same case use a circular and the observed non-circular failure surface (see Figure 5.3) and show that the back-calculated factor of safety for the circular failure surface is slightly greater (FS=1.02) than that back-calculated for the observed failure surface (FS=1.0). Thus, available inclinometer data can be used to establish a circular or noncircular slip surface and the best representation of the field slip surface should be used for the back-analysis.

2) Stark et al. (2005b) use a back-analysis of a 70 m deep-seated landslide along a highway cutslope in the San Francisco Bay area to show that available

information/data is appropriate and yields the best estimate of the actual failure surface. More importantly all of the information/data, e.g. inclinometer data and observed toe of the slide, should be used to estimate the actual failure surface and not be discarded. Figure 5.6 presents an aerial view of the cutslope and Figure 5.7 presents a cross-section for this cutslope. In this case all of the available information/data was used to develop the deep-seated failure surface shown in Figure 5.7. The opposing expert in the case omitted the slope inclinometer installed by the State Highway Department that showed a failure surface at a depth of 10 m (30 ft.). This resulted in the expert using a shallow failure surface on the cutslope for the back-analysis and developing a rainfall induced failure mechanism instead of a toe excavation mechanism that implicate the Highway Department. In addition to omitting the inclinometer data, the fact that the inclinometer was "sheared off" at a depth of 10 m (30 ft.) at the slope toe was not considered. As a result, the opposing expert concluded that the periodic heave of the highway pavement was caused by expansive soils, differential settlement due to a transition from natural to fill material, and/or poor pavement construction instead of the toe of a deep-seated landslide. This might be a reasonable hypothesis if the inclinometer at the cutslope toe had not been sheared off at a depth of 10 m (30 ft.). Because the inclinometer was sheared off, the failure surface must pass through the inclinometer and terminate in the highway where the pavement heave was observed as shown in Figure 5.7. Figure 5.7 shows that a deep bedrock failure surface can incorporate/explain the heave of the highway pavement, the sheared inclinometer, the distress of the residence, the failure surface found in large diameter borings, BA-2, near the residence, and the sheared inclinometer installed adjacent to the residence. A shallow failure surface along the cutslope does not explain all of the observed movement and should not be used for the back-analysis.

3) In the third case, the use of slope inclinometers and interpretation of the subsurface data was confirmed using the numerical model FLAC Stark et al. (2010). Between 1988 and 1989, a housing development with about 50 units was completed on an undeveloped hillside near Novato, California and is referred

herein as the Knolls. An 11 unit housing development was constructed upslope of the Knolls and is referred herein as the Vista. Only 7 of the 11 Vista lots were developed at the time of the 1996 landslide.

Figure 5.8 presents an aerial view of these housing developments, the subsequent upslope development referred to as the BC Development, and an outline of the slide mass. Only a portion of the housing units in the Knolls and Vista development are shown in Figure 5.8. A landscape screen fill with a height of at least 22 m above the adjacent natural terrain and a length and width of about 165 and 80 m, respectively, was constructed just downslope of the BC Development (see Figure 5.8). The volume of the landscape screen when fill placement ceased was approximately 76,600 cubic meters of soil created from the BC Development.

Various geotechnical engineers employed for the BC Development drilled almost 80 borings across the site and none of the borings exceed a depth of about 15 m within the slide limits shown in Figure 5.8. The slope inclinometers installed in the Visa development after homeowner complaints of damage show the depth of sliding to be 40 to 45 m. Thus, none of the initial borings drilled within the slide limits were deep enough to uncover the problematic serpentinite. As a result, the designers probably were not aware of the weak layer underlying the site although the serpentinite is outcropping at numerous locations across the project site. Nine of the fifteen slope inclinometers installed after the initial report of distress provided useful information on location of the failure surface but the other six are either too shallow or outside the slide limits shown in Figure 5.8 and do not provide direct information on the location of the actual failure surface. Each of the nine useful inclinometers show only one slide plane at depths ranging from 5 m near the landslide toe to 40 m near the middle of the slide mass. The failure surface in Figure 5.9 (see dashed line) was developed by connecting the location of shear movement in the inclinometers, following the various material types, and passing the failure surface through the cracks observed at the top of the landslide and the housing distress observed at the landslide toe. Slope stability software was

used to search for the critical failure surface between point of known location, e.g., inclinometer location.

The installation of inclinometers to a depth below the failure surface is important to locate the failure surface, however, inclinometers installed at shallower depths should also be considered because the actual failure surface must be below these inclinometers. The presence of nine useful inclinometers and surface observation of movement did not clearly define the entire failure surface. Figure 5.9 shows a large gap in inclinometers from under the fill to under the sandstone or a horizontal distance of about 130 m to about 370 m. Limit equilibrium analyses were then used to search for the failure surface in only this range of horizontal distance to locate the depth in the serpentinite that yielded the lowest factor of safety. This failure surface (see Figure 5.9) resulted in the lowest factor of safety and the best combination of the observed movement and inclinometer data. To clarify the location of the failure surface in the serpentinite in this area, the numerical model FLAC was used to confirm the location of high shear stresses within serpentinite to verify locate the actual failure surface.

In summary, a common problem observed in practice is searching for the critical failure surface during a back-analysis instead of forcing the failure surface to pass through the sheared inclinometers and the observed surface features. It is proper to conduct a search for the failure surface that yields the lowest back-calculated friction angle between the inclinometers and the observed surface and subsurface features. This can be accomplished by fixing the failure surface in the slope stability software at the location of the inclinometers and the observed features and allowing the software to search the critical failure surface between these fixed points. The resulting slip surface can be verified using numerical methods, e.g., FLAC.

5.2.7 Tension Crack in the Back-Analysis

Landslides usually involve cohesive materials and the failure is usually preceded by formation of a tension crack at the top of the slope which usually delineates the extent of the

initial slide mass. Usually the opening of the tension crack(s) is followed by sliding along a well-defined failure surface unless the slope is quickly stabilized (Terzaghi et al., 1996).

Once the tension crack is formed, all strength along the failures surface through the crack is lost (Duncan and Wright, 2005). If a tension crack develops, shear resistance is only developed along the length of slip surface below the tension crack depth at the time of sliding. Thus including the depth of the tension crack in the failure surface is likely to result in an underestimate of the back-calculated shear strength of the problematic soil. Duncan and Wright (2005) suggest introducing a tension crack into slope stability analysis by terminating the failure surface at the bottom of a vertical slice at an appropriate depth below ground surface as shown in Figure 5.10. To account for the tension cracks in the back-analysis, the depth of the tension crack (d_{crack}) at the time of failure must be known. The depth of a tension crack can be estimated by measuring the vertical or near vertical part of slip surface at the top of the slope or it can be estimated using shear strength parameters, *c* and ϕ, in following equation presented by Duncan and Wright (2005):

$$d_{crack} = \frac{2c}{\gamma \tan(45 - \frac{\phi}{2})}$$

Because materials with a high cohesive strength are sensitive to the assumption of a tension crack in the back-analysis and this sensitivity increases when the tension crack is partially or completely filled with water (Deschamps and Yankey, 2006), a detailed parametric study was performed to determine the effect of a tension crack on the back-analysis of landslides.

5.2.7.1 Analysis of Northolt Landslide in London Clay

In an attempt to determine the effect of a tension crack on the back-calculated effective stress friction angle, ϕ'_{back} herein, the Northolt Landslide (Skempton, 1964) was used because the failure surface at the top of the slope is almost vertical for a considerable depth, 1.45 meters, as shown in Figure 5.2. Skempton (1964) uses Bishop's (1954) stability method for circular slip surface as shown in Figure 5.2.

For the Northolt landslide, the tension crack depth of 1.45 meters with a fully specified failure surface as represented by slip surface 'E' in Duncan and Stark (1992) shown in Figure 5.3

was selected to investigate the impact of a tension crack on the back-calculated strength. Three slope stability software packages XSTABL, UTEXAS3, and SLOPE/W and Spencer's (1967) stability method as coded in each software package was used to investigate the impact of a tension crack. The results of the study are presented in Tables 5.2 and 5.3.

The strength parameters used for both Brown and Blue London clays present in the Northolt slide are also shown in Tables 5.2 and 5.3. Skempton (1964) reports a water content (w_0) of 30% for the London clay below the water surface involved in the slide. Saturated unit weight (γ_{sat}) of 19.9 kN/m^3 reported by Nishimura et al. (2007) is used for both Brown and Blue London clays below the water surface whereas a moist unit weight (γ_{moist}) of 17.6 kN/m^3 is used for the soil above the water surface. Because the Northolt landslide is a first-time slide, the fully softened strength will govern the strength of the London Clay (Skempton, 1970). As established earlier the back-calculated friction angle is in close agreement with the fully softened secant friction angle obtained from empirical correlation presented by the present study (see Figure 6.36).

Although all the three slope stability packages have an option for computing the factor of safety while incorporating a tension crack with a fully specified slip surface, the calculated factors of safety are not in agreement. The effect of the type of material, the ratio of depth of tension crack in relation to the length of the failure surface, and the accuracy of the three stability packages are discussed in subsequent sections.

5.2.7.2 Effect of Type of Material

The effect of a tension crack is a function of the effective stress cohesion (c') of the material in which the tension crack has developed as a result two categories of materials are used in the back-analysis: (1) purely frictional ($c' = 0$) and (2) cohesive material ($c' > 0$). A summary of the results of the parametric analysis is presented below:

5.2.7.2.1 Purely Frictional Material (c' = 0)

If the soil at the top of the slope, i.e., the soil in the tension crack zone, is non cohesive, all three stability packages yield similar factors of safety with or without a tension crack depth (d_{crack}) of 1.45 m (Table 5.2). Therefore, in the back-analysis of a reactivated landslide where the tension crack is thought to have developed in cohesionless soil, e.g., desiccated and weathered

clays, sand and gravel, the tension crack has no effect on the back-calculated shear strength parameter ϕ' when using these three slope stability packages and thus can be neglected because the strength is controlled by the effective normal stress along the depth of the tension crack. The low effective normal stress (σ'_n) and short length of the crack results in similar factors of safety because the shear strength is calculated by $\sigma'_n.\tan \phi'$.

5.2.7.2.2 Cohesive Material (c' > 0)

If an effective stress cohesion greater than zero, i.e., $c' > 0$, is used to represent the tension crack and assuming the soil strength parameters shown in Table 5.3, the presence of a tension crack impact the results. A maximum value of the effective cohesion, $c' = 2.4$ kPa, is considered practical for unweathered overconsolidated London Clay (Duncan and Stark, 1992). The factor of safety calculated with a tension crack is lower than the value calculated without a tension crack because there is a shorter length of the failure surface that is assigned a shear resistance. But the difference is so small that it does not significantly affect the back-calculated shear strength. Based on the results of this analysis it can be concluded that when the soil in the tension crack zone exhibits a small value of cohesion (less than 2.4 kPa), a tension crack may be neglected in the back-analysis of landslides.

5.2.7.3 Effect of Tension Crack Depth to the Length of Failure Surface Ratio (d_{crack}/L)

To study the effect of varying depths of tension crack (d_{crack}), as compared to the entire length of the failure surface (L), the Northolt landslide in the London clay is also used (Figure 5.2). Analyses are conducted by varying the depth of tension crack and making adjustments in the upper portion of the failure surface. Table 5.2 shows the results for five different depths of the tension crack using XSTABL. Based on Duncan and Stark (1992), the values of effective stress cohesion for the Brown and Blue London clays are taken as zero and 0.48 kPa, respectively, whereas, the friction angle of 24° is considered for both of the clays. Results show that even when the tension crack depth is up to almost 15% of the length of the failure surface, the effect of incorporation of the tension crack in the back-analysis is negligible. Therefore, in the back-analysis of the landslides while conducting a drained analysis and using Spencer's (1967) stability method, the tension crack can be neglected up to a d_{crack}/L ratio of 1/6.

5.2.7.4 Comparison of Stability Packages with Tension Cracks

During present study, the factors of safety yielded by the three stability software packages are not in agreement. Therefore, the main objective of this section is to determine the accuracy of these packages when a tension crack is used. The results of the study are summarized below:

5.2.7.4.1 **UTEXAS3**

UTEXAS3 can incorporate a tension crack with a fully specified circular or noncircular failure surface. The capabilities and limitations of UTEXAS are summarized by Pockoski and Duncan (2000). The input commands required to include a tension crack are complex and the user may have to execute the program several times to debug the input parameters. UTEXAS3 yields similar factors of safety with or without a tension crack when the soil in the tension crack zone has no effective stress cohesion ($c' = 0$). However, when a small value of effective stress cohesion is used for the soil in the tension crack zone, the effect of tension crack starts appearing in the results (Table 5.3) but the difference is insignificant. For example, soil in the tension crack zone with c'=0.48 kPa, UTEXAS3 yields a lower factor of safety for a tension crack than the case with no tension crack. UTEXAS3 yielded lower factors of safety in all of the cases as compared to the other two stability packages i.e. XSTABL and SLOPE/W, and the difference is up to about 6% (see Tables 5.2 and 5.3) which is in agreement with the finding of Duncan (1996).

5.2.7.4.2 **XSTABL**

XSTABL can also incorporate a tension crack with a fully specified circular or noncircular failure surface. Although XSTABL has a provision to input the maximum crack depth and water depth in the crack and the user's manual explains the corresponding theory, it does not adequately describe the procedure to input the failure surface in combination with a tension crack. During the present study it was determined that if a tension crack is used in combination with a fully specified failure surface that terminates at the bottom of the tension crack; XSTABL calculates a factor of safety by adjusting failure surface near to bottom of the tension crack. Thus, a parametric study was conducted to determine the proper means for describing the failure surface in combination with a tension crack. The analyses are performed

with a tension crack while terminating the failure surface at the following four different locations to determine the effect on the factor of safety:

- ***Case I***: Terminating the failure surface at the bottom of the tension crack and considering the weight of soil above the end of the failure surface as a surcharge.
- ***Case II***: Terminating the failure surface at the bottom of the tension crack and incorporating the tension crack depth in the input data.
- ***Case III***: Extending the failure surface vertically along the tension crack to the ground surface.
- ***Case IV***: Extending the failure surface up to a point selected slightly behind the location of the tension crack at the ground surface and incorporating the tension crack depth in the input data.

Case I: The Northolt landslide was modeled using the weight of soil above the bottom of the tension crack as surcharge as proposed by Pockoski and Duncan (2000) and the results are used for comparison with the other three cases (Table 5.5).

Case II: Even though the fully specified failure surface terminates exactly at the bottom of the tension crack, XSTABL still searches for the failure surface in the tension crack area above the point of termination of the failure surface. This search may be caused by termination of the failure surface within the soil and not at the ground surface. In addition, XSTABL may not be able to join the point of termination of the failure surface with the bottom of the tension crack so it searches for a failure surface in the area above the point of termination of the failure surface. In the process, XSTABL for some reason makes adjustments in the specified failure surface close to the point of termination at the bottom of the tension crack that results in the failure surface not connecting to the bottom of the tension crack. For example, the specified failure surface connects with the ground surface in front of the tension crack. Therefore, the factor of safety reported in this case is different from the value reported for Case I. Because XSTABL automatically searches for the failure surface from the bottom of specified crack depth even with a fully specified failure surface, the factor of safety reported is not representative of the failure surface terminating at the bottom of the tension crack.

Case III: This analysis shows that the effective stresses and thrust line in the vertical portion of the failure surface in the vicinity of the tension crack are somewhat unusual i.e., shows negative effective stress and the thrust line extends beyond the soil mass. Negative effective stresses are usually encountered for cases that involve high pore water pressures, a combination of thin slices with a low self-weight, a high "*c*'-value", and steep slice-base angles (Sharma, 1995). The limit equilibrium method can sometimes lead to numerical difficulties that are manifested by negative normal effective stresses calculated along the failure surface. Therefore, when the top soil in the slope is a purely frictional material, i.e., *c*'=0, the factors of safety calculated are similar to Cases I and IV. Whereas, when the top soil exhibits a little cohesion, the factor of safety differs from the values in Cases I and IV. Although XSTABL is designed to neglect the effect of negative effective stresses for a slice within the last 5% of the slices near the slope crest, it still affects the results (see Table 5.5). If the effective stresses are negative, the shear strength contribution is neglected by XSTABL for these slices (Sharma, 1995). Thus, the vertical portion of the failure surface should not be made part of the failure surface when using XSTABL; instead a tension crack in combination with a fully specified failure surface extended up to a point selected behind top scarp on the ground surface should be used because it yields a better estimate of factor of safety.

Case IV: The results obtained for Case IV are similar to Case I for purely frictional material (*c*'=0) and cohesive material (*c*' >0). The results of the analysis performed in this case show that the failure surface was terminated at the bottom of the tension crack by XSTABL and also the tension crack was properly incorporated in the analysis. This study also shows that extending the failure surface to any reasonable point behind the location of the tension crack up to the ground surface yields similar results (see Table 5.5). Thus, a point behind the tension crack on the ground surface can be selected for a fully specified failure surface and the failure surface is extended up to this point and yields a good estimate of the factor of safety. A tension crack is used as an input to the desired depth and extending the failure surface to the ground surface to a point selected behind the top scarp. Such a failure surface in combination with inputting the tension crack depth yields an accurate value of factor of safety.

5.2.7.4.3 **SLOPE/W**

SLOPE/W is a popular slope stability package with practitioners and can incorporate a tension crack. A fully specified failure surface with and without a tension crack was analyzed and the results are shown in Tables 5.2 and 5.3. The analyses performed using SLOPE/W yield similar results with and without a tension crack for both the top soil being a purely frictional material and a cohesive material. The results of SLOPE/W are close to the results of XSTABL using the Case IV failure surface. But the factors of safety obtained using SLOPE/W, are almost 6% higher than the values of factors of safety obtained from UTEXAS3.

In summary, a tension crack is an important assumption in the back-analysis of a landslide which needs careful consideration. Based on the parametric study conducted herein it is determined that a tension crack that has a depth less than 15% of the length of the failure surface in the back-analysis can be neglected when using Spencer's (1967) stability method and UTEXAS3, XSTABL, or SLOPE/W. Procedures described in the slope stability packages e.g., UTEXAS3 and SLOPE/W, for modeling a tension crack in the analysis are elaborate and must be followed carefully. XSTABL Reference Manual does not provide a detailed description on modeling a tension crack with a specified failure surface. To model the tension crack in the XSTABL, the specified failure surface should not terminate at the bottom of the tension crack but should extend to the ground surface to a point behind the tension crack and a tension crack should also be included in the analysis.

5.3 Methods of Stability Analysis and Stability Software Package

There are three main types of slope stability methods, i.e., limit equilibrium, finite element, and finite difference methods, which are being used in practice. These slope stability methods are coded in different commercially available software which are being used in research and practice. Although each method has its own advantages and limitations all can yield reliable results. A brief discussion of the three methods is presented below:

5.3.1 Limit Equilibrium Method

Limit equilibrium methods involving vertical slices are the most commonly used method for slope stability analyses because of simplicity, ease of use and long history. Limit equilibrium

methods are based on static equilibrium. These methods satisfy some or all of the conditions of equilibrium such as moment and/or horizontal and vertical force equilibrium. Some of the well know and widely used stability methods are: Fellenius (1936), Taylor (1937), and Bishop (1955), Lowe and Karafiath (1960), Morgenstern-Price (1965), Spencer (1967), Janbu (1968), US Army Corps of Engineers (1970) etc. Fredlund and Krahn (1977) and Furuya (2004) present a detailed comparison between different limit equilibrium methods. Duncan (1996) concludes that the factors of safety (FS) obtained from stability analysis methods that satisfy all limit equilibrium conditions are within $\pm$6% of each other. Slope stability software using limit equilibrium methods include CLARA/W, SLIDE, SLOPE/W, UTEXAS3/UTEXAS4, XSTABL, WINSTABL, etc. Oliphant and Horne (1992), Pockoski and Duncan (2000), and Alkasawneh et al. (2007) present a detailed description and comparison of some of the commercially available slope stability software that use the limit equilibrium method.

5.3.2 Finite Element Method

Finite element method (FEM) is used for finding approximate solutions of partial differential equations as well as integral equations. FEM is able to simulate physical behavior using computational tools without the need to simplify the problem. The most attractive feature of the FEM is its ability to handle complex geometries (and boundaries) with relative ease. The finite element method was introduced to geotechnical engineering profession by Clough and Woodward (1967) in which they used nonlinear stress-strain relationship in the analysis of an embankment dam. The principal difference between limit equilibrium and finite element (FE) methods is in the analysis approach to slope stability problems because limit equilibrium methods are based on various equilibrium conditions whereas FEMs utilize a constitutive law to model soil behavior. Some of the FEM software being used for slope stability analyses are ABACUS, FLEADAM, GeoFEAP, PLAXIS, SIGMA/W, Z-SOIL, etc. Alkasawneh et al. (2007) present a comparison between limit equilibrium and FEM method and also between some of the commercially available slope stability software.

5.3.3 Finite Difference Method

Finite difference method (FDM) is an alternative way of solving the differential equations. FDM is an approximation of the differential equation whereas FEM is an

approximation of the solution. FDM in its basic form is restricted to rectangular shapes and simple alterations. The most attractive feature of the FDM is that it is easy to implement and can accommodate large displacements which are relevant to landsldies.

The finite difference software FLAC (Fast Lagrangian Analysis of Continua), developed by Itasca Consulting Group, is commonly used in geotechnical engineering. FLAC is a two-dimensional explicit finite difference program for engineering mechanics computation. FLAC simulates the behavior of structures built of soils, rock, or other materials that may undergo plastic flow when their yield limits are reached. Materials are represented by elements, or zones, which form a grid that is adjusted by the user. Each element behaves according to a prescribed linear or nonlinear stress/strain relationship in response to the applied forces or boundary restraints. The material can yield and flow and the grid can deform and move with the material that is represented. FLAC uses a shear strength reduction (SSR) technique for a stability analysis which reduces the shear strength of the soil until collapse to simulate a post-peak strength loss. The resulting factor of safety is the ratio of soil shear strength to the reduced shear strength at failure (Dawson et al., 1999). This shear strength reduction technique was developed by Zeinkiewics et al. (1975) and has been applied by various researchers.

The shear strength reduction technique has a number of advantages over the method of slices for slope stability analysis, such as the increase in movement with the corresponding decrease in shear strength. In addition, the critical failure surface is found automatically by locating and connecting the zones of highest shear stress (Dawson et al., 1999). Although FLAC has an option to incorporate an interface to simulate a failure surface, the observed failure surface cannot be modeled directly which is a limitation with the software. But FLAC can effectively locate the critical failure surface for a first-time landslide by showing the zones of highest shear stress and maximum strain rates. During the present study the Northolt landslide was analyzed using FLAC and the results are shown in Figure 5.12. The zone of maximum strain rate is shown in Figure 5.12 which represents the critical failure surface. This failure surface is in close agreement with the observed failure surface reported by Skempton (1964) and shown in Figure 5.2. Thus, FLAC may be used for performing a back-analysis of a first-time landslide because it predicts a failure surface that is in agreement with the field failure surface. However,

at present it may not be useful for the back-analysis of reactivated or preexisting landslides because FLAC has not been successful in modeling the field preexisting failure surface.

5.4 Back-Analysis Procedure for Landslides

Based on the uncertainties with back-analysis described previously, a comprehensive back-analysis procedure for landslides was developed during the present study. The back-analysis procedure includes:

1) Understanding the subsurface conditions (type of soils/materials, thickness and shear strength of various layers, ground water surface, surface water sources, external water sources, porewater pressures, slope geometry, tension cracks etc.).
2) Defining representative cross-sections that is located and oriented parallel to the direction of maximum movement. The cross-section should include all relevant materials and structures.
3) Defining the type and location of the failure surface based on ground surface observation, slope inclinometer data, and subsurface features.
4) Selecting the appropriate stability method and software for the back-analysis.
5) Varying the shear strength of the problematic/weak layer until the factor of safety equals approximately unity (FS≈1.0) to determine the back-calculated shear strength of the problematic layer.
6) Comparing the back-calculated shear strength parameter (ϕ') with the results of laboratory strength testing on representative samples to ensure agreement.
7) Comparing the back-calculated shear strength parameter (ϕ') with empirical correlations, such as shown in Figure 6.24 and 6.36, to ensure agreement. If the landslide is a first-time landslide, i.e., no slide occurred previously at the site, empirical correlations for the fully softened shear strength should be used to verify the back-calculated shear strength depending on the level of progressive failure that contributed to the landslide. In a first-time slide, the back-calculated shear strength is at or slightly below the measured or estimated fully softened strength. If the landslide is a reactivation of a prior slide, laboratory testing or an empirical correlation for the residual strength should be used to verify the back-

calculated strength. The back-calculated residual shear strength should be in agreement with the measured or estimated residual shear strength.

8) If the back-calculated shear strength is not in agreement with the appropriate empirical correlation and/or laboratory strength testing, there could be an error in the back-analysis. This should be investigated by checking the input parameters and the entire process should be repeated until the back-calculated shear strength is in agreement with the appropriate empirical correlation and/or laboratory strength testing.

9) Reconduct back-analysis with revised parameters and verify results are in agreement with empirical correlations and test results.

5.5 Summary and Discussion

The back-analysis of landslides involves many uncertainties. Therefore, experience and judgment should be used in selecting the input parameters and assumptions for the other materials involved in the back-analysis. The assumptions made in the back-analysis have different effects than those made in the design and even experienced engineers make incorrect assumptions for the back-analysis.

Slope geometry at the time of failure can be determined from prior topographic surveys/maps or aerial photographs, satellite images and by site observation after failure. Observations of surrounding slopes are also helpful in understanding the subsurface conditions at the time of failure.

In the absence of adequate subsurface information/data, large diameter borings can be used to obtain more representative samples than conventional borings, helpful in visual inspection of the soil stratigraphy, and beneficial in locating the failure surface by lowering down the experts in the borings. Type of material involved in the landslide can be determined from borings and/or insitu tests. Properties of each material present in the slide mass should be determined with as much accuracy as possible to minimize the uncertainty to the material properties.

Back-analysis can provide a better estimate of the shear strength parameters than the laboratory tests for remedial designs. Fully softened shear strength is mobilized in a first-time

landslide whereas residual shear strength is mobilized in a reactivated or preexisting landslide. Although the fully softened shear strength mobilized in a first-time landslide, the residual shear strength will be available for remedial designs because of the induced shear displacement. Therefore, the residual shear strength of slip surface material is important and should be determined in a laboratory ring shear testing. A conservative estimate of a soil shear strength parameter will yield an unconservative result in the back-analysis. Therefore, the best estimate of the shear strength parameters is necessary to economize the repair measures. The back-calculated shear strength parameters should be verified using laboratory test results and existing empirical correlations. If the back-calculated strength seems unreasonable then adjustments should be made to the back-analysis assumptions. Furthermore, a stress dependent strength envelope should be used in the back-analysis for both fully softened and residual shear strengths.

Available piezometer data can provide useful information about the porewater pressure conditions present at the time of failure that must be incorporated in the back-analysis. Varying the phreatic surface changes the FS, therefore, a good estimate of the groundwater/phreatic surface is required for a good estimate of shear strength parameters. Assuming the groundwater/ phreatic surface at the time of failure should be avoided because using a high groundwater/ phreatic surface will result in a higher back-calculated shear strength to achieve a FS of unity. If there is large uncertainty in the groundwater/phreatic surface or porewater condition, it may be more appropriate to back-calculate the phreatic surface rather than shear strength using measured shear strengths.

The effect of rainfall on the groundwater surface should be incorporated using available rainfall data of the area. This data can be used to establish using the rainfall thresholds required to activate slide movement. Intense rainfall can trigger shallow landslides while sustained rainfall is required to activate movement of a deep-seated landslide. Therefore, both intense and progressive/cumulative rainfall should be recorded for areas prone to landslides and used in the investigation. The effect of rainfall should be considered in the back-analysis to achieve a good estimate of back-calculated shear strength.

Instead of searching for the critical failure surface, the field failure surface should be used in the back-analysis. Inclinometers should be installed to a depth below the failure surface and available inclinometer data should be used to locate the failure surface. The failure surface can

also be located from excavations made after the failure and/or large diameter boreholes. The observed points of the failure surface should be fixed in the stability package and a search for the critical surface in between these points should be made. Therefore, selection of a suitable stability package which forces the slip surface to pass through fixed points and method of stability analysis for the back-analysis are important. The commercially available stability packages XSTABL, UTEXAS3, and SLOPE/W based on limit equilibrium methods yield reasonable back-analysis results. Finite difference computer software, e.g., FLAC, can be used to estimate the location of the critical failure surface from the zone of highest shear stress. The main limitation with FLAC for landslides is the actual/observed failure surface cannot be modeled in the software. Although FLAC has an option to input a weak interface, it cannot be incorporated along the observed failure surface. This can result in the zone of the highest shear stress and maximum strain rate may be at different location than the observed failure surface in a reactivated and preexisting landslide, especially in a deep-seated landslide. For a first-time landslide, FLAC has been able to locate a critical surface that is in close agreement with the observed failure surface. Thus, FLAC may be effectively used for performing a back-analysis of a first-time landslide but it is still being evaluated for the back-analysis of reactivated or preexisting landslides.

A landslide is usually preceded by opening of a tension crack near the upslope end of the slide mass. The soil shear strength along the tension crack is lost because of the open gap in the soil. If a tension crack develops, shear resistance is only developed along the length of slip surface below the tension crack depth at the time of sliding. Including the depth of the tension crack in the failure surface is likely to result in an underestimate of the back-calculated shear strength of the problematic layer. Therefore a tension crack is important in the back-analysis of landslides. The depth of tension crack can be estimated by measuring the vertical or near vertical part of slip surface at the top of the slope or can be measured by making excavation at the top of the slide mass. This depth is important because this depth is not assigned a shear strength along shear surface.

Back-analysis of the Northolt landslide showed that a tension crack with a depth up to 15% of the length of the failure surface can be neglected when using Spencer's (1967) method and any of the slope stability packages from UTEXAS3, XSTABL and/or Slope/W because there

is little impact on the back-calculated strength. However, additional analyses are required to generalize this finding to all landslide geometries. All three stability packages used herein, i.e., XSTABL, UTEXS3, and SLOPE/W, have provisions to specify a tension crack in the analysis and yield reasonable results if a tension crack is properly included in the analysis. For example, XSTABL requires extending the failure surface to the ground surface in combination with a tension crack, if a tension crack is to be accurately modeled in the back-analysis.

5.6 Tables and Figures

Table 5.1. *c*' and ϕ' values for the London clay, determined by various methods.

	c', kPa (psf)		ϕ'	τ_{bc}, kPa (psf)	Failure Surface	Method	FS
Back-analysis (Using Linear Strength Failure Envelope)							
Skempton, 1964	6.7 (140)		18°	*18.4 (383.7)	Circular	Bishop's 1955	1.0
Duncan and Stark, 1992	0.72 (15)		25°	*17.5 (364.7)	Non-circular	Spencer's 1967	1.02
Current Study	Brown clay	0	24.4°	*16.3 (340.0)	Non-circular	Spencer's 1967	1.0
	Blue clay	0.48 (10)	24.4°	*16.8 (350.5)			
New Correlation - Figure 6.36 (Stress Dependent Envelope)							
Fully softened strength	0		26°	24.4 (509.3)	LL = 79%, CF = 55% σ_n' = 50 kPa (1044psf)		
Residual strength	0		12.5°	11.1 (231.5)			
Measured strength from reversal direct shear test (Skempton, 1964)							
Residual strength	0		16°	10.3 (215)	σ_n' = 35.9 kPa (750 psf)		
Peak strength	15.3 (320)		20°	28.5 (595)	σ_n' = 35.9 kPa (750 psf)		

*Back-calculated shear strength, $\tau_{bc}' = c' + \sigma_n' \tan \phi'$ at effective normal stress (σ_n')=35.9 kPa (750 psf)

Table 5.2. Tension crack in back-analysis for purely frictional material (c'=0).

Trial #	d_{crack}	Brown London Clay		Blue London Clay		FS Spencer (1967) Method
		c'	Φ'	c'	Φ'	
	m	kPa	degree	kPa	degree	
UTEXAS3						
1	0	0	24	0.48	24	0.931
2	1.45	0	24	0.48	24	0.931
XSTABL						
1	0	0	24	0.48	24	0.983
2	1.45	0	24	0.48	24	0.983
SLOPE/W						
1	0	0	24	0.48	24	0.986
2	1.45	0	24	0.48	24	0.986

Table 5.3. Tension crack in back-analysis of cohesive material.

Trial #	**d_{crack}**	**Brown London Clay**		**Blue London Clay**		**FS Spencer (1967) Method**
		***c*'**	**ϕ'**	***c*'**	**ϕ'**	
	m	**kPa**	**degree**	**kPa**	**degree**	
UTEXAS3						
1	0	0.48	24	0.48	24	≈ 0.94
2	1.45	0.48	24	0.48	24	≈ 0.94
3	0	2.4	24	2.4	24	≈ 1.05
4	1.45	2.4	24	2.4	24	≈ 1.04
XSTABL						
1	0	0.48	24	0.48	24	≈ 0.99
2	1.45	0.48	24	0.48	24	≈ 0.99
3	0	2.4	24	2.4	24	≈ 1.10
4	1.45	2.4	24	2.4	24	≈ 1.10
SLOPE/W						
1	0	0.48	24	0.48	24	≈ 0.99
2	1.75	0.48	24	0.48	24	≈ 0.99
3	0	2.4	24	2.4	24	≈ 1.10
4	1.45	2.4	24	2.4	24	≈ 1.10

Table 5.4. Effect of tension crack depth on a back-analysis.

Trial #	Vertical Part of Failure Surface at top of failure surface, d_{crack} (m)	d_{crack} (m)	Length of Failure Surface, L (m)	d_{crack}/L	FS, Spencer (1967) Method
1	0.84	0	26.0	0	0.99
2		0.84	26.0	1/31	0.99
3	1.45	0	25.4	0	0.98
4		1.45	25.4	1/20	0.98
5	2.74	0	24.36	0	1.01
6		2.74	24.36	1/9	1.01
7	3.96	0	23.68	0	1.13
8		3.96	23.68	1/6	1.13
9	4.57	0	22.86	0	0.99
10		4.57	22.86	1/5	1.10

Table 5.5. Results of tension crack analyses performed using XSTABL.

Case #	Brown London Clay		Blue London Clay		FS Spencer Method (1967)
	c'	ϕ'	*c*'	ϕ'	
	kPa	degree	kPa	degree	
I	0	24	0.48	24	0.983
II	0	24	0.48	24	0.989
III	0	24	0.48	24	0.983
IV	0	24	0.48	24	0.983
I	0.48	24	0.48	24	0.991
II	0.48	24	0.48	24	0.996
III	0.48	24	0.48	24	0.990
IV	0.48	24	0.48	24	0.991

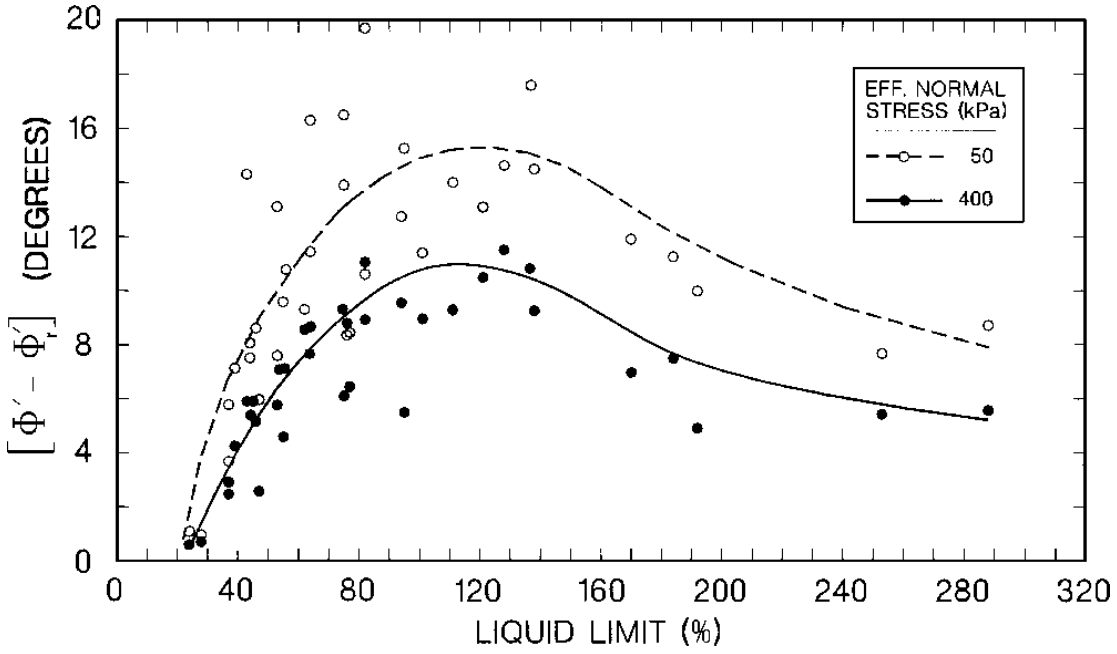

Figure 5.1. Difference between secant fully softened and residual friction angles as function of liquid limit (from Stark et al. 2005a)

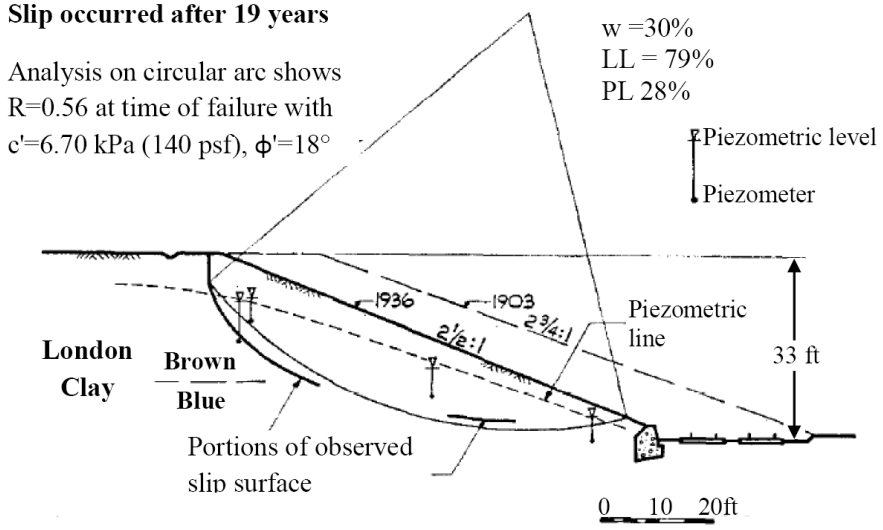

Figure 5.2. Northolt 1955 landslide in London clay with circular failure surface (from Skempton, 1964).

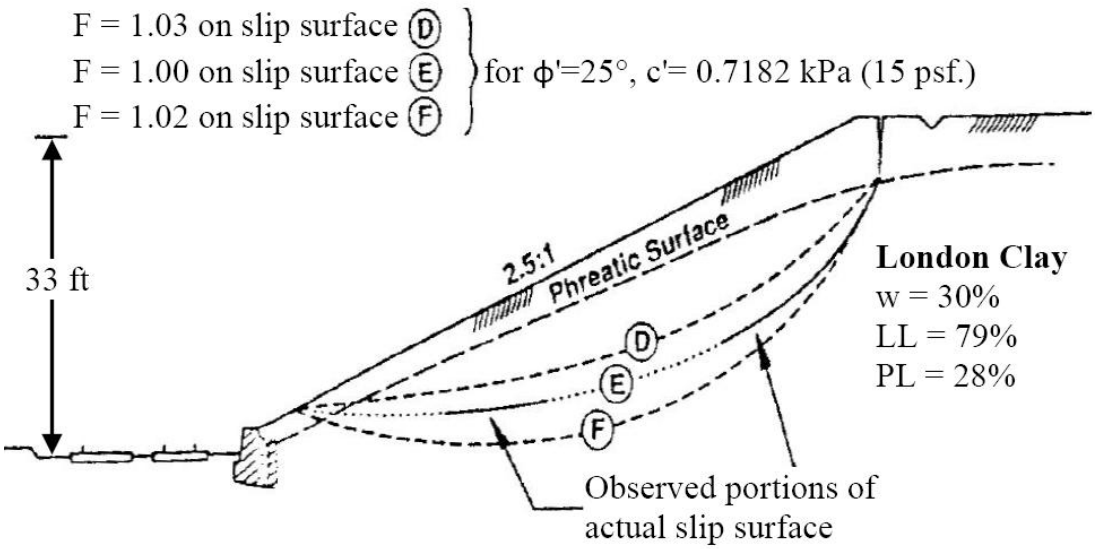

Figure 5.3. Cross-section and failure surface used by Duncan and Stark (1992) (from Duncan and Stark, 1992).

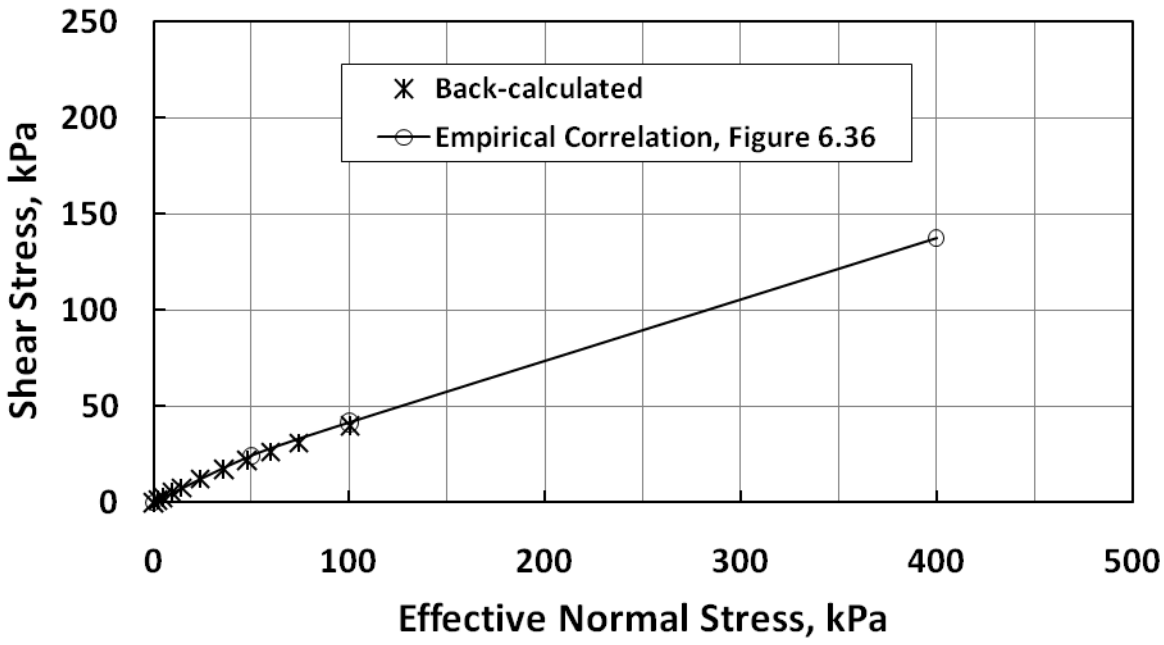

Figure 5.4. Stress dependent fully softened strength envelope developed from empirical correlation shown in Figure 6.36 for the Northolt landslide.

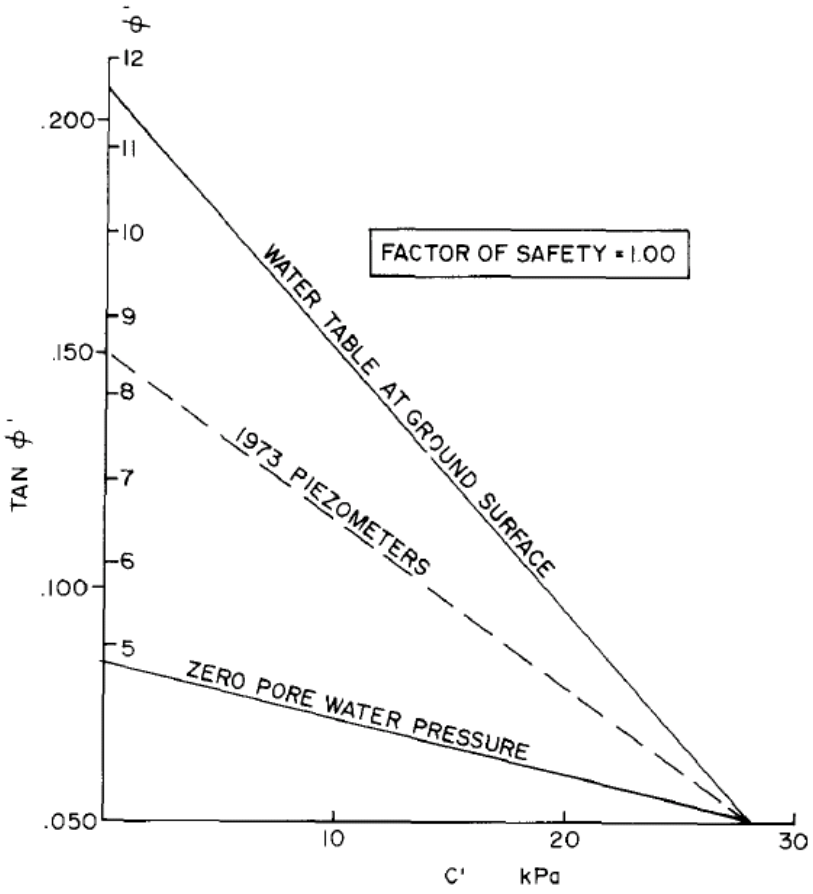

Figure 5.5. Effect of porewater pressure on back-calculated combination of *c'* and ϕ' (from Sauer, 1984).

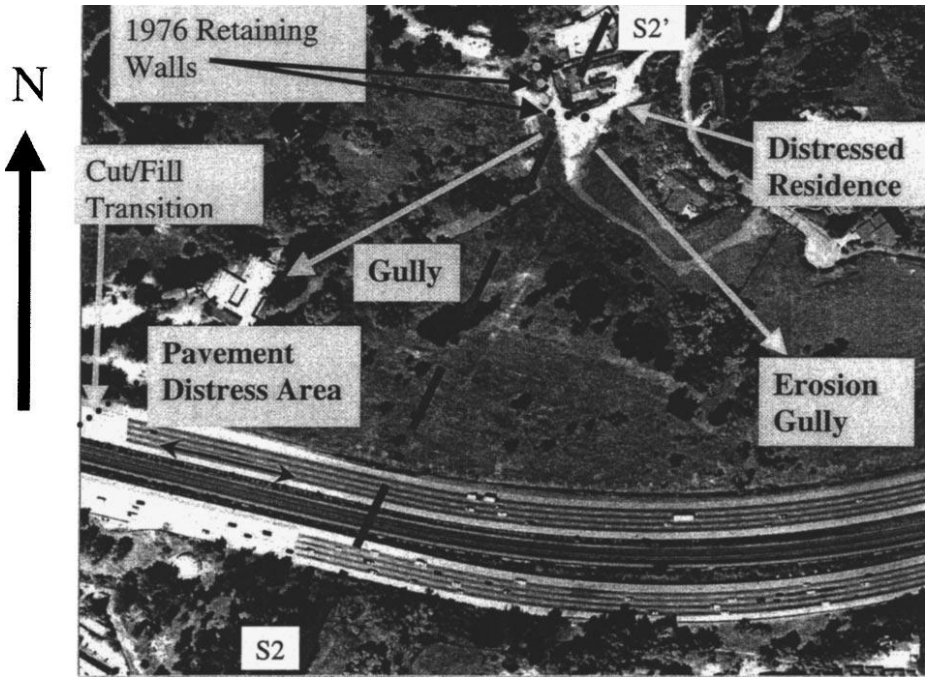

Figure 5.6. Aerial photograph of cutslope and distressed residence in 1999 (from Stark et al., 2005).

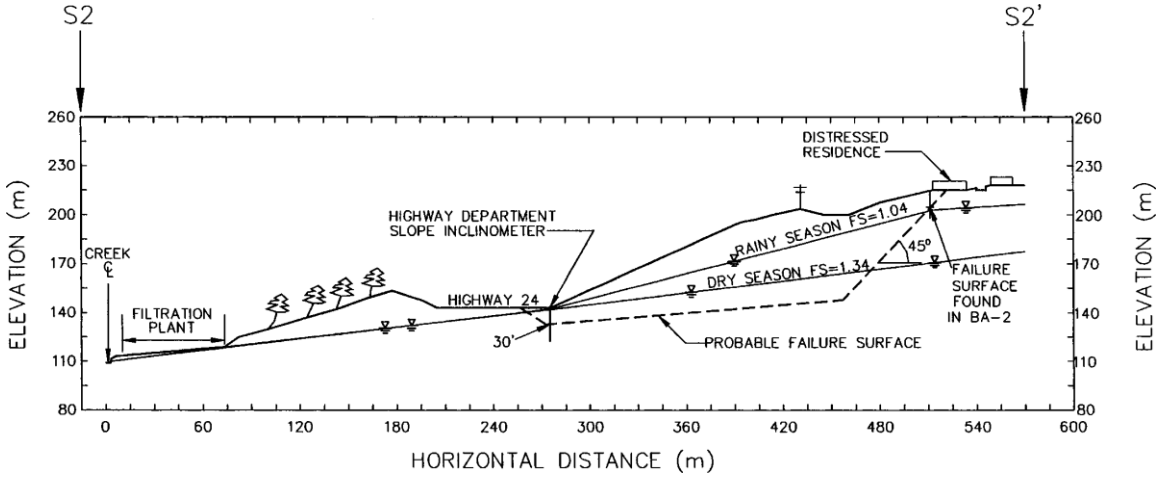

Figure 5.7. Postexcavation stability analysis for cross section S2-S2' (from Stark et al., 2005).

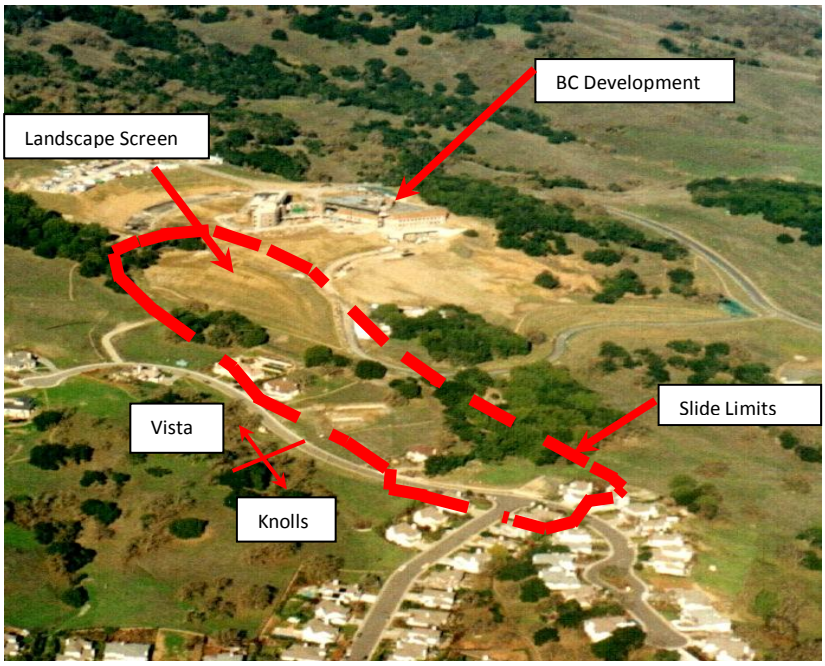

Figure 5.8. Aerial view of housing developments, BC Development, and an outline of the slide mass.

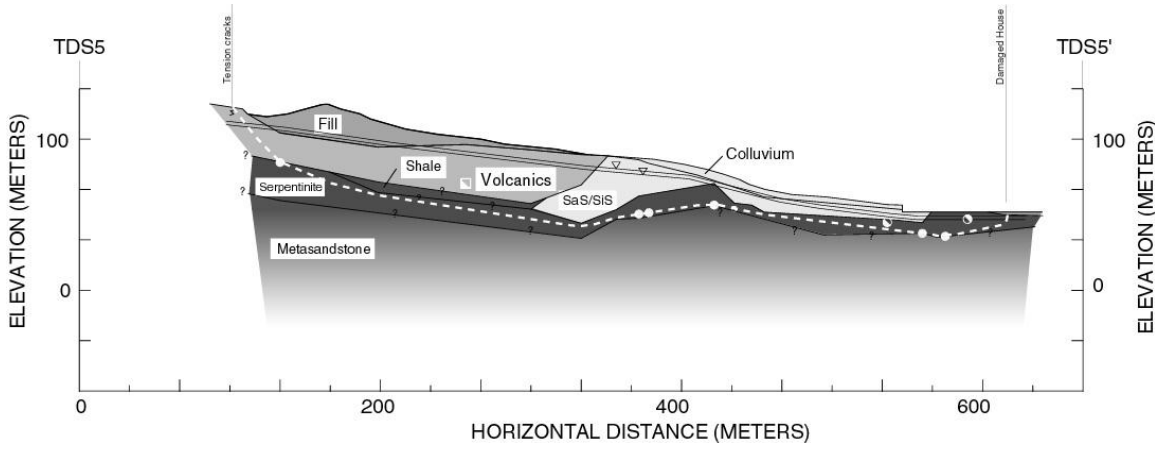

Figure 5.9. Cross-section TDS 5 through the western portion of the landslide after surficial grading and placement of the landscape screen.

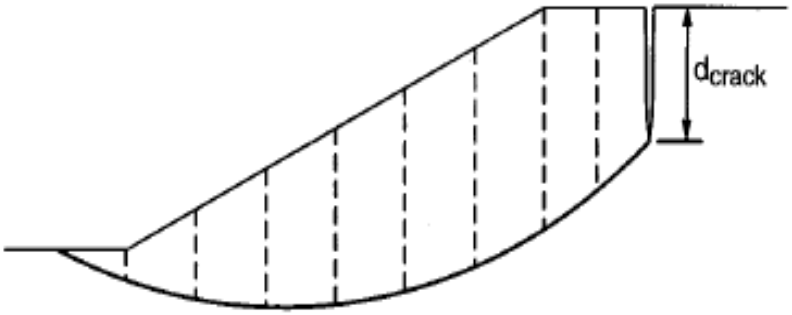

Figure 5.10. Location of the tension crack and its depth.

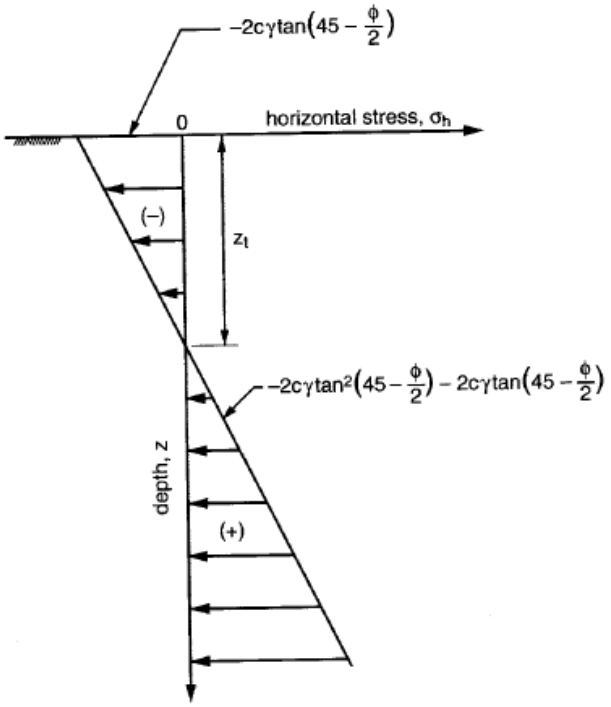

Figure 5.11. Use of d_{crack} to estimate *c*.

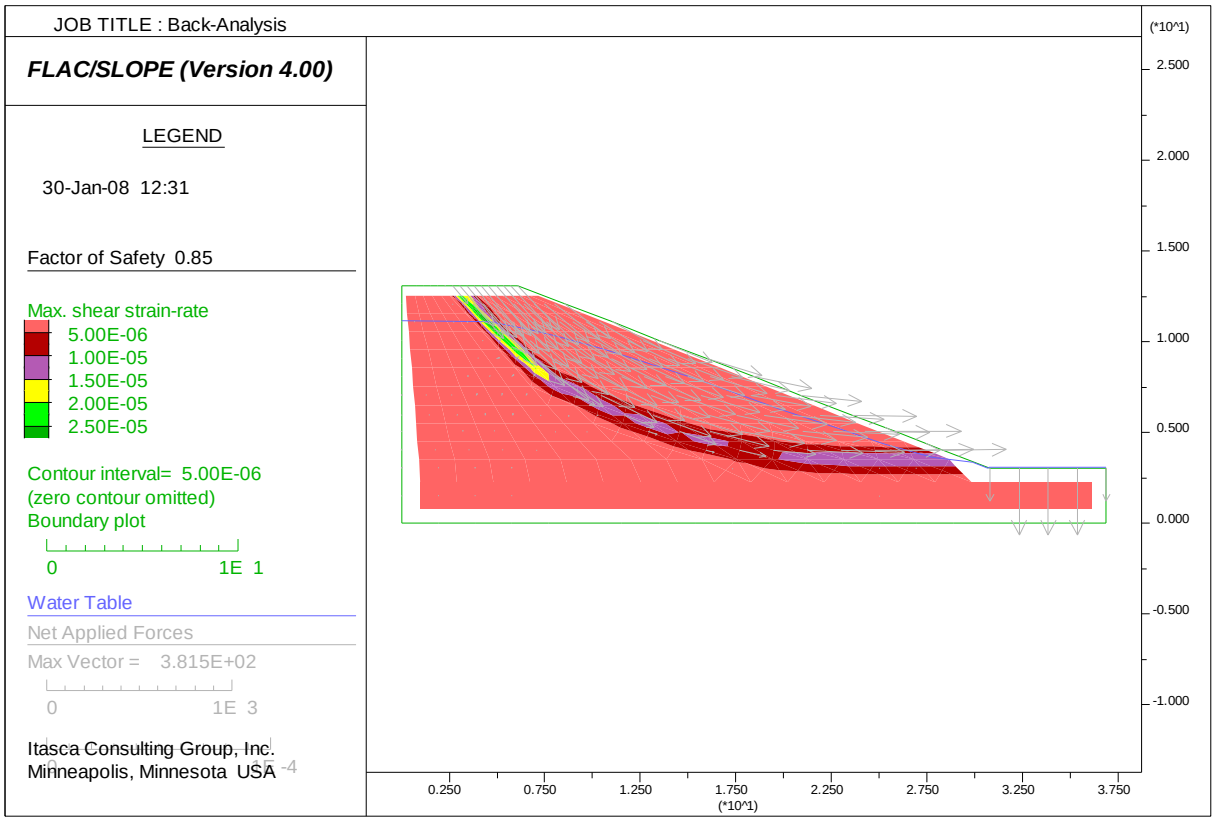

Figure 5.12. Results of analysis of the Northolt landslide performed using FLAC.

CHAPTER 6: DRAINED SHEAR STRENGTHS AND EMPIRICAL CORRELATION

6.1 Introduction

The shear strength of the soil is the maximum value of shear stress that the soil can withstand. Drained shear strength is the applicable strength when the soil is loaded slowly enough so excess porewater pressures, i.e., pore pressures that exceed the hydrostatic value, are not induced by the applied loading. Drained conditions are also applicable when loads are applied slowly to a mass of soil, or where they persist for a long enough time that the soil can drain the excess porewater pressure (Duncan and Wright, 2005).

Overconsolidated clays show a significant reduction in drained shearing resistance when sheared to large displacements. When the clay is sheared, the shear stress usually reaches a peak value at a small shear displacement. When the shear displacement is increased to a larger value, the clay undergoes a post-peak strength loss until a constant minimum or residual value is reached.

Different shear devices and test methods are being used to measure the drained residual and fully softened shear strengths of cohesive soils. Two shear devices being used in practice and research are the direct shear box and torsional ring shear device. Because of limited axial deformation, a triaxial compression test is not suitable to measure the drained residual strength parameters of cohesive soils, however, it can yield a reliable drained fully softened shear strength parameters.

In geotechnical engineering, the word “empirical correlation” is frequently used and so far many methods of parameter measurement and design procedures are primarily founded on experience and observation (Ladd et al., 1977). The empirical correlations with which we are primarily concerned are between drained residual and fully softened friction angles and information obtained from routine index tests, i.e., LL, CF, and PI. These correlations play an important role in practice by providing estimates of parameter values for use in preliminary design and also by serving as a check on data obtained from laboratory tests.

Different empirical correlations for the drained fully softened and residual shear strengths have been proposed by different researchers and are a function of clay-size fraction (CF), plasticity index (PI), and liquid limit (LL) and CF. The fully softened shear strength corresponds to the random arrangements of clay particles of normally consolidated clay soils and numerically equals the drained peak strength of a normally consolidated specimen (Skempton, 1970). Therefore, particle size, shape, interlocking, and degree of orientation is important in measuring the fully softened shear strength of clays. The residual shear strength is primarily dependent on mineral composition, which is related to plasticity, and grain size characteristics, such as clay-size fraction (Kenney, 1967 and Stark and Eid, 1997). Therefore, the empirical correlations based on LL and CF of the soil are considered more relevant and appropriate. Stark and Eid (1994 and 1997) and Stark et al. (2005a) propose empirical correlations for drained residual and fully softened friction angles based on LL and CF. These empirical correlations were developed using torsional ring shear test results and verified with the back-analysis of case histories. These empirical correlations have been widely accepted and are being used in practice and research with confidence. A stress dependent failure envelope is recommended for analysis of slopes and back-analysis of landslides (Stark and Eid, 1994 and 1997). Because a stress dependent failure envelope exhibits the maximum curvature or stress dependency at low effective normal stresses, i.e., effective normal stresses of less than 100 kPa, it is desirable to plot the failure envelop for an effective normal stress of 50 kPa. Therefore, the empirical correlation for drained residual friction angles suggested by Stark et al. (2005a) is extended to an effective normal stress of 50 kPa herein.

Shales are highly overconsolidated clays with varying degree of induration resulting in aggregation of particles. The degree of shale induration (aggregation) may influence the measurement of physical properties such as LL and CF (Mesri and Cepeda-Diaz, 1986). Townsends and Banks (1974) and Mesri and Cepeda-Diaz (1986) recommend using a specimen that passes the Number 200 sieve to measure the LL, CF and drained friction angles for indurated shales. The soil is ball milled so it can pass the Number 200 sieve. The ball milling breaks down the aggregated particles. Ball milling results in maximum disaggregation of clay particles without using a chemical dispersing agent (Mesri and Cepeda-Diaz, 1986). For indurated shales, Stark et al. (2005a) used ball milled specimens processed through Number 200 sieve to measure the LL, CF, and drained residual friction angles using a torsional ring shear

device. Where it was expected that the ball milling would change the texture and gradation of the soil, Stark et al. (2005a) just remolded the soil and processed it through the Number 40 sieve (not ball milled) and conclude that the results are in agreement with developed empirical correlations for drained residual and fully softened friction angles.

During the present study seven new soil specimens were tested to determine for the drained residual friction angles and three new specimens for the drained fully softened friction angles. The new results were added to the existing correlation. All of these specimens were processed through Number 40 sieve and not ball milled because ball milling is not necessary for soils that are not highly overconsolidated clays and shales. The LL and CF measured using ASTM D4318 and D422 (2008a and 2008b) can be used to establish a stress dependent drained residual and fully softened strength failure envelope using empirical correlations suggested by Stark et al. (2005a) and/or presented in the present study for soils that are not highly overconsolidated clays and shales.

This chapter briefly describes the various shear devices and test procedures used to measure the drained residual and fully softened shear strength of clay soils, the effect of sample preparation on LL, CF, and drained residual and fully softened friction empirical correlations. Some improvements in the empirical correlations for drained residual and fully softened friction angles suggested by Stark et al. (2005a) are suggested by adding a trend line for an effective normal stress of 50 kPa and providing equations for each CF group and effective normal stress. The spreadsheet developed using the equations in MS Excel and also coded in VB 6.0 for estimating the values of drained residual and fully softened friction angles is also discusses in this chapter.

6.2 Measurement of Drained Residual Shear Strength of Cohesive Soils

The residual shear strength is primarily dependent on mineral composition and is not related to plasticity index or grain size characteristics including clay-size fraction (Kenney, 1967). The residual shear strength condition can be established in the laboratory when a clay specimen is sheared at slow rate to a large displacement. In the field, the residual strength condition may be obtained when a clay mass undergoes a large shear displacement up to several feet (Skempton, 1964) due to landsliding, tectonic movement, solifluction, etc. The residual

shear strength of clay soils is commonly determined by shearing a normally consolidated intact or remolded specimen using a torsional ring shear, direct shear, or possibly a triaxial device.

6.2.1 Torsional Ring Shear Test

The importance of residual strength and its effects on slope stability was not widely understood by the geotechnical engineering profession until the mid 1960's, so the practical importance of the pioneering work by Hvorslev (1939), Haefeli (1951), and other early researchers was not appreciated until many years later. To overcome the limitation of a direct shear test, Bishop et al. (1971) introduce a torsional ring shear device which is designed to shear a soil specimen in the laboratory to an unlimited shear displacement in a single direction.

The Bishop et al. (1971) torsional ring shear device uses an annular specimen with 152 mm and 101 mm outer and inner diameters, respectively, and a specimen height of 19 mm. The specimen is sheared near the specimen mid-height and shearing occurs only in one direction. Thus, the specimen can be sheared to an unlimited continuous shear displacement without changing the direction of shear. The specimen is confined radially by upper and lower confining rings and a gap is opened and maintained after consolidation near specimen mid-height where shearing occurs with the aid of a gap control mechanism. The Bishop et al. (1971) ring shear test device usually results in a substantial amount of soil extrusion during testing and the extrusion is difficult to control. The specimen is contained in the two confining rings so it is difficult to observe shearing directly which makes it difficult to control the extrusion or adjust the gap if extrusion is occurring. Presently some torsional ring shear devices use the basic design of the Bishop et al. (1971) ring shear device. ASTM D6467 (2008c) provide a test procedure to measure the drained residual shear strength of clay soils using a torsional ring shear apparatus. The Bishop et al. (1971) ring shear device can be used to measure the drained residual shear strength of an undisturbed specimen obtained from the shear surface and a remolded specimen prepared the shear surface sample.

A torsional ring shear test performed using an intact specimen containing the shear surface is referred to as a "slip surface" test. Skempton (1985) concludes that a slip surface test can provide a good estimation of the field residual strength. However, obtaining a natural slip surface sample, transporting to the laboratory, trimming, and transferring it to the shearing

device is difficult and requires special consideration. The residual shear strength of cohesive soils is independent of stress history (Skempton, 1964, Petley, 1966, Bishop et al., 1971, Townsend and Gilbert, 1976, Morgenstern, 1977) which allows the use of a remolded specimen obtained from a shear surface sample to measure the drained residual shear strength of a soil. La Gatta (1970) also supports using a remolded specimen for measuring the drained residual shear strength of clays. Thus, a reconstituted soil specimen can be prepared from the shear surface sample after air drying, pulverizing, processing through Number 40 or 200 sieve, mixing with water, rehydrating, and transferring to the shearing device for consolidation and shearing. The advantages of obtaining a soil sample from the failure surface are that it represents the index properties and mineralogy of the problematic layer along which failure has occurred and the measured drained residual strength is a good representation of the field residual strength.

A shear surface can be formed in the laboratory by preshearing a remolded specimen after consolidation as described in ASTM D6467 (2008c). The preshearing occurs at a faster rate to minimize the time required to reach the residual strength value. After equalization of porewater pressures, which may have resulted because of shearing at a faster rate, the presheared specimen is sheared at a slow/drained rate to obtain the residual strength of the specimen. The shear surface also can be formed without preshearing using the torsional ring shear device to shear an "intact" remolded specimen at a slow/drained rate to a large enough displacement to achieve a drained residual strength. The disadvantage of not preshearing a specimen is that a significant amount of time is required to reach the residual condition which requires a large shear displacement to orient the clay particles along the shear surface in the direction of shear.

Bromhead (1979) proposes a ring shear device similar to the Bishop-type ring shear device except the shearing occurs at the top of a specimen (a smear type shearing) and not at specimen mid-height. The Bromhead torsional ring shear device is widely used because of its simplicity, practicality, shorter test time, and small amount of soil specimen required (Bromhead, 1979, Lupini et al., 1981, Tika et al., 1996, Stark and Eid, 1994, Eid 1996, Tiwari and Marui, 2005, Meehan, 2006). The Bromhead ring shear device uses an annular specimen with 100 mm and 70 mm outer and inner diameters, respectively, and a specimen height of 5 mm. Stark and Eid (1993 and 1994) suggest modification to the Bromhead ring shear specimen mold which allows the specimen to be raised so it is flush with the top of the specimen container by removing

the settlement resulting from specimen consolidation. The raising minimizes the effect of wall friction on the test results which makes the device more suitable/reliable than the Bishop et al. (1971) device. Stark and Eid (1994 and 1997) and Stark et al. (2005a) conclude that the modified Bromhead ring shear device provides a good estimate of the drained residual shear strength of cohesive soils. The Bromhead ring shear device can be used to measure the drained residual shear strength of a remolded specimen prepared from a shear surface sample. The Bromhead ring shear device is also suitable for testing an undisturbed slip surface specimen as discussed by Stark and Contreras (1996).

The torsional ring shear test can be performed using a new specimen at each effective normal stress or the same specimen can be used to perform a multistage test at various effective normal stresses to develop a stress dependent residual strength envelope (Anderson and Hammoud, 1988, Stark and Vettel, 1992, Stark and Eid, 1994, Eid, 1996).

Bromhead and Curtis (1983), Stark and Eid (1994), Mesri and Shahien (2003), Stark et al. (2005a), and Tiwari et al. (2005) conclude that the drained residual shear strength measured in a ring shear test is in agreement with the back-calculated drained residual shear strength for a landslide slip surface.

6.2.2 Direct Shear Test

Different test methods are being used to try to measure the drained residual shear strength of cohesive soils in a direct shear box. Skempton (1964) introducing the residual shear strength suggested a reversal direct shear test procedure to measure the drained residual shear strength. To obtain the residual strength condition in the field the slide mass may have to undergo several feet of shear displacement (Skempton, 1964). Skempton (1964) acknowledges that to obtain the residual strength condition in the laboratory, the soil specimen is required to undergo a large shear displacement and ideally the shearing should be in one direction. The direct shear box can be displaced in one direction to a limited shear displacement of only about 6 mm. This is problematic because a large shear displacement in one direction is required to orient the clay particles parallel to the direction of shear. Skempton (1964) proposes a reversal direct shear test in which the specimen is subjected to large shear displacement by changing the direction of movement of the shear box. This results in changing the orientation of previously aligned clay

particles upon reversing the shearing direction and results in a peak strength being measured on the shear stress-displacement relationship at the start of each reversal. Residual shear strength, a constant value on a shear stress-displacement relationship, may be obtained after completion of 4 to 6 reversals cycles as suggested by Skempton and Petley (1967). Skempton (1964) acknowledges that direct shear reversal technique is not perfect and ideally the specimen should be sheared in one direction which resulted in Bishop developing a ring shear device in the late 1960's and early 1970's.

Apart from the limitation of shear displacement in one direction, there are many other problems associated with a direct shear test that include, soil extrusion during shearing, offset of the top half of the shear box from the bottom half during shearing, the shear surface moving below the top of the bottom half of the shear box especially in the case of a multistage test, chances of slurrying at the shear surface upon changing the direction of shear as identified by Skempton (1964), continuously changing the shear surface cross-sectional area during shearing, creating and maintaining the gap between the top and bottom halves of the shear box during the entire shearing process, etc.

A direct shear test can be performed using an intact "slip surface" specimen containing a shear surface and is preferred to reduce the shear displacement in the test. As discussed earlier obtaining a natural slip surface sample, transporting to the laboratory, trimming, and properly aligning the specimen in the shearing device with the gap in the shear box, and orienting the specimen so shearing continues in the same direction as in the field are all difficult. Because the residual shear strength of cohesive soils is independent of stress history, this allows the use of a remolded specimen obtained from the shear surface to measure the drained residual shear strength. Thus, a reconstituted soil specimen similar to that discussed for the torsional ring shear can be used for the direct shear test but some form of preshearing is required to reduce the required shear displacement.

In a direct shear, a shear surface can be formed by shear displacement upon shearing of an "intact" remolded specimen. The major disadvantage of this test procedure is that to reach the residual strength condition, a large shear displacement is usually required to orient the clay particles along the shear surface in the direction of shear. The shear surface formed in the direct

shear box by shearing an intact specimen may not be perfect and may result in excessive soil extrusion and damage to the direct shear specimen. In addition, continuous shear displacement in one travel of the shear box is limited to almost 6 mm.

A shear surface can also be formed by precutting a remolded specimen prior to shearing (Kenney, 1967). A thin wire can be used for precutting of a direct shear specimen in an assembled shear box. Kenney (1967) performed a series of reversal direct shear box tests to measure the residual strength of natural soils, pure clay minerals, and mineral mixtures following the approach outlined by Skempton (1964) after precutting. Use of this test procedure is supported by tests conducted on precut specimens that gave more regular and reproducible results than tests conducted on intact specimens. Kenney (1967) found that residual strengths of natural soils are primarily dependent on the clay minerals that are present in the soil. Kenney (1967) concludes that residual strength does not correlate well with plasticity index or grain size. Skempton (1985) also recommends using a precut specimen to measure the residual shear strength of the soils.

The process of specimen precutting in an assembled direct shear box is difficult and is dependent on the expertise of the person performing the test. Mesri and Cepeda-Diaz (1986) suggest using a remolded precut specimen consolidated separately in the two halves of a shear box in two separate oedometers. The faces of the both halves of a direct shear box are consolidated against a smooth surface so that clay particles along the faces are aligned as much as possible during the consolidation process. This allows consolidation of the specimen at high consolidation pressures in separate halves of the shear box. To align the clay particles along the shear surface in the direction of shear, a surgical blade is used to preshear the surface of each shear box after consolidation and before combining both halves together. After preshearing, the full or assembled specimen is shifted to the shear box and shearing is commenced to obtain the residual strength value after equalization of porewater pressure. The precutting results in obtaining the residual strength value after a relatively small shear displacement as compared to an intact remolded specimen because a shear surface was formed by connecting the smooth faces of separately consolidated specimens in the two halves of the shear box. Although this method results in obtaining the residual value after relatively small shear displacement, as compared to

the intact specimen, the effort, time, and resources required to consolidate the specimen in two separate halves of the direct shear box in two separate oedometers are large.

The direct shear test can be a single stage in which a specimen is used to measure the drained residual shear strength at a single effective normal stress. The direct shear test can also be a multistage in which a single soil specimen is used to measure the residual shear strengths at different effective normal stresses to obtain a stress dependent failure envelope. But special caution is required to ensure that the shear surface does not move away from the gap between the two shear box halves because of loading and unloading in a multistage test. New standard test method for measuring the drained residual shear strength of cohesive soils by using a reversal direct shear test are being considered by ASTM WK#3822 (ASTM, 2010b).

6.2.3 Triaxial Compression Test

Chandler (1966) suggests a method to measure the drained residual shear strength of clays in a triaxial compression test. Because shearing in a triaxial compression test to large axial strains results in cross-sectional area changes therefore Chandler (1966) proposes corrections for change in the contact area and the restraint of the rubber membrane in triaxial compression tests. An intact or unsheared specimen cannot be used in the triaxial compression test to obtain a reasonable estimate of the drained residual shear strength of clays, however, a specimen containing a natural shear surface may be used for such testing. Patton and Hendron (1974) conclude that limited amount of axial deformation in a triaxial compression test makes it unsuitable to measure the drained residual shear strength. Also Meehan (2006) conclude that the triaxial compression test is not suitable to measure the drained residual shear strength along preexisting shear surfaces (slickensided discontinuities).Thus, a consolidated-drained triaxial compression test to measure the drained residual shear strength is not considered suitable to measure the drained residual strength of clays and is used the least for such testing.

6.3 Measurement of Drained Fully Softened Shear Strength of Cohesive Soils

The drained fully softened shear strength of overconsolidated clay may develop under highly fissured and jointed conditions without presence of a preexisting shear surface (Terzaghi et al., 1996). The fully softened shear strength corresponds to the random arrangements of clay

particles of normally consolidated clay soils. Skempton (1970) suggests that numerically the fully softened shear strength of clays equals the drained peak strength of a normally consolidated specimen. Therefore, particle size, shape, interlocking, and degree of orientation is important in measuring the fully softened shear strength of clay soils.. The fully softened shear strength of clay soils is commonly determined by shearing a normally consolidated intact/undisturbed or remolded specimen using a direct shear, ring shear, or a triaxial device.

6.3.1 Torsional Ring Shear Test

The fully softened shear strength of normally consolidated remolded clay specimen can also be measured in a torsional ring shear device. Professor Stark has proposed standards for ASTM (2010a) for measuring the fully softened shear strength of a normally consolidated clay specimen in a torsional ring shear device which is scheduled for re-balloting by D18 committee. A remolded specimen prepared from air drying, pulverizing, and processing through the Number 40 sieve can be consolidated in the torsional ring shear device to a desired effective normal stress and sheared at a slow/drained rate to measure the drained fully softened shear strength of the clay specimen. The peak strength observed in a ring shear device on a normally consolidated clay specimen numerically equals the fully softened shear strength of the soil specimen.

As discussed above the fully softened shear strength of soils is stress dependent (Stark and Eid, 1997 and Mesri and Shahien, 2003), therefore, the drained fully softened should be measured at minimum three effective normal stresses to develop a stress dependent fully softened strength failure envelop. After observing the peak strength in a torsional ring shear device, the specimen can be sheared to a large displacement to measure the residual shear strength of the same specimen at same effective normal stress or the test can be stopped to replace the existing specimen. To measure the fully softened shear strength in a torsional ring shear device at different effective normal stresses, each time a new ring shear specimen is to be used.

A torsional ring shear device is relatively easy to use and requires little/small effort to measure the fully softened shear strength of clay specimens as compared to the other test devices, i.e., direct shear and triaxial devices. Because the fully softened shear strength corresponds to the peak strength of a normally consolidated specimen, it should be ensured that

the shearing starts soon after completion of the primary compression of the specimen to obtain the more representative values. If the specimen is allowed to undergo secondary compression, it may show a higher strength than the actual fully softened shear strength of the specimen.

6.3.2 Direct Shear Test

The direct shear box is used to measure the fully softened shear strength of a normally consolidated clay specimen. The fully softened shear strength of a clay specimen numerically equals the peak strength of a normally consolidated specimen (Skempton, 1970). Therefore, a direct shear box can be used to measure the peak strength of an undisturbed normally consolidated clay specimen obtained from the field and/or remolded normally consolidated specimen prepared in the laboratory. It may not be appropriate and relevant to obtain an undisturbed normally consolidated specimen from the field because mostly the clays and shales are overconsolidated. Thus, a remolded specimen prepared from the soil obtained from the field can be normally consolidated in the laboratory and used to measure the fully softened shear strength of clay soils. The remolded specimen can be consolidated in the assembled direct shear box to the desired normal pressure and sheared after completion of consolidation to measure the peak strength. The remolded specimen, consolidated separately in the laboratory to the desired normal pressure and trimmed into the direct shear box can also be used to measure the fully softened shear strength of the clay soils. The specimen is sheared at a slow/drained rate to ensure that no shear induced porewater pressures develops during the shearing.

The peak strength measured on a normally consolidated specimen is the fully softened shear strength at that effective normal stress. Stark and Eid (1997) establish that the fully softened shear strength of soils is stress dependent which is also augmented by Mesri and Shahien (2003), therefore, the drained fully softened should be measured at minimum three effective normal stresses to develop a stress dependent fully softened strength failure envelop. After observing the peak strength, the specimen can be sheared to a large displacement to measure the residual shear strength of the same specimen at that effective normal stress or the test can be stopped to replace the existing specimen. To measure the fully softened shear strength at different effective normal stresses, each time a new direct shear specimen is to be used. Unfortunately, so far no ASTM standard is available for measuring the fully softened shear strength of soils.

6.3.3 Triaxial Compression Test

A triaxial compression apparatus is frequently used to measure the fully softened shear strength because of its ability to simulate the field stress conditions and large displacement is not required (Eid, 1996). In a triaxial compression test, stresses and strains are sufficiently uniform that a local or progressive shear failure does not significantly affect the test results. A drained triaxial compression and an undrained triaxial compression test with porewater pressure measurements are frequently used to measure the fully softened shear strength of a normally consolidated clay specimen. The triaxial apparatus and test procedures are described in detail by Bishop and Henkel (1962). Triaxial compression tests can be performed on an undisturbed normally consolidated specimen obtained from the field and/or on a remolded specimen prepared from the soil sample obtained from the field. An undisturbed normally consolidated sample without any preexisting shear surface can be used for a triaxial specimen by trimming a specimen from the sample, consolidating to 2 to 2.5 times the field stress condition to create a normally consolidated specimen, and shearing. A triaxial specimen can be also prepared from a remolded soil sample as discussed in the previous section. The remolded specimen is rehydrated, placed in a triaxial compression mold, consolidated to the required effective normal stress, and sheared. The peak strength observed during a drained triaxial compression test corresponds to the drained fully softened shear strength of the soil. A new standard test method for consolidated drained triaxial compression tests are being balloted by ASTM WK#3821 (ASTM, 2010c).

In an undrained triaxial compression test on a normally consolidated undisturbed specimen, the maximum principal stress ratio failure criterion is used to define the peak strength of the specimen. If the failure criterion for stress difference is adopted, then the shearing resistance obtained from undrained tests is generally about 8% less than obtained from a drained test (Simons, 1963). This is attributed to porewater pressure increase even after the point of maximum stress difference is reached. Bjerrum and Simons (1960) show that for an undrained test on a normally consolidated remolded clay specimen, the axial strain at the point of maximum stress difference is generally on the order of 10% and the two failure criteria give peak shear strengths which do not differ appreciably.

Eid (1996) shows little information exists on the comparison of the fully softened shear strength of clay soils measured in triaxial compression test and other shear devices, e.g., direct

shear and ring shear devices. The triaxial compression test is a difficult test and usually requires more time and efforts than the ring shear and direct shear tests. Furthermore, a consolidated drained triaxial compression tests take much more time than an undrained triaxial compression test.

6.4 Empirical Correlation for Drained Residual Friction Angles of Clays

Skempton (1964), while introducing the concept of residual shear strength of clay soils, suggests a relationship between CF and drained residual friction angle. Skempton (1964) also suggests that the residual shear strength is a function of the clay mineral present in the soil. Kenney (1967) used direct shear test results on natural soils and clay minerals to conclude that the residual shear strength is primarily dependent on mineral composition and that it is not related to plasticity or grain size characteristics including CF. Regardless subsequent researchers, such as Voight (1973), Kanji (1974), Seycek (1978), Lupini et al. (1981), Skempton (1985), Mesri and Cepeda-Diaz (1986), Collotta et al. (1989), Mesri and Shahien (2003), proposed different empirical correlations for the drained residual friction angles using CF and/or plasticity index (PI). of clays which include. Although Mesri and Cepeda-Diaz (1986) present their direct shear test data along with data from Kenney (1967) on a LL versus drained residual friction angles without incorporating the effect of stress dependency on the shear strength of cohesive soils. Stark and Eid (1994) present ring shear drained residual friction angles as a function of LL and incorporate the effect of CF and effective normal stress in a single correlation. Thus, the empirical correlations presented by Stark and Eid (1994) and refined by Stark et al. (2005a) are widely accepted in the geotechnical community because these reduce the scatter in ϕ'_r by using the relevant parameters, LL, CF, and σ'_n.

This section covers the historical development of the empirical correlations for the drained residual shear stress presented by various researchers and the new residual strength empirical correlations developed herein using data from Stark and Eid (1994), Stark et al. (2005a), and data generated during the study. The new correlation includes equations for each CF group and effective normal stress with an additional effective normal stress of 50 kPa. A spreadsheet was developed to plot the stress dependent drained residual and fully softened failure envelopes by specifying only LL and CF.

6.4.1 Previous Empirical Correlations for Drained Residual Friction Angles of Clays

Prior drained residual shear strength correlations are divided into three distinct groups based on LL, CF, and PI, which are discussed below.

6.4.1.1 Empirical Correlations Based on Liquid Limit

6.4.1.1.1 Mitchell (1976)

Mitchell (1976) presents empirical correlations compiled by Deere (1974) in which a relationship between drained residual friction angle and LL is presented. Mitchell (1974) cites personal communication with Deere (1974) as the source for Figure 6.1. Mitchell (1976) also presents a relationship between drained residual friction angle (ϕ'_{res}) and plasticity index (PI) derived from Deere (1974) which is also shown in Figure 6.1. Figure 6.1shows that the drained residual friction angle decreases with an increase in either LL or PI. The correlations shown in Figure 6.1 do not present any test data but present lower and upper bounds with an average curve for ϕ'_{res} versus PI and ϕ'_{res} versus LL.

Both of these relationships show the range of ϕ'_{res} is almost 12° for a single value of PI or LL for the entire range of PI and LL. Mitchell (1976) does not provide any explanation or reason for the large range of ϕ'_{res} values. Because the correlations presented by Mitchell (1976) are not supported by any data and are not widely used, these relationships are not included in Mitchell (1996) and Mitchell and Soga (2005).

6.4.1.1.2 Mesri and Cepeda-Diaz (1986)

Most researchers present a relationship between secant residual friction angle and CF or plasticity index (PI). Mesri and Cepeda-Diaz (1986) present a relationship between ϕ'_r and LL based on direct shear tests on 24 shale specimens and data from Kenney (1967) (see Figure 6.2). They also plot the same test results versus CF to obtain the relationship in Figure 6.3. Mesri and Cepeda-Diaz (1986) refer to Kenney (1967) and conclude that the residual shear strength is primarily dependent on mineral composition and that it is not related to plasticity or grain size characteristics including CF.

Chandler (1977) and Bromhead (1978) use on the back-analysis of landslides involving Lias and London clays, respectively, to conclude that the mobilized residual shear strength decreases with increasing effective normal stress and thus is effective stress dependent. However, Mesri and Cepeda-Diaz (1986) do not include effective normal stress at which the direct shear tests were performed in their correlations. Furthermore, Mesri and Cepeda-Diaz (1986) also present their test results in terms of CF (see Figure 6.3) with an argument that the correlation between secant residual friction angle and either LL, CF, and mineralogy is expected because each is directly or indirectly related to particle size and/or platyness. This suggests that the importance of LL, CF, and effective normal stress was not fully understood when establishing the relationship for drained residual friction angle of clay soils.

6.4.1.1.3 Stark and Eid (1994)

Stark and Eid (1994) present the empirical correlation for drained residual friction angle of cohesive soils based on ring shear test on 32 clays and shales shown in Figure 6.4. Stark and Eid (1994) conclude that the drained residual failure envelope is stress dependent (nonlinear) and incorporate this effect in the empirical correlation. Stark and Eid (1994) giving due consideration to the conclusion of Kenney (1967) that the residual shear strength is primarily dependent on mineral composition, incorporated the effect of LL, CF and effective normal stress in a comprehensive correlation for drained residual friction angle. The LL describes the clay mineralogy, CF quantifies the amount of the clay minerals, and σ'_n captures the stress dependent values of the failure envelope.

Skempton (1985) concludes that clay mineralogy has a little effect on the residual strength when CF is less than 20% because the strength is then controlled largely by the sand and silt particles. Skempton (1985) also concludes that if CF exceeds 50%, residual strength depends almost entirely on sliding friction of clay particles and therefore depends on clay mineralogy. Therefore, Stark and Eid (1994) use three CF groups to capture the impact of CF groups on ϕ'_r. The empirical correlation shows a relationship between LL and ϕ'_r for three distinct CF groups, i.e., CF $\leq$ 20%, 25% $\leq$ CF $\leq$ 45%, and CF $\geq$ 50% (see Figure 6.4). Stark and Eid (1994) also show three different values of drained residual friction angle corresponding to LL and CF for three different effective normal stresses, i.e., 100, 400, and 700 kPa. The values of drained

residual friction angle for the three different effective normal stresses can be used to develop a stress dependent drained residual strength failure envelope for use in stability analyses.

Stark and Eid (1994) use samples processed through the Number 200 sieve for highly overconsolidated clays. The soil is ball milled prior to reduce the aggregation of the overconsolidated clay particles so they can be processed through the Number 200 sieve. ASTM D4318 and D422 test methods are used to estimate LL and CF, respectively, for the material processed through the Number 200 sieve. If the clay is not highly overconsolidated, i.e., without significant induration (aggregation), the samples are only processed through the Number 40 sieve and thus not ball milled. The method for sample preparation using ball milling of highly overconsolidated clays was proposed by Mesri and Cepeda-Diaz (1986) and used to measure LL and CF because most of the highly overconsolidated clays, mudstones, claystones, and shales possess varying degrees of induration. La Gatta (1970) shows disc milling of Cucaracha shale increases the LL from 49% to 156% by disaggregating the clay particles. Townsend and Bank (1974) show a similar increase in LL with milling using a high speed food blender on Bearpaw shale sample in which the LL increased from 132% to 152% and 196% after 2 and 15 minutes of blenderizing, respectively.

In summary, a disaggregated estimate of LL and CF of a clay is required to estimate values of drained residual friction angle from the empirical correlation suggested by Stark and Eid (1994). The estimated values of drained residual friction angles can be used to develop a stress dependent residual strength failure envelope which can be used in a slope stability analysis. Because the empirical correlations presented by Stark and Eid (1994) were developed using LL, CF, and effective normal stress, the correlation show good agreement with back-calculated drained residual friction angles. Because of the reliability of ring shear test data of Stark and Eid (1994) and its verification from the case histories, other researchers, such as Mesri and Shahien (2003), have used this data to develop their correlations.

6.4.1.1.4 Stark et al. (2005a)

Stark et al. (2005a) refine the ϕ'_r correlation of Stark and Eid (1994) based on ring shear tests on 66 clays and shales. The empirical correlation proposed by Stark et al. (2005a) is shown

in Figure 6.5. Because the empirical correlation by Stark and Eid (1994) was widely accepted at the time, Stark et al. (2005a) refined the correlation by adding test results for additional 34 soils.

Stark et al. (2005a) use ball milled samples processed through the Number 200 sieve for highly overconsolidated clays and ASTM D4318 and D422 standards to estimate LL and CF, respectively, for clays with induration (aggregation). For non-indurated materials the material was not ball milled and only processed through the Number 40 sieve and ASTM D4318 and D422 were used to measure LL and CF, respectively. The resulting empirical correlation is shown in Figure 6.5. Because Stark and Eid (1994) used ball milled soils to estimate LL and CF and only LL and CF are required to use the empirical correlation, the effect of sample preparation raised some questions. Therefore, Stark et al. (2005a) present a detailed description of the effect of sample preparation and ball milling on determining the index properties of a soil. The ball milling of indurated (aggregated) claystones, mudstones and shales results in an increase in LL and CF. Because ball milled values of LL and CF were used to develop Figure 6.5, the users while consulting the correlation should also use ball milled or disaggregated values of LL and CF for highly overconsolidated clays, i.e., mudstones, claystones, and shale.

Stark et al. (2005a) emphasize that the clay specimens which are not indurated (aggregated) do not require particle disaggregation by ball milling for processing through Number 200 sieve instead a specimen processed through Number 40 sieve as suggested by ASTM can be used for measuring LL and CF. The ball milling of such clay specimens which are not indurated (aggregated) will result in changing the texture and gradation of the soil. Stark et al. (2005a) suggest using judgment to decide whether or not a material should be ball milled. This decision can be made after examination of the chunks of claystone, mudstone, shale, or overconsolidated clay and determining whether the chunks can be sufficiently broken down with a mortar and pestle to disaggregate the clay particles.

Because the commercial laboratories primarily, if not exclusively, utilize the ASTM standard procedure (ASTM, 2008a and 2008b) to measure the LL and CF, respectively, Stark et al. (2005a) proposed empirical correlations for estimating ball milled derived value of LL and CF from ASTM derived value of LL and CF (see Figures 6.6 and 6.7). Stark et al. (2005a) use 15 samples of highly overconsolidated clays to establish these relationships by measuring LL and

CF with and without ball milled material. Figures 6.6 and 6.7 have facilitated estimating the values of drained residual friction angle from the empirical correlation shown in Figure 6.5 for highly overconsolidated clays, i.e., mudstones, claystones, and shales.

In summary, a disaggregated estimate of LL and CF is required to use the empirical correlation for drained residual friction angle proposed by Stark et al. (2005a). Only highly overconsolidated clay samples need to be disaggregated so these materials should be ball milled to estimate the values of LL and CF whereas ASTM D4318 and D422 test methods can be used to estimate values of LL and CF, respectively, for the other clay samples. Even for the highly overconsolidated clay samples, disaggregated values of LL and CF can be estimated using the correlation in Figures 6.6 and 6.7 ASTM D4318 and D422, respectively, to measure non-disaggregated values of LL and CF. Because the empirical correlations presented by Stark et al. (2005a) were developed using LL, CF, and effective normal stress, and have been verified using case histories, these correlations are widely used in the geotechnical community.

The scatter for each CF group on Figure 6.5 is maximum of 3-4° compared to 6-7° for other proposed correlations, such as Mesri and Shahien (2003), using the same data set but plotting ϕ'_r versus PI. Thus, the Mesri and Cepeda-Diaz (1986) and Mesri and Shahien (2003) statement that "A correlation between ϕ'_r and LL or PI is expected because each is directly or indirectly related to one or both of the fundamental factors of particle size and platyness" does not appear to be supported. Instead the empirical correlation presented by Stark et al. (2005a) provides a relationship between ϕ'_r and LL while incorporating the effect of CF and effective normal stress (see Figure 6.5) results in a reliable estimate of ϕ'_r.

6.4.1.2 Empirical Correlations based on Clay-Size Fraction

6.4.1.2.1 Skempton (1964)

Skempton (1964) concludes that the residual shear strength is a function of the clay minerals present in the soil. Skempton (1964) considered it appropriate to correlate the drained residual friction angle with clay mineralogy. Skempton (1964) uses direct shear test results of nine natural soils and three clay minerals to establish the relationship between CF and ϕ'_r shown

in Figure 6.8. Skempton (1964) concludes that drained residual friction angle decreases with increasing the CF.

6.4.1.2.2 Lupini et al. (1981)

Lupini et al. (1981) presents ring shear test results for a number of natural soils. The ring shear test results along with previously published results suggest that the residual shear strength changes significantly as the clay content of the soil increases. This change in ϕ'_r occurs due to a change in shearing mechanism as the CF increases. The test results for 52 different soils were complied and plotted by Lupini et al. (1981) to develop a relationship between ϕ'_r and CF as shown in Figure 6.9. The same test results are also used by Lupini et al. (1981) for a relationship between ϕ'_r and plasticity index (PI or I_p) that is shown in Figure 6.10. Lupini et al. (1981) conclude that a change in shearing resistance occurs at a CF of about 35% or a PI of 30% (see Figures 6.9 and 6.10). Lupini et al. (1981) show that a number of test results fall outside any reasonable correlation band on both plots and conclude that some of the degradable mudstone and shale materials show atypically low residual friction angles, particularly when they are correlated with plasticity index. Thus, Lupini et al. (1981) suggest that simple correlations with index properties are inadequate for the prediction of residual strength for engineering purposes.

Lupini et al. (1981) conclude that the residual strength behavior changes significantly as the clay content of the soil increases and that correlation between residual strength and soil index properties and gradation cannot be generalized. The correlation may be valuable in studying the residual strength of a particular variable soil deposit, provided that they properly reflect changes in particle shape, gradation, mineralogy, porewater chemistry, etc., but not for soils for a wide range of sites.

6.4.1.2.3 Skempton (1985)

Skempton (1985) shows a relationship between CF and ϕ'_r for different soils with the values of activity, A_c (PI/CF) between 0.5 and 0.9 (see Figure 6.11). Figure 6.11 shows ϕ'_r decreases with increasing CF. Skempton (1985) concludes that clay mineralogy has little effect on residual strength when the CF is less than 20% because the strength is controlled largely by the sand and silt particles or sliding shear. Skempton (1985) also concludes that when CF

exceeds 50%, residual strength depends almost entirely on sliding friction a “sliding shear” of the clay particles and therefore depends on their character or mineralogy. The effects of particle reorientation are important in clays containing platy clay minerals and having a CF exceeding about 20-25%.

6.4.1.2.4 Mesri and Cepeda-Diaz (1986)

Mesri and Cepeda-Diaz (1986) use direct shear test results of twenty four shales to present a relationship between CF and ϕ'_r (see Figure 6.3). The ball milling method of sample preparation described by Mesri and Cepeda-Diaz (1986) is discussed above and not repeated here. Mesri and Cepeda-Diaz (1986) also present a relationship between LL and ϕ'_r and conclude that a correlation between ϕ'_r and either LL, CF, or mineralogy is expected because each is directly or indirectly related to one or both of the fundamental factors of particle size and platyness. Mesri and Cepeda-Diaz (1986) also conclude that their findings are in agreement with the findings of Skempton (1965).

6.4.1.2.5 Others

Borowicka (1965), Binnie et al. (1967), and Kenney (1977) present data on ϕ'_r and a correlation between ϕ'_r and CF. Chandler (1984) also presents data to reinforce the empirical correlation suggested by Lupini et al. (1981).

6.4.1.3 Empirical Correlations based on Plasticity Index

6.4.1.3.1 Voight (1973)

Voight (1973) present a relationship between plasticity index and residual strength coefficient, referred as μ'_r, as shown in Figure 6.12. The relationship was developed using data from other researchers. Voight (1973) argued that “mineralogical factors affect Atterberg index parameters, so it does not seem surprising that strength and plasticity can be correlated.”

Voight (1973) presents an argument that the scatter in Figure 6.12 may be caused by the low plasticity measured for some of the soils, such as Cucaracha shale. Voight (1973) attributes it to either flocculation or to insufficient breakdown of particle aggregates. Voight (1973) concludes that the plasticity index appears to be a useful guide to residual strength of natural

soils but he recommends further examination of the correlation presented in Figure 6.12. Voight (1973) does not show agreement with back-analysis of some case histories or provide sufficient data to verify his conclusion.

6.4.1.3.2 Kanji (1974)

In response to the empirical correlation suggested by Voight (1973) between plasticity index and residual shear strength of natural soils. Kanji (1974) presents a summary of previous research on peak and residual shear strength and plotted these friction angles versus PI of each soil as shown in Figure 6.13. Kanji (1974) endorses the Voight (1973) findings that the index property of a soil can be correlated to the residual friction angle. Kanji (1974) endorses the work by Voight (1973) without showing any agreement with the back-calculated values and without performing any laboratory tests to support his conclusion.

6.4.1.3.3 Seycek (1978)

Seycek (1978) mentions studying the correlation between residual friction angle and LL, CF, plasticity index (PI), and activity (A_c). Seycek (1978) suggests that the best correlation appeared to be between ϕ'_r and plasticity index (PI) as shown in Figure 6.14. Seycek (1978) also mentions performing 195 tests on different soils but no test results are presented. Based on data shown in Figure 6.14, Seycek (1978) concludes that the best correlation appeared to be between residual shear strength and PI. But Seycek (1978) acknowledges that this correlation is not sufficient to enable the simple index tests to be substituted for residual shear strength testing. The scatter on Figure 6.14, especially at plasticity index of 20%, shows that there is a large variation in residual friction angle up to 20°. In the presence of such a huge difference in ϕ'_r with PI, the conclusion presented by Seycek (1978) that the best correlation exists between the residual friction angle and PI is not justified. Figure 6.14 shows that the difference in ϕ'_r vales for PI between 20 to 80% is so large that no useful conclusion can be made.

6.4.1.3.4 Lupini et al. (1981)

As discussed earlier, Lupini et al. (1981) present ring shear test results for a number of natural soils. The test results for fifty two different soils are plotted in Figure 6.10 and present a

relationship between ϕ'_r and PI. Lupini et al. (1981) suggest that simple correlations with index properties are inadequate for the prediction of residual strength for engineering purposes.

In summary, correlations between residual strength and soil index properties and gradation cannot be generalized according to Lupini et al. (1981). They may be valuable in studying the residual strength of a particular variable soil deposit, provided that they properly reflect changes in the more fundamental properties of particle shape, gradation, mineralogy, porewater chemistry, etc., but not for a range of soil deposits

6.4.1.3.5 Mesri and Shahien (2003)

Mesri and Shahien (2003) using the data of Stark and Eid (1994 and 1997) and Eid (1996) suggest new correlations between friction angles, both ϕ' and ϕ'_r, and index properties (PI) as shown in Figure 6.15. Mesri and Shahien (2003) acknowledge the precision of Stark and Eid (1994 and 1997) test data and empirical correlations by stating that the correlation includes less scatter because the testing used a consistent sample preparation and includes the influence of σ'_n. However, Mesri and Shahien (2003) reason that the absence of reliable data on CF for some case histories they analyzed so the Stark and Eid (1994 and 1997) data was plotted using PI instead of LL and CF. Mesri and Shahien (2003) show three different plots one each for effective normal stresses of 50, 100, and 400 kPa but each plot shows the relationship for both drained residual and fully softened friction angles.

Mesri and Shahien (2003) acknowledge the scatter in data by previous researchers who relate residual friction angle with PI. But the scatter in Figure 6.15 for drained residual friction angle values especially for the PI < 50% is still greater than 7° which suggests that only using PI does not provide a reliable estimate of drained residual friction angle for cohesive soils. In other words, PI does not encapsulate the influence of LL (clay mineralogy) and CF (amount of clay minerals) in the correlation.

Further, Mesri and Shahien (2003) suggest that for many clay and shale compositions, PI ≈ LL*CF which implies that PI does encapsulate both LL and CF. Additional explanation is not presented.

6.4.1.3.6 Others

Other researchers who developed a drained residual friction angle - PI correlation include Vaughan et al. (1979), Chandler (1984), and Lambe (1985). Chandler (1984) plots his data on the empirical correlation suggested by Lupini et al. (1981) and has not specifically suggested this as an empirical correlation for ϕ'_r.

6.4.1.4 Empirical Correlations based on Other Parameters

Some other researchers present empirical correlations for drained residual friction angle of cohesive soils based on different parameters besides LL, CF, PI, A_c, and/or σ'_n, which are discussed below.

6.4.1.4.1 Collotta et al. (1989)

Collotta et al. (1989) suggest that the residual friction angle is function of a parameter called as CALIP. Collotta et al. (1989) relates CALIP which includes LL, CF, and PI of the soil and suggests Equation 6.1 to estimate CALIP. The value of CALIP is then used to estimate the value for drained residual friction angle as shown in Figure 6.16.

$$CALIP = (CF^2 * LL * PI * 10^{-5}) \quad (6.1)$$

Collotta et al. (1989) also present a relationship between drained residual friction angle and CF using the same data to provide a comparison with the empirical correlation in Figure 6.16. Collotta et al. (1989) determine that the relationship between ϕ'_r and CALIP shown in Figure 6.16 shows less scatter than the scatter observed in the relationship between ϕ'_r and CF.

The correlation presented by Collotta et al. (1989) considers all of the index properties, i.e., LL, CF, and PI, making it complex to calculate CALIP and then estimate ϕ'_r from Figure 6.16. Although CALIP considers LL, CF, and PI, there is still considerable scatter in Figure 6.16 and more scatter than observed in the empirical correlations suggested by Stark and Eid (1994) and Stark et al. (2005a). The additional scatter in Collotta et al. (1989) is probably due to the effect of stress dependency on the residual shear strength or drained residual friction angle not being incorporated. Furthermore, Collotta et al. (1989) do not show any verification of their

correlation with case histories. Thus, the empirical correlation suggested by Collotta (1989) appears less reliable than Stark and Eid (1994) and Stark et al. (2005a).

6.4.1.4.2 Wesley (2003)

Wesley (2003) suggests a new method of comparing ϕ'_r with a parameter termed ΔPI. Wesley (2003) proposes calculating ΔPI using PI and LL which is given in Equation 6.2 and uses the A-line from the plasticity chart suggested by Casagrande (1948) to develop the ϕ'_r relationship shown in Figure 6.17.

$$\Delta PI = PI - 0.73(LL - 20) \quad (6.2)$$

Wesley (2003) suggests that ΔPI is the distance on the plasticity chart from the A-line for a given soil. The value of ΔPI is positive or negative if a soil lies above or below A-line, respectively. Although Wesley (2003 and 2004) concludes that his proposed correlation shows less scatter, Figure 6.17 shows that for the same ΔPI value the variation in ϕ'_r values is 8-10°. Furthermore, Wesley (2003) presents data for clays mostly for ΔPI < 20 and only three points show ΔPI > 25 of which only one point represents ΔPI > 50. Also, Wesley (2003) has not incorporated the stress dependent nature of ϕ'_r. Thus, even after complicating the use of simple index parameters with ΔPI, the correlation does not yield a better correlation than Stark and Eid (1994) and Stark et al. (2005a).

6.4.1.4.3 Tiwari and Marui (2005)

Tiwari and Marui (2005) compare the residual friction angle with the mineralogical composition of a soil. Tiwari and Marui (2005) suggest using the mineralogical composition determined from x-ray diffraction instead of using more common index properties of a soil. Tiwari and Marui (2005) suggest the biggest advantage of this method is the small quantity of soil (almost 30 g) required to perform the x-ray diffraction test. The empirical correlation suggested by Tiwari and Marui (2005) may be useful for theoretical studies but may not be useful for the practitioners because of difficulties in performing x-ray diffraction tests.

The purpose of an empirical correlation is to estimate the desired soil property using common index parameters, such as LL, PI, and CF which can be reliably and conveniently measured and understood by the practitioners.

6.4.2 New Proposed Empirical Correlation for Drained Residual Friction Angle

The empirical correlation for drained residual friction angle suggested by Stark et al. (2005a) is widely used in geotechnical engineering because it contains small scatter as compared to all other similar empirical correlations and incorporates the three main factors, clay mineralogy (LL), amount of clay mineral (CF), and effective normal stress. The only parameters required to estimate the drained residual friction angle are LL and CF which are conveniently measured. The correct estimate of LL, and CF can help in estimating a reliable ϕ'_r value for that soil. Thus, the correlation suggested by Stark et al. (2005a) plays an important role in practice by providing estimates of ϕ'_r values for use in preliminary design and also serving as a check on data obtained from laboratory tests.

The empirical correlation suggests three different CF groups, i.e., CF $\leq$ 20%, 25% $\leq$ CF $\leq$ 45%, and CF $\geq$ 50% which account for three different shearing behaviors, i.e., rolling, transitional, and sliding, respectively, as suggested by Lupini et al. (1981) and Skempton (1985).

Stark et al. (2005a) use ball milled soil samples processed through Number 200 sieve for highly overconsolidated clays and for all other soils pulverized using a mortar and pestle and processed though Number 40 sieve. Ball milling of highly overconsolidated clays such as shales, claystones, and mudstone that contain a high degree of induration (aggregation), results in a sample disaggregated clay particles (Mesri and Cepeda-Diaz, 1986) that facilitates measurement of the residual strength. The clay samples that are not highly overconsolidated or aggregated should not be ball milled because the ball milling would change the texture and gradation of the soil (Stark et al., 2005a). Because most of commercial laboratory may not have a ball milling facility available, Stark et al. (2005a) provide empirical correlations for ball milled LL and CF, using ASTM derived LL and CF values. However, these correlations contain limited data and additional data was developed herein to reinforce the correlations. The present study also uses additional data for seventeen soils from Eid (2006) to improve the LL and CF correlations presented by Stark et al. (2005a).

Stark et al. (2005a) present a separate trend line for each effective normal stress of 100, 400, and 700 kPa in each CF group. Thus, CF identifies the CF group and LL determines ϕ'_r for three different effective normal stresses. Therefore, the correct estimate of LL and CF can be used to estimate ϕ'_r at various effective normal stresses to develop a stress dependent residual strength failure envelope. This stress dependent envelop can be used directly in stability analyses of preexisting landslides. Because a nonlinear residual strength failure envelope has more curvature at low effective normal stress, it was decided to add data for an effective normal stress less than 100 kPa. Thus, the Stark et al. (2005a) correlation was extended during the present study by adding data for effective normal stress of 50 kPa in all three CF groups and suggesting new trend lines for the other effective normal stresses to reflect new data in all three CF groups.

The empirical correlation proposed by Stark et al. (2005a) are available in graphical form which makes it difficult to incorporate in computer based applications such as in the slope stability software. As a result, the present study developed separate equation for each trend line of the newly proposed correlation which can be used to estimate ϕ'_r using LL only. The CF value decides the required equation to be used and the LL value is the only input parameter to estimate ϕ'_r from the equations.

6.4.2.1 Effect of Sample Preparation on Drained Residual Friction Angle

The residual strength is a fundamental property because the soil structure, stress history, particle interference, and diagenetic bonding have been removed by continuous shear displacement in one direction. As a result, the residual strength is controlled by the frictional resistance of individual clay particles, oriented primarily face-to-face, sliding across one another. The frictional shear resistance induced by sliding along individual clay particles is controlled by the fundamental characteristics of the clay particles, e.g., type of clay mineral(s) and the quantity or percentage of the clay mineral(s). Ball milling of the sample simply facilitates the measurement of the residual strength of remolded overconsolidated clays, mudstones, claystones, and shales in the laboratory by expediting the disaggregation process that occurs in the field over many years and a lot of shear displacement. This results in smaller shear displacements, and thus time, required to achieve a residual strength condition in laboratory ring shear testing on remolded material.

In the field, the residual strength condition is achieved after a movement on the order of several feet has occurred (Skempton, 1964). The shearing results in increasing the fine contents along the shear surface by pushing the silt and sand away from the shear surface. Mesri and Cepeda-Diaz (1986) conclude that "the shearing process itself disaggregates and orients even the clay plates at the surface of aggregates adjacent to the shear plane." Chandler (1969) measured a higher CF in the shear surface than the overall specimen indicating disaggregation during shear. Thus, during the process of reaching the residual condition in the field, the aggregated clay particles are broken down to close to the original clay particle size. The disaggregation of the clay particles in the laboratory is facilitated by ball milling or pulverizing by some other means to process the soil sample through the Number 200 sieve to simulate the field conditions. As discussed before, a remolded soil sample is preferred for laboratory residual shear strength testing because of difficulties in sampling, orienting, and shearing in the field direction undisturbed shear surface specimens. However, the use of a remolded specimen results in a larger shear displacement being required in the laboratory than an undisturbed shear surface specimen unless the sample is ball milled and processed through the Number 200 sieve and the specimen is presheared prior to drained shearing. This applies to heavily overconsolidated clays, claystones, mudstones, shales, and other highly aggregated materials. Non-aggregated material does not form a well defined shear surface so a remolded specimen is usually used anyways. The value of drained residual friction angle is not affected by sample preparation procedure if the true residual shear strength is reached because the particles are disaggregated and oriented parallel to the direction of shear. Thus, sample preparation is not likely to affect the drained residual shear strength or drained residual friction angle but it does affect the measurement of index properties, such as LL and CF, as discussed below. Because the empirical correlations for drained residual friction angle developed herein uses LL and CF, a correct estimate of LL and CF is necessary to estimate the drained residual friction angle.

6.4.2.2 Effect of Sample Preparation on Liquid Limit, Clay-Size Fraction

Preparation of a remolded specimen can influence the measurement of liquid limit (LL) and clay-size fraction (CF). Mesri and Cepeda (1986) conclude that most of the heavily overconsolidated clays, mudstones, claystones, and shales possess varying degrees of induration. This induration involves diagenetic bonding between clay mineral particles by carbonates, silica,

alumina, iron oxides, and other ionic complexes. The degree of induration (aggregation) that survives a particular sample preparation procedure will influence the measurement of the index properties (La Gatta, 1970, Townsend and Banks, 1974). To simulate the field conditions under which the residual strength is mobilized the material should be disaggregated before measuring LL and CF. Mesri and Cepeda (1986) suggest ball milling highly overconsolidated clay specimens to "free" or disaggregate the clay particles. Ball milling is suggested only for highly overconsolidated clays, mudstones, claystones, and shales because they possess substantial diagenetic bonding that are usually not destroyed using a mortar and pestle. Because LL and CF are used herein to infer clay mineralogy and quantity of particles smaller than 0.002 mm, respectively, the mudstone, claystone, and shale particles should be disaggregated and processed through the Number 200 sieve. To facilitate processing the soil through the Number 200 sieve, ball milling is used to disaggregate the clay particles. A representative air-dried sample is used for ball milling (Mesri and Cepeda, 1986).

Ball milling of highly overconsolidated clays results in a better estimate of the actual LL than the ASTM standard test method (2008a), because more of the diagenetic bonding and induration is eliminated which allows more particle surface area to be exposed and to hydrate than if the clay particles are not disaggregated. Ball milling usually results in a higher LL than that obtained using the ASTM standard test method (2008a). For example, La Gatta (1970) shows an increase in LL from 49% to 156% using disc milling of Cucaracha shale for six minutes. The higher LL is caused by the ball milling causing more particle disaggregation than the ASTM standard method and thus more water adsorption. Commercial laboratories or other testing facilities where ball milling facility is not available, other means can be used to pulverize the material and process it through the Number 200 sieve for the estimating LL.

The clay specimens which are not indurated (aggregated) do not require disaggregation of clay particles by ball milling or any other means to process through Number 200 sieve instead a specimen processed through Number 40 sieve as suggested by ASTM can be used for measuring LL and CF. The ball milling of such clay specimens which are not indurated (aggregated) would result in changing the texture and gradation of the soil. Stark et al. (2005a) suggest using judgment to determine on whether or not a material should be ball milled. This decision can be made after examination of the chunks of claystone, mudstone, shale, or overconsolidated clay

and determining whether the chunks can be sufficiently broken down with a mortar and pestle to disaggregate the clay particles and process the material through Number 200 sieve.

Stark et al. (2005a) present a relationship between ball milled derived LL and ASTM derived LL using 14 soil samples of highly overconsolidated clays (see Figure 6.6). The correlation suggested by Stark et al. (2005a) facilitated estimating the ball milled derived LL from the ASTM derived LL because ball milling requires special equipment and extra effort that may not be available in practice. Because commercial laboratories primarily, if not exclusively, utilize the ASTM standard procedure (ASTM, 2008a) to measure LL, this correlation can be used to estimate the ball milled derived LL and thus compare ring shear test results with the empirical correlation for drained residual friction angle presented by Stark et al. (2005a) to assess agreement.

Because the relationship between ball milled and ASTM derived LL suggested by Stark et al. (2005a) has limited data, new data was developed herein to enhance the relationship. Test results of two more soils tested during present study along with test results of 12 more soils tested by Eid (2006) were used to determine the new relationship. Table 6.1 shows 28 soil samples tested by Stark et al. (2005a), Eid (2006), and during the present study to augment the LL empirical correlation suggested by Stark et al. (2005a). A relationship between the ASTM derived LL, referred herein as $LL_{\#40}$, and the ratio of LL measured on a sample processed through Number 200 sieve, referred herein as $LL_{\#200}$, was developed using the data shown in Table 6.1. The resulting relationship is shown in Figure 6.18 and can be used with an ASTM derived value of LL ($LL_{\#40}$) to estimate the $LL_{\#200}$ value for a particular soil. This should reduce the need for commercial laboratories to ball mill or pulverize claystones, shales, and mudstones and process them through the Number 200 sieve and facilitate usage of the empirical relationships. The relationship shown in Figure 6.18 can be expressed using Equation 6.3 and can be used to estimate the ratio of the liquid limit values. The relationship presented in Equation 6.1 is in agreement with the equation suggested by Stark et al. (2005a).

$$\frac{LL_{\#200}}{LL_{\#40}} = 0.003\left(LL_{\#40}\right)+1.23 \qquad (6.3)$$

Figure 6.18 shows the LL is affected by sample preparation procedure. This is in agreement with the results reported by La Gatta (1970) for Cucaracha shale from the Panama Canal in which LL increased from 49% to 156% by crushing the shale for 6 min in a disc mill. It is anticipated that the higher the LL, the greater the bonding between clay particles, the more difficult disaggregation of the clay particles becomes, and the higher the difference between the values of $LL_{\#40}$ and $LL_{\#200}$. Thus, high plasticity claystones, shales, and mudstones should be processed through Number 200 sieve before measuring LL.

Preparation of a remolded specimen also can influence the measurement of CF as well as LL. Stark and Eid (1994 and 1997) and Stark et al. (2005a) suggest that the material should be disaggregated before measuring CF to simulate the field conditions under which the residual strength is mobilized, i.e., disaggregated clay particles which results in a higher value of CF. Therefore, Stark et al. (2005a) suggest using soil processed through the Number 200 sieve for highly overconsolidated clays to measure CF.

Because commercial laboratories primarily utilize the ASTM standard procedure (ASTM, 2008b) to measure the CF, the empirical correlation shown in Figure 6.7 has facilitated use of the empirical correlations for drained residual friction angle presented by Stark et al. (2005a). Stark et al. (2005a) use 14 samples of highly overconsolidated clays establish this relationship. Test results for 18 additional soils obtained from Eid (2006) were used to augment the CF relationship suggested by Stark et al. (2005a) and are shown in Table 6.1.

A relationship between the ASTM derived values (ASTM, 2008b) of CF, called herein $CF_{\#40}$, and the ratio of CF measured using material processed through Number 200 sieve, called herein $CF_{\#200}$, to $CF_{\#40}$ values is shown in Figure 6.19. Because an increase in CF results in lower values of ϕ'_r, it is important to select the correct CF group to estimate ϕ'_r values from the empirical correlations developed during present study. Correct estimation of CF may be important for CF group 1 and 2 but is not important for CF group 3. Because for $CF_{\#40} > 50\%$, $CF_{\#200}$ will also be greater than 50%, it will not affect the ϕ'_r values estimated from the empirical correlation presented by Stark et al. (2005a) with both values being in the highest CF group.

Figure 6.19 shows that the $CF_{\#200}/CF_{\#40}$ ratio decreases as $CF_{\#40}$ increases. It is anticipated that the decrease is caused by $CF_{\#40}$ value being in better agreement with the $CF_{\#200}$

value at higher values of CF. This may be attributed to the dispersing agent, sodium hexametaphosphate, being more effective in high plasticity soils than low plasticity soils.

The relationship in Figure 6.19 can be used to estimate the $CF_{\#200}$ using $CF_{\#40}$. This value of $CF_{\#200}$ can be used to estimate the drained residual friction angle from the empirical correlations suggested in the present study. The relationship in Figure 6.19 can be expressed by Equation 6.4. $CF_{\#40}$ can be used to estimate the value of $CF_{\#200}$ which can be used to estimate drained residual friction angle from the empirical correlation presented in the following section.

$$\frac{CF_{\#200}}{CF_{\#40}} = 0.0002\left(CF_{\#40}\right)^2 - 0.0278\left(CF_{\#40}\right) + 2.15 \qquad (6.4)$$

In summary, the most important factor in disaggregating the material is the level to which the clay bonding is removed. The soil sample processed through Number 200 sieve results in a greater amount of disaggregation than the ASTM sample preparation procedure that requires processing through the Number 40 sieve and index properties that better represent the residual strength of the material (Townsend and Banks, 1974, Mesri and Cepeda, 1986). To facilitate use of the empirical correlation for drained residual friction angle in practice, adjustment factors for LL and CF are presented in Figures 6.18 and 6.19, respectively, to adjust ASTM derived values of LL and CF, respectively.

6.4.2.3 Inclusion of σ'_n = 50 kPa in Drained Residual Friction Angle Correlation

Many researchers have suggested a stress dependent relationship between residual shear and effective normal stress (Chandler, 1977, Bromhead, 1978, Lupini et al., 1981, Stark and Eid, 1994 and 1997, and Stark et al., 2005a). Stark and Eid (1994) and Stark et al. (2005a) recommend using a stress dependent residual strength failure envelope in stability analyses. The nonlinear residual strength failure envelope is most pronounced, i.e., have greater curvature, at low effective normal stresses, e.g., σ'_n < 100 kPa, and it becomes nearly linear at higher effective normal stresses.

Stark and Eid (1994) and Stark et al. (2005a) present a relationship between LL and drained residual friction angle for effective normal stresses of 100, 400, and 700 kPa for three CF groups. However, Stark and Eid (1994) and Stark et al. (2005a) do not present a trend line for an

effective normal stress less than 100 kPa. Review of data generated herein indicated significant curvature of the residual failure envelope for σ'_n between zero and 100 kPa. To capture this nonlinearity, it was decided to develop and include a trend line for σ'_n = 50 kPa so a residual failure envelope could be developed using σ'_n equal to 0, 5, 100, 400, and 700 kPa. Figure 6.20 illustrates the stress dependent residual strength failure envelope at lower effective normal stresses. Therefore, the present study extended the correlation of Stark et al. (2005a) by adding data and a trend line for σ'_n = 50 kPa in all three CF groups, CF $\leq$ 20%, 25% $\leq$ CF $\leq$ 45%, and CF $\geq$ 50%, respectively. Figure 6.21 through Figure 6.23 present the data and trend lines for CF groups Figure 6.24 presents the new residual strength correlation for all values of σ'_n and the three CF groups.

During the present study, the ring shear data for an effective stress of 50 kPa was collected by Eid (1996) for 36 soils from the data generated by Stark et al. (2005a), and data generated for fine soils during the present study.

The empirical correlation in Figure 6.24 can be used to estimate the drained residual friction angles for effective normal stresses of 50, 100, 400, and 700 kPa using CF and LL of the soil. The estimated drained residual friction angle for each value of σ'_n can be used to calculate the residual shear stress which can be used to plot the drained residual failure envelopes. The stress dependent envelope developed from the empirical correlation can be used in the stability analysis of preexisting landslides. Figure 6.20 presents an excellent comparison of the stress dependent residual strength failure envelope obtained from the ring shear test results and from new empirical correlation in Figure 6.24. Other comparisons between ring shear data and empirical correlation in Figure 6.24 made during this study are also in agreement.

In summary, the addition of data and a trend line for an effective normal stress of 50 kPa in the empirical correlation shown in Figure 6.24 provides a better stress dependent residual strength failure envelope than prior correlations for use in stability analyses.

6.4.2.4 Equations for New Drained Residual Friction Angle Empirical Correlations

Stark and Eid (1994) and Stark et al. (2005a) present a relationship between LL and drained residual friction angle in graphical form. This required consulting the figure to obtain values of drained residual friction angles for a given LL. Because the empirical correlation

proposed by Stark et al. (2005a) is widely used by the geotechnical community and consulted frequently it was decided to develop an expression for each trend line to facilitate use of the correlation in practice.

The present study considered each CF group separately and developed an equation for all four effective normal stresses, i.e., 50, 100, 400, and 700 kPa, trend lines. The mathematical expressions developed herein are in excellent agreement with the trend lines suggested by Stark et al. (2005a). The coefficient of determination (R^2) which is the total variation in the dependent variable explained by the independent variable in statistical language has also been calculated by performing the regression analysis. Because the trend lines by Stark et al. (2005a) were developed based on the engineering judgment and considering the behavior of natural soils, the R^2 value determined using statistical tools for each trend line is below unity (see Figures 6.21 to 6.23). Although lower the R^2 values show scatter in the data developed from ring shear testing in the laboratory but still the empirical correlation gives a good estimate of residual friction angle for a natural soil. Furthermore, availability of limited data for CF Group 1 and 2 and variation in the test results result in a lower value for R^2.

A set of four equations was developed for each CF group. The empirical correlation for drained residual friction angles of CF group 1 and for LL values ranging from 24% to less than 80% ($24\% \leq LL < 80\%$) are given below as Equations (6.5). The limit for LL is specified because no ring shear data is available out of this LL range. The ring shear data along with the trend lines sketched by Stark et al. (2005a) for CF Group 1, and the new equations are plotted in Figure 6.21. The trend lines sketched from the newly developed Equations (6.5) are also plotted on Figure 6.21 to compare the prior trend line with the equation generated trend line. Figure 6.21 shows that the trend lines plotted using Equations (6.5) are in excellent agreement with the trend lines suggested by Stark et al. (2005a). Thus, a second degree polynomial can best represent the trend lines for CF Group 1 for all four effective normal stresses.

$$\left(\phi_r\right)_{\sigma_n'=50\text{kPa}} = 39.71 - 0.29(\text{LL}) + 6.63\text{x}10^{-4}(\text{LL})^2 \quad (6.5a)$$

$$\left(\phi_r\right)_{\sigma_n'=100\text{kPa}} = 39.41 - 0.298(\text{LL}) + 6.81\text{x}10^{-4}(\text{LL})^2 \quad (6.5b)$$

$$(\phi_r)_{\sigma_n'=400kPa} = 40.24 - 0.375(LL) + 1.36x10^{-3}(LL)^2 \quad (6.5c)$$

$$(\phi_r)_{\sigma_n'=700kPa} = 40.34 - 0.412(LL) + 1.683x10^{-3}(LL)^2 \quad (6.5d)$$

Another set of four equations was developed for CF Group 2 and LL values ranging from 30% to less than 130% (30% $\leq$ LL < 130%) are given below in Equations (6.6). Again the limit for LL is specified because ring shear data is available only for this specific LL range. The ring shear data along with the trend lines sketched by Stark et al. (2005a) for CF Group 2 are plotted in Figure 6.22. The trend lines sketched from the newly developed equations are also plotted on Figure 6.22 for comparison. Figure 6.22 shows that the trend lines plotted by using Equations (6.6) are in good agreement with the trend lines suggested by Stark et al. (2005a). Thus, a third degree polynomial can be used to represent the trend lines for CF Group 2 and for all four effective normal stresses.

$$(\phi_r)_{\sigma_n'=50kPa} = 31.4 - 6.79x10^{-3}(LL) - 3.616x10^{-3}(LL)^2 + 1.864x10^{-5}(LL)^3 \quad (6.6a)$$

$$(\phi_r)_{\sigma_n'=100kPa} = 29.8 - 3.627x10^{-4}(LL) - 3.584x10^{-3}(LL)^2 + 1.854x10^{-5}(LL)^3 \quad (6.6b)$$

$$(\phi_r)_{\sigma_n'=400kPa} = 28.4 - 5.622x10^{-2}(LL) - 2.952x10^{-3}(LL)^2 + 1.721x10^{-5}(LL)^3 \quad (6.6c)$$

$$(\phi_r)_{\sigma_n'=700kPa} = 28.05 - 0.2083(LL) - 8.183x10^{-4}(LL)^2 + 9.372x10^{-6}(LL)^3 \quad (6.6d)$$

The trend lines in CF Group 3, i.e., CF $\geq$ 50%, is divided into two parts to develop the equations to ensure that new trend lines are in agreement with the trend lines suggested by Stark et al. (2005a). Two equations are required to capture the complicated slope of each trend line. Figure 6.23 shows that the left portion of each trend line, i.e., for LL < 120%, can be represented by a polynomial expression. However, right portion of trend line, i.e., LL $\geq$ 120%, can best be represented by a linear relationship. This necessitated using separate equations for LL values ranging between 40% and less than 120% and LL values ranging between 120% and 300%. The upper and lower limits for LL values are specified because of the availability of ring shear test data for this range.

The ring shear data along with the trend lines sketched by Stark et al. (2005a) for CF Group 3 are plotted in Figure 6.23. The trend lines sketched using Equations (6.7 and 6.8) are also plotted on Figure 6.23 for comparison purposes. Figure 6.23 shows that the trend lines plotted by using Equations (6.7 and 6.8) are in close agreement with the trend lines suggested by Stark et al. (2005a). Thus, a third degree polynomial can represent the trend lines for CF Group 3 and for all four effective normal stresses and for 30% $\leq$ LL < 120%. Whereas, the trend lines for CF Group 3 and for 120% $\leq$ LL $\leq$ 300% can be represented using a linear relationship (straight line).

$$(\phi_r)_{\sigma_n'=50kPa} = 33.5 - 0.31(LL) + 3.9x10^{-4}(LL)^2 + 4.4x10^{-6}(LL)^3 \quad (6.7a)$$

$$(\phi_r)_{\sigma_n'=100kPa} = 30.7 - 0.2504(LL) - 4.2053x10^{-4}(LL)^2 + 8.0479x10^{-6}(LL)^3 \quad (6.7b)$$

$$(\phi_r)_{\sigma_n'=400kPa} = 29.42 - 0.2621(LL) - 4.011x10^{-4}(LL)^2 + 8.718x10^{-6}(LL)^3 \quad (6.7c)$$

$$(\phi_r)_{\sigma_n'=700kPa} = 27.7 - 0.3233(LL) + 2.896x10^{-4}(LL)^2 + 7.1131x10^{-6}(LL)^3 \quad (6.7d)$$

$$(\phi_r)_{\sigma_n'=50kPa} = 12.03 - 0.0215(LL) \quad (6.8a)$$

$$(\phi_r)_{\sigma_n'=100kPa} = 10.64 - 0.0183(LL) \quad (6.8b)$$

$$(\phi_r)_{\sigma_n'=400kPa} = 8.32 - 0.0114(LL) \quad (6.8c)$$

$$(\phi_r)_{\sigma_n'=700kPa} = 5.84 - 0.0049(LL) \quad (6.8d)$$

The empirical correlation for drained residual friction angle developed during the present study and is shown in Figure 6.24. The mathematical relationships between LL and ϕ'_r, in Equations (6.5 to 6.8), along with the conditions discussed above, i.e., for CF and LL, can be used to develop a stress dependent residual strength failure envelope for a cohesive soil instead of Figure 6.24. This may facilitate slope stability software developers in incorporating the empirical correlation in their software and use a nonlinear strength envelop in stability analyses.

6.5 Empirical Correlation for Drained Fully Softened Friction Angles of Clays

6.5.1 Previous Empirical Correlations for Drained Fully Softened Friction Angles

The history of comparing fully softened friction angle (ϕ' or ϕ'_{fs}) with PI can be traced back to the late 1950's. Bjerrum and Simons (1960) present a relationship, which they call the Skempton-Gibson-Bjerrum curve, that relates ϕ'_{fs} to PI of normally consolidated soils. Kanji (1974), while suggesting the relationship between ϕ'_r and PI, stated that the correlations between ϕ'_{fs} and PI published by Kenney (1959), Holt (1962), Brooker and Ireland (1965), Mitchell (1965), Bjerrum (1967) and Deere (1967) had considerable scatter. Skempton (1970) states that the fully softened shear strength of a soil corresponds to the random arrangement of clay particles and it equals the peak strength of a normally consolidated soil sample. Therefore, all of the prior work on fully softened shear strength may have incorporated the effect of consolidation pressure and stress history because remolded specimens were not used. This may have contributed to the large scatter in prior correlations and stated by Kanji (1974) as shown in Figure 6.13. Therefore, all of the empirical correlations on fully softened shear strength and/or ϕ'_{fs} presented by researchers prior to Skempton (1970) are not considered reliable. Empirical correlations for drained fully softened friction angle suggested by various researchers after that are being used in geotechnical engineering are discussed below.

6.5.1.1 Empirical Correlations based on Liquid Limit

6.5.1.1.1 Stark and Eid (1997)

Stark and Eid (1997) present an empirical correlation for drained fully softened friction angle of clays by establishing a relationship between drained fully softened friction angle and LL incorporating the effect of CF. The empirical correlations shown in Figure 6.25 were developed using ring shear test results for 24 clays and shales. It was observed that the drained fully softened friction angle also decreases with increasing LL and increasing CF. The liquid limit and clay-size fraction provide an indication of particle shape (clay mineralogy) and particle size (CF), respectively. Increasing the platyness of the clay particles results in greater tendency for face-to-face interaction and hence resulting in a smaller fully softened shear strength.

Stark and Eid (1997) conclude that the drained fully softened strength failure envelope is also stress dependent (nonlinear) and they incorporate the stress dependent effect in the empirical correlation. Therefore, Stark and Eid (1997) consider mineral composition, CF, and effective normal stress on the drained fully softened friction angle. Stark and Eid (1997) use three CF groups, i.e., CF $\leq$ 20%, 25% $\leq$ CF $\leq$ 45%, and CF $\geq$ 50% (see Figure 6.25), for the correlation. Stark and Eid (1997) show three different values of drained fully softened friction angle corresponding to a given LL and CF for three different effective normal stresses, i.e., 50, 100, and 400 kPa. The values of drained fully softened friction angle for three different effective normal stresses can be used to develop a stress dependent drained fully softened strength failure envelope for stability analysis of a first-time landslide or a slope with no prior sliding.

Stark and Eid 91997) used ASTM D4318 and D422 derived values of LL and CF for clays with little or no induration (aggregation) and disaggregated derived LL and CF values for highly overconsolidated clays, mudstones, claystones, and shales to suggest the correlation in Figure 6.25.

In summary, the correct estimate of LL and CF for a clay sample is required to estimate the values of drained fully softened friction angle from empirical correlation suggested by Stark and Eid (1997). The estimated values of drained fully softened friction angles can be used to develop a stress dependent fully softened strength failure envelope which can be used in a slope stability analysis. Because the empirical correlation presented by Stark and Eid (1997) were developed using LL, CF and effective normal stress, the correlation has shown an agreement with back-calculated drained fully softened friction angles. Therefore, the correlation is widely used in geotechnical community. Because of the reliability of the ring shear test data presented by Stark and Eid (1997) and its verification with case histories, other researchers, e.g., Mesri and Shahien (2003), have used this data to develop similar correlations.

6.5.1.1.2 Stark et al. (2005a)

Stark et al. (2005a) extended the work of Stark and Eid (1997) which proposed an empirical correlation for drained fully softened friction angle of cohesive soils based on the ring shear test results on 36 clays and shales. The empirical correlation proposed by Stark et al.

(2005a) is shown in Figure 6.26. Stark et al. (2005a) augmented the Stark and Eid (1997) correlation with test results for twelve additional soils.

Stark et al. (2005a) use ball milled samples processed through Number 200 sieve for highly overconsolidated clays to estimate LL and CF and ASTM D4318 and D422 test methods to estimate LL and CF, respectively, for clays without any induration (aggregation) to develop the empirical correlation shown in Figure 6.26. Stark and Eid (1997) provide a detailed description of the effect of sample preparation and ball milling on determining the index properties of a soil which is described under the empirical correlation for drained residual friction angle and not repeated here.

Because commercial laboratories primarily utilize the ASTM D4318 and D422 test methods (ASTM, 2008a and 2008b) to determine the LL and CF, respectively, Stark et al. (2005a) proposed empirical correlations, discussed above, for estimating ball milled derived values of LL and CF from ASTM derived LL and CF (see Figures 6.6 and 6.7).

The scatter for each CF group in Figure 6.26 is only up to 3-4° compared to 6-10° found using other correlations, such as Mesri and Abdel-Ghaffar (1993) and Mesri and Shahien (2003) even though the same data is used but plotted versus PI. Thus, an empirical correlation presented by Stark et al. (2005a) showing a relationship between ϕ'_{fs} and LL while incorporating the effect of CF and effective normal stress shown in Figure 6.26 provides the most reliable estimate of ϕ'_{fs}.

6.5.1.2 Empirical Correlations based on Plasticity Index

6.5.1.2.1 Kenney (1959)

Kenney (1959) suggests a relationship between *sin* (ϕ' or ϕ'_{fs}) and PI for normally consolidated soils as shown in Figure 6.27. Earlier, Gibson (1953) presented a relationship between ϕ' and PI based on his triaxial compression test results which led to the Skempton-Gibson-Bjerrum correlation. Figure 6.27 shows the plot by Kenney (1959) and the data for pure clays from Olsen (1974) and by Mitchell and Soga (2005). Figure 6.27 shows a lot of scatter which suggests that correlating *sin* ϕ'_{fs} with PI may not provide a correct correlation.

6.5.1.2.2 Bjerrum and Simons (1960)

Bjerrum and Simons (1960) state that the value of ϕ' or ϕ'_{fs} for any given clay varies with many different factors, so a correlation with only one parameter cannot be expected. Bjerrum and Simons (1960) present a correlation that, which they call the Skempton-Gibson-Bjerrum curve, which relates ϕ'_{fs} to PI of normally consolidated soils (see Figure 6.28). The history of this curve can be traced back to Gibson (1953) where he presents a relationship between ϕ'_{fs} to PI. Bjerrum and Simons (1960) show that the greater the plasticity, the smaller the angle of shearing resistance with respect to effective stress. Therefore, Bjerrum and Simons (1960) present a relationship between ϕ'_{fs} at $(\sigma'_1/\sigma'_3)_{max}$ from triaxial compression test result and the plasticity index as shown in Figure 6.29. Bjerrum and Simons (1960) acknowledge that the scatter from the trend line is appreciable but still a rough correlation with the plasticity index is present. Bjerrum and Simons (1960) do not include quick clays in the correlation because these clays generally exhibit low plasticity index due to a reduction in the liquid limit by leaching out of porewater salt and the corresponding values of ϕ'_{fs} fall below the trend line shown in Figure 6.29.

Figure 6.29 shows considerable scatter for PI < 40% and the scatter is a maximum (18°) for PI ≈ 30%. Thus, relating fully softened friction angle to plasticity index may not be a good choice.

6.5.1.2.3 NAVFAC (1971) and Ladd et al. (1977)

Ladd et al. (1977) present an empirical correlation between friction angle ϕ' or ϕ'_{fs} and plasticity index (PI) from triaxial compression tests on normally consolidated undisturbed clay specimens. Ladd et al. (1977) refers to NAVFAC (1971) for this empirical correlation and presents the correlation on a semi-log scale. Figure 6.30 was obtained by replotting NAVFAC (1971) and Ladd et al. (1977) on an arithmetic scale instead of semi-log scale. The empirical correlation shown in Figure 6.30 uses data from Kenney (1959) and Bjerrum and Simons (1960) with data compiled by other researchers that Ladd et al. (1977) refer to as “General Reporters.”

Ladd et al. (1977) acknowledges considerable scatter in the data for PI of 15-40% where most of the data exist but suggest that the empirical correlation is still useful in estimating engineering properties of soils using simple index properties.

6.5.1.2.4 Mesri and Abdel-Ghaffar (1993)

Mesri and Abdel-Ghaffar (1993) present a correlation for fully softened friction angle using PI and is the first correlation that incorporates a PI greater than 100 % (see Figure 6.31). Figure 6.31 shows considerable scatter for PI $\leq$ 60 %, the range in which most of the data lies. The variation in ϕ' or ϕ'_{fs} is more than 10° for a single value of PI. Furthermore, limited data is available for PI > 60%. Eid (1996) determined that considerable scatter in ϕ'_{fs} versus PI plots may have resulted because of omitting the effect of CF. Furthermore, Mesri and Abdel-Ghaffar (1993) do not incorporate the stress dependent effect of the fully softened strength envelope in the empirical correlation and suggest a single best-fit trend line for all effective normal stresses. Mesri and Abdel-Ghaffar (1993) conclude that "the friction angle ϕ'_{fs}, which is determined by the composition of soil (mainly mineralogy), may decrease slightly at very high effective stresses, but it is a constant in the effective stress ranges encountered in most earth structures." But later on, Mesri and his coworkers include the stress dependent effect of the fully softened strength failure envelope suggested by Stark and Eid (1997) which is discussed subsequently.

6.5.1.2.5 Stark and Eid (1997)

Stark and Eid (1997) propose an empirical correlation for ϕ'_{fs} that uses PI, CF, and effect of σ'_n on one graph as shown in Figure 6.32. Stark and Eid (1997) compare their data by plotting the trend line suggested by Mesri and Abdel-Ghaffar (1993) for PI values of up to 100% as shown in Figure 6.32. Stark and Eid (1997) conclude that this trend line is in agreement with the median of the ring shear data and the scatter present in prior correlations is due to not including CF and σ'_n in the correlations. Stark and Eid (1997) conclude that fully softened friction angle should not be estimated from a single index property such as PI or LL instead CF and σ'_n should also be incorporated to capture the parameters that significantly impact ϕ'_{fs}. This has reduced the scatter in the ϕ'_{fs} versus PI correlation which can be seen for each curve corresponding to a CF group and effective normal stress.

Thus, using CF, σ'_n, and either PI or LL appears to yield a better correlation of ϕ'_{fs}. Estimating different values of ϕ'_{fs} for different values of σ'_n can also facilitate obtaining a stress dependent failure envelope that can be used in stability analysis.

6.5.1.2.6 Mesri and Shahien (2003)

Because Mesri and Shahien (2003) suggest combined correlations for drained residual and fully softened friction angles, discussion of these correlations is already presented while describing empirical correlations for drained residual friction angle. The empirical correlations suggested by Mesri and Shahien (2003) are shown in Figure 6.15.

Stark and Eid (1994 and 1997) conclude that residual and fully softened shear strength failure envelopes are stress dependent and this effect should be incorporated in stability analyses of a reactivated or first-time lanslide, respectively. As discussed before, Mesri and Abdel-Ghaffar (1993) conclude that ϕ' may decrease slightly at very high effective stresses and remains constant in the effective stress ranges encountered in most earth structures. But Mesri and Shahien (2003), while accepting the conclusions of Stark and Eid (1994 and 1997), now conclude that "the relationships between shear strength and effective normal stress for all conditions of stiff clays and shales - intact, fully softened, and residual - are curved….."

Although Mesri and Shahien (2003) suggest three different plots for three different effective normal stresses of 50, 100, and 400 kPa to incorporate the stress dependent effect on the fully softened friction angle, they still only use PI for the correlations which results in considerable scatter (see fully softened friction angle plots in Figure 6.15). For a single value of PI < 60 %, a difference of about 6° in ϕ'_{fs} values can be seen from Figure 6.15. This scatter in ϕ'_{fs} value has been reduced from 10° to 6° by incorporating the effect of effective normal stress as evident by comparing Figures 6.15 and 6.31. The large scatter in ϕ'_{fs} in Figure 6.15 may be attributed to omitting the effect of CF from the empirical correlation. Thus, using only one basic index property of the soil, e.g., PI or LL, does not yield the result. It is recommended that CF be included in such correlations with and σ'_n either PI or LL.

6.5.2 New Empirical Correlation for Drained Fully Softened Friction Angle

The empirical correlation for drained fully softened friction angle suggested by Stark et al. (2005a) is being used in the geotechnical engineering because it contains less scatter than other empirical correlations described above. The only information required to estimate the drained fully softened friction angle, referred herein as ϕ'_{fs}, is LL and CF which are measured routinely. Thus, the correlation suggested by Stark et al. (2005a) provides a reliable estimates of ϕ'_{fs} for use in preliminary design and serves as a check on data obtained from laboratory testing.

The empirical correlation suggests three different CF groups, i.e., CF $\leq$ 20%, 25% $\leq$ CF $\leq$ 45%, and CF $\geq$ 50%, which are similar to the drained residual friction angle empirical correlation and accounts for the effect of CF and σ'_n on ϕ'_{fs} values.

Stark et al. (2005a) suggest the empirical correlation for drained fully softened friction angle using samples processed through the Number 200 sieve for highly overconsolidated clays and samples processed though the Number 40 sieve for all other clays. The effect of ball milling and processing the soil sample through the Number 200 sieve has already been discussed previously in this chapter.

Stark et al. (2005a) suggest a separate trend line for each effective normal stress of 50, 100, and 400 kPa and for each CF group. Thus, CF identifies the CF group and LL helps in estimating ϕ'_{fs} values for three different effective normal stresses. Therefore, a reliable estimate of LL and CF are needed to estimate ϕ'_{fs} for the various effective normal stresses to develop a stress dependent fully softened strength failure envelope. Such a stress dependent envelope can be used in stability analyses of first-time landslides.

The drained fully softened friction angle empirical correlation suggested by Stark et al. (2005a) are available in graphical form which makes it difficult to incorporate it in computer based applications, such as in slope stability software. The present study suggests a different equation for each trend line of the new correlation which can be used to estimate ϕ'_{fs} values, and a stress dependent failure envelope, using LL and CF.

6.5.2.1 Effect of Sample Preparation on Drained Fully Softened Friction Angle

The fully softened shear strength corresponds to a random arrangement of particles and reflects the ability of particles to establish short range interaction and interlocking (Mesri and Cepeda-Diaz, 1986). Mesri and Cepeda-Diaz (1986) conclude that a correlation between drained fully softened friction angle and clay mineralogy should be expected. To explain this, Mesri and Cepeda-Diaz (1986) present the examples of kaolinite and montmorillonite stating that "the stiff plates of kaolinite, ……, are able to establish short range edge-to-face interaction and interference…. highly flexible films of montmorillonite are capable of doing neither." Mesri and Cepeda-Diaz (1986) suggest that as the particle platyness increases, even in random arrangement of particles, the predominant particle interaction is through face-to-face interaction because particle edges can easily bend.

Because the fully softened shear strength corresponds to the peak strength of a normally consolidated specimen, a remolded soil sample is prepared from the soil sample obtained from the field and is normally consolidated in the laboratory to estimate ϕ'_{fs}. The fully softened shear strength is measured at a small shear displacement so particle size and shape will affect the measured value. Development of a first-time shear surface in the field, along which the fully softened shear strength is mobilized, does not correspond to a material with greater fine contents or CF as usually observed along a preexisting shear surface. It is anticipated that during mobilization of the fully softened shear strength in the field, the clay particles remain in their natural structure. Thus, the particles will be probably still aggregated in mudstone, claystone, and shale deposits and disaggregated in weathered clays and silts. Thus, at the time of mobilization of the fully softened strength in the field, particles will probably still be aggregated instead of disaggregated at the residual strength condition. Thus, soil does not have to be processed through the Number 200 sieve.

The soil sample processed through the Number 200 sieve yields a lower fully softened shear strength value than soil processed through the Number 40 sieve using ASTM procedures. Thus, the fully softened shear strength measured in the laboratory using soil processed through the Number 200 sieve is likely to underestimate the fully softened shear strength mobilized in the field. In addition, the mode of shear affects the measured value of ϕ'_{fs}. Eid (1996), Stark and Eid

(1997) and Stark et al. (2005a) used ball milled specimens of highly overconsolidated clays in ring shear tests and determined that the ring shear yields ϕ'_{fs} values about 2.5° lower than those measured in a triaxial compression test with ball milled material. This difference of 2.5° in ϕ'_{fs} was attributed to difference in the mode of shear and stress states in the triaxial and ring shear testing and a 2.5° correction was applied to the ring shear results.

During the present study an investigation to determine the ring shear test procedure for measuring the fully softened shear strength was conducted. Three soil samples were processed through the Number 40 sieve after air drying using a mortar and pestle. This material was used to estimate the ϕ'_{fs} values using a ring shear device. The remolded specimens were consolidated to the required effective normal stress and sheared soon after completion of primary consolidation. For each effective normal stress, a new specimen was prepared and sheared. The results were compared with the empirical correlation suggested by Stark et al. (2005a) and found to be in agreement so the correction of 2.5° was not required as suggested by Eid (1996), Stark and Eid (1997), and Stark et al. (2005a). Thus, sample preparation does impact measured values of ϕ'_{fs}. In particularly, the three soils tested during the present study consist of one shale and two clays. In the ring shear testing of a normally consolidated specimen, shearing must start at the end of primary consolidation. If a specimen is still undergoing primary consolidation, a lower value of ϕ'_{fs} will be measured while an overconsolidated specimen may give a higher value of ϕ'_{fs}. Thus, sample preparation affects the drained fully softened shear strength and friction angle and a soil sample processed through the Number 40 sieve is recommended to measure ϕ'_{fs} using a ring shear device.

The values of ϕ'_{fs} adjusted by adding 2.5° to the values measured in ring shear testing of soil samples processed through Number 200 sieve by Eid (1996), Stark and Eid (1997), and Stark et al. (2005a) is considered herein as analogous to values of ϕ'_{fs} measured using soil samples processed through Number 40 sieve.

For consistency between the empirical correlations for drained residual and fully softened friction angles, ϕ'_{fs} values are plotted against LL and CF measured using a similar procedure as used for drained residual friction angle correlation. The values of LL and CF were measured using soil processed through the Number 200 sieve for highly overconsolidated clays and

processed through the Number 4o sieve for silts and clays are to be used to estimate the value of ϕ'_{fs} from the empirical correlation being suggested herein.

6.5.2.2 Equations for New for Drained Fully Softened Friction Angle Correlations

Stark and Eid (1997) and Stark et al. (2005a) present a relationship between LL and drained fully softened friction angle in a graphical form with separate trend lines for each effective normal stress and in three different CF groups. This requires consulting the figure to estimate values of drained fully softened friction angles for the LL of the clay. Because the empirical correlation proposed by Stark et al. (2005a) are widely accepted by the geotechnical community and being consulted frequently in practice, it was decided to develop a representative equation for each trend line.

The present study, considered each CF group separately while developing an equation for each trend line for three effective normal stresses considered, i.e., 50, 100, and 400 kPa. New trend lines for each σ'_n value consider the data and trend line suggested by Stark et al. (2005a) and the new data created during the present study. During the present study it was determined that the trend lines suggested by Stark et al. (2005a) are in agreement with the trend lines those could have been sketched using the data developed during this study. Thus, the mathematical expressions represent the trend lines developed by Stark et al. (2005a). Because the trend lines by Stark et al. (2005a) were developed based on the engineering judgment and considering the behavior of natural soils, the R^2 value determined by performing regression analysis for each trend line is below unity (see Figures 6.33 to 6.35). Although lower the R^2 values show scatter in the data developed from ring shear testing in the laboratory but still the empirical correlation gives a good estimate of fully softened friction angle for a natural soil.

A set of three equations was developed during the present study for the empirical correlation for drained fully softened friction angles of CF Group 1 and for LL values ranging from 20% to less than 80% ($20\% \leq LL < 80\%$) and is given below as Equations (6.9). The limit for LL is specified because the ring shear data is available only for this LL range. The ring shear data along with the trend lines sketched by Stark et al. (2005a) for CF Group 1are plotted in Figure 6.33. The trend lines sketched from the Equations (6.9) are also plotted on Figure 6.33 to 6.35 to compare the results. Figure 6.33 shows that the trend lines plotted using Equations (6.9)

are in close agreement with the trend lines suggested by Stark et al. (2005a). Thus, a second degree polynomial can be used to represent the trend lines for CF Group 1 and for all three effective normal stresses.

$$(\phi_r)_{\sigma_n'=50kPa} = 34.85 - 0.0709(LL) + 2.35x10^{-4}(LL)^2 \quad (6.9a)$$

$$(\phi_r)_{\sigma_n'=100kPa} = 34.39 - 0.0863(LL) + 2.66x10^{-4}(LL)^2 \quad (6.9b)$$

$$(\phi_r)_{\sigma_n'=400kPa} = 34.76 - 0.13(LL) + 4.71x10^{-4}(LL)^2 \quad (6.9c)$$

A set of three equations was also developed during the present study for the CF Group 2 and for LL values ranging from 30% to 130% (30% $\leq$ LL $\leq$ 130%) and is given below as Equations (6.8). The upper and lower limits for LL are specified because of ring shear data is only available for this LL range. The ring shear data along with the trend lines sketched by Stark et al. (2005a) for CF Group 2 are plotted in Figure 6.34. The trend lines obtained from Equations (6.10) are also plotted on Figure 6.34 for comparison purposes. Figure 6.34 shows that the trend lines plotted by using Equations (6.10) are in agreement with the trend lines suggested by Stark et al. (2005a). Thus, a second degree polynomial also can be used to represent the trend lines for CF Group 2 and for all three effective normal stresses.

$$(\phi_r)_{\sigma_n'=50kPa} = 36.18 - 0.1143(LL) - 2.354x10^{-4}(LL)^2 \quad (6.10a)$$

$$(\phi_r)_{\sigma_n'=100kPa} = 33.11 - 0.107(LL) + 2.2x10^{-4}(LL)^2 \quad (6.10b)$$

$$(\phi_r)_{\sigma_n'=400kPa} = 30.7 - 0.1263(LL) + 3.442x10^{-4}(LL)^2 \quad (6.10c)$$

A set of three equations was also developed during the present study for the CF Group 3 and for LL values ranging from 30% to 300% (30% $\leq$ LL $\leq$ 300%) and is given below as Equations (6.11). The upper and lower limits for LL are specified because ring shear data is available for this LL range. The ring shear data along with the trend lines sketched by Stark et al.

(2005a) for CF group 3 are plotted in Figure 6.35. The trend lines obtained from the newly developed Equations (6.11) are also plotted on Figure 6.35 for comparison purposes.

Figure 6.35 shows that the trend lines plotted by using Equations (6.11) are in close agreement with the trend lines suggested by Stark et al. (2005a). Thus, a third degree polynomial can be used to represent the trend lines for CF Group 3 and for all three effective normal stresses.

$$(\phi_r)_{\sigma_n'=50kPa} = 33.37 - 0.11(LL) + 2.344x10^{-4}(LL)^2 - 2.96x10^{-7}(LL)^3 \quad (6.11a)$$

$$(\phi_r)_{\sigma_n'=100kPa} = 31.17 - 0.142(LL) + 4.678x10^{-4}(LL)^2 - 6.762x10^{-7}(LL)^3 \quad (6.11b)$$

$$(\phi_r)_{\sigma_n'=400kPa} = 28.0 - 0.1533(LL) + 5.64x10^{-4}(LL)^2 - 8.414x10^{-7}(LL)^3 \quad (6.11c)$$

The empirical correlation for drained fully softened friction angle developed herein is shown in Figure 6.36 and can be represented by mathematical equations as discussed above. The mathematical relationship between LL and ϕ'_{fs}, represented by Equations (6.9) to (6.11), along with the CF and LL discussed above, can be used to develop a stress dependent fully softened strength failure envelope for a cohesive soil. This may allow the work of slope stability software developers to code these relationships in their software so a stress dependent failure strength envelope can be used in stability analyses.

6.6 Computer Aided Stress Dependent Failure Envelopes

During the present study a spreadsheet was developed using the Microsoft Excel spreadsheet which utilizes only two parameters, CF and LL, as input and generates the values of ϕ'_r and ϕ'_{fs} for effective normal stresses, i.e., 50, 100, 400, and 700 kPa (see Figure 6.37). The stress dependent residual and fully softened shear strength failure envelopes are plotted on the same page and on a single figure with the spreadsheet (see Figure 6.37). The advantage of showing both drained residual and fully softened strength failure envelopes on the same graph is that the user can compare the difference between the fully softened and residual strengths in a single figure.

The methodology used in developing this spreadsheet was also used to develop Visual Basic (VB 6.0) program for the correlations. Similar to the spreadsheet, the user only needs to

specify two input parameters, i.e., LL, and CF, to estimate the values of ϕ'_r and ϕ'_{fs} and values of shear stress for each value of σ'_n. The user can export the results to any desirable format such as MS Excel, MS Word, and PDF for further use.

Most of the stability software allow the use of a stress dependent failure envelope but values of the stress dependent failure envelope are obtained from the graphical correlation manually. With the introduction of an equation for each trend line relationships between ϕ'_{fs} and LL and ϕ'_r and LL for all three CF groups and different effective normal stresses, a user can quickly obtain the values to generate a stress dependent failure envelope for use in a stability analysis.

6.7 Summary and Discussion

The residual strength is the fundamental property of soil because the soil structure, stress history, particle interference, and diagenetic bonding have been removed by continuous shear displacement in one direction. In the field, the shearing process results in disaggregating the clay particles and a higher CF being present along the shear surface as compared to the soil above or below (Chandler, 1969). A highly overconsolidated clay sample disaggregated either by ball milling or another technique and processed through the Number 200 sieve will result in obtaining the residual strength value with a smaller shear displacement than a non-disaggregated sample. In other words, a highly overconsolidated clay processed through the Number 40 sieve will usually require a larger shear displacement to reach the residual strength than material processed through the Number 200 sieve. In summary, sample preparation does not affect the measured residual shear strength of a highly overconsolidated clay but it does reduces the shear displacement and time to achieve a drained residual strength condition in laboratory testing of a remolded specimen.

The fully softened shear strength corresponds to a random arrangement of particles and reflects the ability of particles to establish short range interaction and interlocking. The fully softened shear strength is measured at a small shear displacement so particle size and shape will affect the measured value. During the mobilization of the fully softened shear strength in the field, the clay particles remain in their natural structure and aggregated particles of highly overconsolidated clays are not likely to disaggregate. Thus, the fully softened shear strength can

be measured using a remolded normally consolidated specimen prepared from soil processed through the Number 40 sieve.

Because values of LL and CF are usually measured in practice using ASTM test methods (ASTM, 2008a and 2008b), empirical correlations for LL and CF using soil processed through the Number 40 sieve and processed through the Number 200 sieve are presented. The empirical correlations were developed using data for 28 and 32 natural soil samples for LL and CF, respectively. Thus, these empirical correlations allow commercial laboratories to measure LL and CF using soil processed the Number 40 sieve, i.e., ASTM test methods, instead of having to disaggregate the highly overconsolidated clay by processing it through the Number 200 sieve.

New residual and fully softened empirical correlations presented by the present study relates both ϕ'_r and ϕ'_{fs} to LL, CF and σ'_n. For consistency between the residual and fully softened empirical correlations, ϕ'_r and ϕ'_{fs} are plotted against LL and CF measured using a similar procedure. The values of LL and CF should be estimated using soil processed through the Number 200 sieve for highly overconsolidated clays and processed through the Number 40 sieve for all other clays. CF is used to select the proper CF group and ϕ'_r and ϕ'_{fs} are estimated using the LL.

Because a stress dependent failure envelope exhibits the maximum curvature at low values of σ'_n and the residual empirical correlations suggested by Stark et al. (2005a) do not show data or a trend line for an effective normal stress of less than 100 kPa, new data and new trend lines for each CF group are suggested for σ'_n equal to 50 kPa.

The new residual and fully softened empirical correlations are modeled using mathematical expressions to facilitate their use in practice. A separate equation is developed for each trend line in each CF group. The mathematical expressions reduce the need to utilize the graphical version of the empirical correlations.

A spreadsheet was developed during the present study using Microsoft Excel that incorporates the mathematical expression for each trend line. The spreadsheet requires two input parameters, LL and CF, and generates values of ϕ'_r and ϕ'_{fs} for different effective normal stresses. The stress dependent residual and fully softened strength failure envelopes are plotted

on a single graph by the spreadsheet for comparison purposes. The methodology used to develop the spreadsheet was also incorporated in a Visual Basic (VB 6.0) program fto facilitate use in practice. The user can export the results of the program to any desirable format, such as MS Excel, MS Word, and PDF.

Table 6.1. Soil samples used in liquid limit (LL) and clay-size fraction testing.

Soil No.	Clay, mudstone, shale, and claystone samples	Clay, mudstone, shale, and claystone locations	ASTM LL (%)	Ball-milled LL (%)	Ratio Ball-milled/ASTM LL	ASTM CF (%)	Ball-milled CF (%)	Ratio Ball-milled/ASTM CF
(1)	(2)	(3)	(4)	(5)	(6)	(7)	(8)	(9)
From Stark et al. (2005a)								
1	Batestown till	Batestwon, Ill.	21	29	1.38	-	-	-
2	Duck Creek shale	Fulton, Ill.	29	37	1.28	19	31	1.63
3	Crab Orchard	Peoria, Ill.	36	44	1.22	19	32	1.68
4	Claystone	Big Bear, Calif.	48	75	1.56	40	54	1.35
5	Shear surface	Brillant, Ohio	44	-	-	28	39	1.39
6	Illinois Valley shale	Peru, Ill.	45	56	1.24	35	45	1.29
7	Shear surface	Novato, Calif.	95	-	-	54	61	1.13
8	Shear surface	Los Angeles, Calif.	55	62	1.13	17	27	1.59
9	Dike shale	Cairo, Egypt	52	91	1.75	47	58	1.23
10	Makattam shale	Cairo, Egypt	68	103	1.51	24	43	1.79
11	Shear surface (LD-8)	Orange County, Calif.	69	-	-	30	41	1.37
12	Shear surface (LD-15)	Orange County, Calif.	75	97	1.29	48	52	1.08
13	Shear Surface (depth 8.4m)	San Diego, Calif.	82	119	1.45	73	81	1.11
14	Pierre shale	New Castle, WY	103	137	1.33	44	54	1.23
15	Panoche clay gouge	San Francisco, Calif.	125	219	1.75	-	72	-
16	Otay Bentonitic claystone	Chula Vista, Calif.	133	216	1.62	43	53	1.23
17	Bentonitic shale	San Diego, Calif.	141	239	1.70	-	-	-
18	Claystone	May City, Egypt	-	-	-	15	29	1.93

Table 6.1 (cont.)

Soil No.	Clay, mudstone, shale, and claystone samples	Clay, mudstone, shale, and claystone locations	ASTM LL (%)	Ball-milled LL (%)	Ratio Ball-milled/ASTM LL	ASTM CF (%)	Ball-milled CF (%)	Ratio Ball-milled/ASTM CF
(1)	(2)	(3)	(4)	(5)	(6)	(7)	(8)	(9)
From Eid (2006)								
19	Shear surface	1st of May City, Egypt	25	30	1.20	15	29	1.93
20	Maali shale	Cairo, Egypt	27	30	1.11	23	23	1.35
21	Slide plane	Randolph. Ill.	-	-	-	24	46	1.92
22	Red sea white shale	Elsokhna, Egypt	43	55	1.28	38	50	1.32
23	Slide plane	Los Angeles, Calif.	49	55	1.12	17	27	1.59
24	Patapaco shale	Wash. D.C.	53	77	1.45	35	59	1.69
25	Pierre shale	Limon , CO.	55	73	1.33	42	49	1.17
26	Red sea gray shale	Elsokhna, Egypt	57	84	1.47	25	44	1.76
27	Upper pepper shale	Waco, Texas	68	89	1.31	58	72	1.24
28	Santiago shale	San Diego, Calif.	70	89	1.27	29	57	1.97
29	Slide plane	San Diego, Calif.	82	119	1.45	73	82	1.12
30	Mokattarin gray shale	Cairo, Egypt	85	134	1.58	53	79	1.49
31	Shear surface	Elhamam, Egypt	130	186	1.43	56	77	1.38
32	Oahe shale	Oahe, SD	-	-	-	76	82	1.08
33	Midra shale	Doha, Qatar	-	-	-	68	84	1.24
34	Lea Park shale	Saskatchwan, Canada	-	-	-	73	76	1.04
35	Otay shale	San Diego, Calif.	-	-	-	56	77	1.38
Present Study								
35	Bentonitic shale (pink)	San Diego, Calif.	90	126	1.40	-	-	-
36	Bentonitic shale (gray)	San Diego, Calif.	112	173	1.54	-	-	-

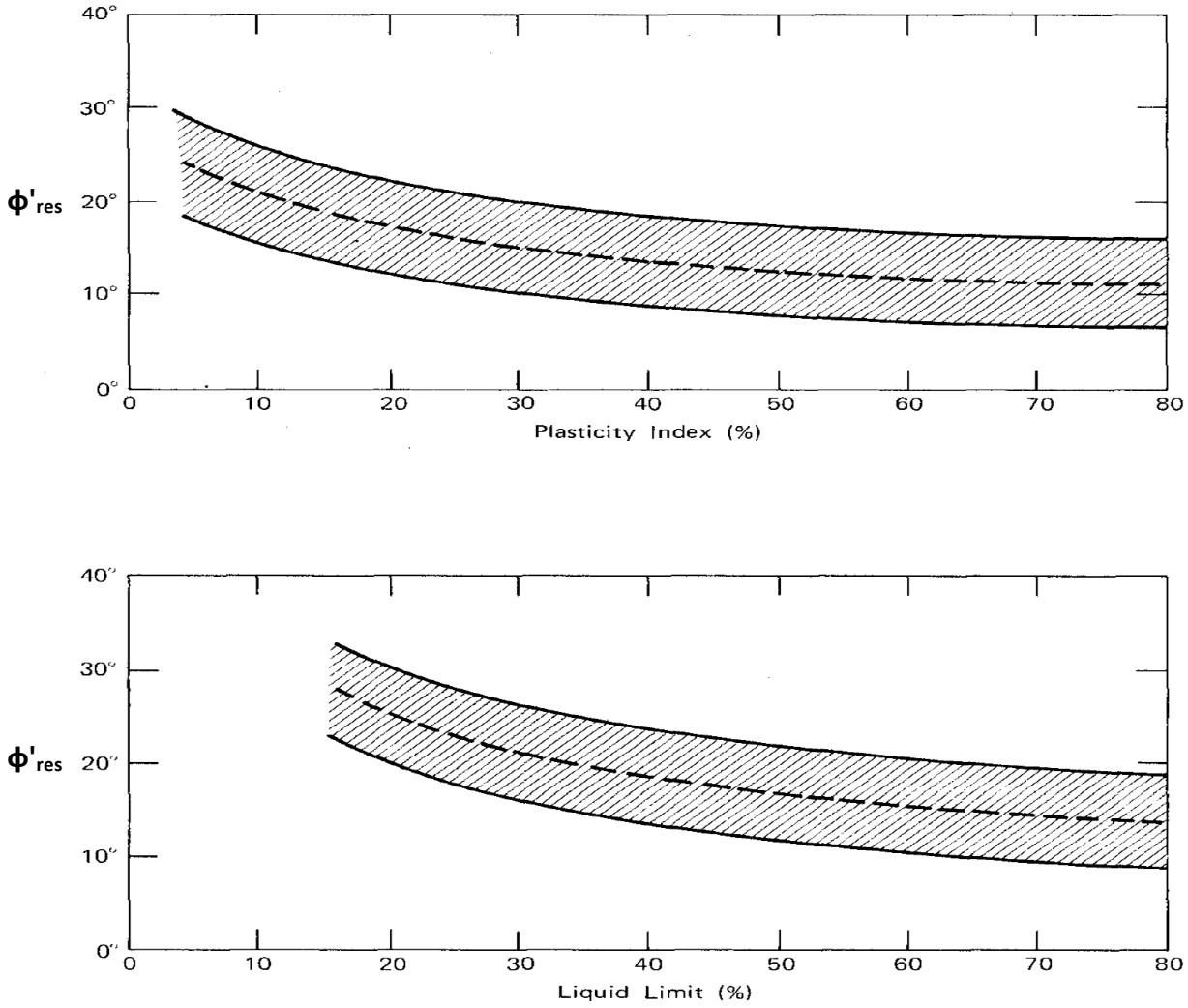

Figure 6.1. Residual between residual friction angle and plasticity, PI and LL (from Mitchell, 1976).

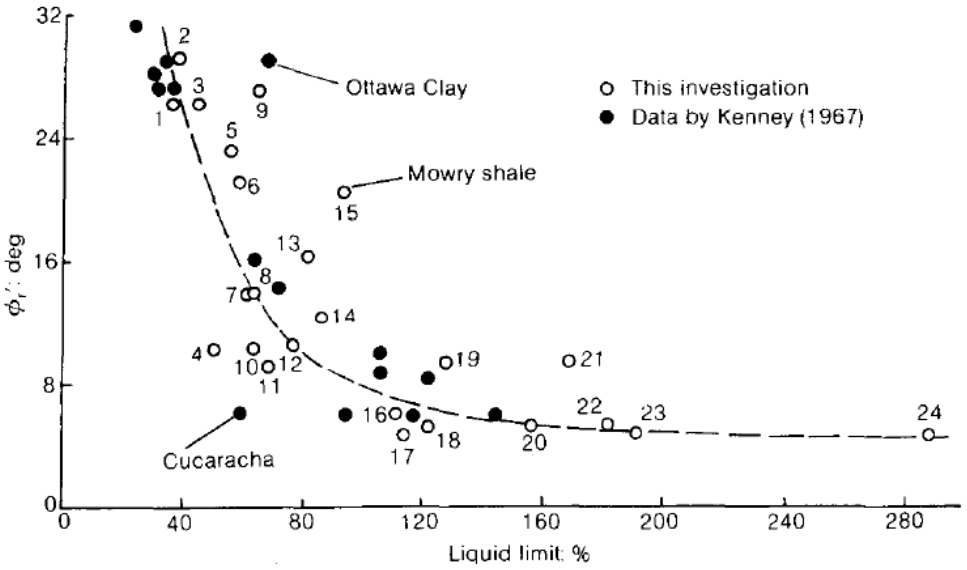

Figure 6.2. Residual friction angle-LL relationship based on the test results of 24 shales (from Mesri and Cepeda-Diaz, 1986).

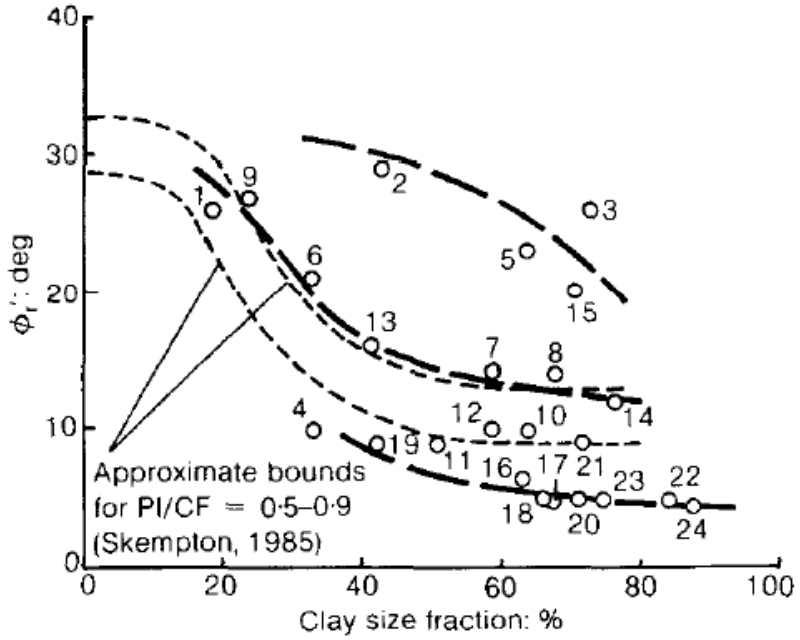

Figure 6.3. Residual friction angle-CF relationship based on the test results of 24 shales (from Mesri and Cepeda-Diaz, 1986).

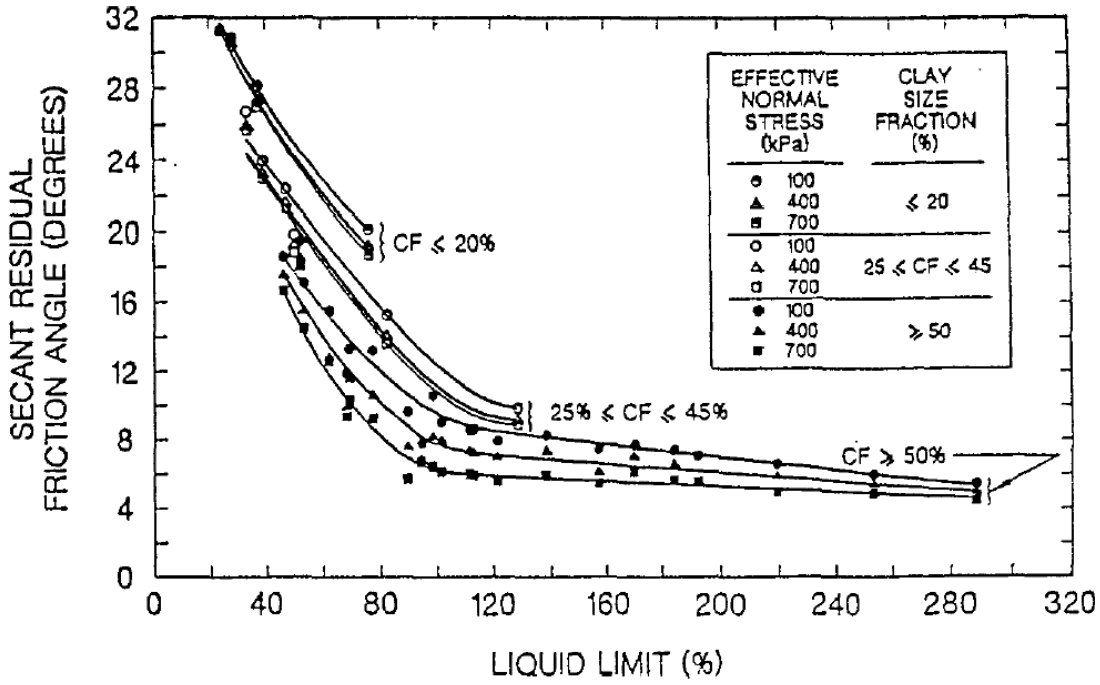

Figure 6.4. Relationship between drained residual friction angle and LL (from Stark and Eid, 1994).

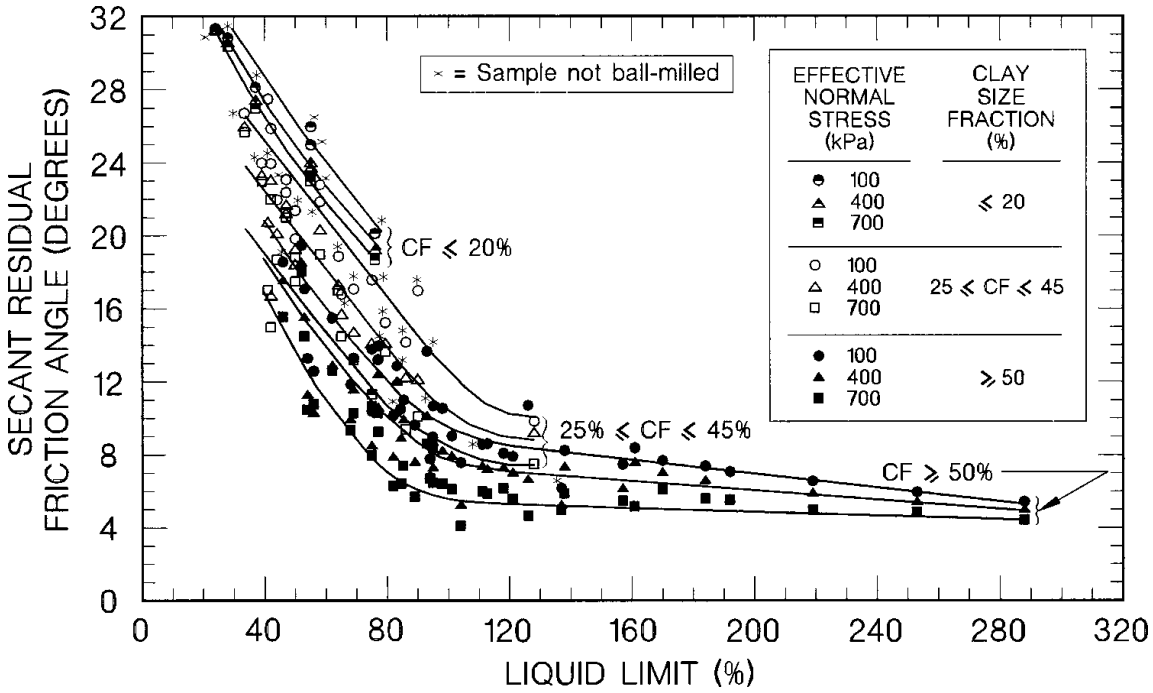

Figure 6.5. Secant residual friction angle relationships with LL, CF, and σ'_n (from Stark et al., 2005a).

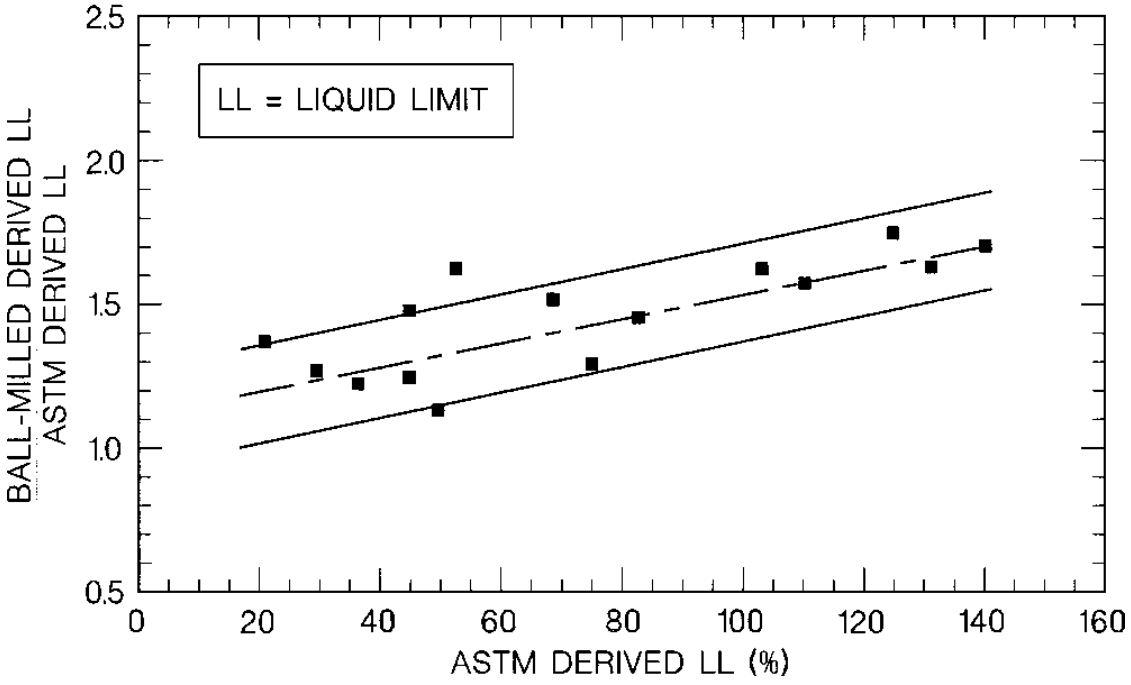

Figure 6.6. Ratios of ball milled and ASTM derived LL values (from Stark et al., 2005a).

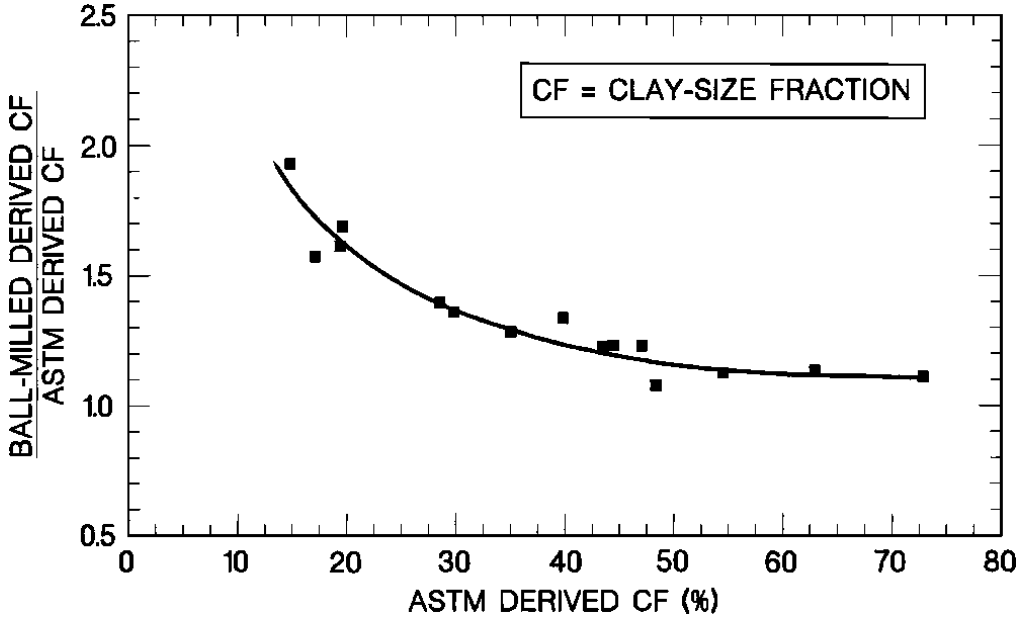

Figure 6.7. Ratios of ball milled and ASTM derived CF values (from Stark et al., 2005a)

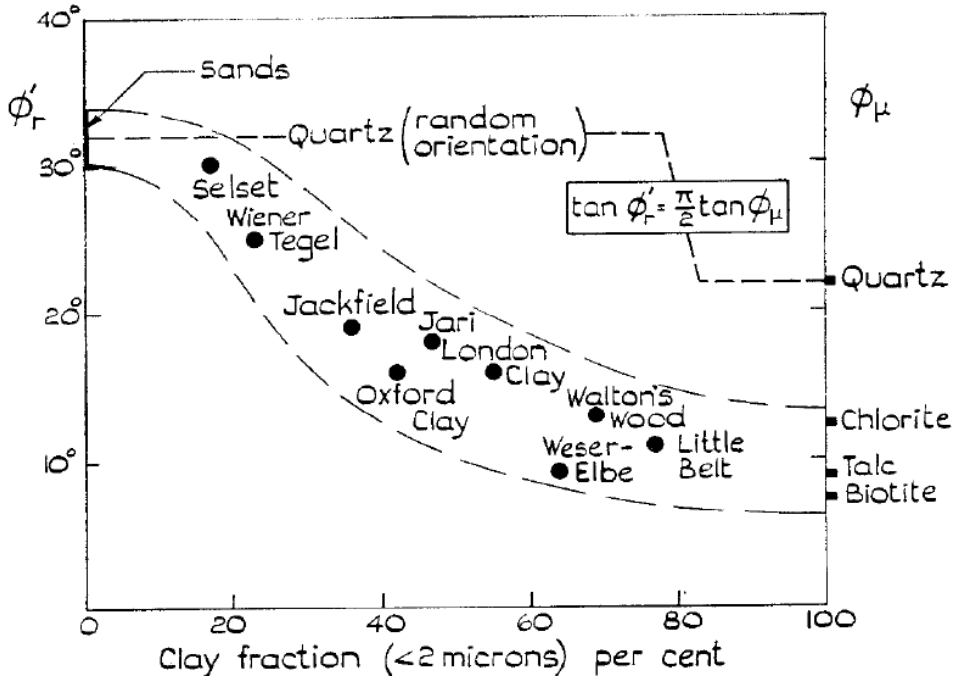

Figure 6.8. Plot showing decrease in ϕ'_r with increase in CF (from Skempton, 1964).

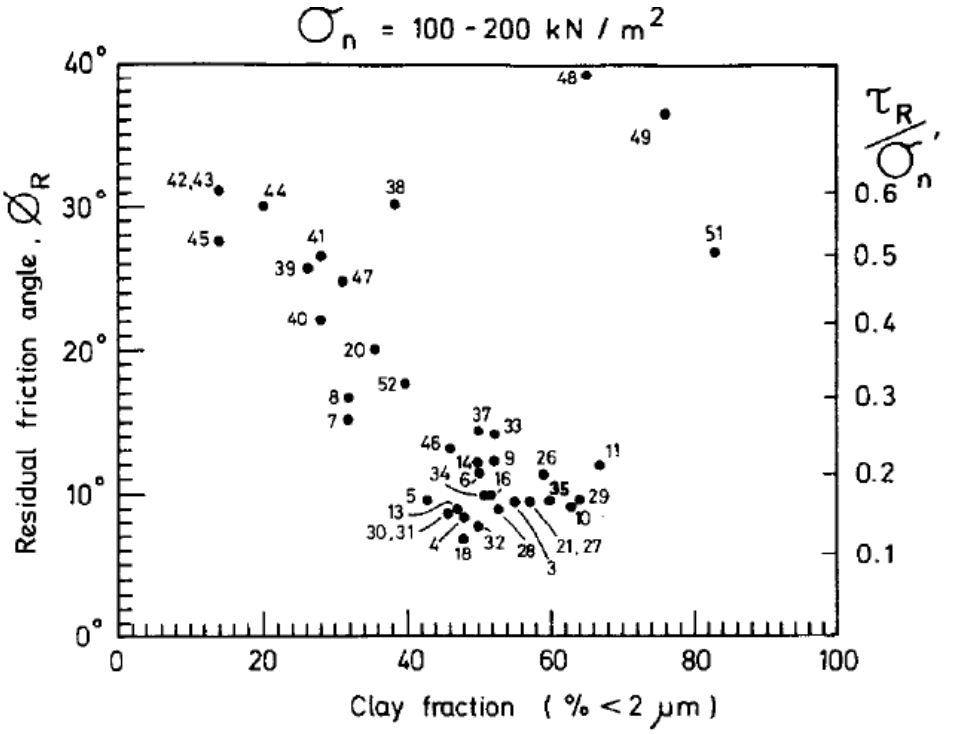

Figure 6.9. Residual friction angles versus CF for natural soils (from Lupini et al. 1981).

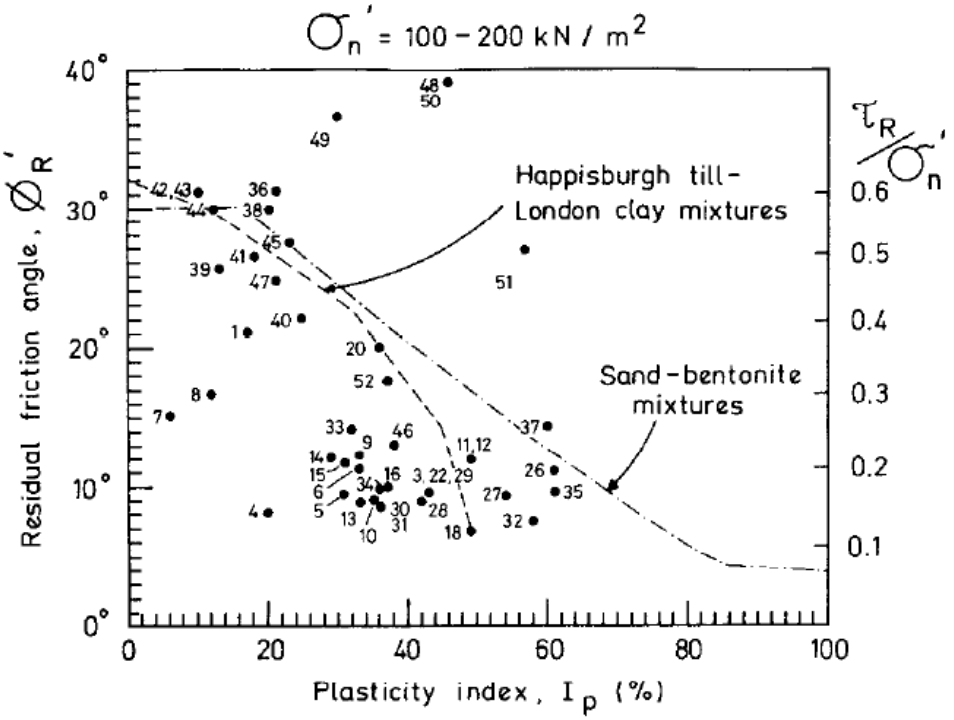

Figure 6.10. Residual friction angles versus plasticity index (PI or I_p) for natural soils (from Lupini et al. 1981).

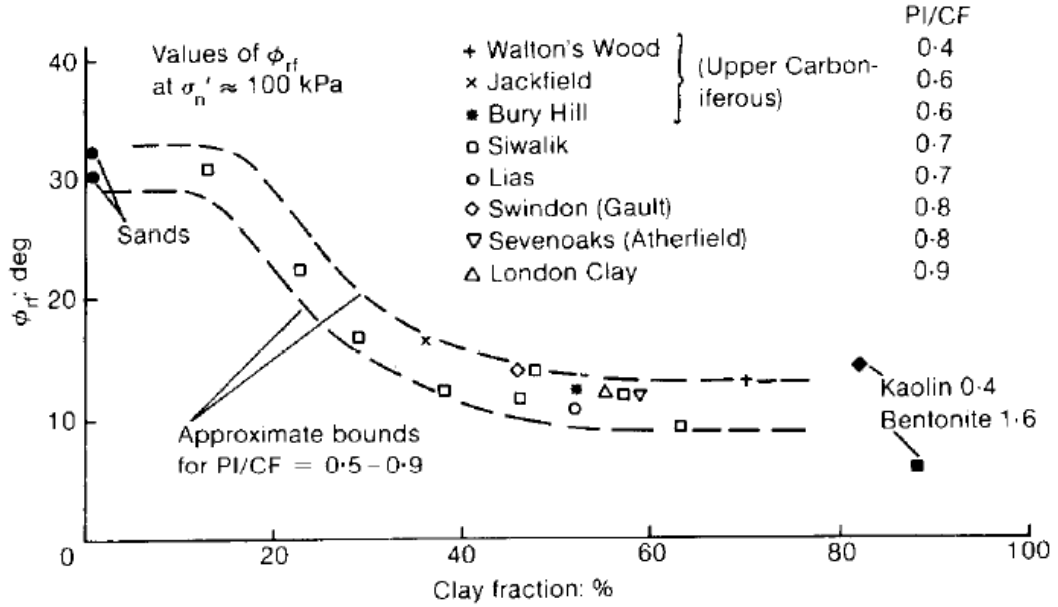

Figure 6.11. Field residual and ring shear tests on sands kaolin and bentonite (from Skempton, 1985).

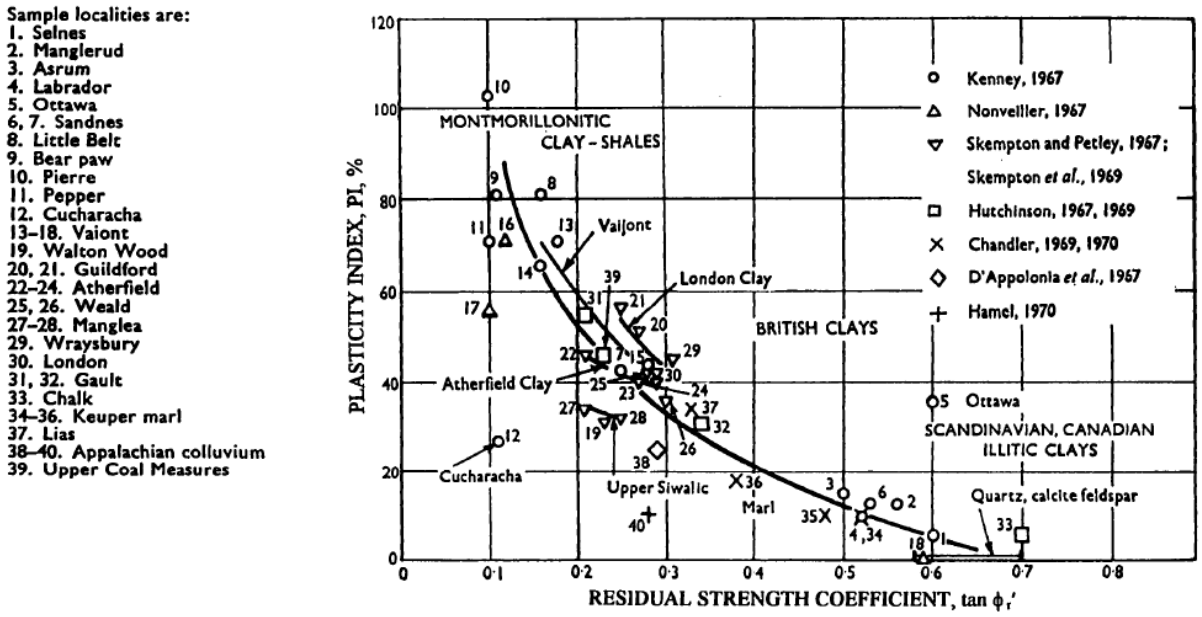

Figure 6.12. Plasticity index, I_p, plotted against residual strength coefficient, μ'_r (from Voight, 1973).

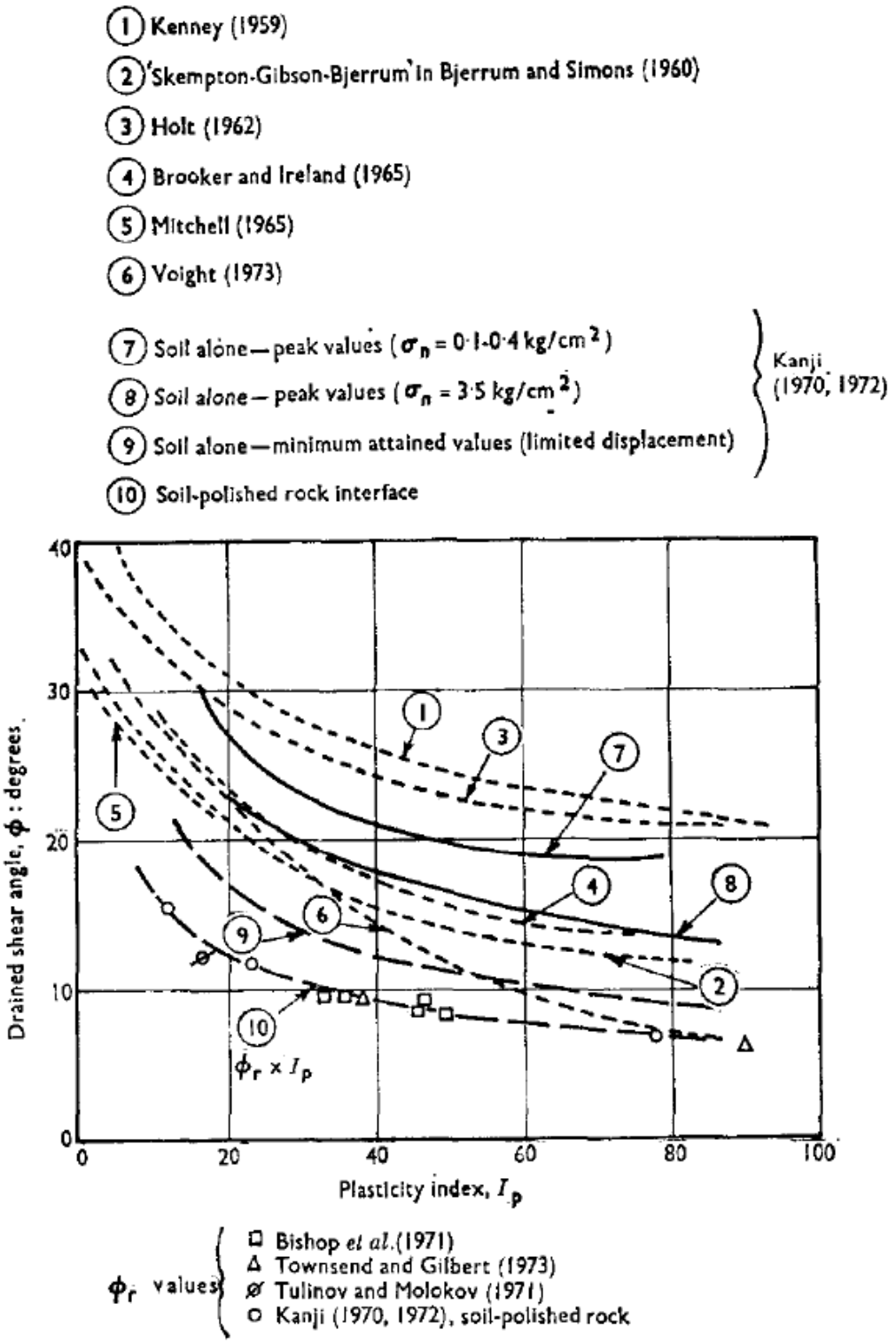

Figure 6.13. Drained shear angle ϕ plotted against plasticity index I_p (from Kanji, 1974).

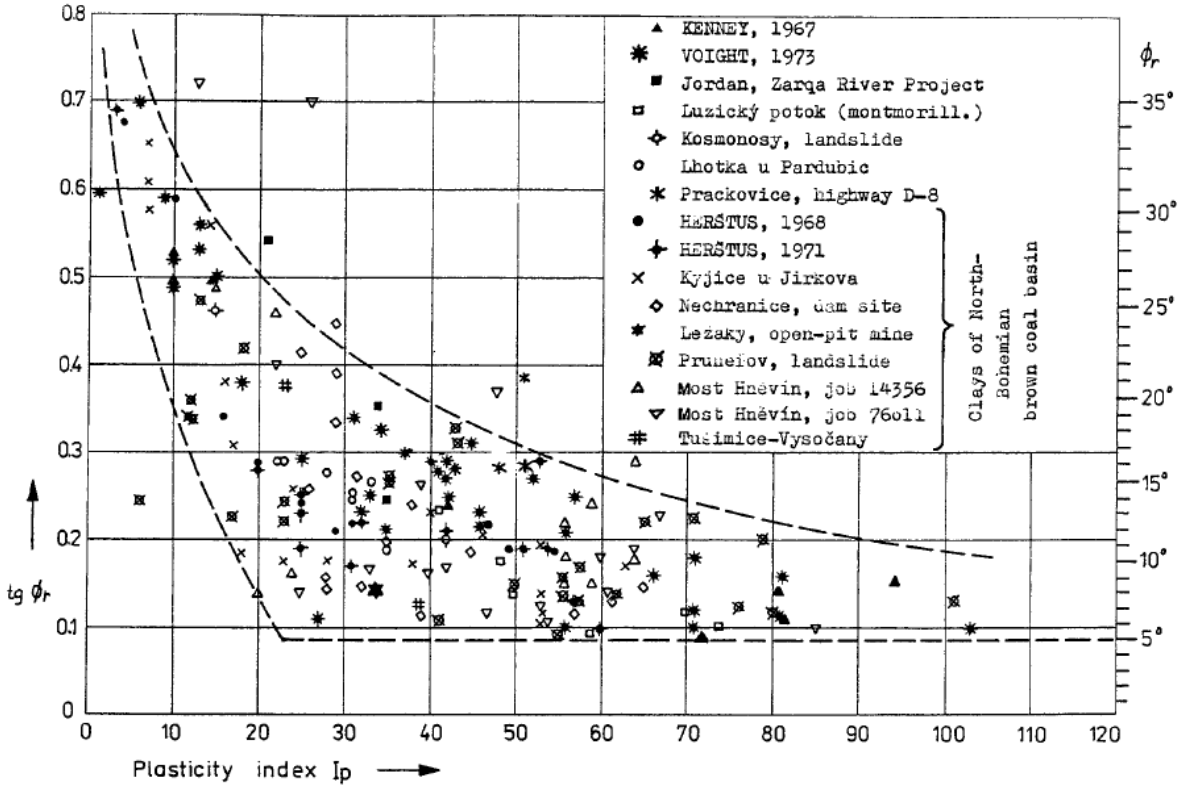

Figure 6.14. Relation of residual angle of internal friction ϕ_r to plasticity index I_p (Atterberg) (from Seycek, 1978).

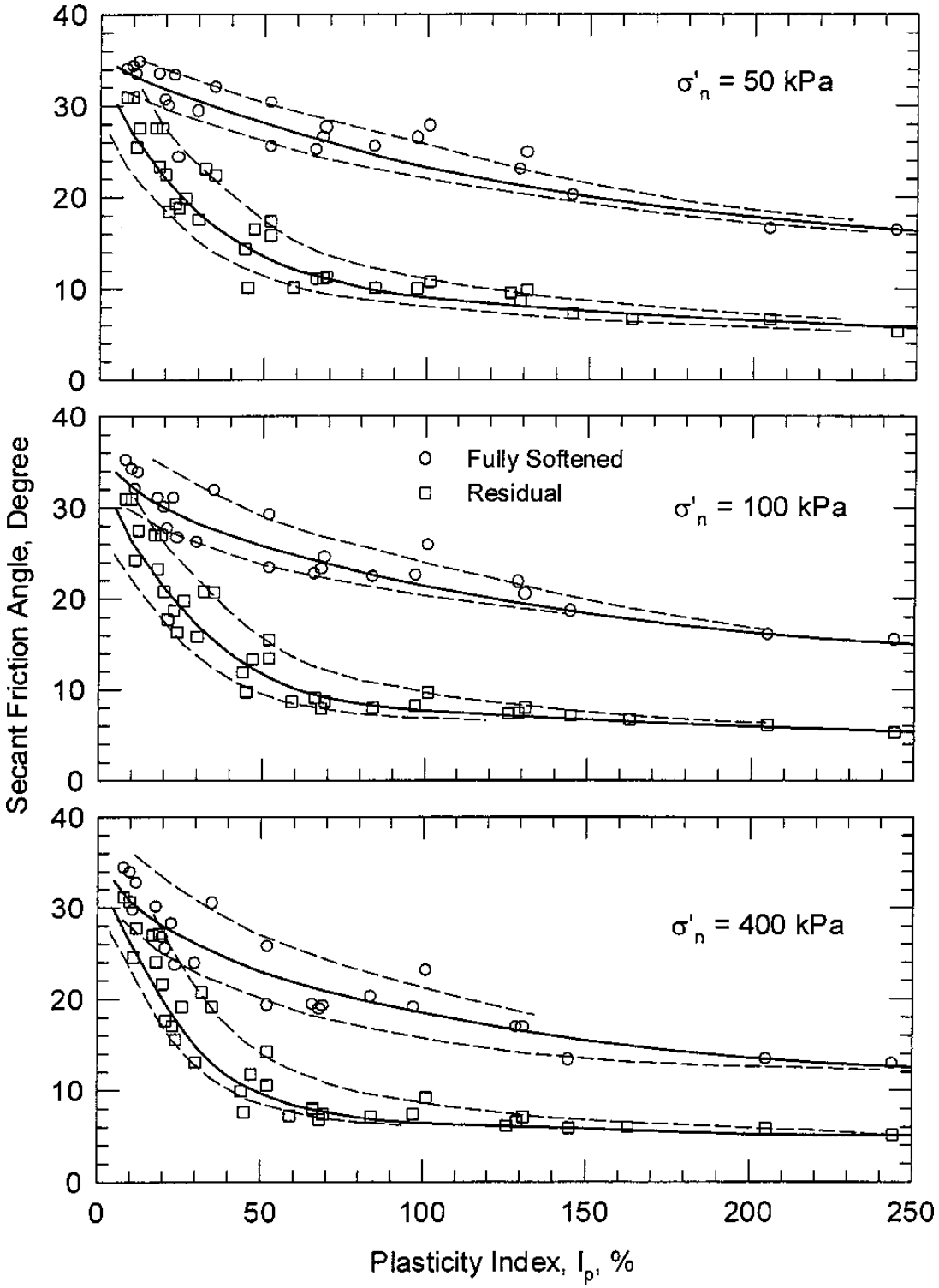

Figure 6.15. Empirical correlations on fully softened strength and residual friction angles developed from the ring shear data of Stark and Eid 1994, Eid 1996, and Stark and Eid 1997 (from Mesri and Shahien, 2003).

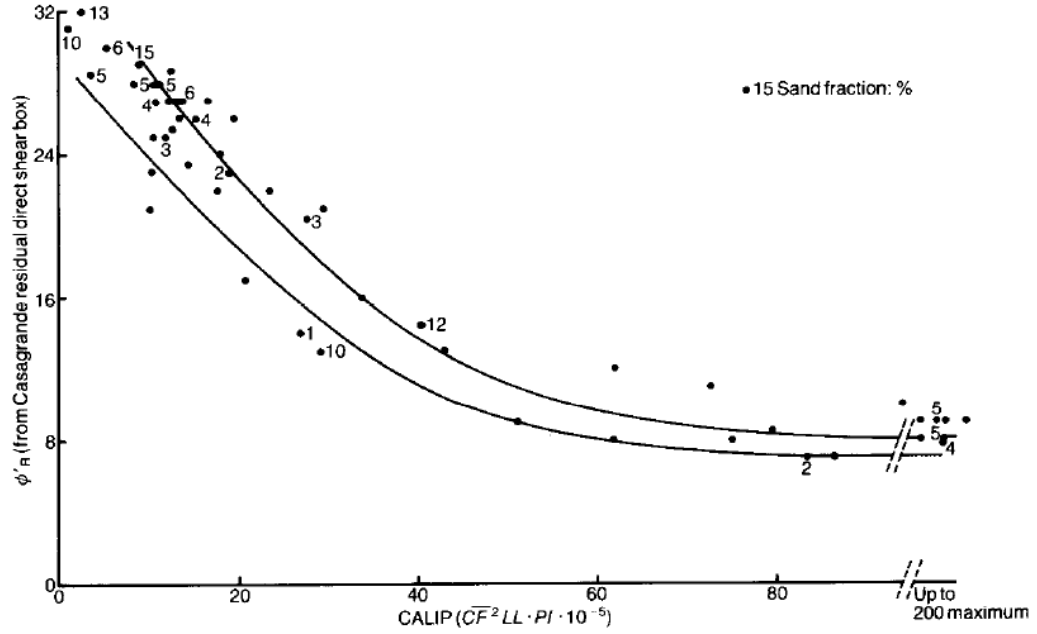

(a)

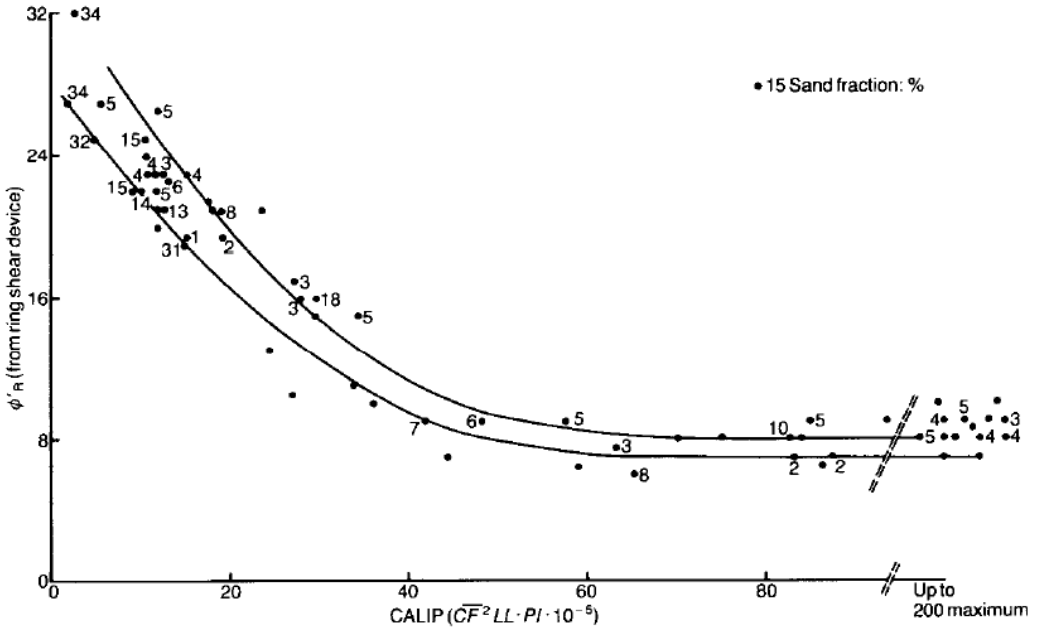

(b)

Figure 6.16. Relationship between CALIP and ϕ'_r applied to (a) direct shear tests (b) ring shear tests (from Collotta et al. 1989).

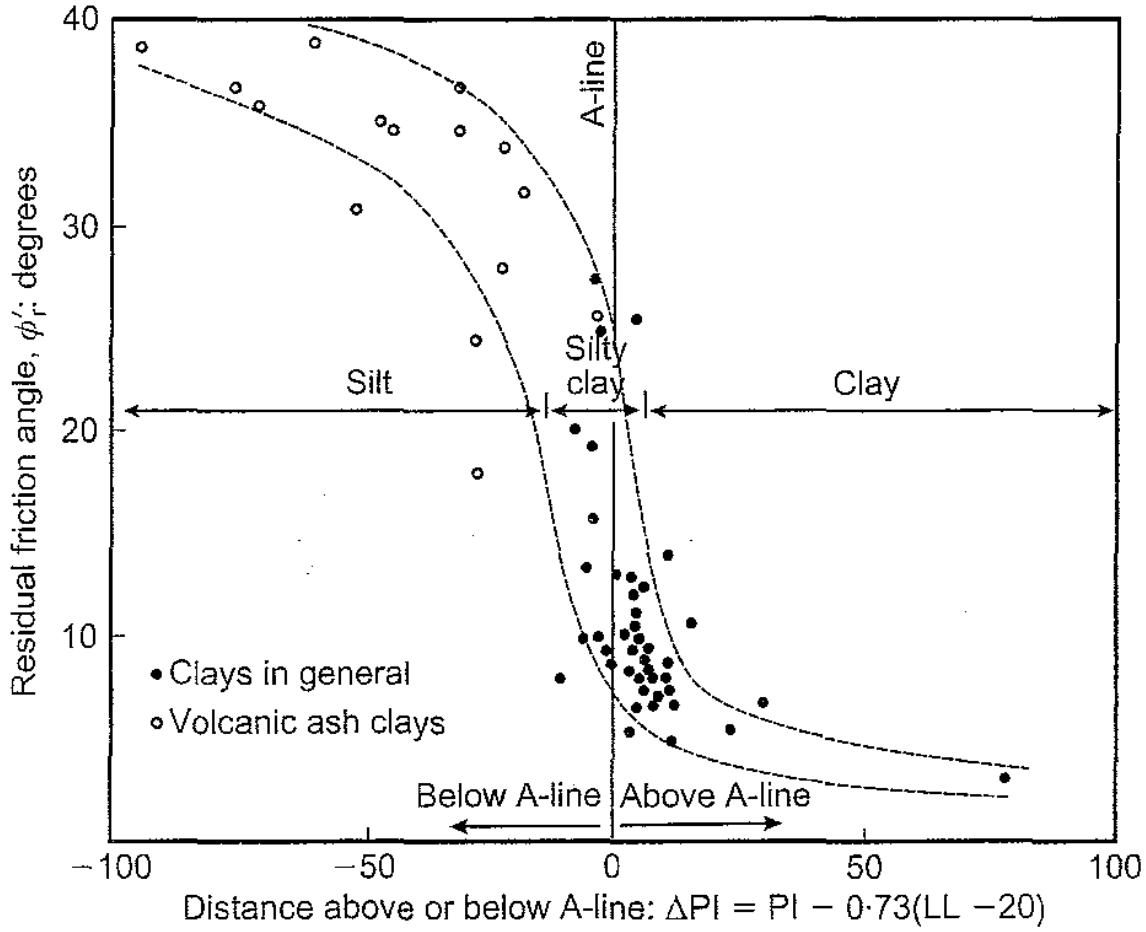

Figure 6.17. Residual fiction angle plotted against distance above or below the A-line (ΔPI) (from Wesley 2003).

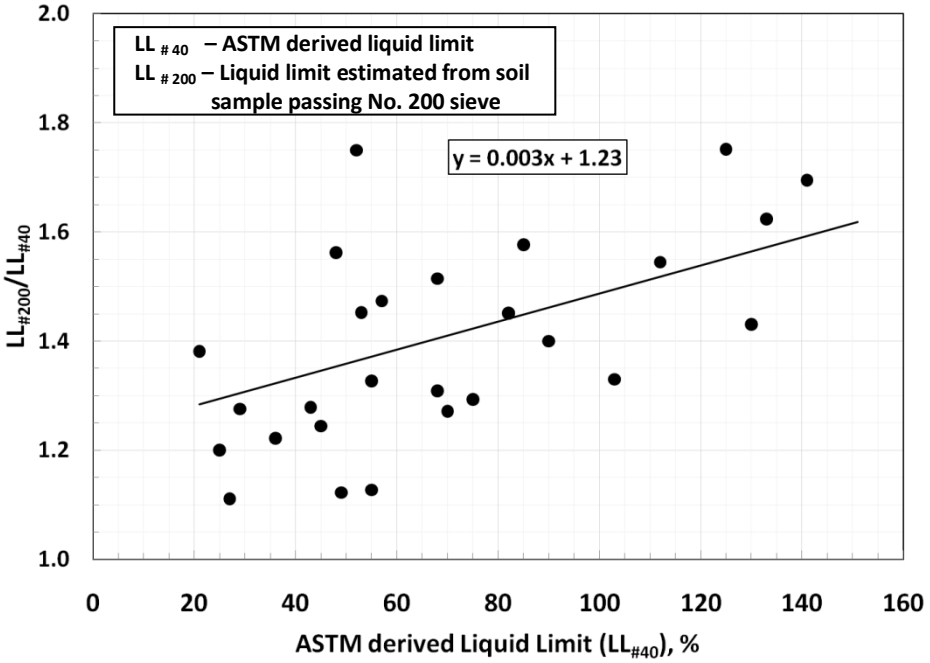

Figure 6.18. Ratio of LL values derived from the material processed through Number 200 sieve ($LL_{\#200}$) and ASTM derived LL values ($LL_{\#40}$) (data from Stark et al., 2005a, Eid 2006 & 2 new soils).

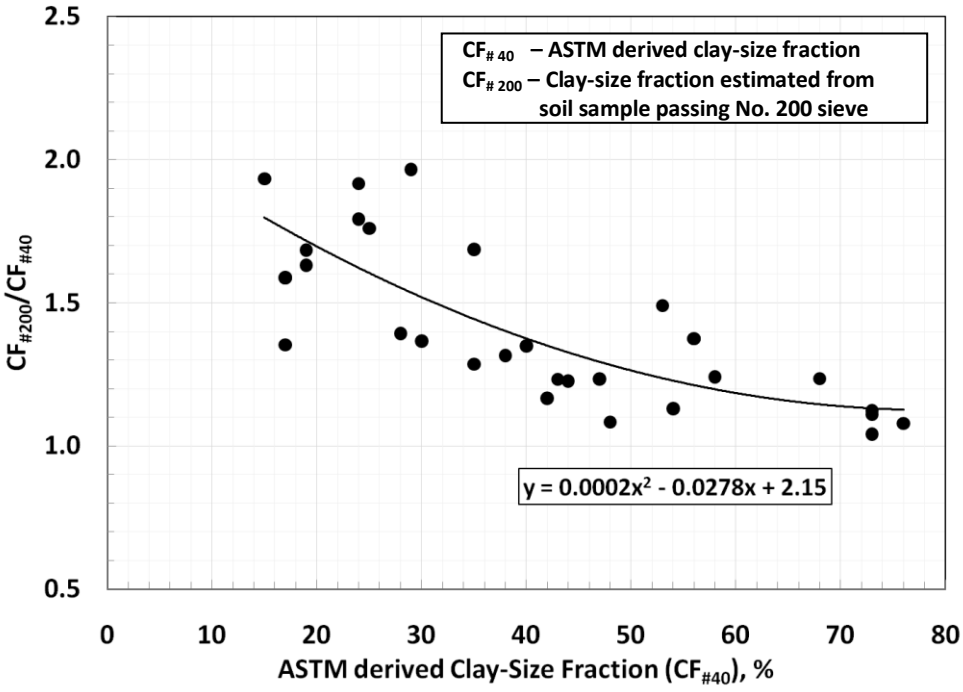

Figure 6.19. Ratio of CF values derived from the material processed through Number 200 sieve ($CF_{\#200}$) and ASTM derived CF values ($CF_{\#40}$) (data from Stark et al., 2005a & Eid 2006).

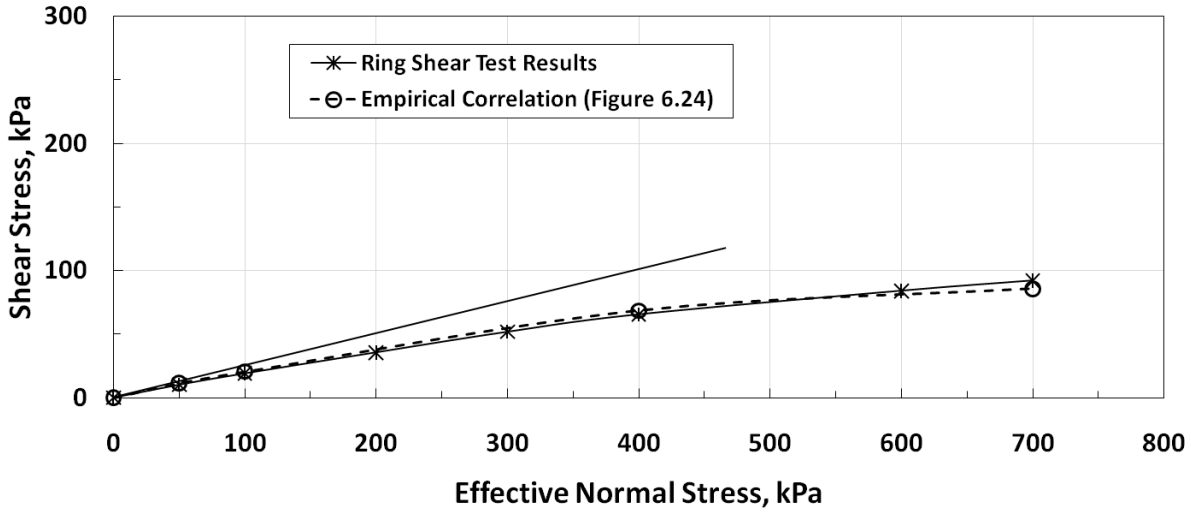

Figure 6.20. Effect of nonlinearity of a stress dependent residual strength failure envelope at low effective normal stress of 50 kPa (ring shear test results of Madisette clay from Los Angeles, Calif.).

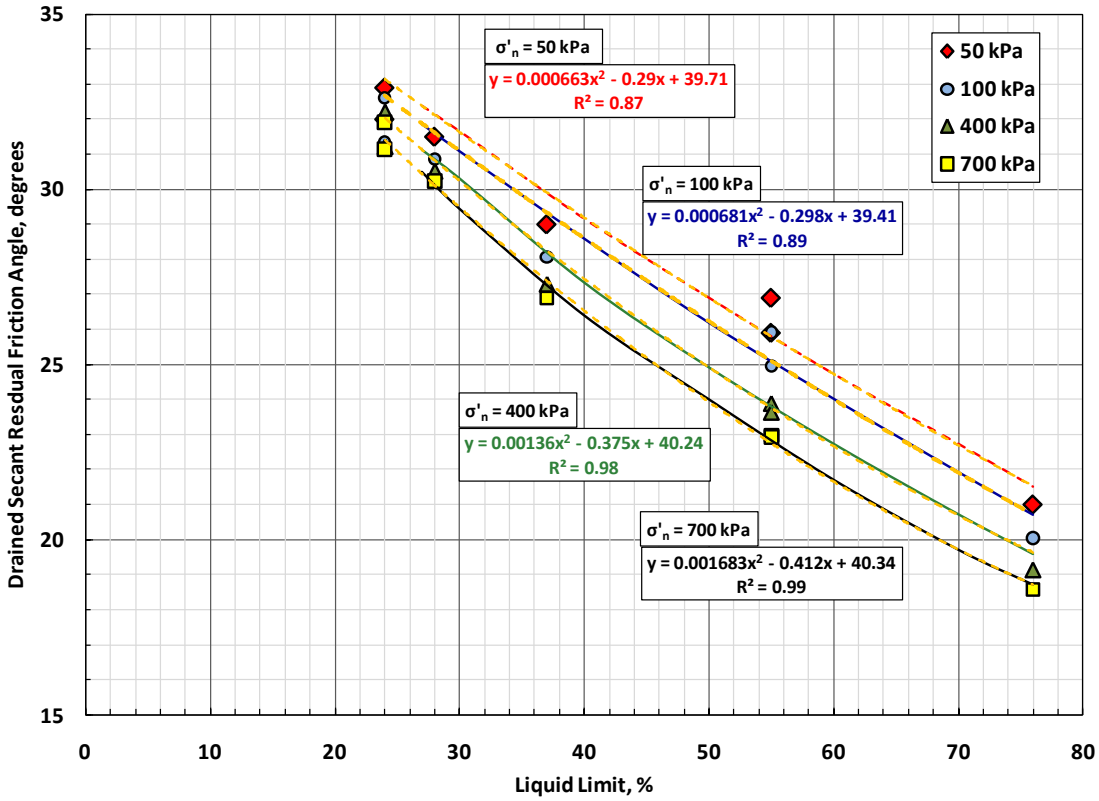

Figure 6.21. Relationship between drained secant residual friction angles and LL for CF Group # 1 (CF $\leq$ 20%).

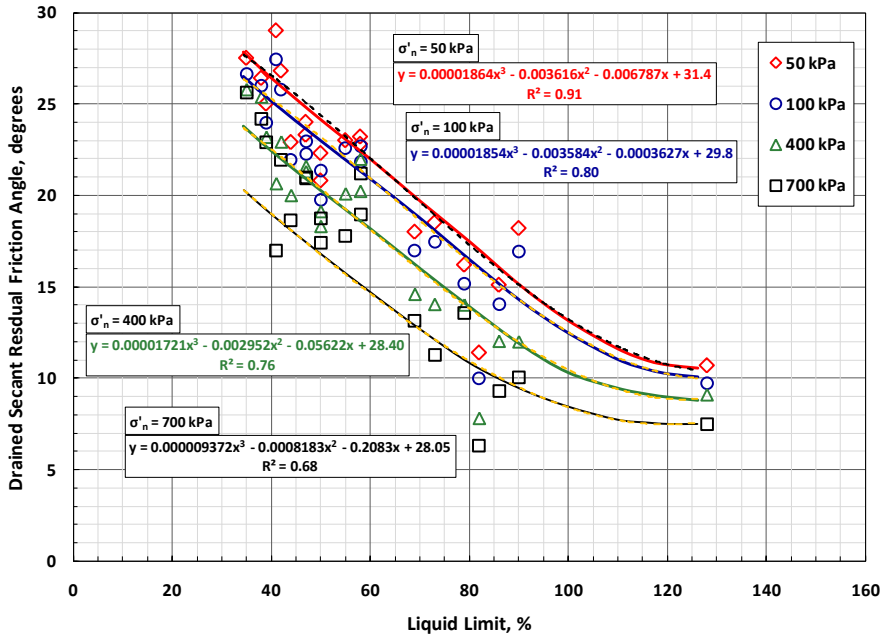

Figure 6.22. Relationship between drained secant residual friction angles and LL for CF Group # 2 (25% ≤ CF ≤ 45%).

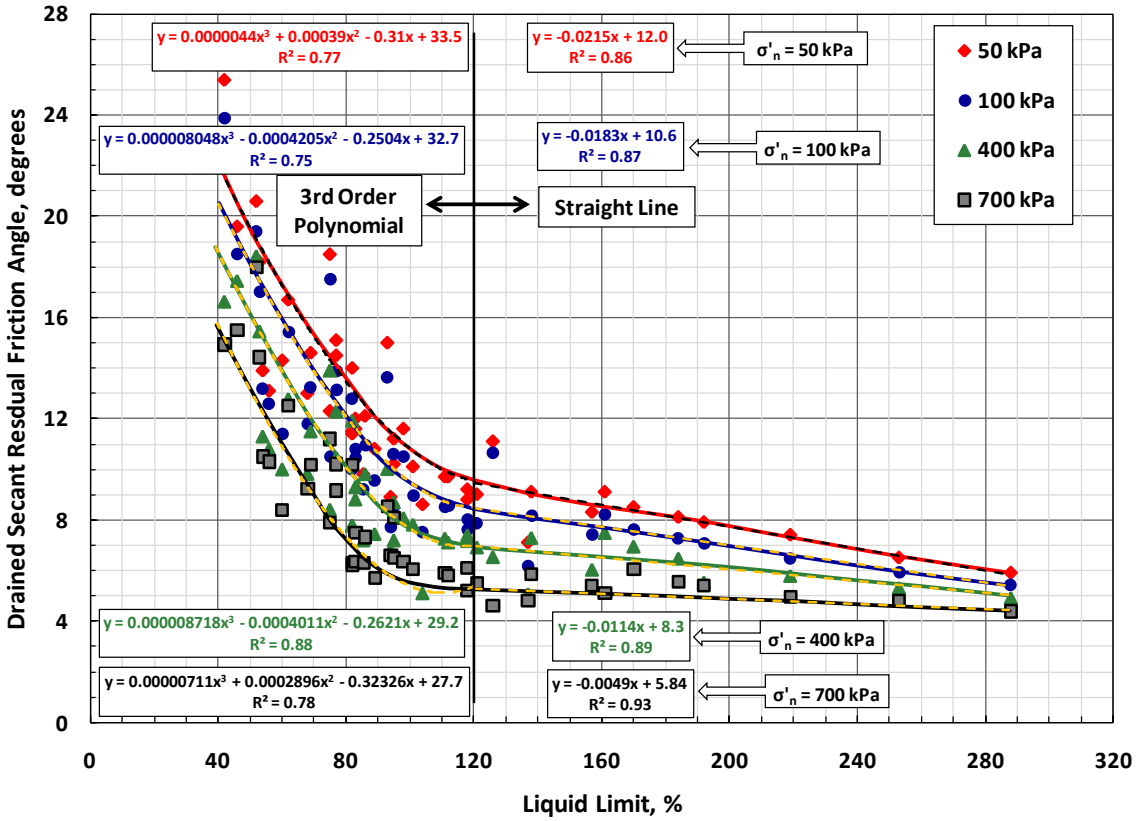

Figure 6.23. Relationship between drained secant residual friction angles and LL for CF Group # 3 (CF ≥ 50%).

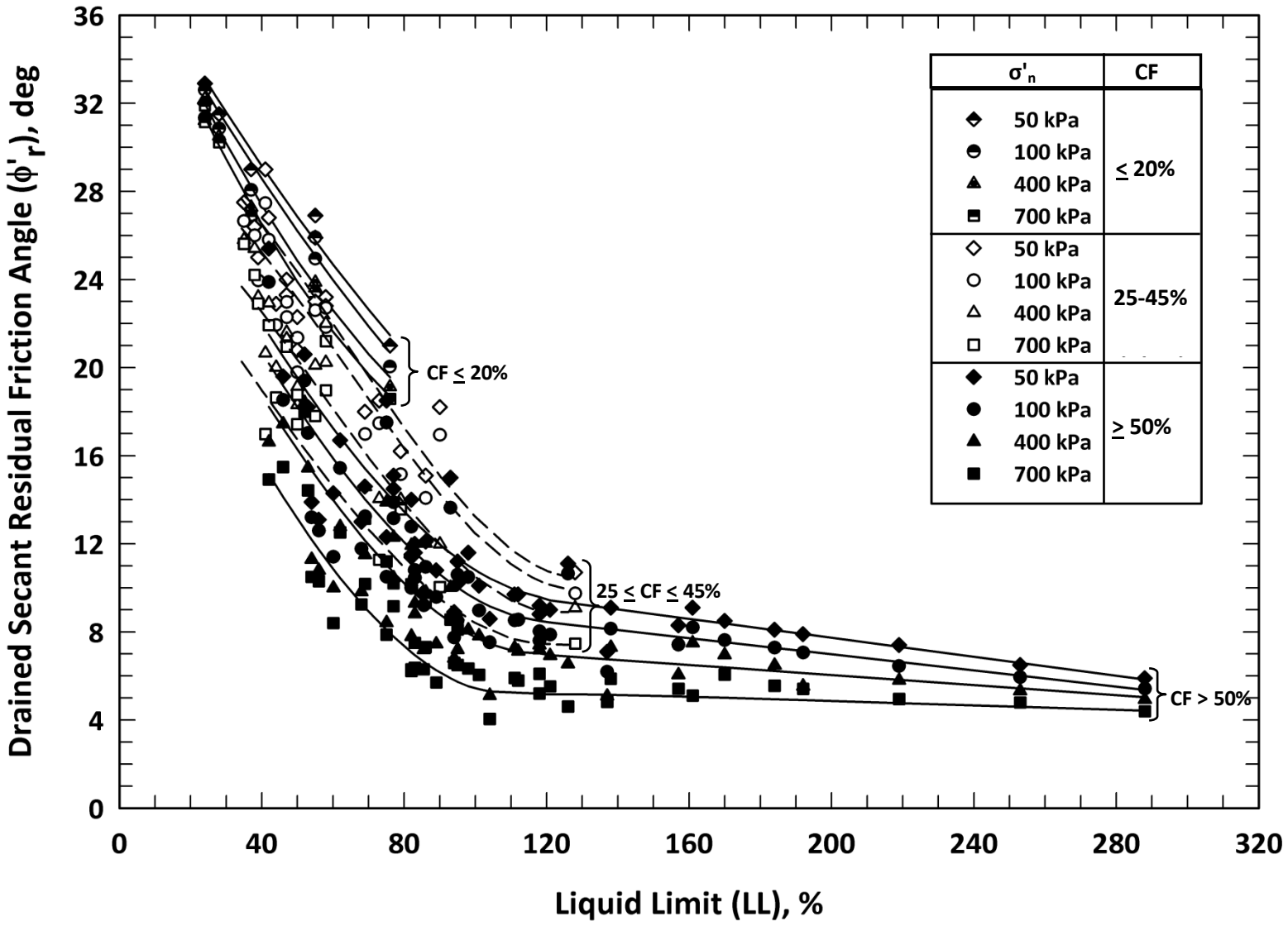

Figure 6.24. New empirical correlations for ϕ'_r based on LL, clay-size fraction (CF) and effective normal stress (σ'_n) (data from Stark and Eid, 1994, Stark et al., 2005a, and seven new soils (total 73 soils)).

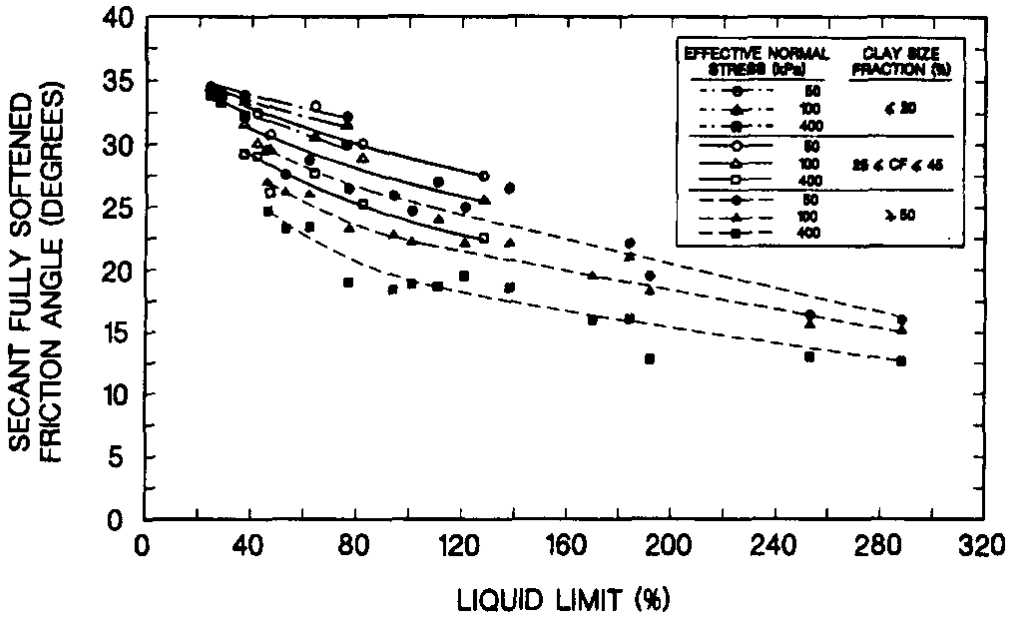

Figure 6.25. Relationship between secant fully softened friction angles and LL for triaxial compression mode of shear (from Stark and Eid, 1997).

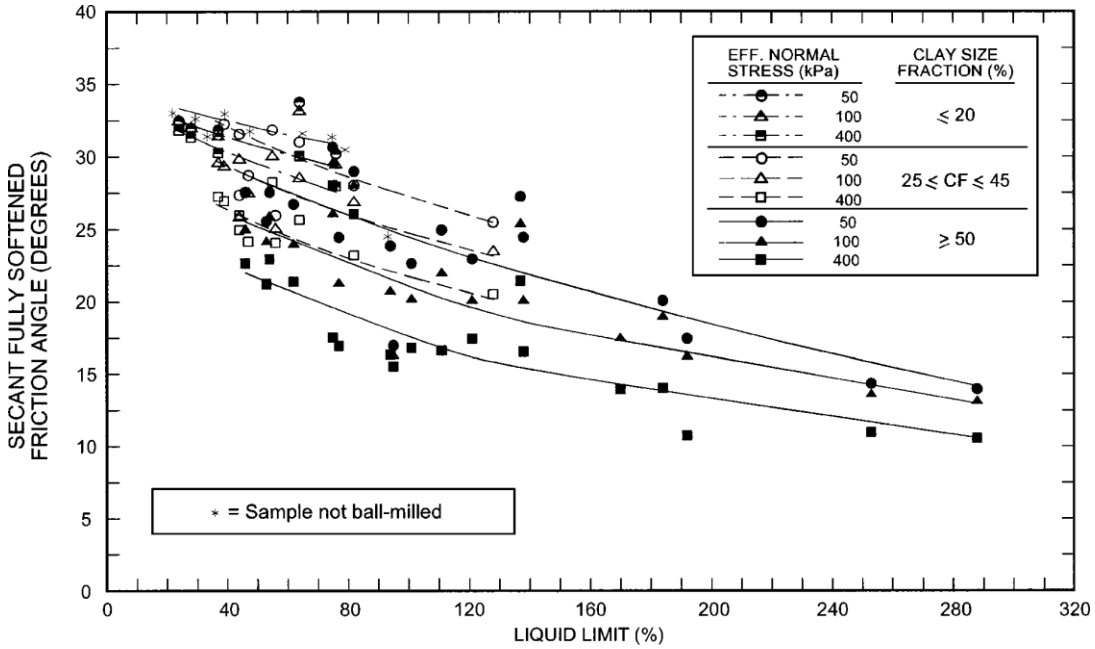

Figure 6.26. Secant fully softened friction angle relationships with LL, CF, and σ'_n (from Stark et al., 2005a).

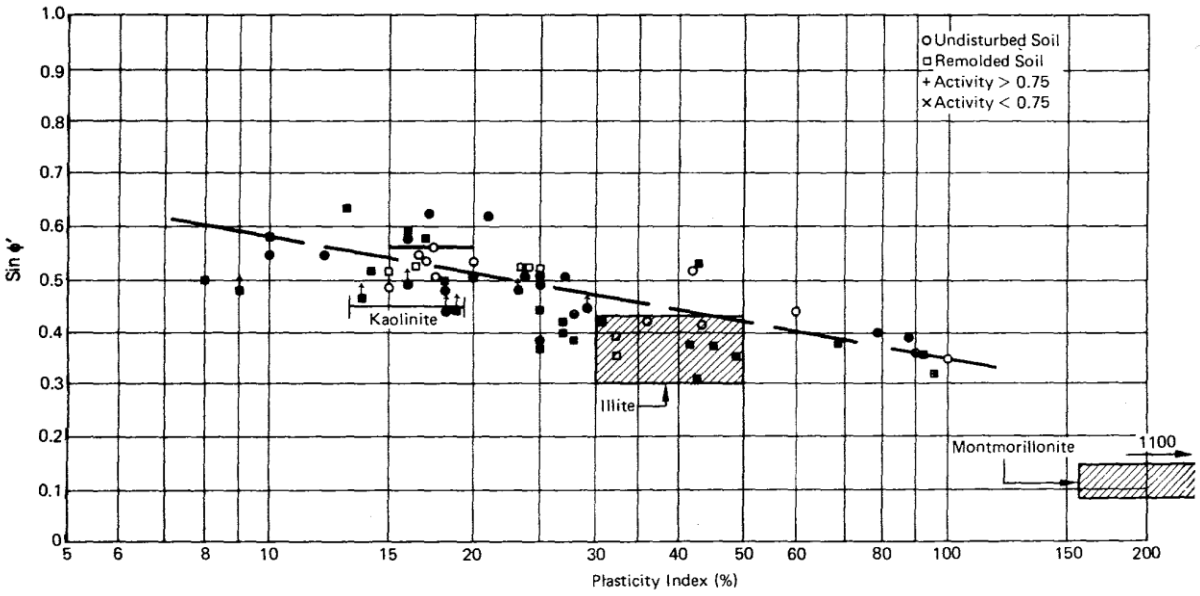

Figure 6.27. Relationship between sin ϕ' and plasticity index for normally consolidated soils (from Mitchel and Soga (2005), figure adapted from Kenney (1959) and data for pure clays from Olsen (1974)).

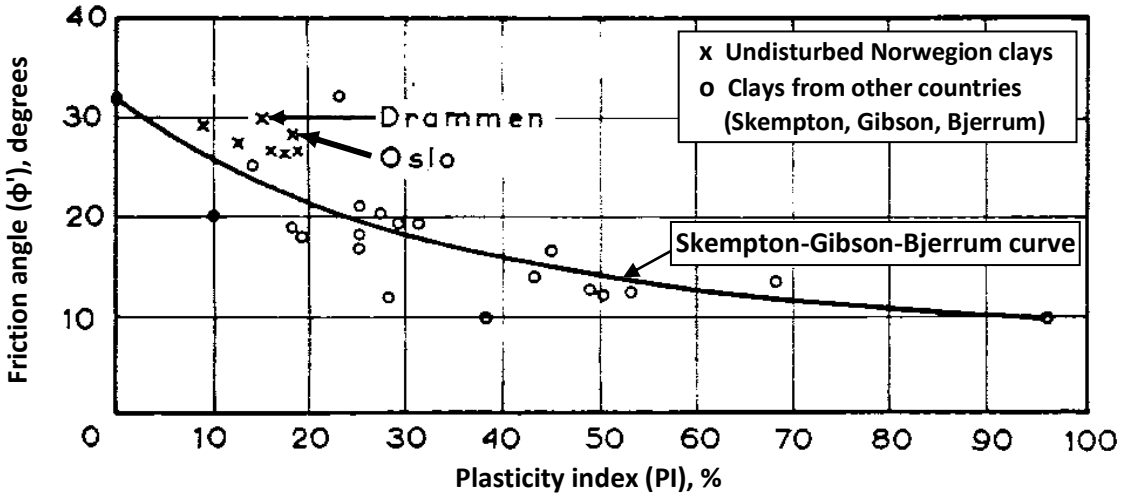

Figure 6.28. Relationship between ϕ' and plasticity index and Skempton-Gibson-Bjerrum correlation (from Bjerrum and Simons, 1960).

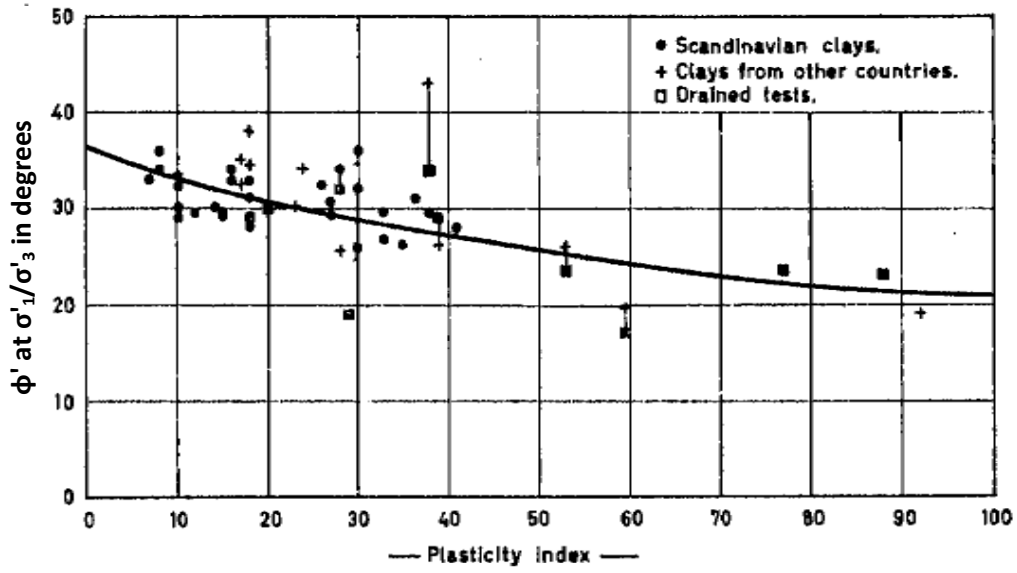

Figure 6.29. Relationship between ϕ' at (σ_1/σ_3) and plasticity index (from Bjerrum and Simons, 1960).

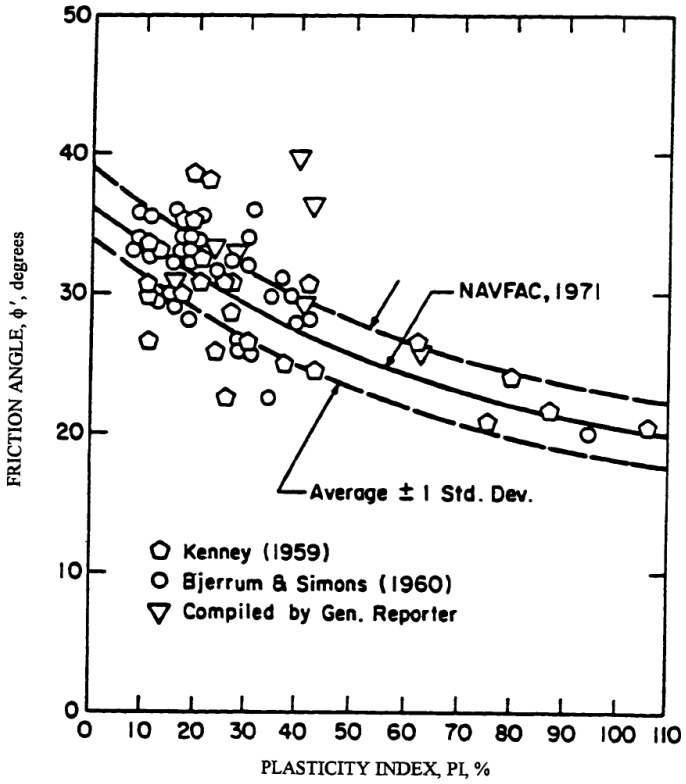

Figure 6.30. Correlation between ϕ' at (σ_1/σ_3) and PI from triaxial tests on normally consolidated clays (after Ladd et al., 1977).

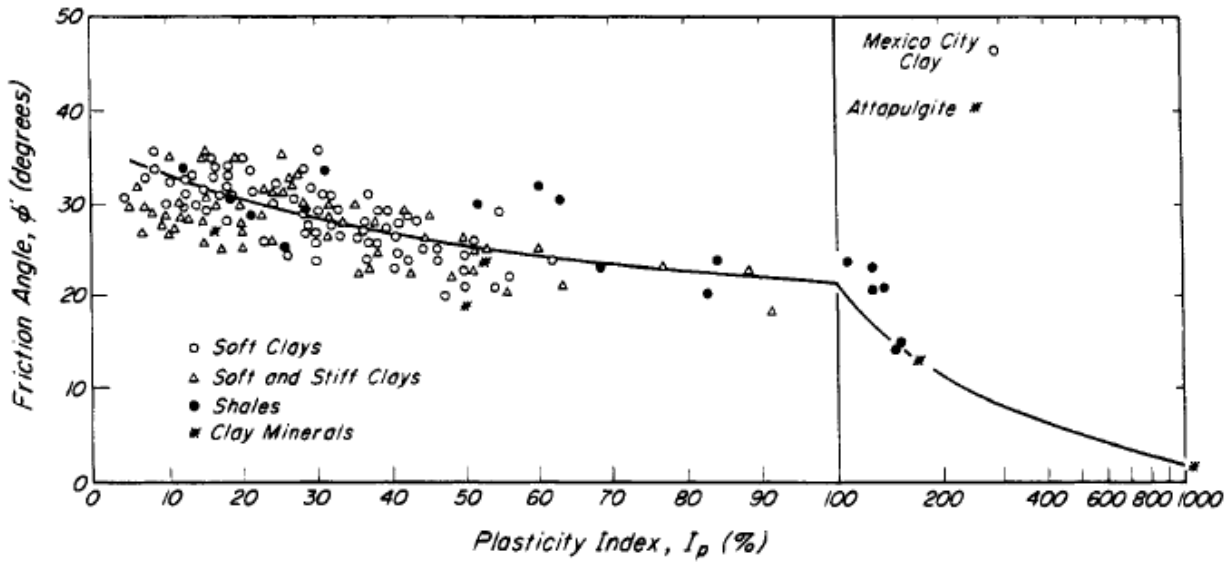

Figure 6.31. Values of secant fully softened secant friction angle for clays of various compositions as reflected in plasticity index (from Mesri and Abdel-Ghaffar, 1993).

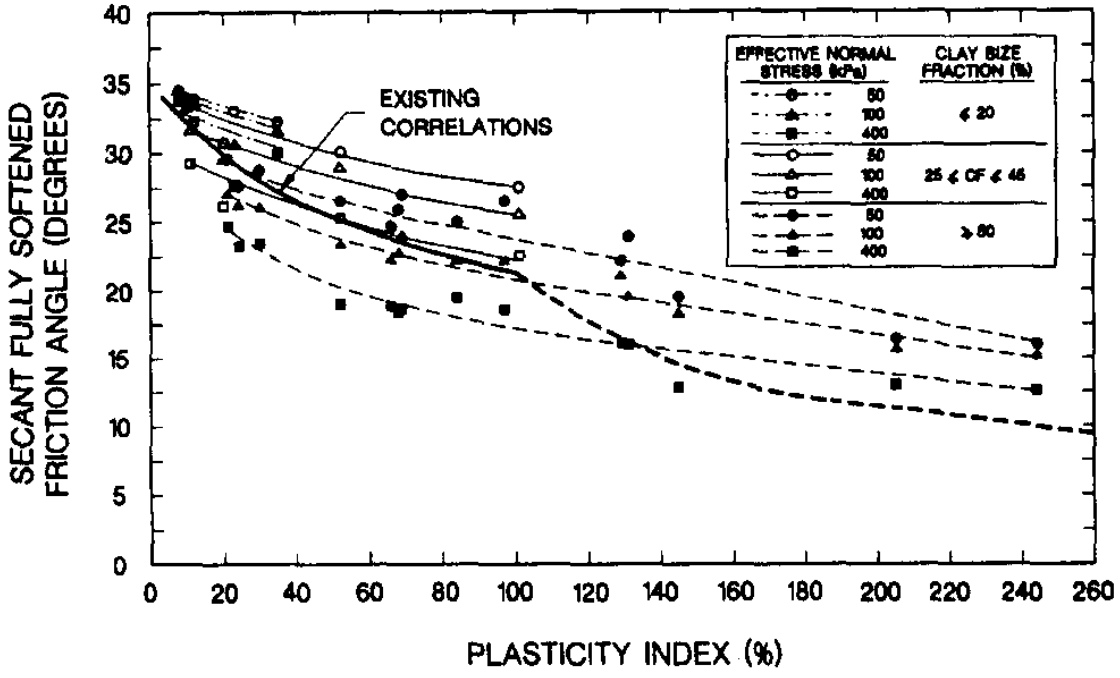

Figure 6.32. Relationship between secant fully softened secant friction angles and PI (from Stark and Eid, 1997).

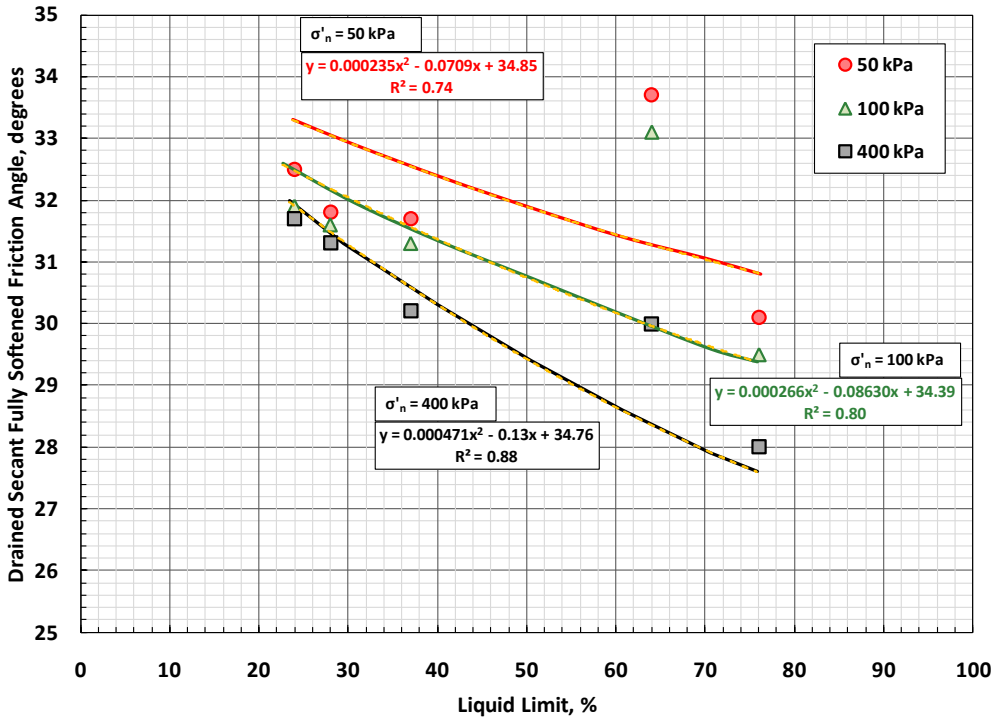

Figure 6.33. Relationship between drained secant fully softened friction angles and LL for CF Group # 1 (CF $\leq$ 20%).

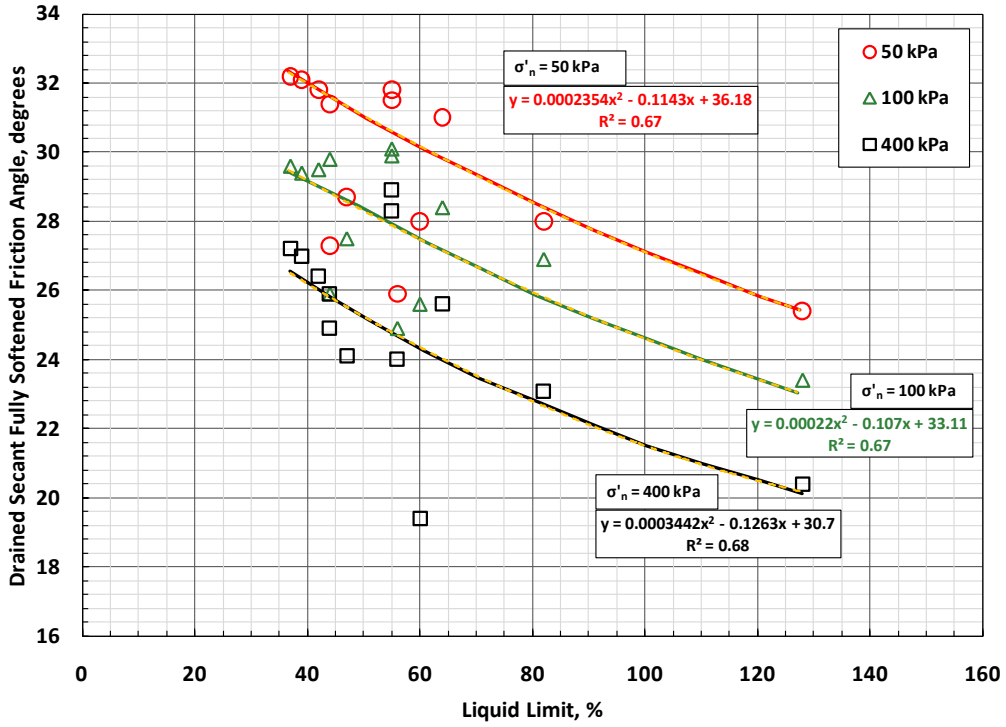

Figure 6.34. Relationship between drained secant fully softened friction angles and LL for CF Group # 2 (25% $\leq$ CF $\leq$ 45%).

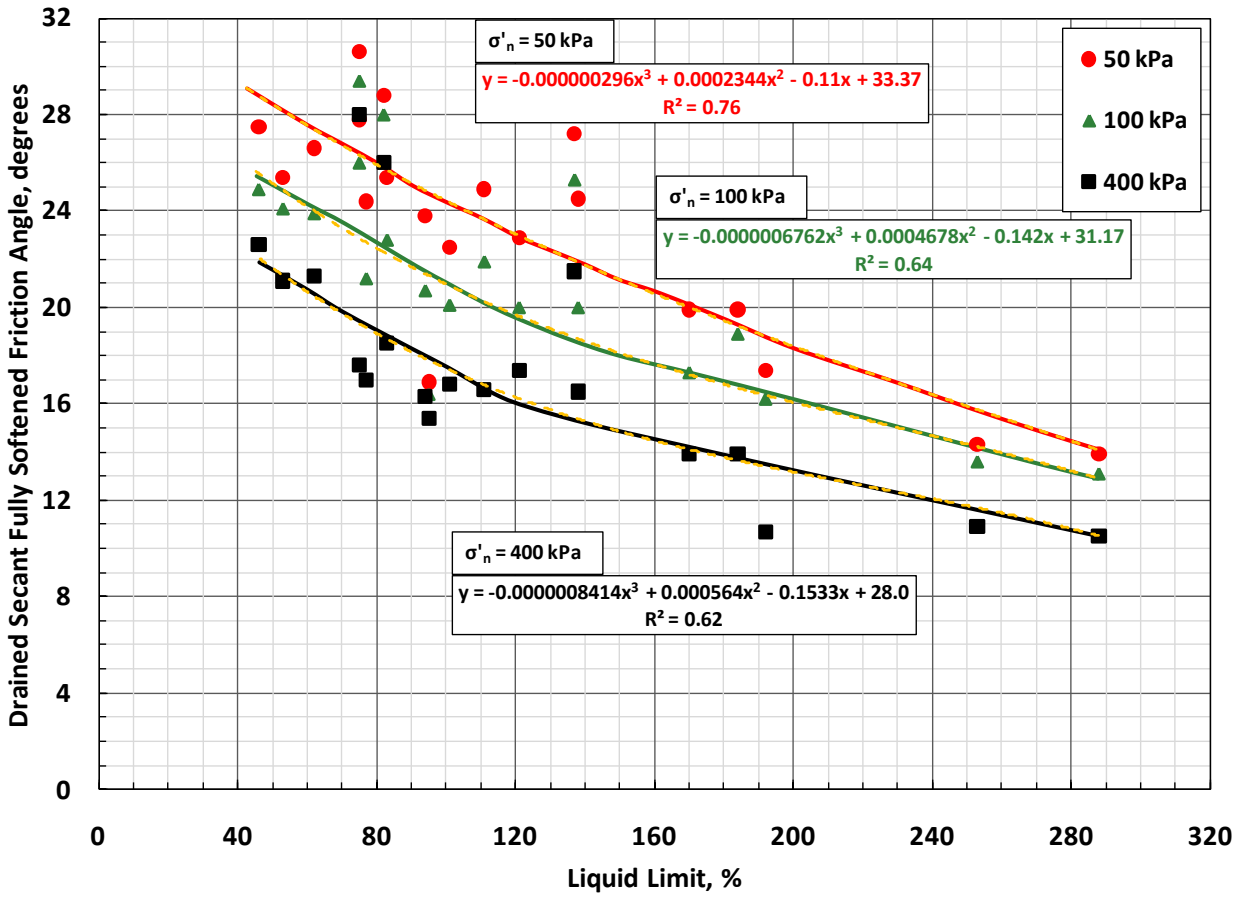

Figure 6.35. Relationship between drained secant fully softened friction angles and LL for CF Group # 3 (CF $\geq$ 50%).

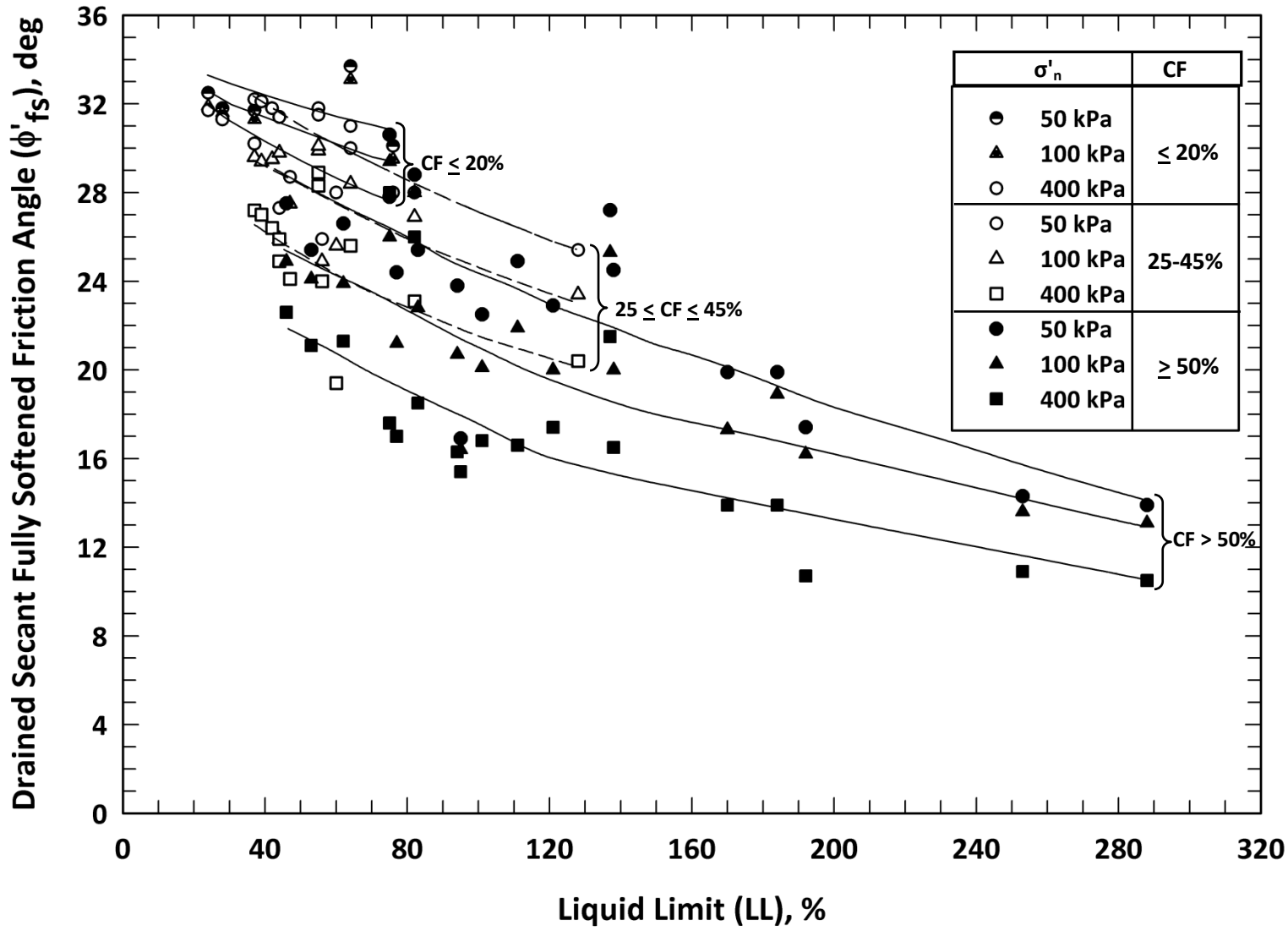

Figure 6.36. New empirical correlation for ϕ'_{fs} based on LL, clay-size fraction (CF) and effective normal stress (σ'_n) (data from Stark and Eid, 1997, Stark et al. 2005a, and three new soils (total 39 soils)).

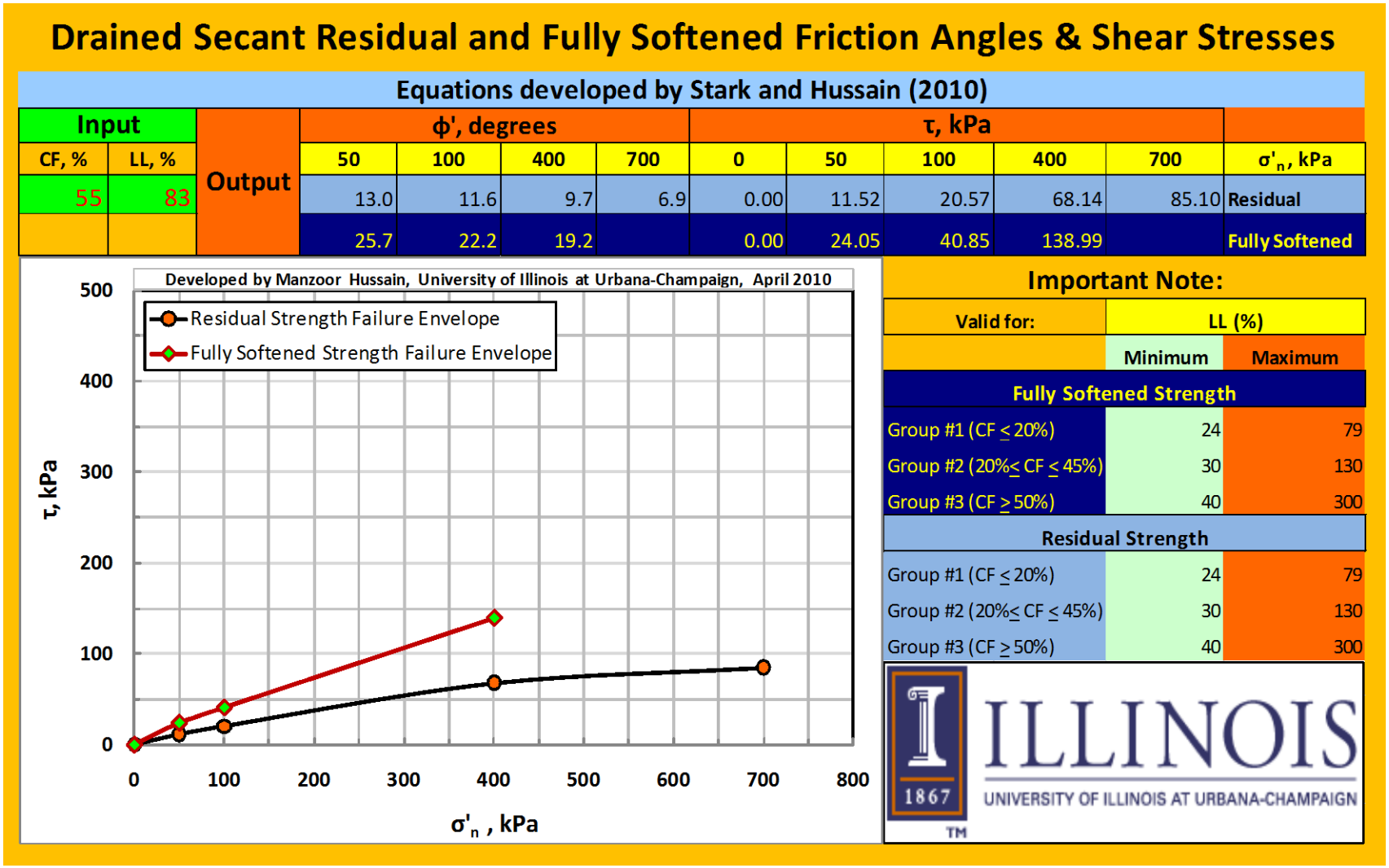

Figure 6.37. Layout of worksheet developed in MS Excel for new empirical correlations for drained secant residual and fully softened friction angles (only LL and CF are used as input to make calculations and plot).

CHAPTER 7: SUMMARY AND CONCLUSIONS

7.1 Summary

The present study presents a review of the importance of drained shear strengths, i.e., residual and fully softened, in the analysis of landslides. A detailed summary and analysis of available laboratory shear devices and various methods to measure the drained residual and fully softened shear strength are presented. The effect of sample preparation on index properties, e.g., LL and CF, and drained residual and fully softened friction angles is also investigated with recommendations for appropriate sample preparation techniques for measuring these index and engineering properties of soils.

Existing literature on strength recovery was reviewed and summarized to develop a new laboratory strength recovery test method for this study. The literature review on shear strength recovery revealed that three different types of shearing devices, i.e., direct shear box, Japanese ring shear device that is similar to the Bishop et al. (1971) ring shear device, and the Bromhead ring shear device, have been used to investigate the possibility of strength recovery along preexisting shear surfaces. Furthermore, all of the researchers who suggest the possibility of strength recovery along a preexisting shear surfaces use different soils, sample preparation procedures, rest periods, and test procedures. Because different test devices, test methods, rest periods, and sample preparation procedures were used, it is difficult to compare the test results reported in the literature. One useful conclusion from the previous test results is that the recovered shear strength is a function of rest time because longer rest periods result in a greater observed recovered shear strength.

The present study uses two laboratory shearing devices to investigate the strength recovery of cohesive soils. A number of strength recovery tests were performed using the modified Bromhead torsional ring shear device on four natural soils and a direct shear box was sued to test one of these natural soils. The laboratory test results suggest that the recovered shear strength may be relevant for shallow landslides or shallow depths (< 5 m) of a deep-seated landslide because the recovered strength was noticeable only at low effective normal stresses. The laboratory test results show that the recovered strength was lost with a small shear

displacement therefore the recovered strength may not be reliable for design of remedial measures. Back-analysis of two case histories suggest that some strength recovery does occur during a period of no movement but the recovered strength can only be used to explain the slope creep behavior and the stability observed during the period of no movement. On renewal of each slide movement, the recovered strength is lost and thus the residual strength is only available to stabilize the landslide.

Back-analysis of landslides is performed to estimate the available shear strength of the problematic layer present along the shear surface because back-analysis can yield a better estimate of the shear strength as compared to laboratory testing. Because the conditions present along the shear surface and in the slide mass at the time of failure are frequently unknown so some assumptions are required for a back-analysis which introduces uncertainties in the analysis. The uncertainties involved in the back-analysis of landslides are discussed herein and illustrated using various case histories. A new back-analysis procedure for preexisting/reactivated and first-time landslides is suggested in the present study which can help practitioners to select input parameters to simulate the conditions at the time of failure. A more reliable back-analysis will help in a better estimate of the strength along the shear surface and a remedial design.

Empirical correlations are useful for geotechnical engineers and play an important role in practice by providing parameter estimates for use in preliminary design and providing a check on data obtained from laboratory and insitu tests. Empirical correlations for residual and fully softened shear strength are relevant to landslides, therefore, a detailed review of previous residual and fully softened empirical correlations was made. Because the empirical correlations proposed by Stark et al. (2005a) for drained residual and fully softened friction angle are widely used in practice and research, an effort was made to update and improve these correlations by adding new data, a trend line for an effective normal stress of 50 kPa, and developing mathematical equation for each trend line to facilitate their use. Because the stress dependent failure envelope has more curvature at low effective normal stresses, new data and trend-lines for an effective normal stress of 50 kPa were added to the drained residual friction angle correlation.

A new MS Excel spreadsheet was developed using the mathematical equation(s) for each trend line which requires only two input parameters, i.e., LL and CF, and calculates the values of drained residual and fully softened friction angles and shear stresses. The spreadsheet output

presents two stress dependent failure envelopes one each for the drained residual and fully softened shear stress on a single graph. The user can estimate the difference in the two values and decide on the appropriate strength for analysis and design. The user can use the relevant stress dependent failure envelope in slope stability software directly to capture the stress dependent nature of the soil. The methodology used in developing the spreadsheet has been coded in computer software Visual Basic, VB 6.0, which allows exporting of the results to a spreadsheet or any other format. Because most of the slope stability software has the option to input a nonlinear or stress dependent failure envelope for the analysis, the equation based empirical correlations may help utilizing stress dependent failure envelopes in practice.

7.2 Conclusions

7.2.1 Conclusions from Shear Strength Recovery Test Results

The present study concludes that a torsional ring shear device is a better device than a direct shear box for performing strength recovery tests because shearing occurs in one direction, unlimited shear displacement can be applied, the effective normal stress is uniformly applied to the entire specimen, and secondary compression results in a uniform vertical movement of the entire shear surface. Furthermore, establishing a residual strength condition in a specimen is necessary for performing a strength recovery test because it is used as the starting point to measure a strength gain. A torsional ring shear device yields more reliable results than a direct shear box because unlimited shear displacement can occur to orient the clay particles parallel to the direction of shear. In a torsional ring shear device the specimen also can be subjected to the normal and shear stresses during the rest period.

It is recommended that the strength recovery tests be conducted using an overconsolidated specimen to reduce the magnitude of secondary compression during the rest period especially for direct shear tests. The specimen should be subjected to the normal and shear stresses that correspond to the residual strength of the soil to simulate field conditions.

The direct shear test should be stopped for a rest period after a constant, minimum strength is achieved. Furthermore, the direct shear test period should be stopped for a rest when the direct shear box is moving in the forward direction so the proving ring is in compression not tension because the proving ring is usually calibrated in compression and performs well in

compression as compared to tension. Caution should be exercised when setting up the direct shear test, during shearing and during the rest periods so the shear surface remains in the gap between the two halves of the shear box and above the top of bottom half.

The laboratory study suggests that the direct shear strength recovery test results differed from the ring shear strength recovery test results for a similar soil at similar effective normal stresses. The difference between the ring shear and direct shear test results may be due to differences in measured drained residual shear strength in each device, difference in test procedures, and different in the state of applied stresses during the rest periods in both devices.

The mechanism(s) involved in strength recovery/healing may be secondary compression of the shear surface material, van der Waals attractions, cation exchange, thixotropic hardening and/or particle reorientation as result of particle unbending at low effective normal stresses. The ring shear specimens tested herein were submerged in distilled and deionized water, and the tests were conducted at a constant temperature of 70ºF so desiccation, water chemistry, and temperature probably did not play a major role in the observed strength increase at an effective normal stress of 100 kPa.

Strength recovery at effective normal stresses of 100 kPa or less, which represents shallow landslides ($\leq$ 5 m depth) or shallow portions along a deep failure surface, is noticeable in the ring shear and direct shear test results. However, strength gain is essentially negligible at effective normal stresses greater than 100 kPa in the ring shear device.

Strength gain at effective normal stresses of 100 kPa or less may be caused by rebounding/reorienting of clay particles previously oriented parallel to the direction of shear. At higher effective normal stresses, the particles are less able to rebound/reorient and therefore the strength gain is negligible.

High plasticity soils, with a large difference between the fully softened and residual strengths, exhibit a higher strength gain from the residual value than low plasticity soils at an effective normal stress of 100 kPa or less.

Even at low effective normal stresses, the recovered strength will not reach the fully softened strength for the soils tested because of the presence of a preexisting shear surface and

clay particles oriented parallel to the direction of shear. The recovered shear strength for low plasticity soils (LL< 50%) is closer to the fully softened strength after long recovery periods than high plasticity soils (liquid limit between 80% and 112%) at an effective normal stress of 100 kPa or less. This is caused by the smaller difference between the fully softened and residual strengths for low plasticity soils than high plasticity soils.

The observed recovered strength in ring shear and direct shear tests even at an effective normal stress of 100 kPa is lost with a small shear displacement so the benefit of this strength for the repair of shallow landslides or the shallower portion of a deep-seated landslide may not be significant. This leads to the conclusion that the observed strength gain has limited practical significance in the analysis and repair of landslides. Therefore, Skempton's (1964 and 1985) suggestion of using the drained residual shear strength for remediation of reactivated landslides and for comparison with back-calculated shear strength parameters still appears applicable. However, the strength gain at $\sigma'_n \leq 100$ kPa may be useful in explaining the behavior of shallow landslides, such as slope creep behavior and stability prior to slide reactivation. It is also concluded that the analysis and design of both shallow and deep-seated landslides should use the drained shear strength measured using ASTM D6467 (2008c) for design purposes.

7.2.2 Back-Analysis of Landslides

The back-analysis procedures presented in the present study can be used in the back-analysis of all landslides, i.e., reactivated/preexisting and first-time landslides. The back-analysis of landslides involves many uncertainties. Therefore, experience and judgment should be used in selecting the input parameters and assumptions for the other slide mass materials. The assumptions made in the back-analysis have different effects than those made for design and sometimes the mechanics of back-analysis are not understood and incorrect assumptions are made for the back-analysis.

Site observations of a landslide are helpful in gaining an understanding of the subsurface conditions at the time of failure. Available piezometer and inclinometer data provides useful information about the conditions present at the time of failure and must be incorporated in the back-analysis. In the absence of adequate subsurface information/data, large diameter borings

can be used to obtain more representative samples than conventional borings and help in visual inspection of the soil stratigraphy and location of the failure surface by downhole inspection.

Accurate estimate of the groundwater surface and effect of rainfall on the groundwater surface should be determined using available rainfall data for the area and developing the rainfall threshold that initiate movement. Rainfall is most important for shallow landslides, therefore, the effect of rainfall should be considered in such back-analyses.

A conservative shear strength parameter for overlying materials yields an unconservative result in the back-analysis. Therefore, the best estimate of the shear strength parameters is necessary to economize the repair measures. The back-calculated shear strength parameters should be verified from laboratory testing or existing empirical correlations and if needed adjustments should be made to the input assumptions.

If a tension crack develops, shear resistance is not developed along the tension crack and is only developed along the length of slip surface below the tension crack depth at the time of sliding. Including a tension crack in the failure surface is likely to result in an underestimate of the back-calculated shear strength of the problematic layer. The depth of tension crack can be estimated by measuring the vertical or near vertical part of the slip surface at the top of the slope or can be measured by excavation at the top of the slide mass. During the present study it was determined that when the tension crack depth is up to 15% of the length of the failure surface, the effect of incorporation of the tension crack in the back-analysis is negligible. However, this result needs to be confirmed for a range of slope geometries.

Instead of searching for the critical failure surface, the back-analysis must use the actual failure surface to back-calculate the strength parameters. Selections of a suitable slope stability software and stability method used for the back-analysis are important. Recommendations are presented herein for both issues.

7.2.3 Effect of Sample Preparation on Index Properties and Drained Friction Angles

The residual strength is a fundamental property of the soil because the soil structure, stress history, particle interference, particle orientation, and diagenetic bonding have been removed by continuous shear displacement in one direction. In the field, the shearing process

disaggregates the clay particles and a higher LL and CF along the shear surface is usually measured compared to the LL and CF of soil above or below the shear surface because these materials are not disaggregated. A highly overconsolidated clay disaggregated either by ball milling or any other technique and processed through the Number 200 sieve will reach the residual strength in a ring shear device after a smaller shear displacement than a sample processed through the Number 40 sieve because the particles are initially more disaggregated. Except for a smaller shear displacement to residual, sample preparation does not affect the measured residual shear strength or friction angle.

The procedure for remolded sample preparation influences the measurement of LL and CF. A highly overconsolidated clay, such as a claystone, mudstone, or shale may possess varying degrees of particle induration (aggregation). The LL of a clay mineral is its ability to hold water and finer particles with more surface area will result in a greater LL as compared to aggregated particles. Because more of the diagenetic bonding and induration is eliminated as a result of processing the soil through the Number 200 sieve by ball milling or some other means, more particle surface area is exposed and able to hydrate than if the clay particles are not disaggregated. Therefore, a soil sample containing aggregated clay particles after crushing and processing through the Number 200 sieve results in a higher LL and CF as compared to the sample processed through the Number 40 sieve as required by ASTM test methods.

Clays that do not have aggregated particles should not be processed through the Number 200 sieve after crushing the particles by ball milling or any other mean. It is anticipated that ball milling of such a clay sample may result in changing the texture and gradation of the soil. Thus, a soil sample processed through the Number 40 sieve for such soils that do not have particle aggregation should be used to measure LL and CF. Therefore, a judgment is required to determine whether or not a material should be processed through the Number 200 sieve for measuring LL and CF.

Because of the effort and equipment needed to process the soil through the Number 200 sieve, it is desirable to facilitate measurement of the LL and CF of heavily overconsolidated clays. Empirical correlations are presented herein that use ASTM derived LL and CF to estimate disaggregated values of LL and CF for highly overconsolidated clays. These disaggregated values of LL and CF are used to estimate ϕ'_r and ϕ'_{fs} for heavily overconsolidated clays.

The fully softened shear strength corresponds to a random arrangement of particles that reflects the ability of particles to establish short range interaction and interlocking. Because the fully softened shear strength corresponds to the peak strength of a normally consolidated remolded specimen, particle disaggregation does not occur as in the case of the residual strength condition. The aggregated particles of highly overconsolidated clays are not likely to disaggregate at the time of mobilization of fully softened shear strength in the field because they have not undergone any shear displacement. Thus, a fully softened shear strength can be the peak strength of a normally consolidated sample prepared from material processed through the Number 40 sieve. This sample preparation does affect the laboratory determined fully softened shear strength especially when using a torsional ring shear device.

7.2.4 Measurement of Drained Residual and Fully Softened Shear Strength

The residual shear strength can be estimated from an intact slip surface or a remolded specimen prepared from a sample obtained from a shear surface. Because of the difficulties involved in obtaining and trimming a representative intact specimen, a remolded specimen prepared from a shear surface sample is preferred to estimate the residual shear strength.

The torsional ring shear device yields a better estimate of residual shear strength than other laboratory shear devices. The modified ring shear device described by Stark and Eid (1993) is simple, easy to use, and gives results that have been verified using case histories. A direct shear box has many limitations but can be used to obtain a rough estimate of residual shear strength by reversing the direction of shear displacement a number of times. A triaxial compression test is not suitable to estimate the residual shear strength because of the limited axial strain available which is not sufficient to establish a residual condition.

The drained residual strength measured using two different precut specimens that were consolidated to different effective normal stresses and sheared at similar effective normal stresses are in agreement and confirms that the residual shear strength is independent of the OCR or loading history. However, the values of drained residual friction angle obtained from direct shear tests are lower than the values obtained from ring shear tests at similar effective normal stresses on the same soil. This difference in ϕ'_r at similar effective normal stresses is greater than

3.5° which reinforces that the direct shear device is not suited for measuring the drained residual strength of cohesive soils.

The fully softened shear strength is the peak strength measured using a normally consolidated soil sample. The fully softened shear strength is measured using a remolded specimen consolidated to the desired effective normal stress. The fully softened shear strength can be measured using a torsional ring shear device, a direct shear box, and/or a triaxial apparatus. A triaxial compression test is usually preferred to measure the fully softened shear strength because it best simulates the field conditions. A torsional ring shear device can also give reliable results while using a remolded soil sample processed through Number 40 sieve.

7.2.5 Empirical Correlations for Drained Residual and Fully Softened Friction Angles

Empirical correlations are frequently used to estimate the engineering properties of a soil from simple index parameters, e.g., LL, CF, and PI. The relevant empirical correlations for landslides and slope stability involve the residual and fully softened friction angles. The drained residual friction angle is correlated with LL, CF, and PI and the drained fully softened friction angle is correlated with LL and PI.

The drained friction angle of a soil is function of soil plasticity, clay-size fraction, and effective normal stress. A detailed review of existing empirical correlations for residual friction angle show considerable scatter ranging from 7° to more than 20° except the Stark and Eid (1994) and Stark et al. (2005a) correlation that shows a scatter of only 2-3°. Similarly, a scatter of 6° to 18° for ϕ'_{fs} is present in the literature except the Stark and Eid (1997) and Stark et al. (2005a) correlation that show a scatter of only 2-3°. The reasons for such considerable scatter in both ϕ'_r and ϕ'_{fs} values by researchers other than Stark and Eid (1994 and 1997) and Stark et al. (2005a) can be attributed to omitting the effect of CF on the these two shear strength parameters. Furthermore, other researchers do not consider the effect of stress dependent failure envelopes on residual and fully softened shear strength parameters. Although Mesri and Shahien (2003) consider the effect of stress dependency on ϕ'_r and ϕ'_{fs}, omitting the effect of CF still results in considerable scatter even though the data from Stark and Eid (1994 and 1997) is used.

Empirical correlations developed herein correlate both ϕ'_r and ϕ'_{fs} to LL, CF, and also the stress dependent nature of both strengths. To maintain the consistency between the two correlations, both ϕ'_r and ϕ'_{fs} are correlated with LL and CF estimated using a similar procedure. The values of LL and CF are estimated using a soil sample processed through the Number 200 sieve for highly overconsolidated clays and a sample processed through the Number 40 sieve for all other clays.

Because a stress dependent failure envelop has more curvature at low effective normal stresses, data for an effective normal stress of 50 kPa has been added to the Stark et al. (2005a) ϕ'_r correlation and new trend-lines were developed for each CF group.

New empirical mathematical expressions were developed for the trend lines for both drained residual and fully softened friction angles. Separate equations are developed for each CF group and each trend line for the four different effective normal stresses in each CF group. The mathematical expressions eliminate the need for consulting with the empirical correlation which is available in graph form. The mathematical expressions have been incorporated in a spreadsheet to facilitate use of the empirical correlations. Only two input parameters, i.e., LL and CF, are required to calculate the values of ϕ'_r and ϕ'_{fs} and also the shear stresses using the new spreadsheet. The stress dependent residual and fully softened failure envelopes are also plotted on a single plot by the spreadsheet for comparison purposes. The methodology used to develop the spreadsheet has been coded in a Visual Basic (VB 6.0) program. The VB based interface also uses two input parameters, i.e., LL and CF, and calculates the values for ϕ'_r and ϕ'_{fs} and also the shear stresses with an option to export the output file in any required format, e.g., MS Excel, MS Word, and pdf.

Most slope stability software allows use of a nonlinear failure envelop using specified pairs of shear and effective normal stress. The new spreadsheet or equations can be used to estimate the pairs of shear and effective normal stress for use in the slope stability software.

7.3 Recommendations for Future Research

The present study makes following recommendations for future research:

- Continue strength recovery tests with a Bishop et al. (1971) ring shear device.

- Investigate the use of computer software FLAC for slope stability analyses.
- Test additional soils for inclusion in the residual and fully softened strength correlations.
- Analyze additional strength recovery case histories.

REFERENCES

Alkasawneh, W., Malkawi, A. I. H., Nusairat, J. H., and Albataineh, N. (2008). "A comparative study of various commercially available programs in slope stability analysis." *Computers and Geotechnics J.,* 35, 428–435.

ASTM, (2008a). "Standard test method for liquid limit, plastic limit, and plasticity index of soil." *(D 4318),* West Conshohocken, Pa.

ASTM, (2008b). "Standard test method for particle-size analysis of soils." *(D 422),* West Conshohocken, Pa.

ASTM, (2008c). "Standard test method for torsional ring shear test to determine drained residual shear strength of cohesive soils." *(D 6467),* West Conshohocken, Pa.

ASTM, (2008d). "Standard test method for one-dimensional consolidation properties of soils using incremental loading." *(D 2435),* West Conshohocken, Pa.

ASTM, (2008e). "Standard test method for direct shear test of soils under consolidated drained conditions." *(D 3080),* West Conshohocken, Pa.

ASTM, (2010a). "Standard test method for torsional ring shear test to determine drained fully softened shear strength of cohesive soils." (WK#18521) scheduled for re-balloting by D-18-05 committee. Available at: http://www.astm.org/DATABASE.CART/WORKITEMS/WK18521.htm

ASTM, (2010b). "New test method for repeated direct shear test of soils under consolidated drained conditions." (WK#3822) negative votes need resolution by D-18-05 committee. Available at: http://www.astm.org/DATABASE.CART/WORKITEMS/WK3822.htm

ASTM, (2010c). "New test method for consolidated drained triaxial compression test for soils." (WK#3821) negative votes need resolution by D-18-05 committee. Available at: http://www.astm.org/DATABASE.CART/WORKITEMS/WK3821.htm

Anderson, W. F., and Hammoud, F., (1988). "Effect of testing procedure in ring shear tests." *Geotechnical Testing Journal,* ASTM, 11(3), 204-207.

Angeli, M.-G., Gasparetto, P., Menotti, R. M., Pasuto, A., and Silvano, S., (1996). "A visco-plastic model for slope analysis applied to a mudslide in Cortina d'Ampezzo, Italy." *Quarterly J. Engrg. Geol.* 29: 233-240.

Angeli,M-G., Gasparetto,P., and Bromhead,E., (2004). "Strength-regain mechanisms in intermittently moving slides." *Proc. IXth Int. Symp. on Landslides, Rio de Janeiro,* vol. 1**,** Taylor and Francis, London (2004): 689-696.

Binnie, M. A., Clark, J. F. F. and Skempton, A. W., (1967). "The effect of discontinuities in clay bedrock on the design of dams in the Mangla project." Trans. 9th Int. Congr. Large Dams, Istanbul, 1, 165-183.

Bishop, A.W. (1955). "The use of the slip circle in the stability analysis of earth slopes." *Geotechnique,* 5(1), 7-17.

Bishop A. W., Green, G. E., Garga, V. K, Andresen, A. and Brown, J. D., (1971). "A new ring shear apparatus and its application to the measurement of residual strength." *Geotechnique* 21(4): 273-328.

Bishop, A.W. and Henkel, D.F., (1962). "The measurement of soil properties in the triaxial test." 2nd ed., Edward Arnold, London.

Bjerrum, L. and Simons, N. E. (1960). "Comparison of shear strength characteristics of normally consolidated clays." *Proc., Conf. on Shear Strength of Cohesive Clays,* ASCE, Boulder, CO, 711-726.

Bjerrum, L., (1967). "Progressive failure in slopes of overconsolidated plastic clays." *Int J. Soil Mech. Eng. Div., ASCE,* SM5,1-49.

Borowicka, H. (1965). "The influence of the colloidal content on the shear strength of clay." Proc. 6th Int. Conf. Soil Mech. Montreal, 1, 175-178.

Bromhead, E. N. (1978). "Large landslide in London Clay at Herne Bay, Kent." *Quarterly. J. Engng. Geol. and Hydrology,* 11, 291–304.

Bromhead, E. N. (1979). "A simple ring shear apparatus." *J. Ground Eng.*, 12(5), 40–44.

Bromhead, E. N., and Curtis, R. D. (1983). "A comparison of alternative methods of measuring the residual strength of London clay." J. *Ground Eng,* 16(4), 39-40.

Brooker, E. W. and Ireland, H. O., (1965). "Earth pressures at rest related to stress history." *Can. Geotech. J.,* 2(1), 1-15.

Carrubba, P., and Del Fabbro, M., (2008). "Laboratory Investigation on Reactivated Residual Strength." *J. Geotech. Geoenviron. Eng.*, 134(3), 302-315.

Casagrande, A., (1948). "Classification and identification of soils." Trans. Am. Soc. Civil Eng. 113, 901-930.

Chandler, R. J., (1966). "The measurement of residual strength in triaxial compression." *Geotechnique,* 16(3), 181-186.

Chandler, R. J., (1969). “The effect of weathering on the shear strength properties of Keuper Marl.” *Geotechnique,* 19(3), 321-334.

Chandler, R. J., (1977). “Back analysis techniques for slope stabilization works: a case record.” *Geotechnique,* 27(4), 479-495.

Chandler, R.J., (1984). “Recent European experience of landslides in over-consolidated clays and soft rocks.” *Proc 4th Int. Symp. on Landslides, Toronto,* vol 1, 61-81.

Chugh, A. K. (1986). "Variable interslice force inclination in slope stability analysis." *Soils and Foundations, Japanese Soc. of Soil Mech. and Fdn. Eng.*, 26(1), 115-121.

Clough, R. W., and Woodward, R. J., (1967). “Analysis of embankment stresses and deformations.” *J. Soil Mech. and Found. Div., ASCE,* 93(4), 529-549.

Collotta, T., Cantoni, R., Pavesi, U., Ruberl, E., and Moretti, P. C. (1989). “A correlation between residual friction angle, gradation and the index properties of cohesive soils.” *Geotechnique*, 39(2), 343-346.

Cruden D. M., (1991). “A simple definition of a landslide.” *Bulletin Intl. Assoc. of Eng. Geolog,* No. 43, 27-29.

Cruden D. M., and Varnes D. J. (1996). “Landslide types and processes.” *In: Turner AK, Schuster RL (eds) Landslides investigation and mitigation, Special Report 247,* Transportation Research Board, National Research Council, Washington, D.C., 36-75.

Czarnecki, J., and Dabros, T., (1980). “Attenuation of the van der Waals Attraction Energy in the Particle/Semi-Infinite Medium System Due to the Roughness of the Particle Surface.” *J. Colloid and Interface Science,* Vol. 78, No. 1, 25-30.

D’Appolonia, E., Alperstein, R., and D’Appolonia, D. J., (1967). “Behavior of a colluvial slope.” *J. Soil Mech. Found. Div.*, 93(4), 447-473.

Dawson, E. M., Roth, W. H., and Drescher, A., (1999). “Slope stability analysis by strength reduction.” *Geotechnique,* 49(6), 835-840.

Dawson, E. M., and Roth, W. H., (1999). “Slope stability analysis with FLAC.” *Proc. Int. FLAC Symp. on Numerical Modeling in Geomechanics,* Minneapolis, Minnesota.

Deere, D. U., (1967). “Shale mylonites-their origin and engineering properties.” Ass. Eng. Geol., Nat. Meeting, Dallas, Texas.

Deschamps, R., and Yankey, G., (2005). “Limitations in the back-analysis of strength from failures.” *J. Geotech. Geoenviron. Eng.,* (132)4, 532–536.

Duncan, J. M., (1996). “State of the art: limit equilibrium and finite element analysis of slopes.” *J. Geotech. Geoenviron. Eng.*, 122(7), 577–596.

Duncan, J. M., and Stark, T., (1992). "Soil strengths from back analysis of slope failures." *Proc., Stability and Performance of Slopes and Embankments II*, ASCE, New York, 890–904.

Duncan, J.M., and Wright, S.G., (2005). "Soil Strength and Slope Stability." *John Wiley and Sons*, New York.

Eid, H.T. (1996). "Drained shear strength of stiff clays for slope stability analyses." *PhD thesis, University of Illinois at Urbana-Champaign, USA.*

Eid, H.T. (2006). "Factors influencing determination of shale classification indices and their correlation to mechanical properties." *J. Geotech. and Geol. Eng.*, 24, 1695-1713.

Fannin, R.J. and Jaakkola, J. ,(1999). "Hydrological response of hillslope soils above a debris-slide headscarp." *Can. Geotech. J.*, 36, 1111–1122.

Fellenius, W., (1936). "Calculation of the stability of earth dams." *Proc. 2nd Congress on Large Dams*, 4, 445–463.

FLAC. (Fast Langragian Analysis of Continua) Software Version 5.0., (2005). "*User's Guide and other manuals."* Itasca Consulting Group, Inc., Minneapolis, Minnesota.

Furuya, T, (2004). "Review and Comparison of Limit Equilibrium Methods of Slices for Slope Stability." *Bulletin of the National Institute for Rural Engineering, Japan*, 43, 1-22

Gibo, S., Inoue, H., Zhou, I., and Nakamura, S., (1997). "Stability analysis in the large moved landslide." *The Science Bulletin of the Faculty of Agriculture. University of the Ryukyus* , No. 44 (1997/12), In Japanese with abstract in English, 275-280. Available at: http://ir.lib.u-ryukyu.ac.jp/bitstream/123456789/3715/1/KJ00000161836.pdf

Gibo, S., Egashira, K., Ohtsubo, M., and Nakamura, S., (2002). "Strength recovery from residual state in reactivated landslides." *Geotechnique*, 52(9), 683–686.

Gilbert, R. B., Wright, S. G., and Liedtke, E., (1998). "Uncertainty in back analysis of slopes: Kettleman Hills case history." *J. Geotech. Geoenviron. Eng.*, 124(12), 1167–1176.

Griffiths, D. V., Lane, P. A., (1999). "Slope stability analysis by finite elements." *Geotechnique*, 49(3), 387–403.

Haefeli, R. (1951). "Investigation and measurements of the shear strengths of saturated cohesive soils." *Geotechnique*, 2(3), 186-208.

Holt, J. K., (1962). "The soils of Hong Kong's coastal waters." *Symp. Hgng Kong Joint Group Committee, Hong Kong: Inst. Civ., Mech. and Elect. Engrs.*, 33-51.

Hutchinson, J. N., (1983). "Methods of locating slip surfaces in landslides." *Bulletin of the Assoc. of Engng. Geol*, 20, 235–252.

Hutchinson, J. N., and Gostelow, T. P., (1976). "The development of an abandoned cliff in London Clay at Hadleigh, Essex." *Phil. Trans. R. Soc. London,* A. 283(1315), 557-604.

Hvorslev, M. J. (1939). "Torsion shear tests and their place in the determination of the shearing resistance of soils." *Proc. of ASTM Symposium on Shear Testing of Soils,* 39, 999-1022.

Janbu, N., (1968). "Slope stability computations." Institutt for Geotknikk og Fundamenteringslære, Norges Tekniske Høgskole. Soils mechanics and foundation engineering, The Technical University of Norway.

Janbu, N., (1973). "Slope stability computations." *In: Hirschfield, Ronald, C., and Poulos, Steve, J., Embankment-Dam Engineering - Casagrande Volume,* John Wiley, New York, 47–86.

Kanji, M. A., (1974). "Relationship between drained friction angles and Atterberg limits of natural soils." *Geotechnique,* 24(4), 671–674.

Kenney, T. C., (1959). "Discussion on Geotechnical properties of glacial lake clays." *J. Soil Mech. Found. Div. ASCE,* 85(1), 67-79.

Kenney, T. C., (1967). "The influence of mineral composition on the residual strength of natural soils." *Proc. Geotech. Conf, Oslo,* 1, 123-129.

Kenney, T. C., (1977). "Residual strength of mineral mixtures." *Proc. 9th Int. Conf. on Soil Mech.,* vol. 1, 155–160.

La Gatta, D.P. (1970). "Residual strength of clays and clay-shales by rotation shear tests." *Harvard Soil Mechanics Series No. 86,* Harvard University, Cambridge, Massachusetts.

Ladd, C.C., Foott, K., Ishihara, K., Schlosser, F., and Poulos, H.G., (1977). "Stress-Deformation and Strength Characteristics." *Proc. 9th Int. Conf. Soil Mech. and Fdn. Eng., Tokoyo,* 2, 421-494.

Lambe, T.W. (1985). Amuay landslides, in *Proceedings of the Eleventh International Conference on Soil Mechanics and Foundation Engineering, San Francisco, Golden Jubilee Volume*, 137-158.

Leonards, G. A., (1982). "Investigation of failures." *J. Geotech. Eng. Div., ASCE,* 108(2), 185–246.

Leroueil, S., and Tavenas, F., (1981). "Pitfalls of back-analysis." *Proc., 10th Int. Conf. on Soil Mechanics and Foundation Engineering*, Balkema, Rotterdam, Netherlands, vol. 1, 185–190.

Lowe, J., and Karafiath, L., (1960). "Stability of earth dams upon drawdown." *Proc. First Pan-Am. Conf. on Soil Mech. and Found Eng.,* vol. 2, 537–52.

Lupini, J. F., Skinner, A. E., Vaughan, P. R. (1981). "The drained residual strength of cohesive soils." *Geotechnique,* 31(2), 181–213.

Meehan, C. L. (2006). "An Experimental Study of the Dynamic Behavior of Slickensided Slip

Surfaces." Ph.D. Thesis, Virginia Polytechnic Institute and State University, USA, Available at: http://scholar.lib.vt.edu/theses/available/etd-01302006-101603/)

Mesri, G., and Cepeda-Diaz, A. F., (1986). "Residual shear strength of clays and shales." *Geotechnique,* 36(2), 269–274.

Mesri, G., and Castro, A., (1987). "C_α/C_c concept and K_0 during secondary compression." *J. Geotech. Eng Div, ASCE,* 113, 230-247.

Mesri, G., and Abdel-Ghaffar, M. E. M., (1993). "Cohesion intercept in effective stress-stability analysis." *J. Geotech. Geoenviron. Eng.*, 119(8), 1229–1249.

Mesri, G., and Shahien, M., (2003). "Residual shear strength mobilized in first-time slope failures." *J. Geotech. Geoenviron. Eng.*, 129(1), 12–31.

Mitchell, J.K., (1960). "Fundamental aspects of thixotropy in soils." *J. Soil Mech. and Found. Div., ASCE,* 86(3), 19-52.

Mitchell, N. W. R. (1965). Direct shear tests on thin samples of remolded shales from the Bighorn Mountains, Wyoming. MS thesis, University of Illinois, pp 49.

Mitchell, J. K., (1976). *Fundamentals of soil behavior*, 1st ed., Wiley, New York.

Mitchell, J. K., (1996). *Fundamentals of soil behavior*, 2nd ed., Wiley, New York.

Mitchell, J. K. and Soga, K., (2005). *Fundamentals of soil behavior*, 3rd ed., Wiley, New York.

Morgenstern, N. R., and Price, V. E., (1965). "The analysis of stability of general slip surfaces." *Geotechnique,* 15(1), 79-93.

Morgenstern, N. R., and Tchalenko, J. S., (1967). "The strength along structural discontinuities in stiff clays." *Proc. Geotech. Conf., Oslo, 1,* 147–152.

NAVFAC, (1971). "Design Manual: Soil Mechanics, Foundations, and Earth Structures, NAVFAC, DM-7." *Department of the Navy, Naval Facilities Engineering Command, Alexandria, VA.*

Nishimura, S., Minh, N. A., and Jardine, R. J., (2007). "Shear strength anisotropy of natural London Clay. " *Geotechnique,* 57(1), 49–62.

Olsen, R. E., (1974). "Shearing strength of kaolinite, illite, and montmorillonite." *J. Soil Mech. And Fdn. Div.*, 100(GT11), 1215-1229.

Patton, F.D. and Hendron, A.J., (1974). "General report on mass movements." *Int. Ass. Eng. Geol. 2nd Int. Congress,* vol. 5, GR1–GR57.

Petley, D.J., (1995). "Laboratory and field measurements of residual shear strength." In: D.H. Bell, Editor, *Proc. 6th Intl. Symp. Landslides,* Christchurch, 1992, *Landslides* vol. 3, 1693–1700.

Palladino, D.J., and Peck, R.B., (1972). "Slope failure in an overconsolidated clay, Seattle, Washington." *Geotechnique,* 22(4), 563-595.

Peck, R.B. (1980). “Where has all the judgment gone?” The 5th Laurits Bjerrum Memorial Lecture, *Can. Geotech. J.,*17(4), 584-590.

Pockoski, M., and Duncan J.M., (2000). “Comparison of computer programs for analysis of reinforced slopes.” *Report of a study performed by the Virginia Tech Center for Geotech, Practice and Research,* Virginia Polytechnic Institute and State University.

Ramiah, B.K., Purushothamaraj, P., and Tavane, N.G., (1973). “Thixotropic effects on residual strength of remoulded clays.” *Indian Geotech. J.* 3(3): 189-197.

Saito, M., (1980). “Reverse calculation method to obtain c' and ϕ' on a slip surface.” *Proc. 3rd Intl. Symp. on Landslides, New Delhi, 1,* 281–284.

Sauer, E. Karl, (1984). “A landslide in clay shale in the north Saskatchewan river valley, Canada.” *Engineering Geology J.,* 20, 279-300.

Schmertmann, J. H., (1991). “The mechanical ageing of soils.” *J. Geotech. Eng.*, 117(12), 1288-1330.

Seed, H. B., and Chan, C. K., (1957). “Thixotropic characteristics of compacted clays.” *Proc. ASCE,* 83(SM4), Paper 1427, 1-35.

Seycek, J., (1978). “Residual shear strength of soils.” *Bull. Intl. Assoc. Engrg. Geol.,* Vol. 17, 73-75.

Sharma, S. K., (1996). “*XSTABL:* An integrated slope stability analysis program for personal computers.” *Reference manual, Version 5,* Interactive Software Designs, Inc., Moscow, Idaho.

Shuster, R. L., (1996). “Socioeconomic significance of Landslides. *In: Turner AK, Schuster RL (eds) Landslides investigation and mitigation, Special Report 247,* Transportation Research Board, National Research Council, Washington, D.C., 12-35.

Simons, N.E., (1963). “The Influence of Stress Path on Triaxial Test Results.” Proc. of ASTM. STP No. 361, 270-278.

Skempton, A. W., (1964). “Long term stability of clay slopes.” Fourth Rankine Lecture, *Geotechnique,* 14(2), 77-101.

Skempton, A. W., (1970). “First time slides in overconsolidated clays.” *Geotechnique,* 20(3), 320-324.

Skempton, A. W., (1977). “Slope stability of cuttings in brown London clay.” *Proc., 9th Int. Conf. on Soil Mech. and Found. Engrg.,* Tokyo, Japan, 3, 261-270.

Skempton, A. W., (1984). “Personal communication with Chandler (1984).”

Skempton, A. W., (1985). “Residual strength of clays in landslides, folded strata and the laboratory.” *Geotechnique,* 35(1), 3–18.

Skempton, A. W., and Northey, R.D., (1952). "The sensitivity of clays." *Geotechnique,* 3(1), 30-53.

Skempton, A. W., and Petley, D. J., (1967). "The strength along structural discontinuities in stiff clays." *Proc. Geotech. Conf., Oslo,* 2, 29–46.

Spencer, E., (1967). "A method of analysis of the stability of embankments assuming parallel inter-slice forces." *Geotechnique,* 17(1), 11-26.

Spencer, E., (1973). "Thrust line criterion in embankment stability analysis." *Geotechnique,* 23(1), 85-100.

Stark, T. D., and Duncan, J. M., (1991). "Mechanisms of strength loss in stiff clays." *J. Geotech. Eng.*, 117(1), 139–154.

Stark, T. D., and Eid, H. T., (1992). "Comparison of field and laboratory residual shear strengths." *Proc., Stability and Performance of Slopes and Embankments II*, No. 31, vol. 1, ASCE, New York, GSP 876-889.

Stark, T. D., and Vettel, J. J. (1992). "Bromhead Ring Shear Test Procedure." *Geotechnical Testing Journal,* ASTM, 15(1), 24-32.

Stark, T. D., and Eid, H. T., (1993). "Modified Bromhead ring shear apparatus." *Geotech. Test. J.*, 16(1), 100-107.

Stark, T. D., and Eid, H. T., (1994). "Drained residual strength of cohesive soils." *J. Geotech. Geoenviron. Eng.*, 120(5), 856-871.

Stark, T. D., and Contreras, I. A., (1996). "Constant volume ring shear apparatus." *Geotech. Test. J.*, 19(1), 3-11.

Stark, T. D., and Eid, H. T., (1997). "Slope stability analyses in stiff fissured clays." *J. Geotech. Geoenviron. Eng.*, 123(4), 335–343.

Stark, T. D., and Eid, H. T., (1998). "Performance of three-dimensional slope stability methods in practice." *J. Geotech. Geoenviron. Eng.*, 124(11), 1049–1060.

Stark, T. D., Choi, H., and McCone, S., (2005a). "Drained shear strength parameters for analysis of landslides." *J. Geotech. Geoenviron. Eng.* 131(5): 575-588.

Stark, T. D., Arellano, W. D., Hillman, R. P., Hughes, R. M., Joyal, N. and Hillebrandt, D., (2005b). "Effect of toe excavation on a deep bedrock landslide." *J. Performance of Constructed Facilities*, 19(3), 244–255.

Stark, T. D., and Choi, H., (2008). "Slope inclinometers for landslides." *Landslides J.*, Springer Berlin/Heidelberg, 5(3), 339-350.

Stark, T. D., and Hussain, M., (2010a). "Shear strength in preexisting landslides." *J.Geotech. Geoenviron. Eng.*, 136(7), *in press.*

Stark, T. D., and Hussain, M., (2010b). “Drained residual strength for landslides.” Geotech Special Publication 199, *ASCE GeoFlorida2010,* 3217-3226.

Tang, W. H., Stark, T. D., and Angulo, M., (1999). “Reliability in back analysis of slope failures.” *Soils and Found.,* Japanese Geotechnical Society, 39(5), 73–80.

Taylor, D. W., (1937). “Stability of earth slopes.” *J. Boston Soc Civil Engineers*, 24, 197–247. *Reprinted in contributions to soil mechanics 1925-1940, Boston Society of Civil Engineers, 1940, 337–86.*

Terlien, M. T. J., (1998). “The determination of statistical and deterministic hydrological landslide-triggering thresholds.” *Environmental Geology*, 35 (2–3), 124-130.

Terzaghi, K. (1950). “Mechanisms Of Landslides.” *Geological Society of America*, Berkley, 83-123.

Terzaghi, K., Peck, R. B., and Mesri, G., (1996). “Soil mechanics in engineering practice.” 3rd ed. John Wiley and Sons, New York.

Tiwari, B., Brandon, T. L., Marui, H., and Tuladhar, G. R., (2005). “Comparison of residual shear strengths from back-analysis and ring shear tests of undisturbed and remolded specimens.” *J. Geotech. Geoenviron. Eng,* ASCE., 131(9), 1071–1079.

Tiwari, B., Marui, H., (2005). “A New Method for the Correlation of Residual Shear Strength of the Soil with Mineralogical Composition.” *J. Geotech. Geoenviron. Eng,* ASCE., 131(9), 1139–1150.

Townsend, F. C., and Gilbert, P. A. (1974). “Preparation effects on clay shale classification indexes.” *Proc., Nat. Meeting on Water Resources Eng.,* ASCE Los Angeles, CA., Jan 21-25, 1-30.

Troncone, A., (2005). “Numerical analysis of a landslide in soils with strain-softening behavior.” *Geotechnique,* 55(8), 585-596.

U.S. Army Corps of Engineers, (1970). “Engineering and design – stability of earth and rock fill dams.” *Engr. Manual EM 1110-2-1902,* Dept. of the Army, Corps of Eng., Ofc. of Engrs.

Vaughan, P. R., Hight, D. W., Sodha, V. G. and Walbancke, H. J., (1979). “Factors controlling the stability of clay fills in Britain.” *London: Institution of Civil Engineers,* 203-217.

Voight, B. (1973)., “Correlation between atterberg plasticity limits and residual shear strength of natural soils.” *Geotechnique,* 23(2), 265-267.

Wesley, L.D. (2003). “Residual strength of clays and correlations using Atterberg limits.” *Geotechnique,* 53(7), 669-672.

Wesley, L. D. (2004). “Residual strength of clays and correlations using Atterberg limits.” *Geotechnique,* 54(7), 503–504.

Wieczoreck G. F., (1996). “Landslide triggering mechanisms.” *In: Turner AK, Schuster RL (eds) Landslides investigation and mitigation, Special Report 247,* Transportation Research Board, National Research Council, Washington, D.C., 76-90.

Wright, S. G., (1990)., “*UTEXAS3:* A computer program for slope stability calculations.” *Reference manual, Version 3,* Shinoak Software, Austin, Texas.

Wykeham-Farrance Engineering Ltd., (1988). “Operators manual: Bromhead ring shear apparatus.” *Engineering Ltd.,* Slough, England.

Zeinkiewcz, O. C., Humpheson, C., and Lewis, R. W., (1975). “Associated and non-associated visco-plasticity and plasticity in soil mechanics.” *Geotechnique,* 25(4), 671-689.

APPENDIX A

(Summary of Strength Recovery Tests Performed)

Table A-1. Laboratory strength recovery tests performed during the present study.

Specimen	Effective Normal Stress	Test No.	Number of Tests
Bromhead Ring Shear Tests:			
(1) Residual Strength and Strength Recovery			
Madisette clay	100 kPa	RS-1	5 (1, 10, 30, 90, 300 days)
Silty clay from Esperanza Dam	100 kPa	RS-2	5 (1, 10, 30, 90, 300 days)
Duck Creek Shale	100 kPa	RS-3	5 (1, 10, 30, 90, 300 days)
Otay bentonitic shale	100 kPa	RS-4	5 (1, 10, 30, 90, 300 days)
Madisette clay	200 kPa	RS-5	4 (1, 10, 30, 90 days)
Madisette clay	300 kPa	RS-6	4 (1, 10, 30, 90 days)
Madisette clay	600 kPa	RS-7	4 (1, 10, 30, 90 days)
Silty clay from Esperanza Dam	300 kPa	RS-8	4 (1, 10, 30, 90 days)
Silty clay from Esperanza Dam	600 kPa	RS-9	4 (1, 10, 30, 90 days)
Silty clay from Esperanza Dam (Relaxed specimen)	100 kPa	RS-10	4 (1, 10, 30, 90 days)
Madisette clay	100 kPa	RS-20	1 (non pre-sheared specimen)
(2) Fully Softened Strength			
Madisette clay	100 kPa	RS-11	2
Silty clay from Esperanza Dam	100 kPa	RS-12	1
Duck Creek Shale	100 kPa	RS-13	1
Otay bentonitic shale	100 kPa	RS-14	1
Madisette clay	200 kPa	RS-15	1
Madisette clay	300 kPa	RS-16	1
Madisette clay	600 kPa	RS-17	1
Silty clay from Esperanza Dam	400 kPa	RS-18	1
Silty clay from Esperanza Dam	700 kPa	RS-19	1
		Total Tests:	**55**
Direct Shear Tests:			
(1) Residual Strength			
Madisette clay	Consolidated to 2700 kPa	DS-1	2 (100 and 300 kPa)
Madisette clay	Consolidated to 2700 kPa	DS-2	2 (100 and 300 kPa)
Madisette clay	Overconsolidated to 700 kPa	DS-3	2 (100 and 300 kPa)
		Total Tests:	**6**

APPENDIX B

(Summary of Soils Tested)

Table B-1. Soil samples for drained residual shear strength testing by Stark and Eid (1994 and 1997), Stark et al. (2005a), and present study.

Soil Number	Clay, mudstone, shale, and claystone samples	Clay, mudstone, shale, and claystone locations	Liquid limit (%)	Plastic limit (%)	Clay-size fraction (%)	Activity (PI/CF)
(1)	(2)	(3)	(4)	(5)	(6)	(7)
From Stark et al. (2005a)						
1	*Glacial till	Urbana, IL	24	16	18	0.44
2	*Loess	Vicksburg, MS	28	18	10	1.00
3	*Bootlegger Cove clay	Anchorage, AL	35	18	44	0.39
4	**Duck Creek shale	Fulton, IL	37	25	19	0.63
5	**Chinle (red) shale	Holbrook, AZ	39	20	43	0.44
6	*Colluvium (B-2)	Vallejo, CA	41	22	28	0.68
7	*Slide debris (B-4)	Vallejo, CA	42	23	27	0.70
8	*Silty clay (B-104)	Gary, IN	42	18	48	0.50
9	*Shear surface	Brillant, OH	44	19	39	0.64
10	**Colorado shale	Montana, MT	46	25	73	0.29
11	Panoche mudstone	San Francisco, CA	47	27	41	0.49
12	Mudstone (B-2)	Vallejo, CA	47	27	41	0.49
13	**Four Fathom shale	Durham, England	50	24	33	0.79
14	*Shear surface (LD-17)	Orange County, CA	50	29	25	0.84
15	Mancos shale	Price, UT	52	20	63	0.51
16	Panoche shale	San Francisco, CA	53	29	50	0.48
17	Colluvium	Marietta, OH	54	25	48	0.60
18	*Shear surface	Los Angeles, CA	55	24	17	1.82
19	*Silty clay (sample 2)	Esperanza Dam, Ecuador	55	40	18	0.83
20	Illinois Valley shale	Peru, IL	56	24	45	0.71
21	*Shear surface (LD-11)	Orange County, CA	58	35	23	1.00
22	*Yellowish brown fat clay	Whittier, CA	58	23	37	0.95
23	**Comanche shale	Proctor Dam, TX	62	32	68	0.44
24	*Silty clay (sample 3)	Esperanza Dam, Ecuador	64	41	21	1.10
25	*Shear surface (LD-1)	Orange County, CA	65	32	22	1.50
26	**Bearpaw shale	Billings, MT	68	24	51	0.86

Table B-1 (cont.)

Soil Number	Clay, mudstone, shale, and claystone samples	Clay, mudstone, shale, and claystone locations	Liquid limit (%)	Plastic limit (%)	Clay-size fraction (%)	Activity (PI/CF)
(1)	(2)	(3)	(4)	(5)	(6)	(7)
27	Slide debris (B-3)	Vallejo, CA	69	22	56	0.84
28	*Shear surface (LD-8)	Orange County, CA	69	34	30	1.17
29	Orinda claystone	Contra Costa County, CA	73	25	27	1.78
30	Claystone	Big Bear, CA	75	22	54	0.98
31	*Shear surface (LD-15)	Orange County, CA	75	37	48	0.79
32	*Bay mud	San Francisco, CA	76	41	16	2.19
33	**Patapsco shale	Washington, D.C.	77	25	59	0.88
34	*Monterey claystone (depth 17.4 m)	Carmel, CA	77	26	58	0.88
35	*Shear surface	Los Angeles, CA	79	32	41	1.15
36	Shear surface (depth 28.7 m)	Los Angeles, CA	82	34	50	0.96
37	**Pierre shale	Limon, CO	82	30	42	1.24
38	*Black clay and olive brown clay	Whittier, CA	82	26	57	0.98
39	*Shear surface	Madisette, CA	83	29	52	1.04
40	Clay gouge	Contra Costa County, CA	86	28	76	0.76
41	*Shear surface	Laguna Niguel, CA	86	40	40	1.15
42	Santiago claystone	San Diego, CA	89	44	57	0.79
43	*Shear surface	Oceanside, Oregon	90	37	43	1.23
44	*Monterey claystone (depth 36.3 m)	Carmel, CA	93	39	69	0.78
45	Lower Pepper shale	Waco Dam, TX	94	26	77	0.88
46	Shear surface (depth 19.8 m)	Los Angeles, CA	95	33	47	1.32
47	*Shear surface	Novato, CA	95	27	54	1.26
48	Altamira Bentonitic tuff	Portuguese Bend, CA	98	37	68	0.90
49	Brown London clay	Bradwell, England	101	35	66	1.02
50	Shear surface	Los Angeles, CA	104	32	58	1.24
51	**Cucaracha shale	Panama Canal	111	42	63	1.10
52	*Otay Bentonitic shale	San Diego, CA	112	53	73	0.81
53	Shear surface (depth 8.4 m)	San Diego, CA	118	36	81	1.01

Table B-1 (cont.)

Soil Number (1)	Clay, mudstone, shale, and claystone samples (2)	Clay, mudstone, shale, and claystone locations (3)	Liquid limit (%) (4)	Plastic limit (%) (5)	Clay-size fraction (%) (6)	Activity (PI/CF) (7)
54	**Denver shale	Denver, CO	121	37	67	1.25
55	*Otay Bentonitic claystone	Chula Vista, CA	126	47	53	1.49
56	**Bearpaw shale	Saskatchewan, Canada	128	27	43	2.35
57	Pierre shale	Newcastle, WY	137	30	54	1.98
58	Oahe Firm shale	Oahe Dam, SD	138	41	78	1.24
59	**Claggett shale	Benton, MT	157	31	71	1.78
60	Shear surface (depth 4.0 m)	San Diego, CA	161	43	84	1.40
61	**Taylor shale	San Antonio, TX	170	39	72	1.82
62	**Pierre shale	Reliance, SD	184	55	84	1.54
63	Bentonitic shale	Oahe Dam, SD	192	47	65	1.96
64	Panoche clay gouge	San Francisco, CA	219	56	72	2.26
65	Lea Park Bentonitic shale	Saskatchewan, Canada	253	48	65	3.15
66	**Bearpaw shale	Ft. Peck Dam, MT	288	44	88	2.77
Soils Tested during Present Study						
67	*Dark color yellow clay (I-9@4.5-6 ft.)	San Antonio, Tex	24	19	20	0.25
68	*Light color yellow clay (B-10)	San Antonio, Tex	38	18	40	0.50
69	*Silty clay	Esperanza Dam, Ecuador	55	40	29	0.52
70	*Bel Air (GMX-1 @ 17 ft. depth)	Los Angeles, Calif.	60	33	45	0.60
71	*Shear surface	Los Angeles, Calif.	83	29	52	1.04
72	*Soledad Landslide (AG-1 @ 36 ft. depth)	Los Angeles, Calif.	86	34	64	0.81
73	*Soledad Landslide (LD-1 @ 25 ft. depth)	Los Angeles, Calif.	118	48	55	1.27
* Samples not ball-milled						
** Index Properties from Mesri and Cepeda-Diaz (1986)						

Table B-2. Soil samples for drained fully softened shear strength testing by Stark and Eid (1994 and 1997), Stark et al. (2005a), and present study.

Soil Number	Clay, mudstone, shale, and claystone samples	Clay, mudstone, shale, and claystone locations	Liquid limit (%)	Plastic limit (%)	Clay-size fraction (%)	Activity (PI/CF)
(1)	(2)	(3)	(4)	(5)	(6)	(7)
From Stark et al. (2005a)						
1	*Glacial till	Urbana, IL	24	16	18	0.44
2	*Loess	Vicksburg, MS	28	18	10	1.00
3	**Duck Creek shale	Fulton, IL	37	25	19	0.63
4	*Slide debris	San Francisco, CA	37	26	28	0.39
5	*Colluvium	Vallejo, CA	39	22	36	0.47
6	Slope-wash material	San Luis Dam, California	42	24	34	0.53
7	Crab Orchard shale	Peoria, IL	44	24	32	0.63
8	*Failure plane debris	Brillant, OH	44	19	39	0.64
9	**Colorado shale	Montana, MT	46	25	73	0.29
10	Panoche mudstone	San Francisco, CA	47	27	41	0.49
11	Panoche shale	San Francisco, CA	53	29	50	0.48
12	Colluvium	Marietta, OH	54	25	48	0.60
13	Slide plane material	Los Angeles, CA	55	24	27	1.15
14	Illinois Valley shale	Peru, IL	56	24	45	0.71
15	**Comanche shale	Proctor Dam, TX	62	32	68	0.44
16	Breccia material	Manta, Ecuador	64	41	25	0.92
17	*Silty clay	La Esperanza Dam, Ecuador	64	41	21	1.10
18	Claystone	Big Bear, CA	75	22	54	0.98
19	*Siltstone/Claystone	Orange County, CA	75	37	48	0.79
20	*Bay mud	San Francisco, CA	76	41	16	2.19
21	**Patapsco shale	Washington, D.C.	77	25	59	0.88
22	**Pierre shale	Limon, CO	82	30	42	1.24
23	Shear surface (depth 19.8 m)	Los Angeles, CA	82	31	50	1.02
24	Lower Pepper shale	Waco Dam, TX	94	26	77	0.88
25	*Serpentinite clay	Marion County, CA	95	27	54	1.26
26	Brown London clay	Bradwell, England	101	35	66	1.00

Table B-2 (cont.)

Soil Number (1)	Clay, mudstone, shale, and claystone samples (2)	Clay, mudstone, shale, and claystone locations (3)	Liquid limit (%) (4)	Plastic limit (%) (5)	Clay-size fraction (%) (6)	Activity (PI/CF) (7)
From Stark et al. (2005a)						
27	**Cucarcha shale	Panama Canal	111	42	63	1.10
28	**Denver shale	Denver, CO	121	37	67	1.25
29	**Bearpaw shale	Saskatchewan, Canada	128	27	43	2.35
30	Pierre shale	Newcastle, WY	137	30	54	1.98
31	Oahe Firm shale	Oahe Dam, SD	138	41	78	1.24
32	**Taylor shale	San Antonio, TX	170	39	72	1.82
33	**Pierre shale	Reliance, SD	184	55	84	1.54
34	Oahe Bentonitic shale	Oahe Dam, SD	192	47	65	2.23
35	Lea Park Bentonitic shale	Saskatchewan, Canada	253	48	65	3.15
36	**Bearpaw shale	Ft. Peck Dam, MT	288	44	88	2.77
Soils Tested during Present Study						
37	*Silty clay	Esperanza Dam, Ecuador	55	40	29	0.52
38	*Bel Air (GMX-1 @ 17 ft. depth)	Los Angeles, Calif.	60	33	45	0.60
39	*Shear surface	Los Angeles, Calif.	83	29	52	1.04
* Samples not ball-milled						
**Index properties from Mesri and Cepeda-Diaz (1986)						

APPENDIX C

(Strength Recovery Ring Shear Test Results)

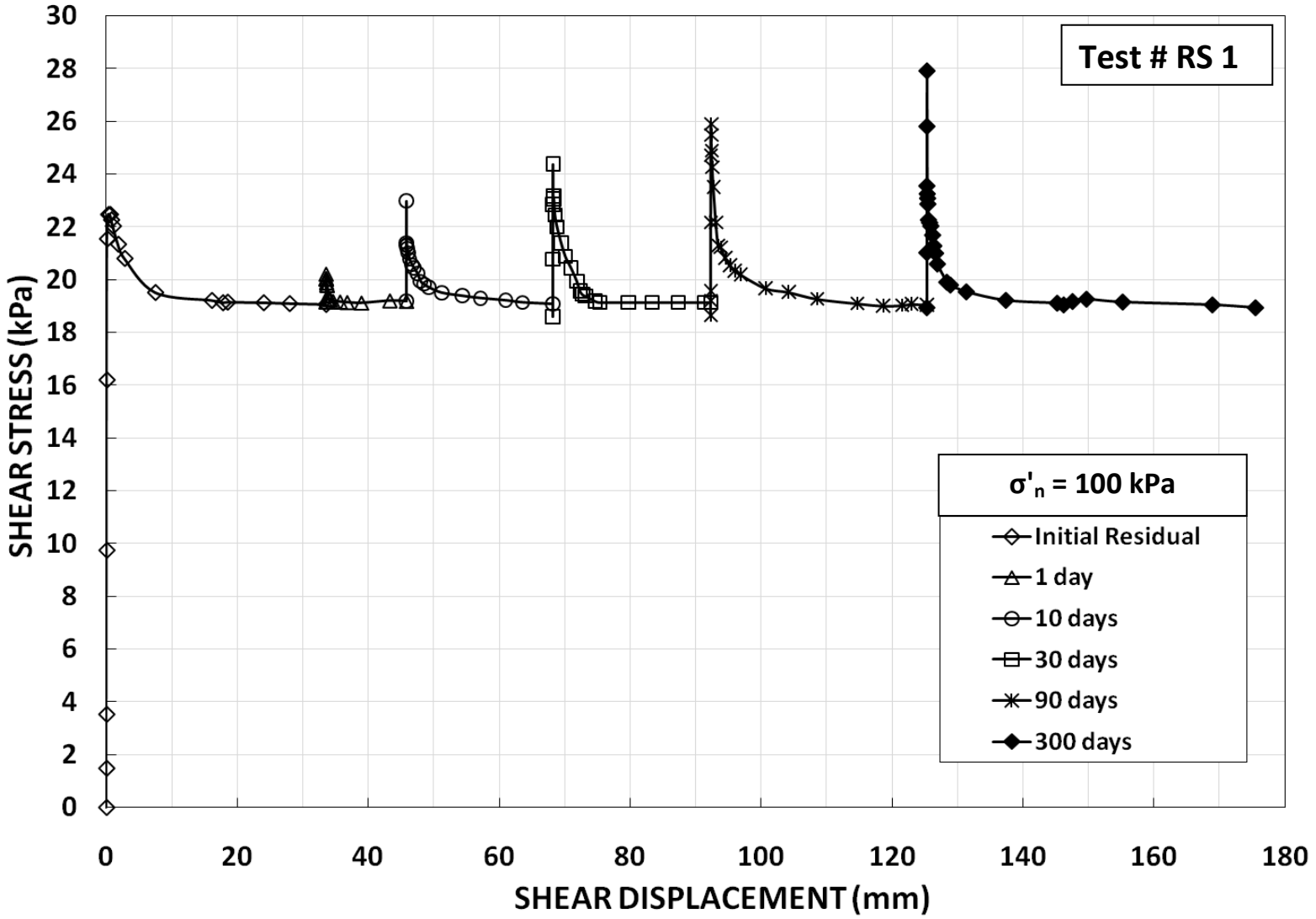

Figure C-1. Schematic diagram showing results of a strength recovery test on Madisette clay at σ'_n = 100 kPa (RS-1 test).

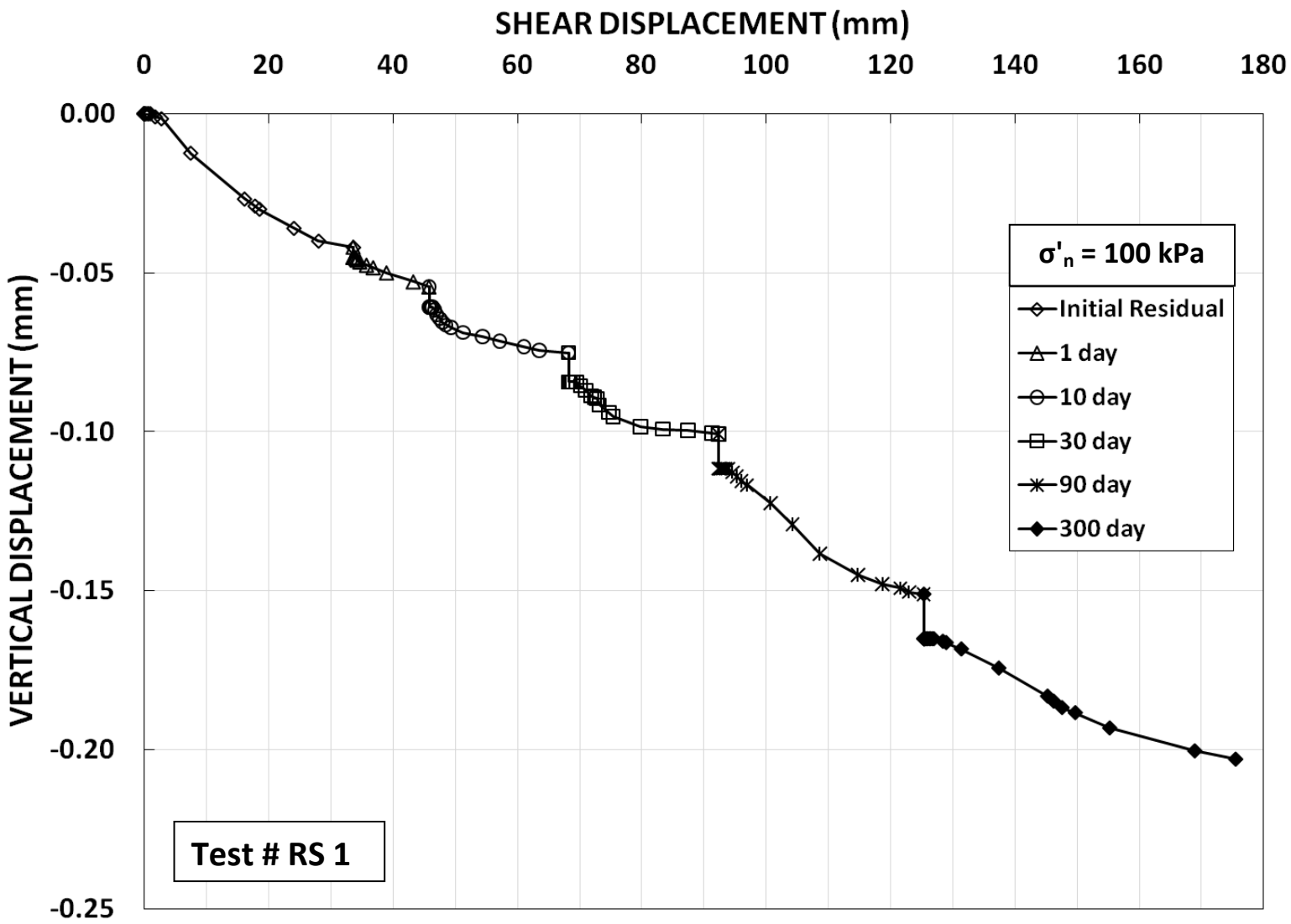

Figure C-2. Schematic diagram showing vertical settlement and shear displacement for strength recovery test on Madisette clay at σ'_n = 100 kPa (RS-1 test).

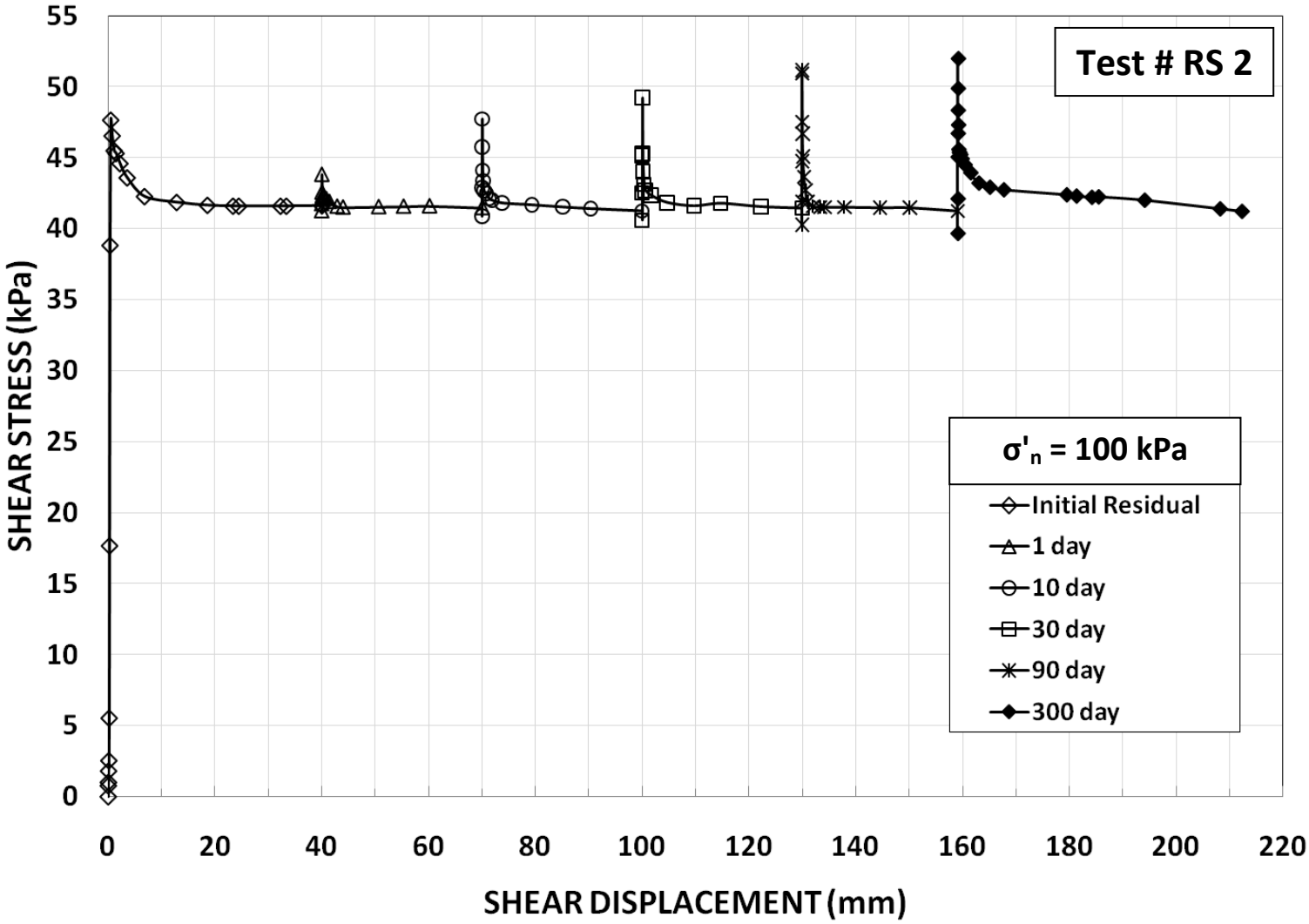

Figure C-3. Schematic diagram showing results of a strength recovery test on silty clay from Esperanza Dam, Ecuador at σ'_n = 100 kPa (RS-2 test).

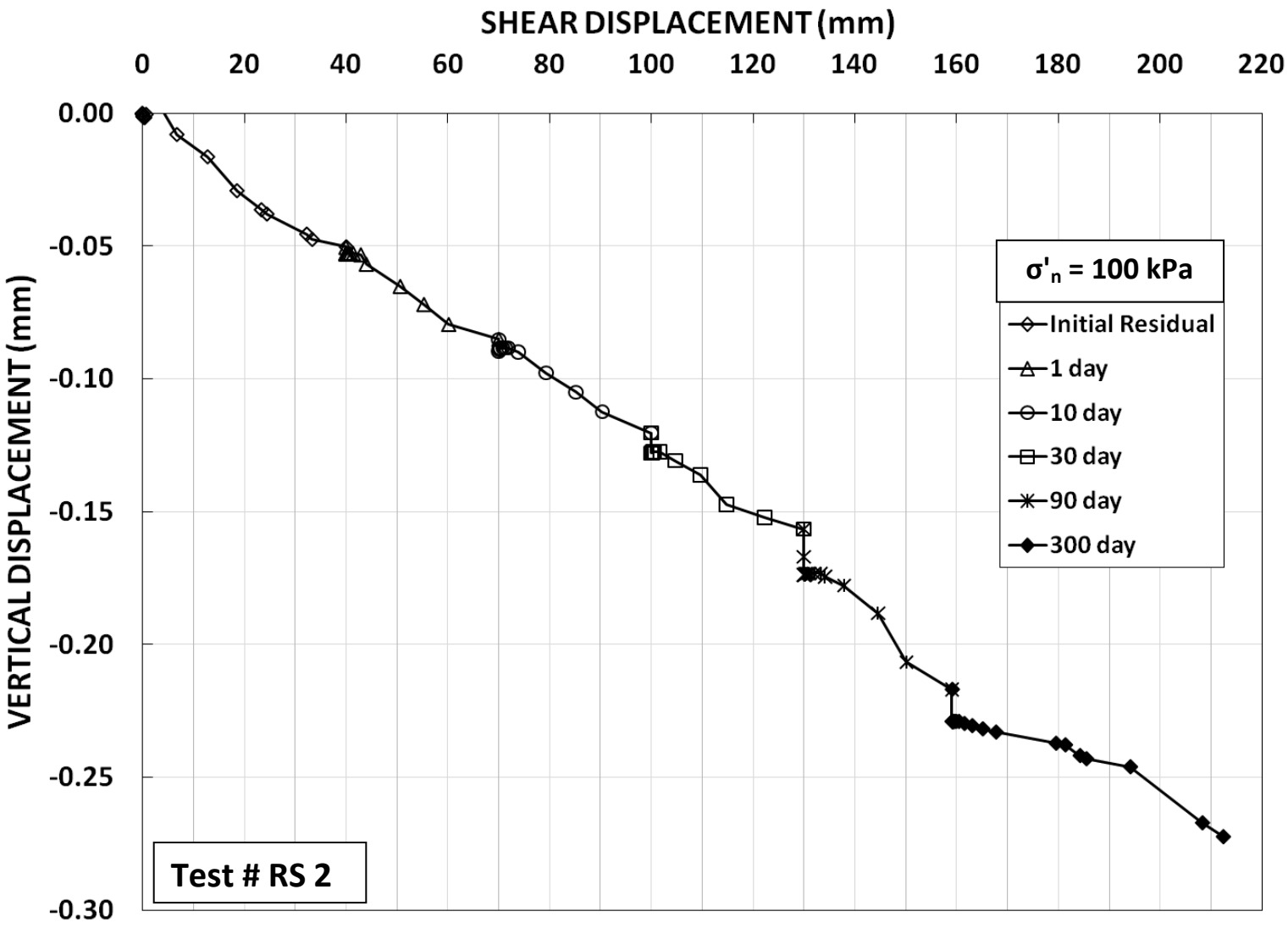

Figure C-4. Schematic diagram showing vertical settlement and shear displacement for strength recovery test on silty clay from Esperanza Dam, Ecuador at σ'_n = 100 kPa (RS-2 test).

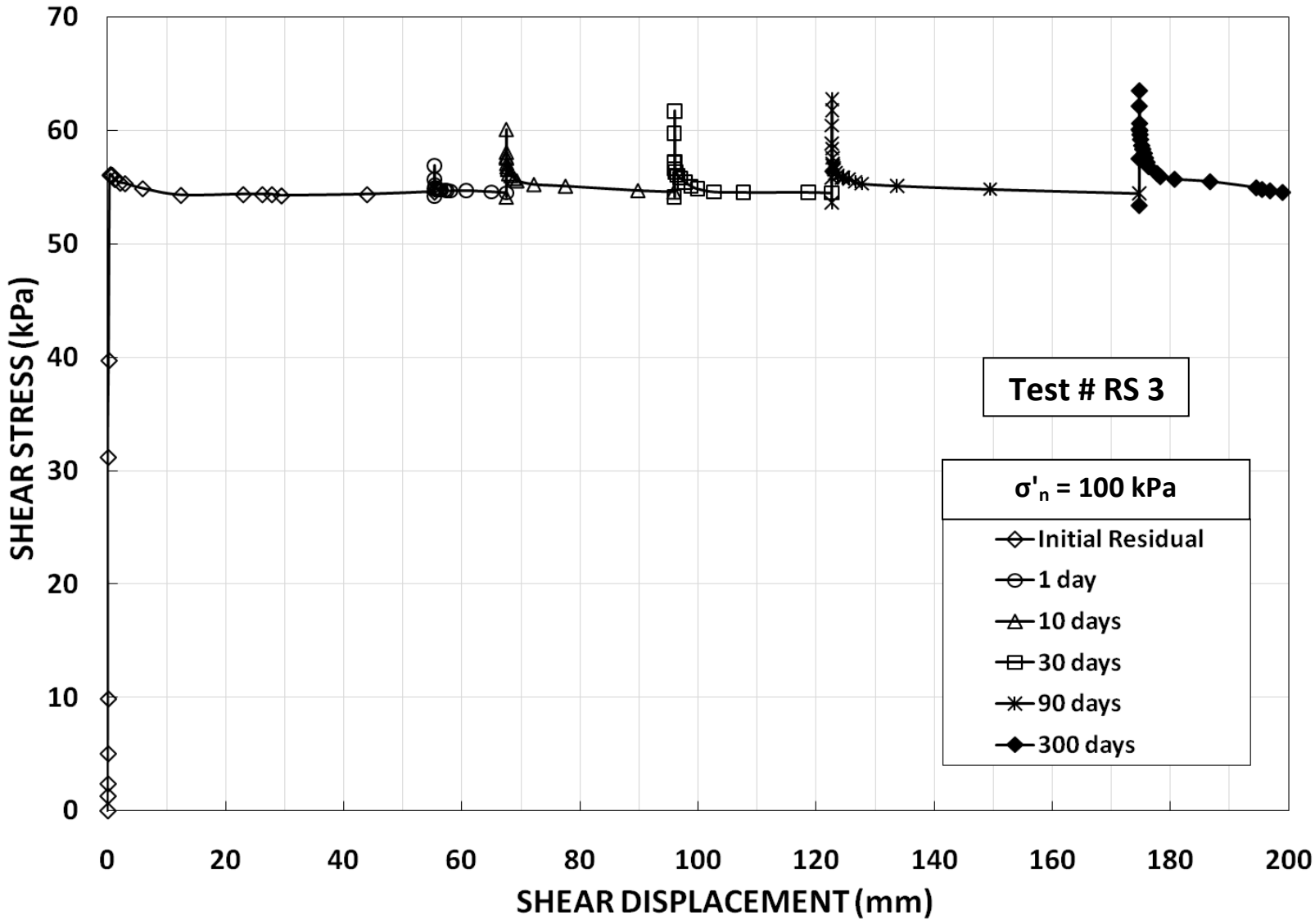

Figure C-5. Schematic diagram showing results of a strength recovery test on Duck Creek shale at σ'_n = 100 kPa (RS-3 test).

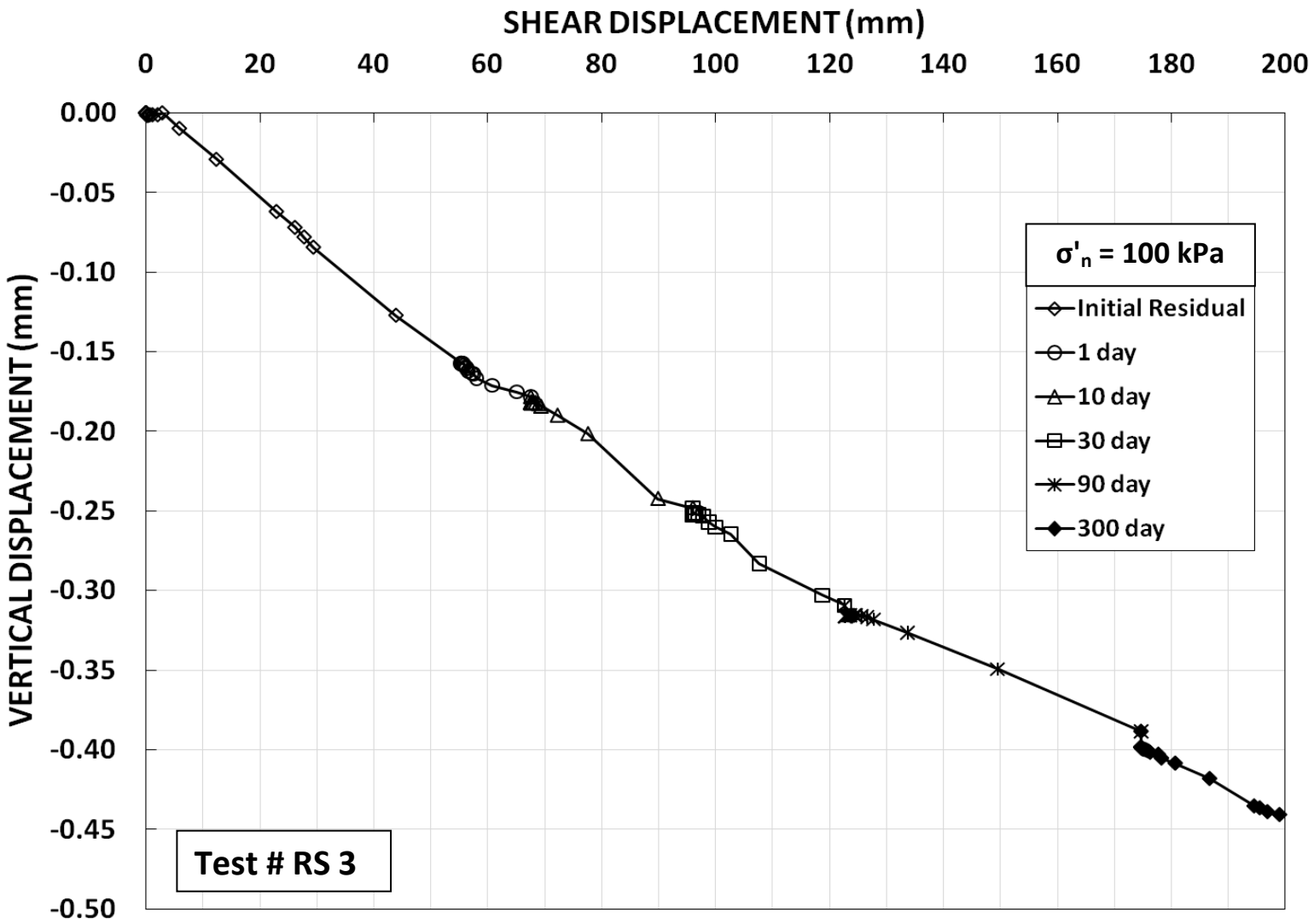

Figure C-6. Schematic diagram showing vertical settlement and shear displacement for strength recovery test on Duck Creek shale at σ'_n = 100 kPa (RS-3 test).

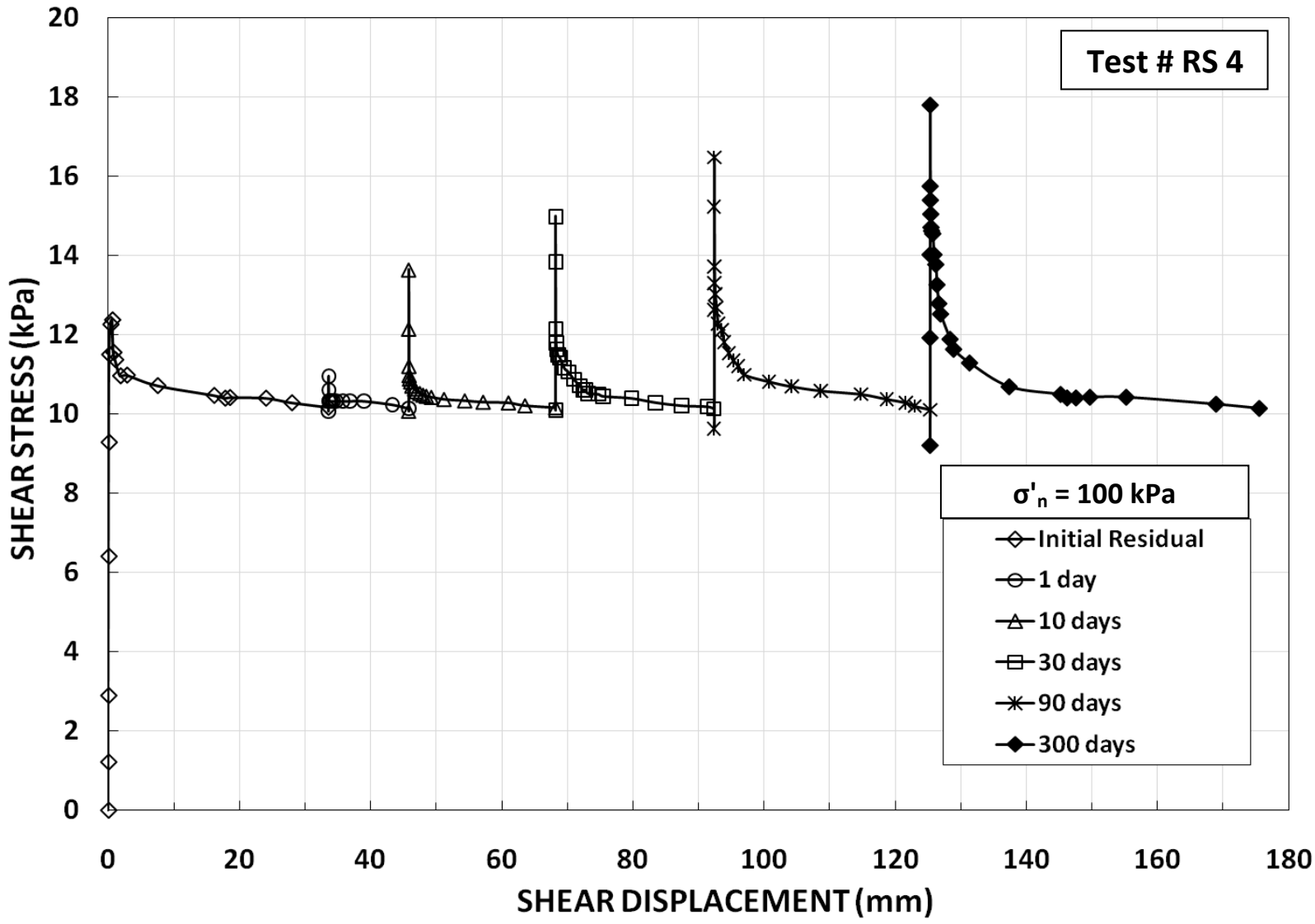

Figure C-7. Schematic diagram showing results of a strength recovery test on Otay Bentonitic shale at σ'_n = 100 kPa (RS-4 test).

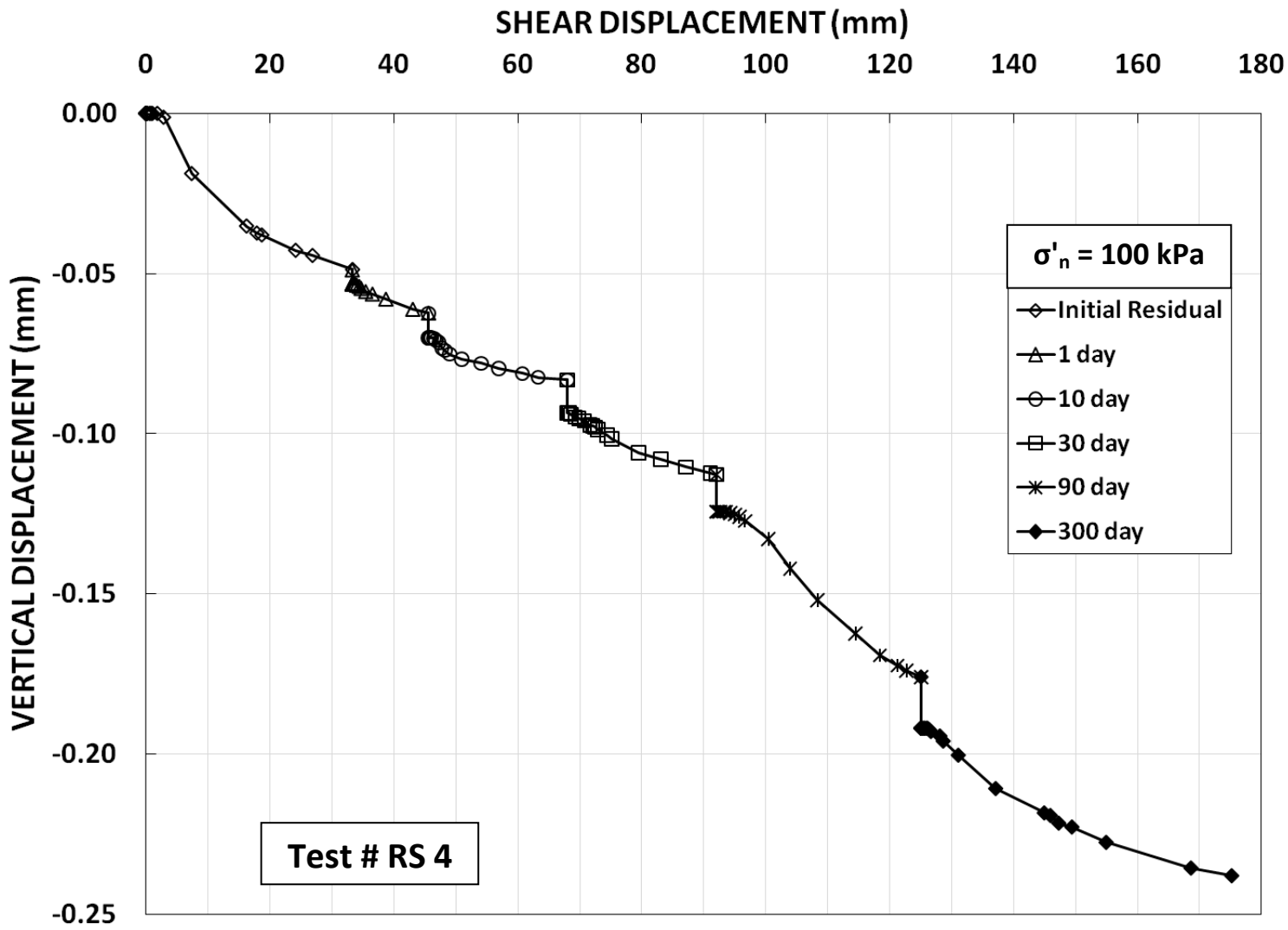

Figure C-8. Schematic diagram showing vertical settlement and shear displacement for strength recovery test on Otay Bentonitic shale at σ'_n = 100 kPa (RS-4 test).

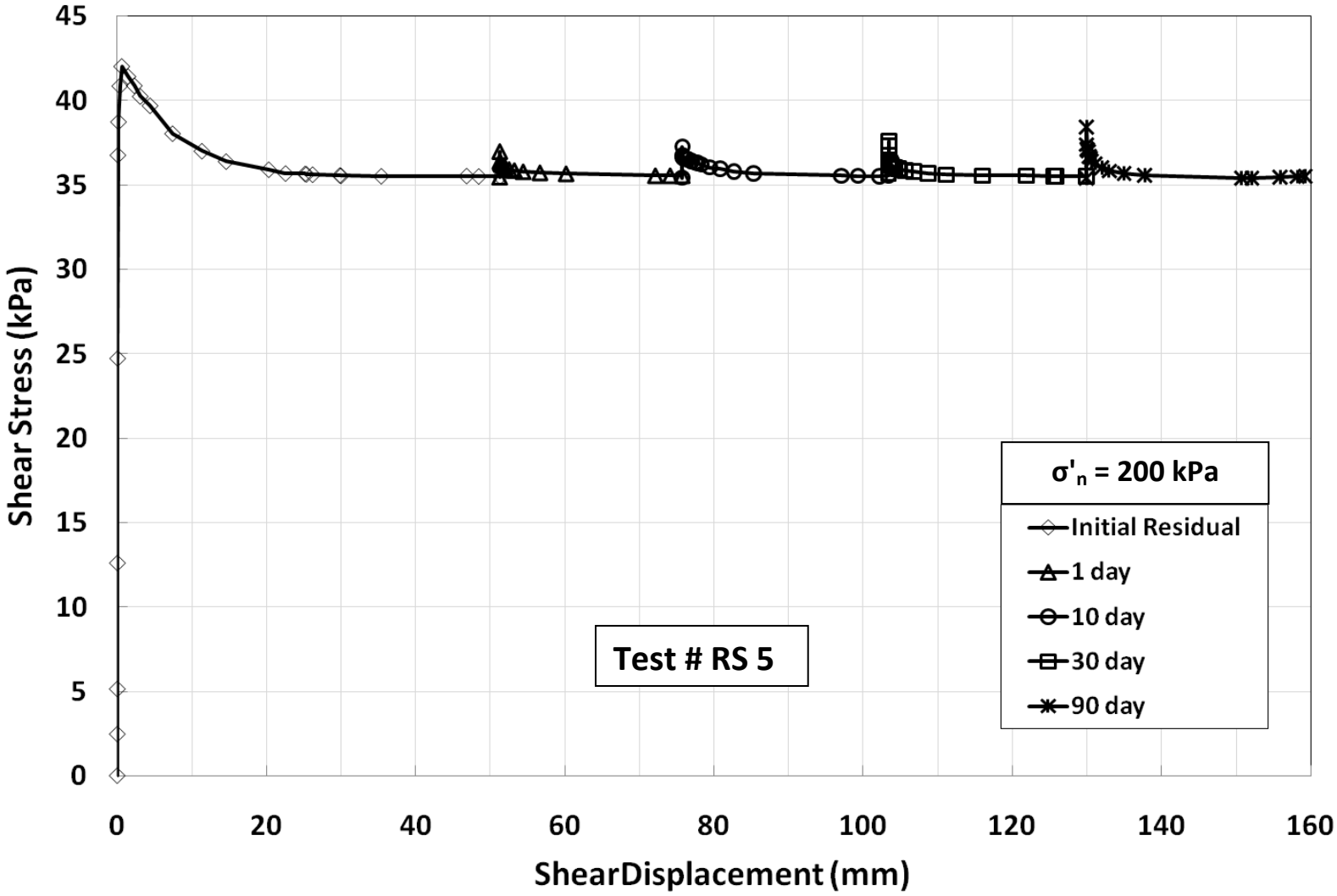

Figure C-9. Schematic diagram showing results of a strength recovery test on Madisette clay at σ'_n = 200 kPa (RS-5 test).

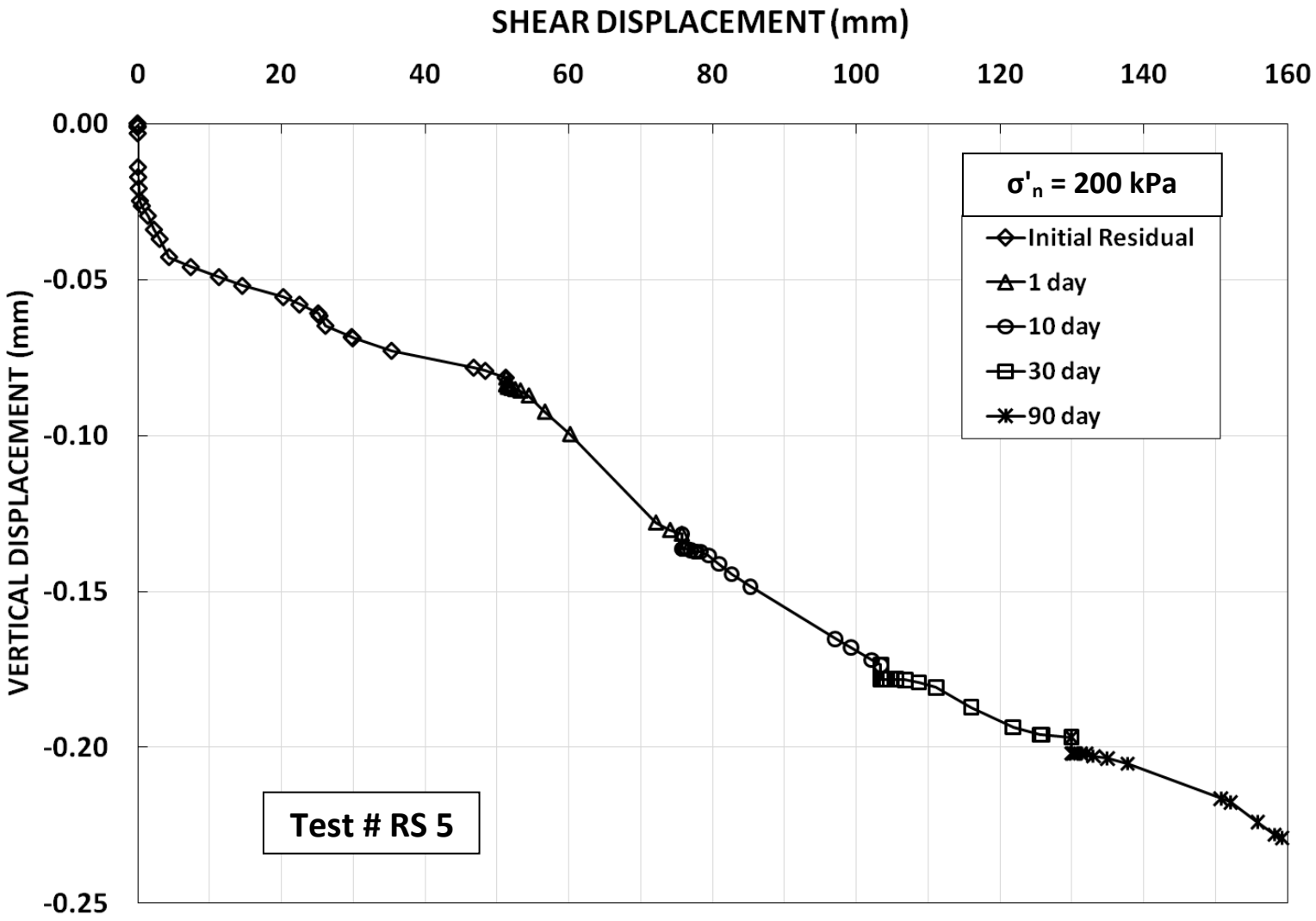

Figure C-10. Schematic diagram showing vertical settlement and shear displacement for strength recovery test on Madisette clay at σ'_n = 200 kPa (RS-5 test).

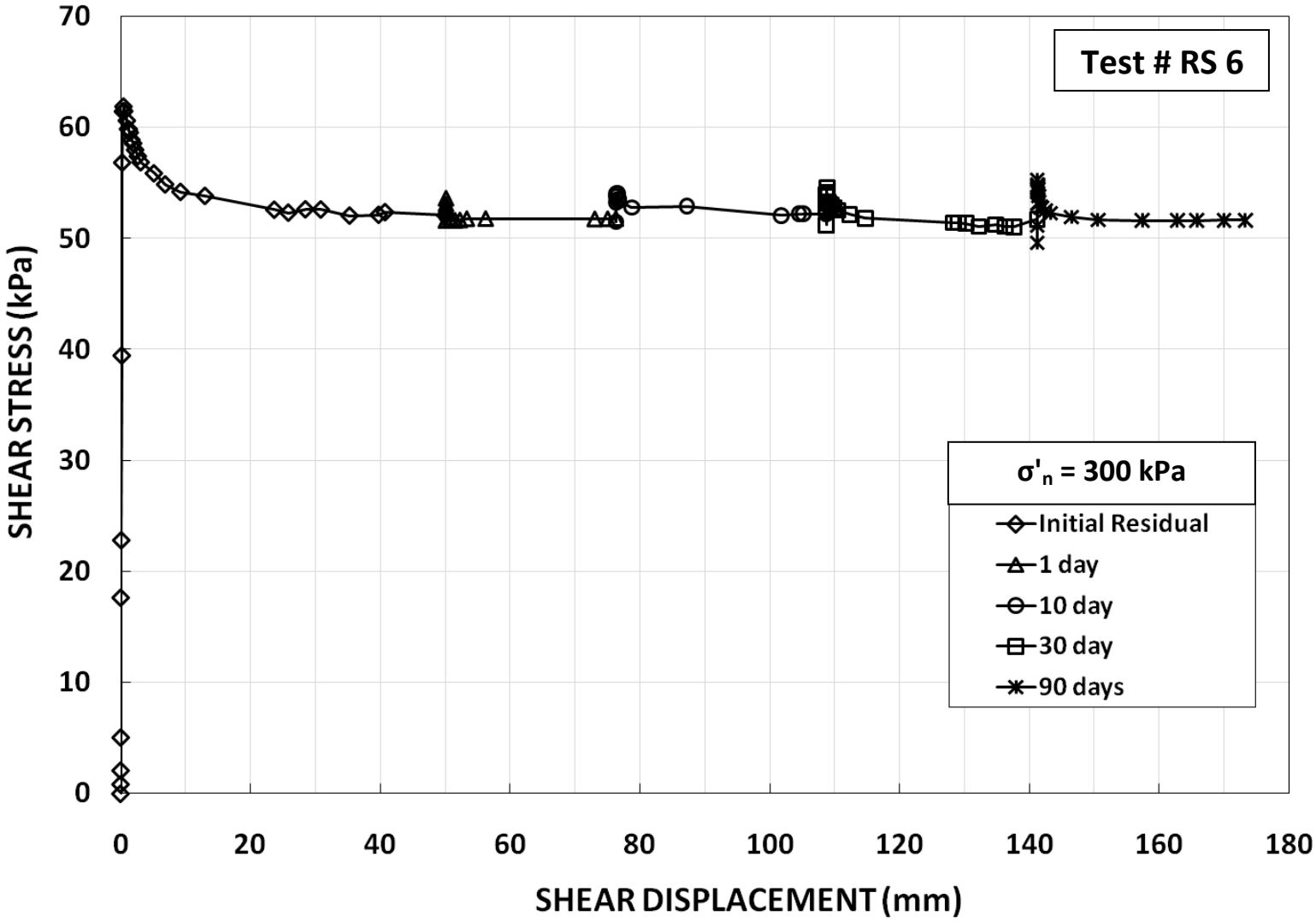

Figure C-11. Schematic diagram showing results of a strength recovery test on Madisette clay at σ'_n = 300 kPa (RS-6 test).

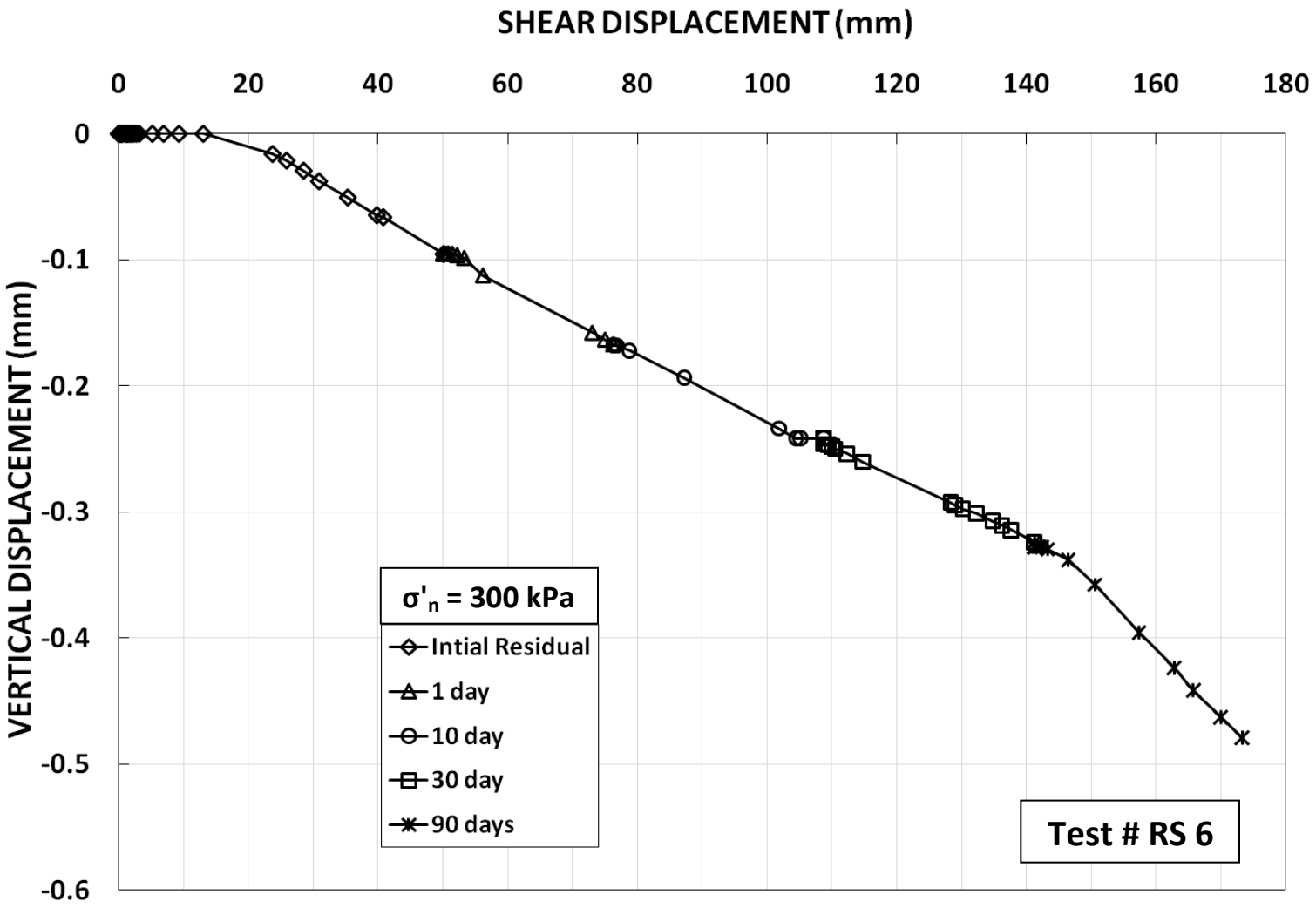

Figure C-12. Schematic diagram showing vertical settlement and shear displacement for strength recovery test on Madisette clay at σ'_n = 300 kPa (RS-6 test).

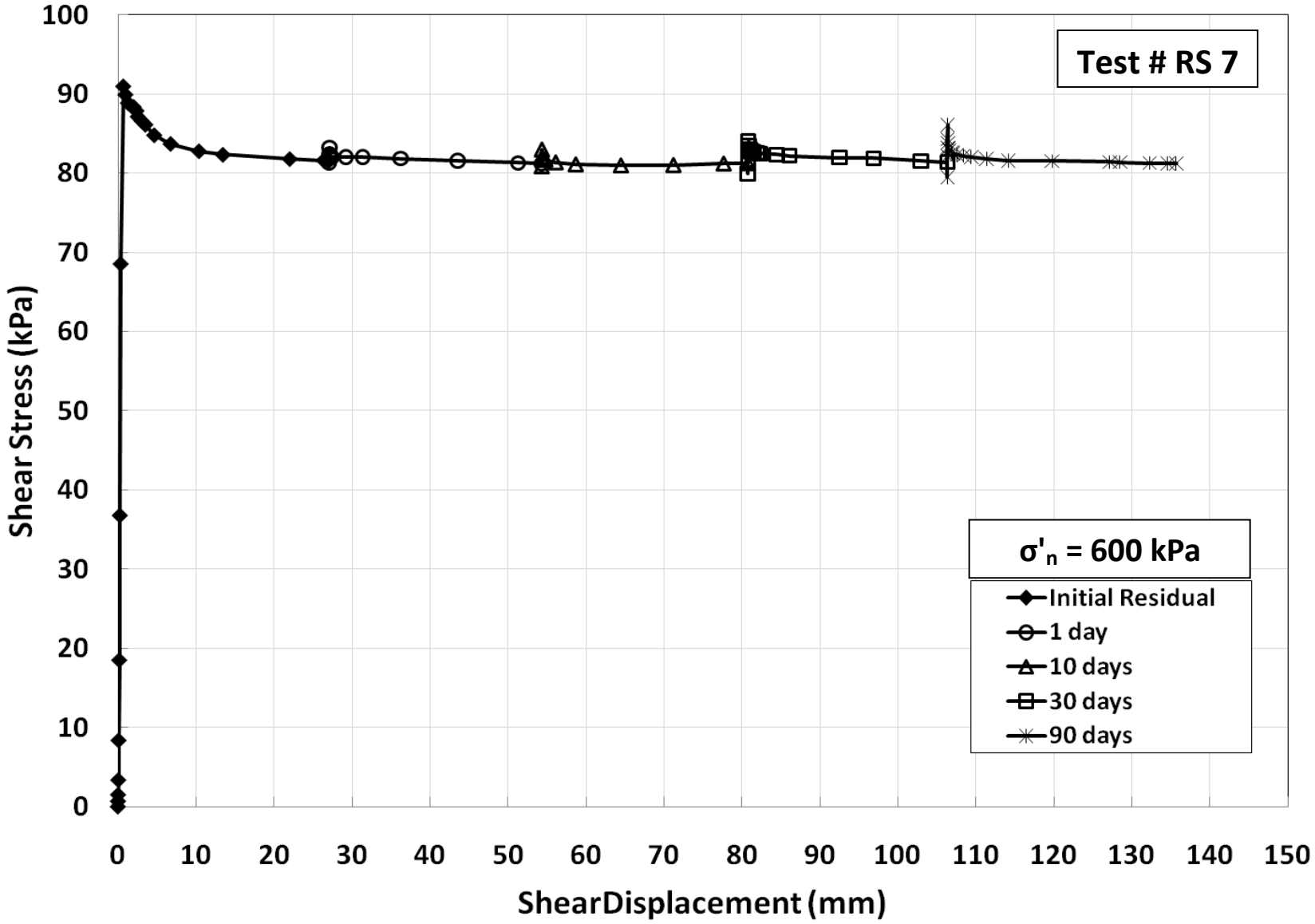

Figure C-13. Schematic diagram showing results of a strength recovery test on Madisette clay at σ'_n = 600 kPa (RS-7 test).

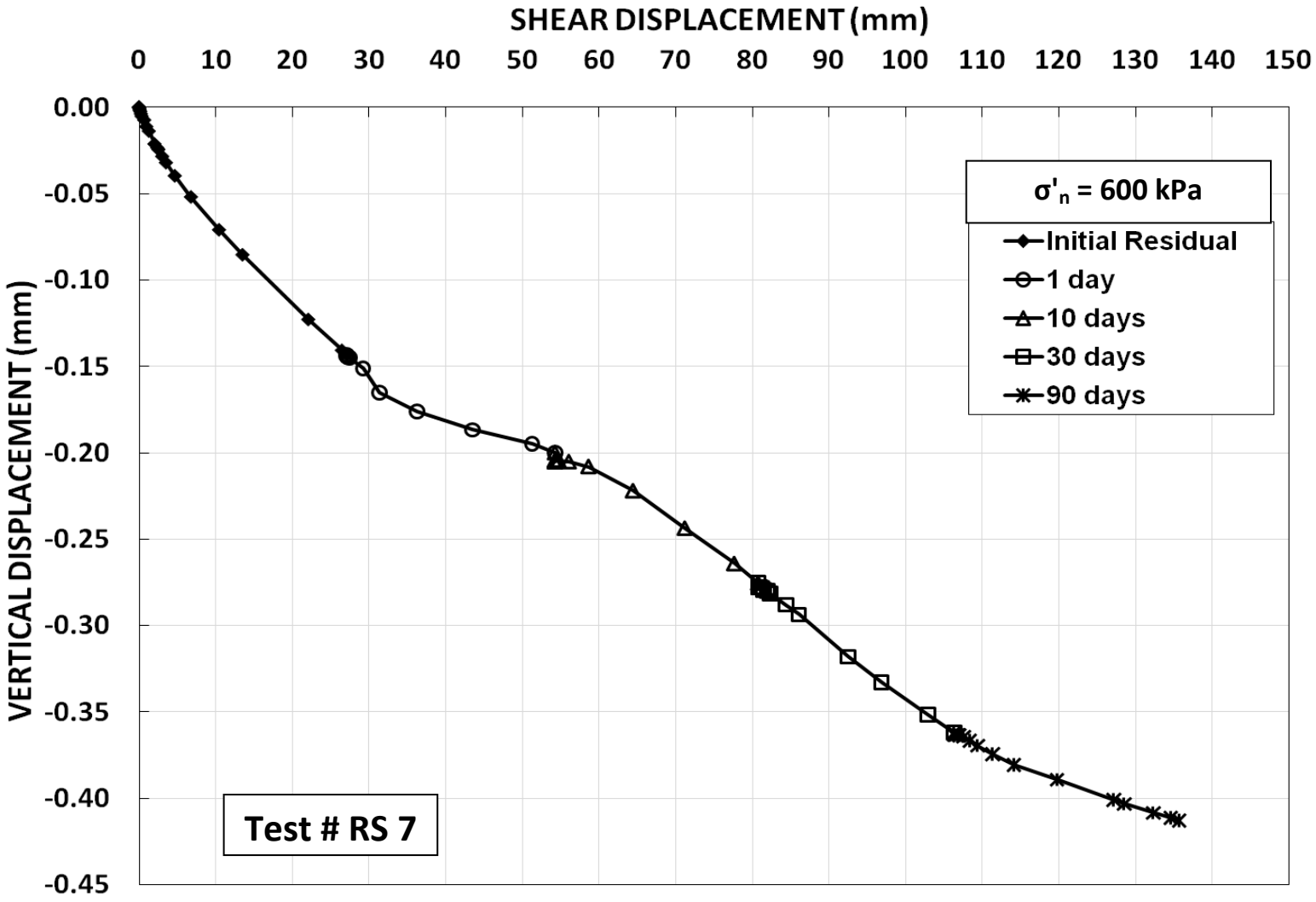

Figure C-14. Schematic diagram showing vertical settlement and shear displacement for strength recovery test on Madisette clay at σ'_n = 600 kPa (RS-7 test).

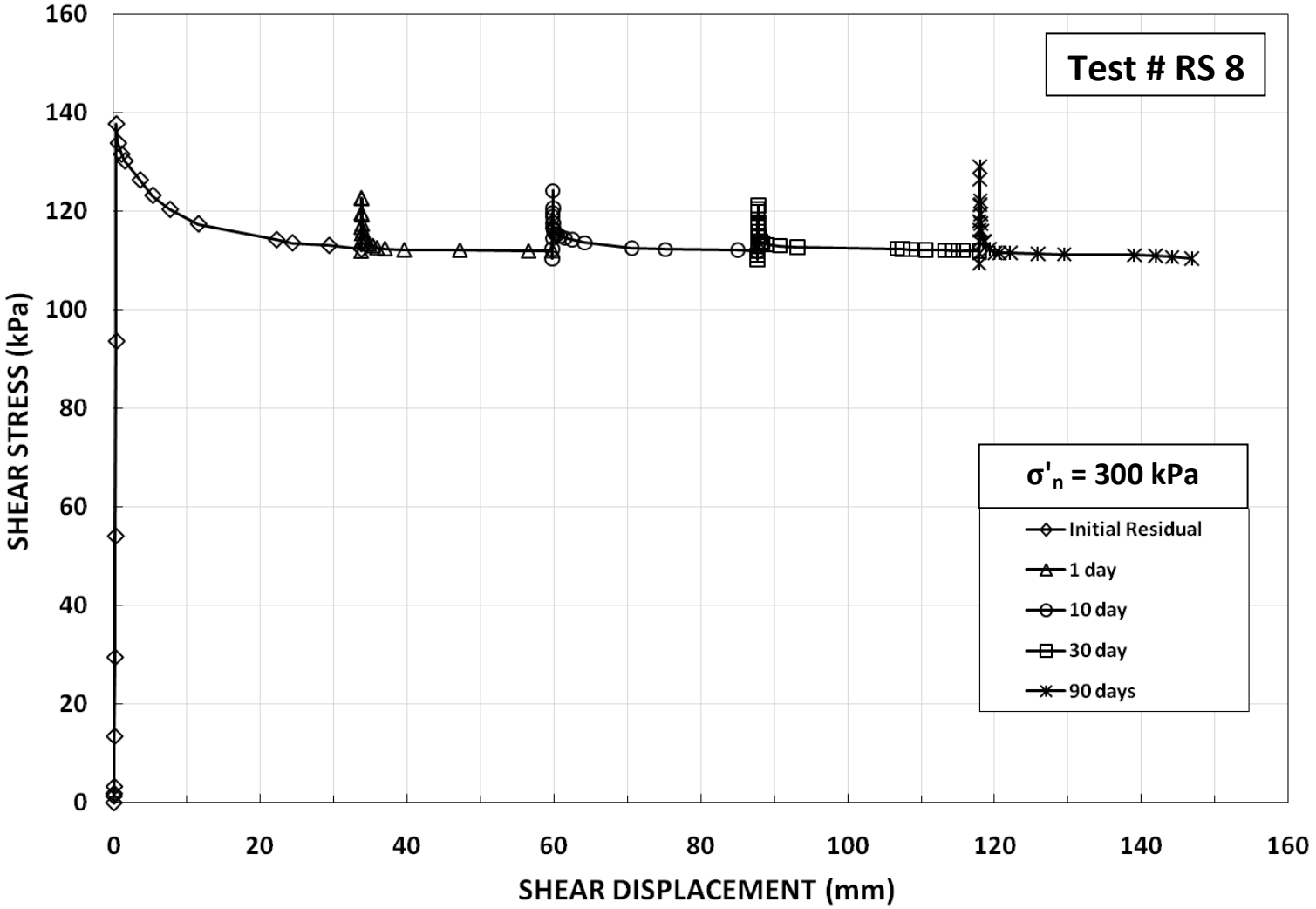

Figure C-15. Schematic diagram showing results of a strength recovery test on silty clay from Esperanza Dam, Ecuador at σ'_n = 300 kPa (RS-8 test).

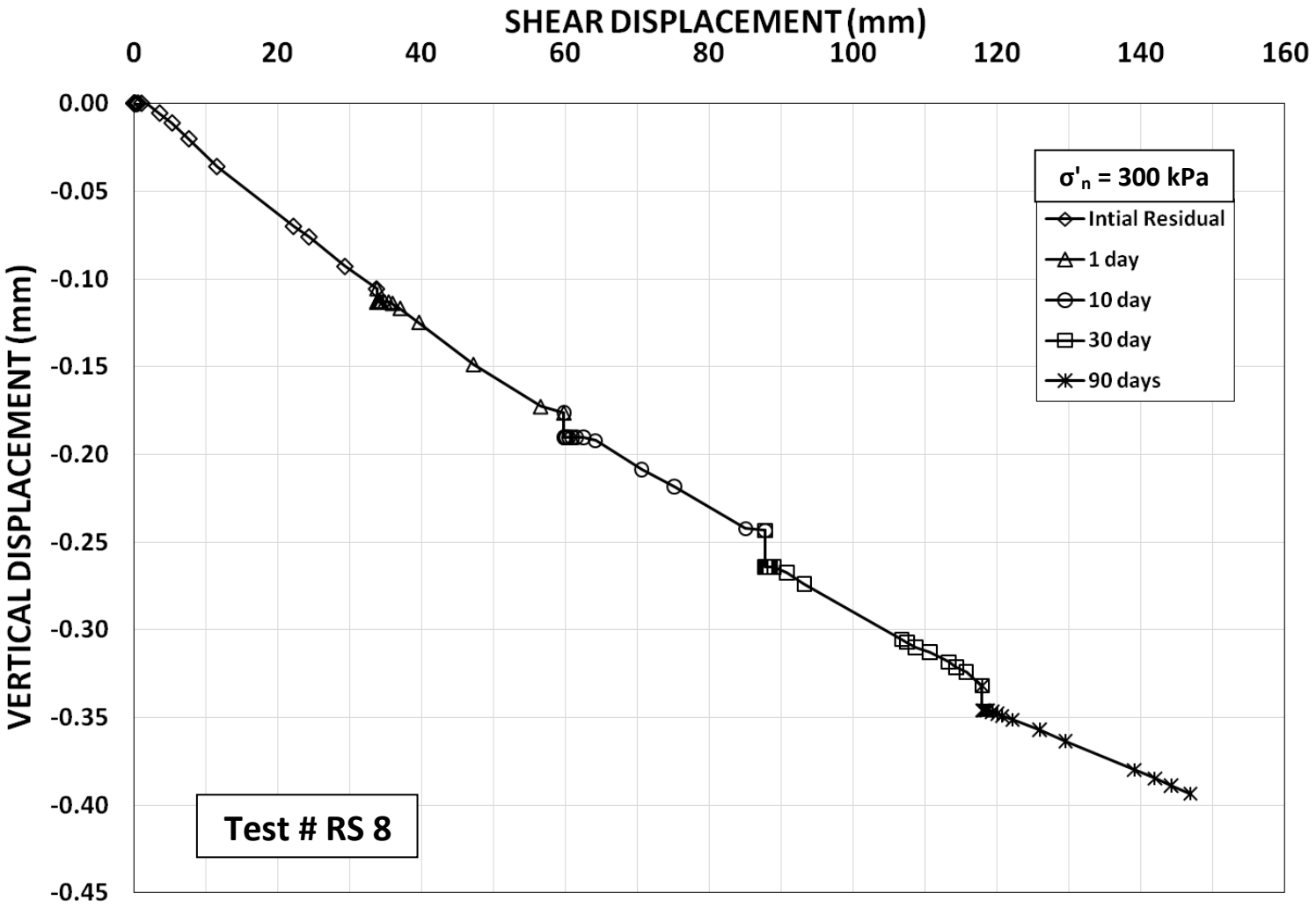

Figure C-16. Schematic diagram showing vertical settlement and shear displacement for strength recovery test on silty clay from Esperanza Dam, Ecuador at σ'_n = 300 kPa (RS-8 test).

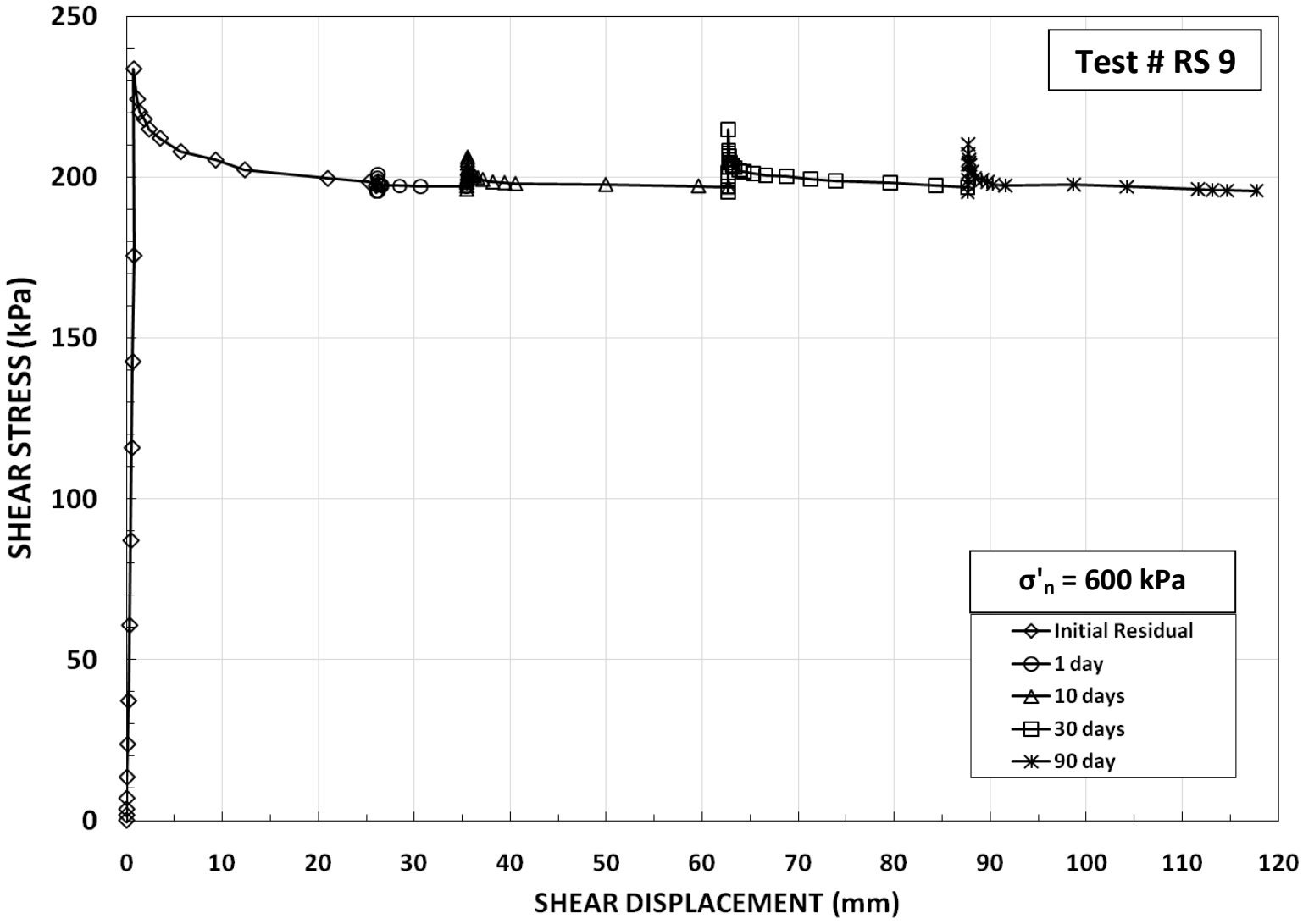

Figure C-17. Schematic diagram showing results of a strength recovery test on silty clay from Esperanza Dam, Ecuador at σ'_n = 600 kPa (RS-9 test).

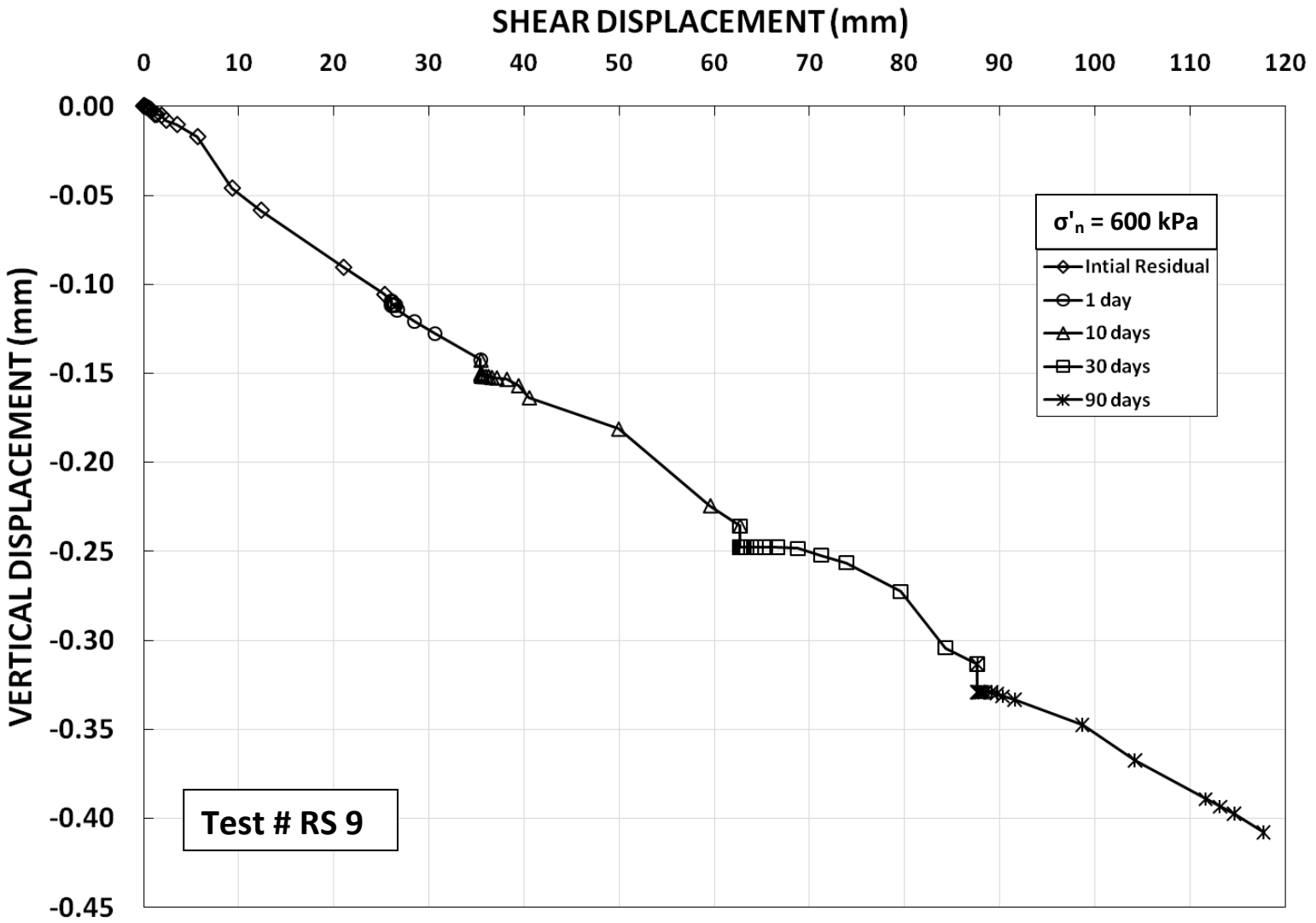

Figure C-18. Schematic diagram showing vertical settlement and shear displacement for strength recovery test on silty clay from Esperanza Dam, Ecuador at σ'_n = 600 kPa (RS-9 test).

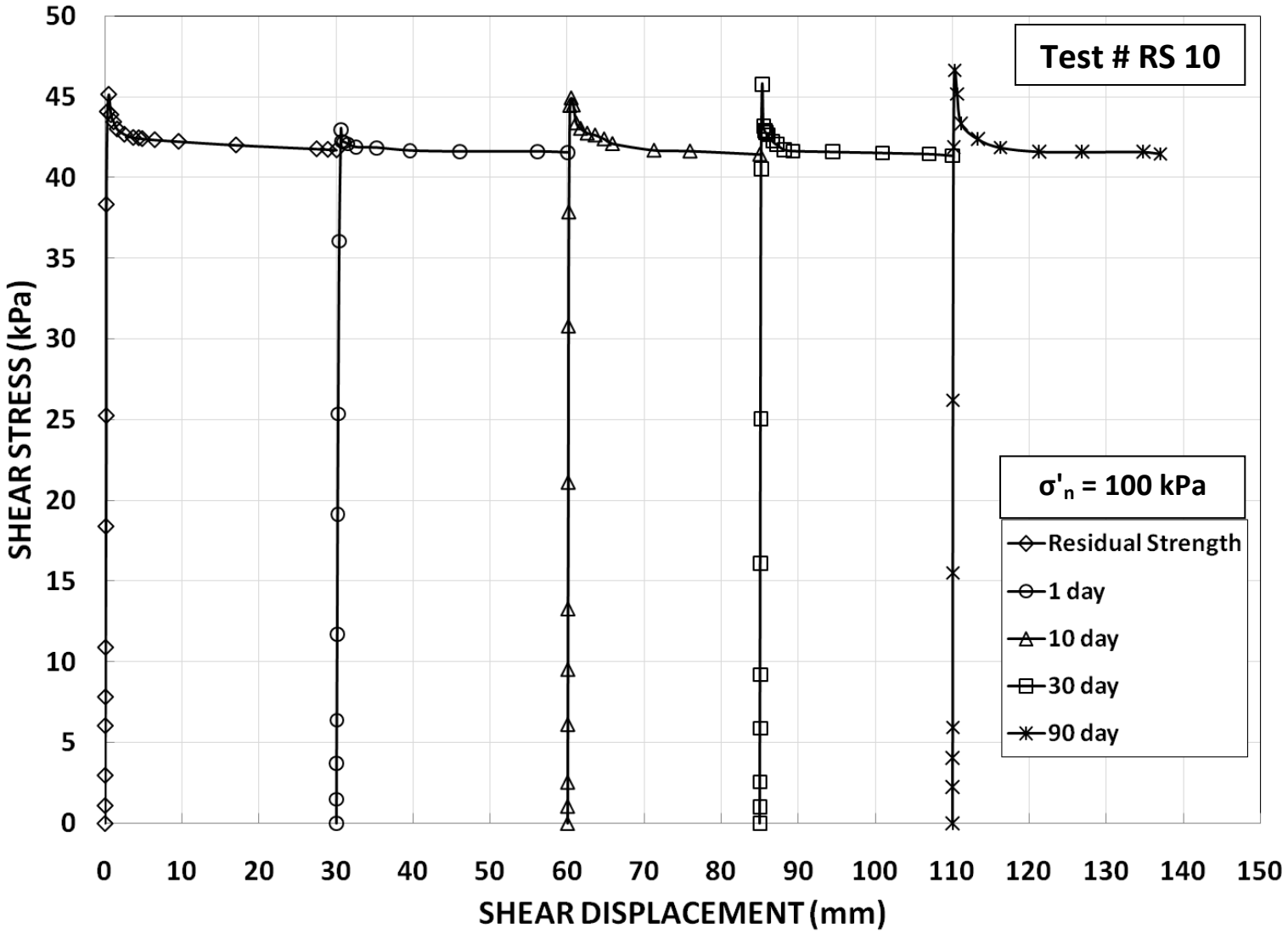

Figure C-19. Schematic diagram showing results of a strength recovery test on silty clay from Esperanza Dam, Ecuador at σ'_n = 100 kPa (RS-10 test).

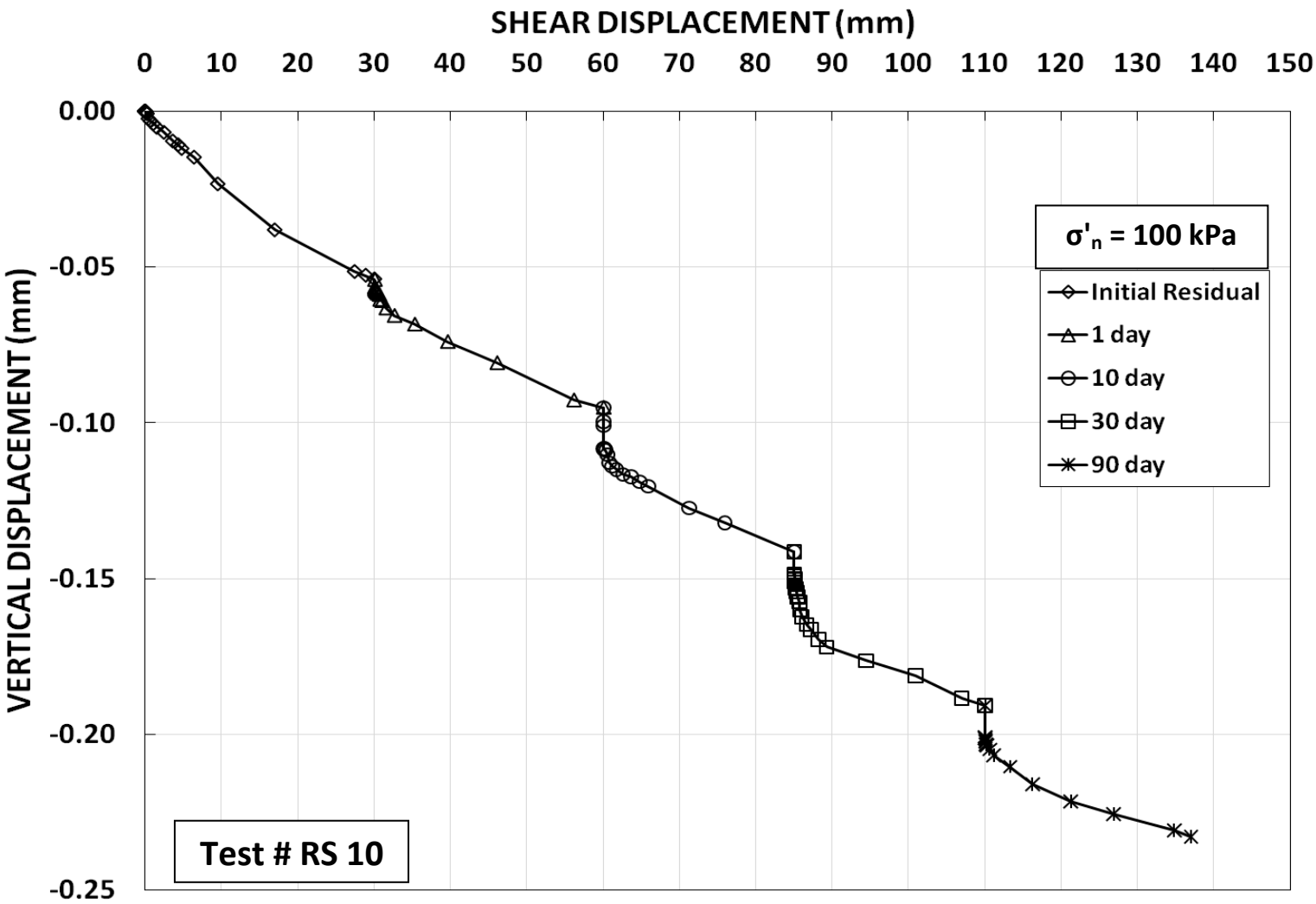

Figure C-20. Schematic diagram showing vertical settlement and shear displacement for strength recovery test on silty clay from Esperanza Dam, Ecuador at σ'_n = 100 kPa (RS-10 test).

APPENDIX D

(Residual and Fully Softened Ring Shear Test Results)

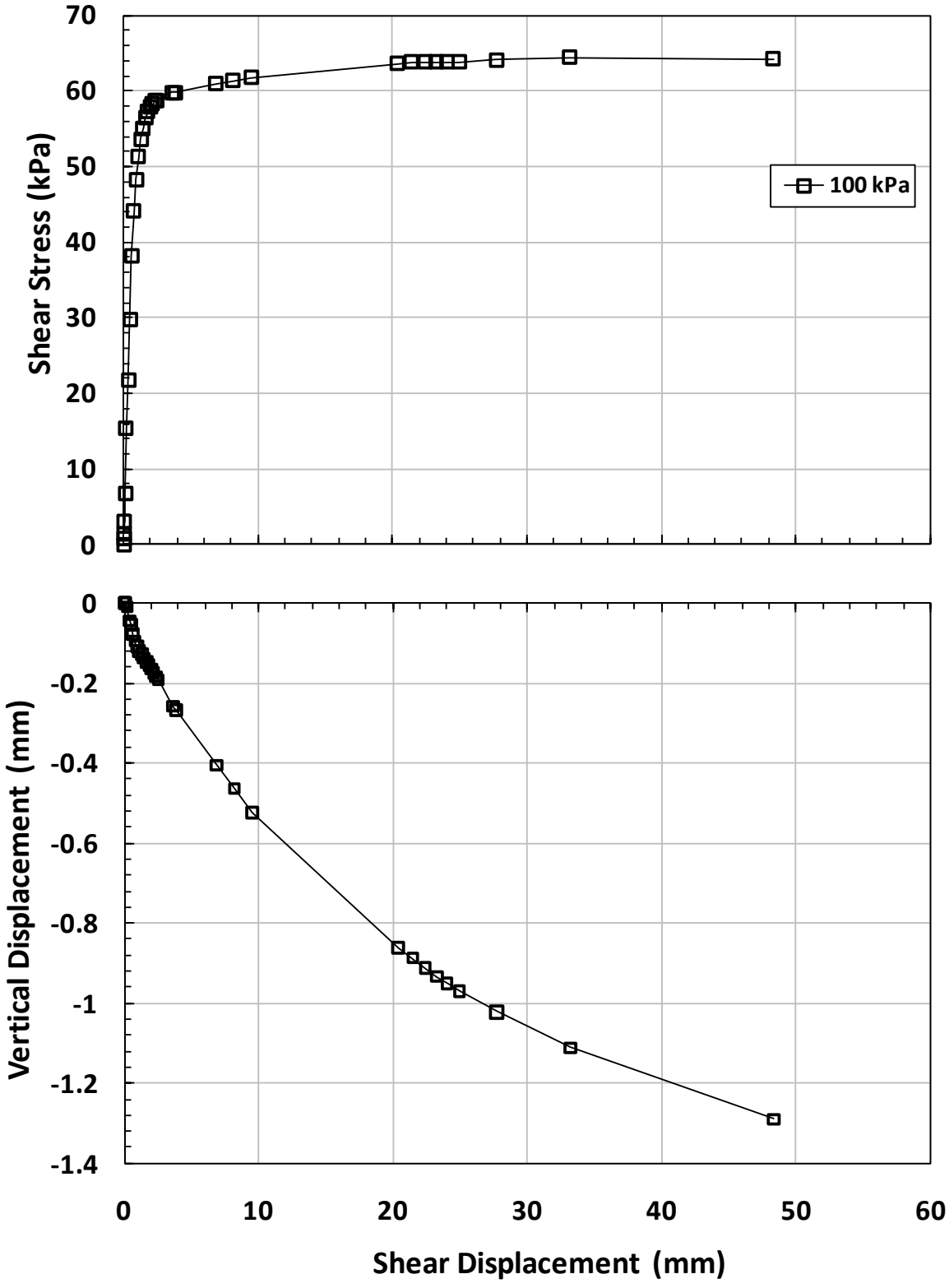

Figure D-1. Residual ring shear test result of light color yellow clay, sample from B-10 (San Antonio, Tex.).

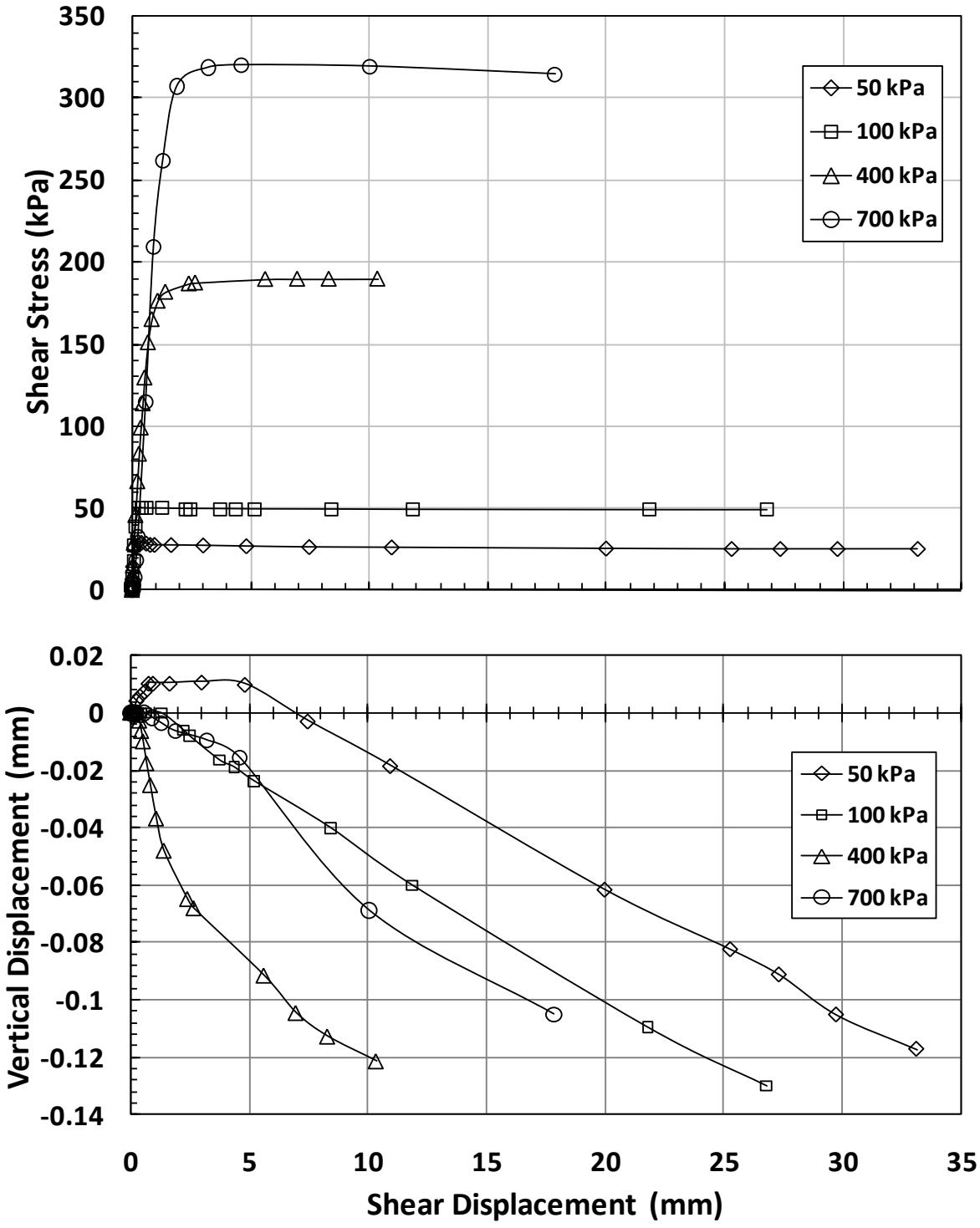

Figure D-2. Residual ring shear test result of dark color yellow clay, sample from I-9 (San Antonio, Tex.).

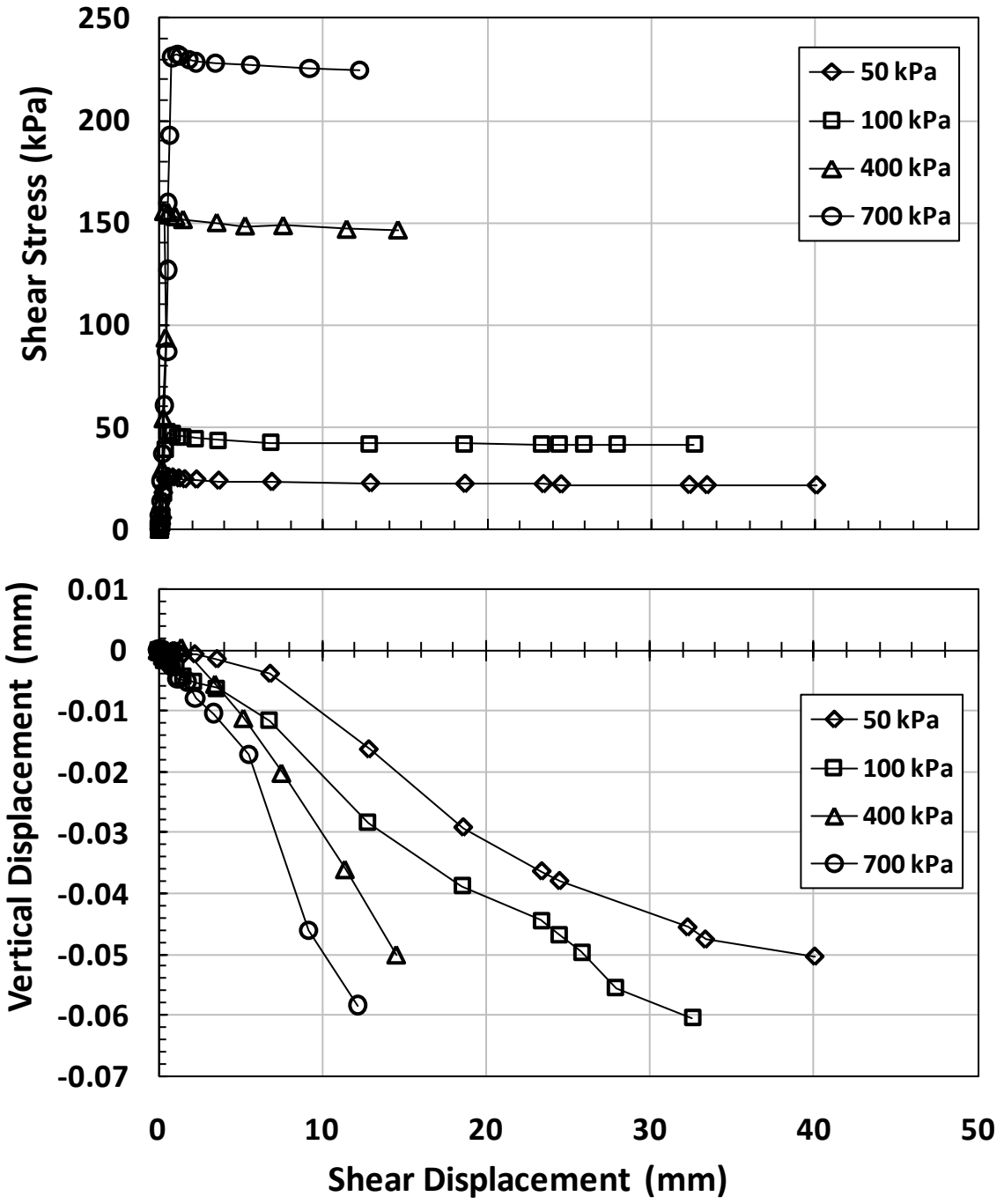

Figure D-3. Residual ring shear test result of silty clay sample from Esperanza Dam (Ecuador).

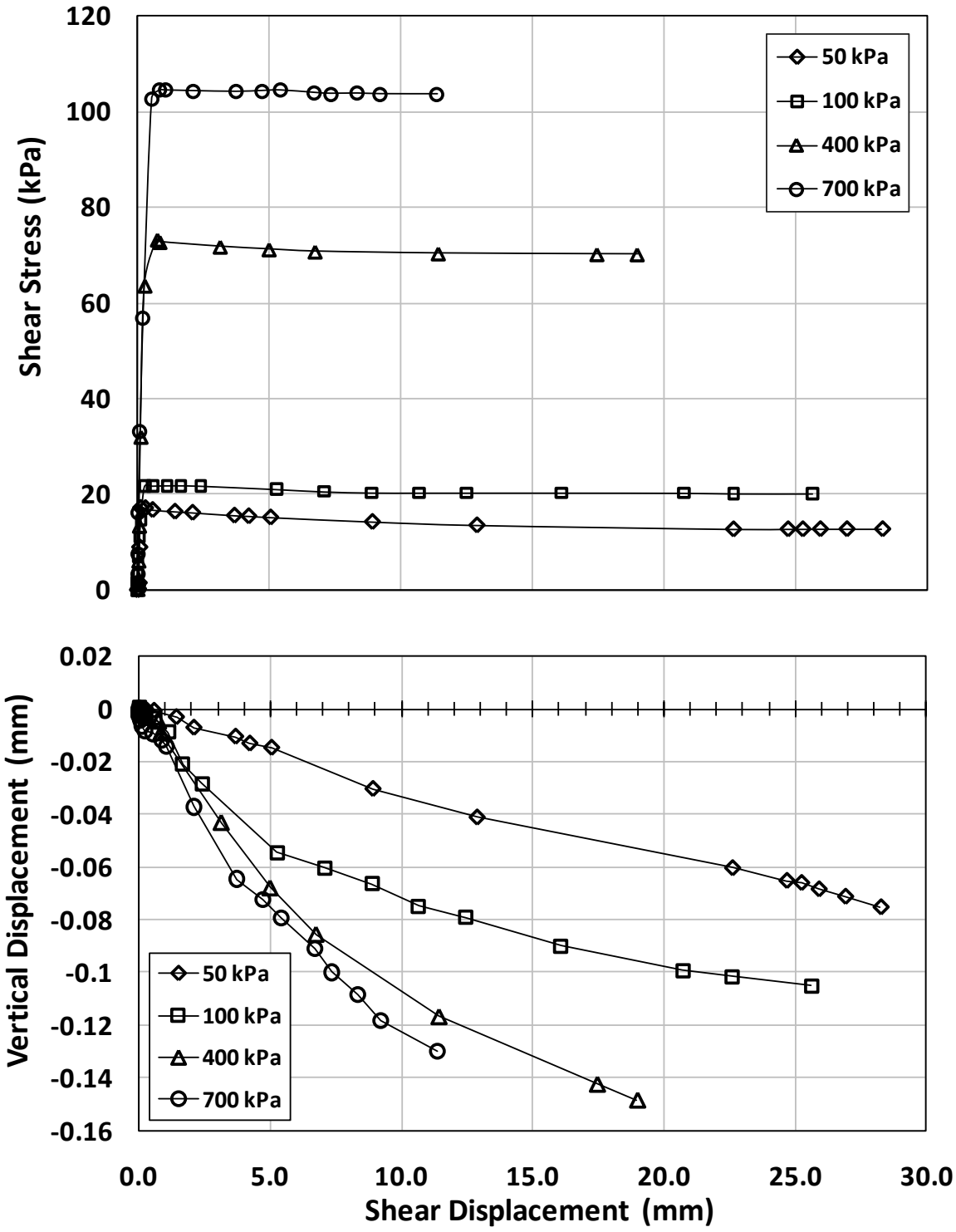

Figure D-4. Residual ring shear test result of Bel Air (GMX-1, @17 ft.) clay sample (Los Angeles, Calif.).

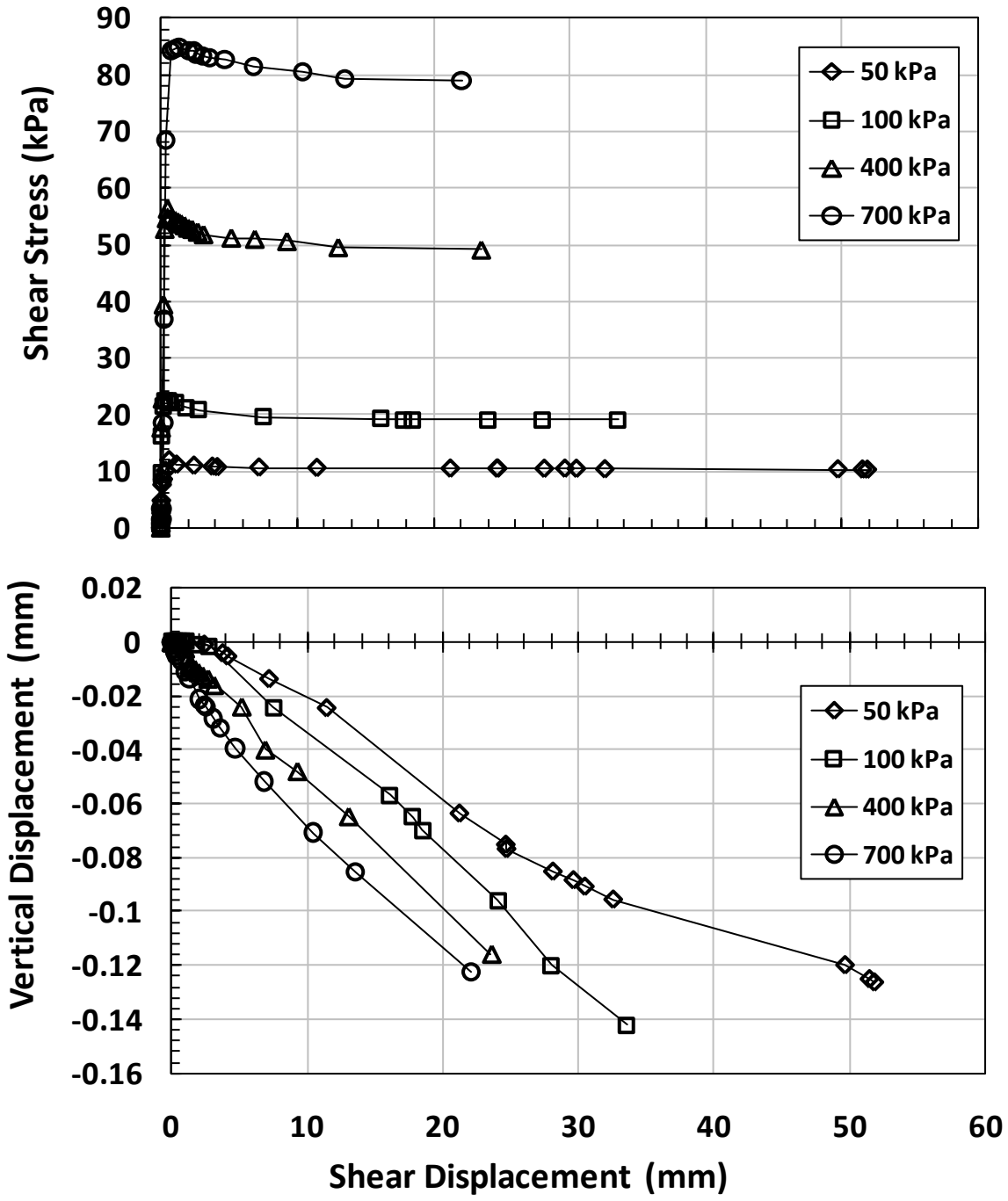

Figure D-5. Residual ring shear test result of shear surface sample of Madisette clay (Los Angeles, Calif.).

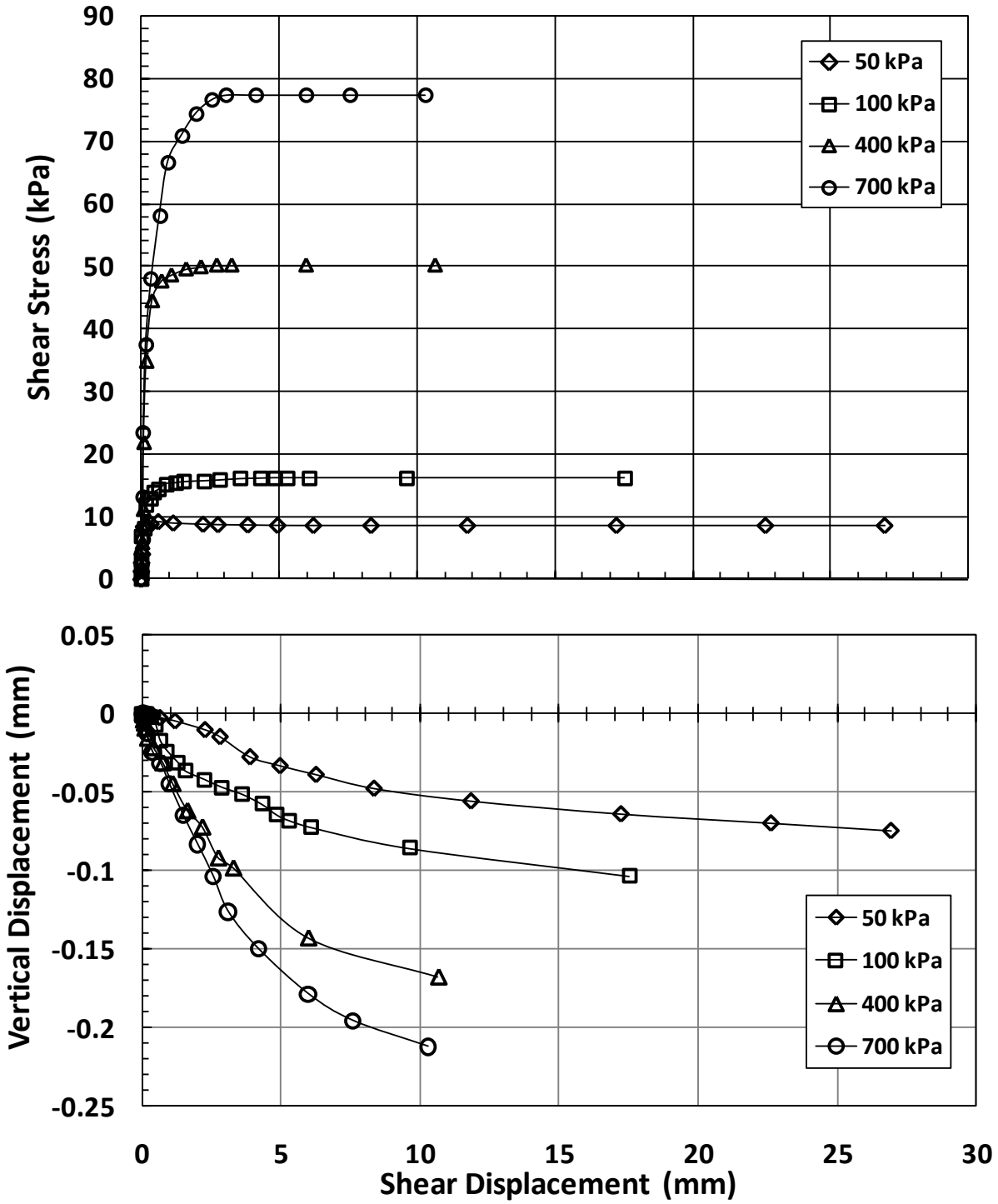

Figure D-6. Residual ring shear test result of shear surface clay sample from Soledad landslide (AG-1 @ 36 ft.) (Los Angeles, Calif.).

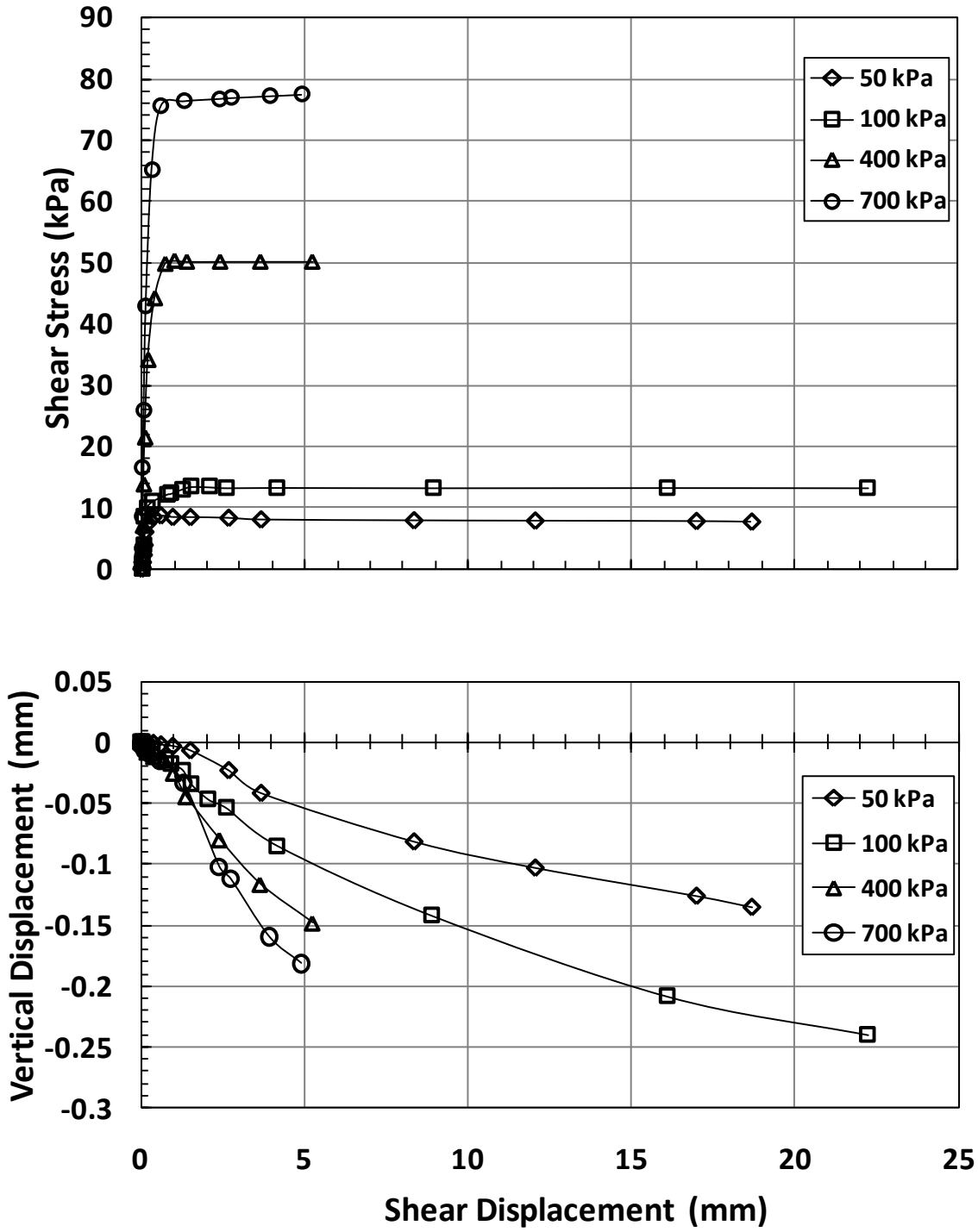

Figure D-7. Residual ring shear test result of Soledad landslide (LD-1 @ 25 ft.) sample (Los Angeles, Calif.).

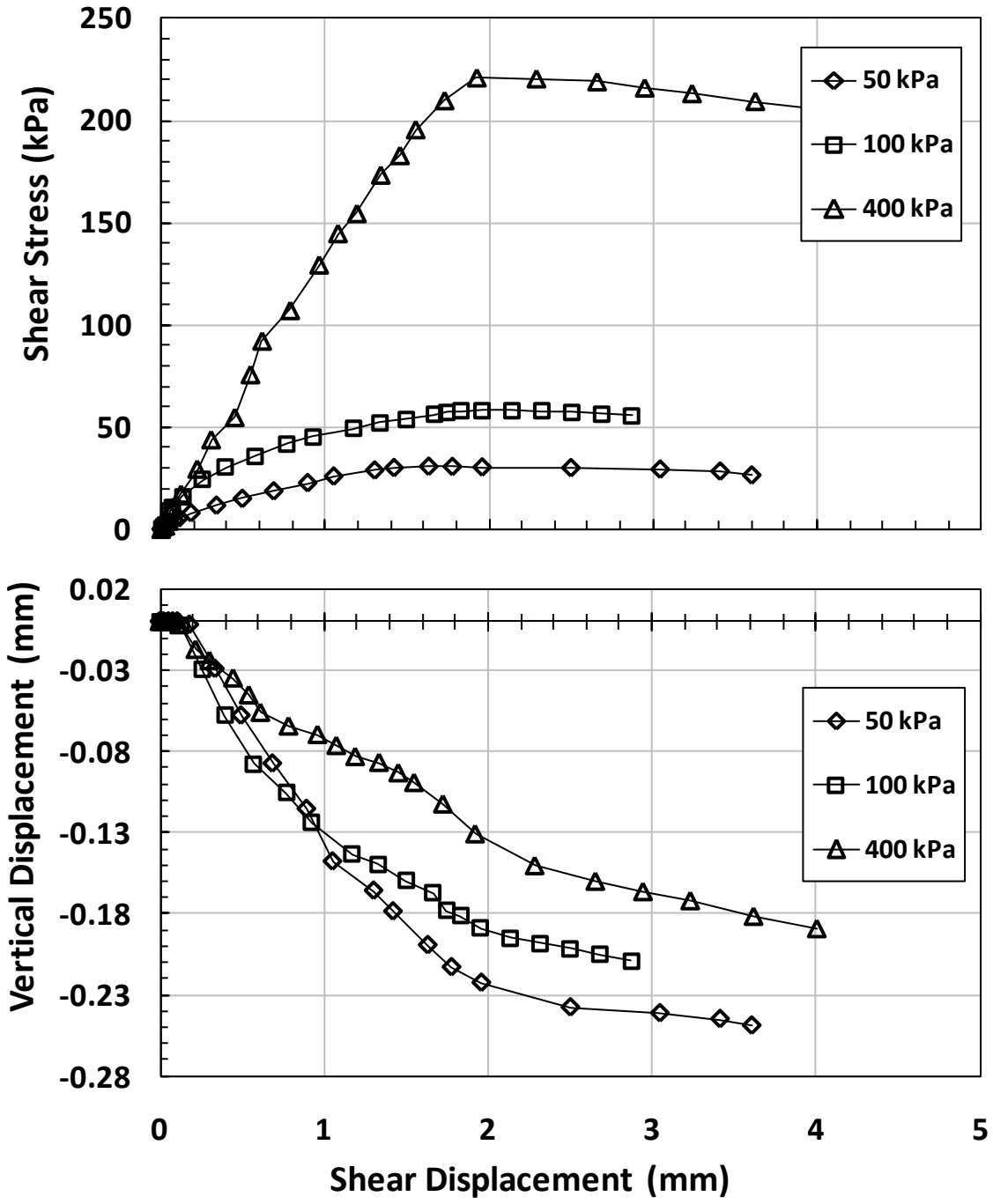

Figure D-8. Fully softened ring shear test result of silty clay sample from Esperanza Dam (Ecuador).

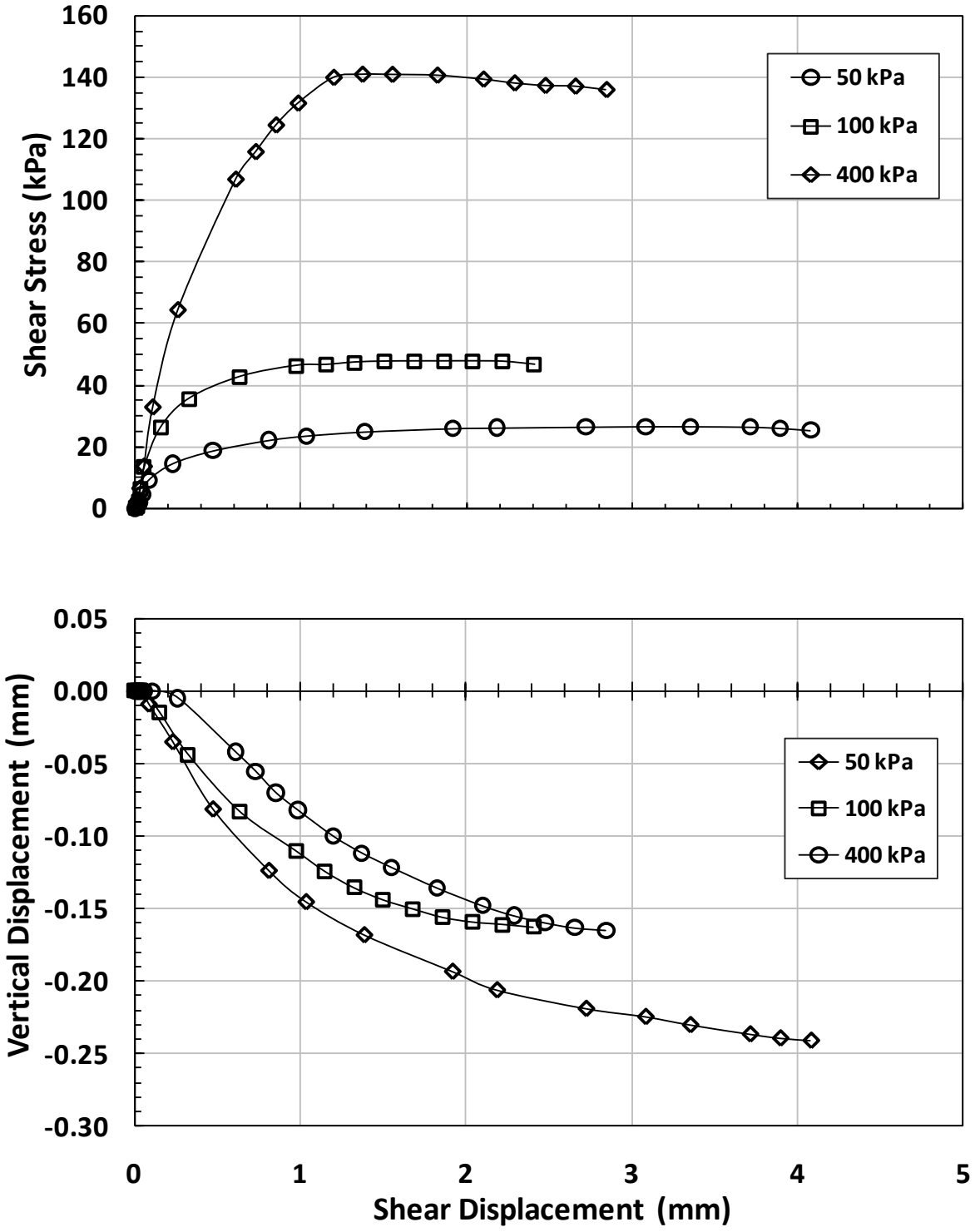

Figure D-9. Fully softened ring shear test result of Bel Air (GMX-1, @17 ft.) clay sample (Los Angeles, Calif.).

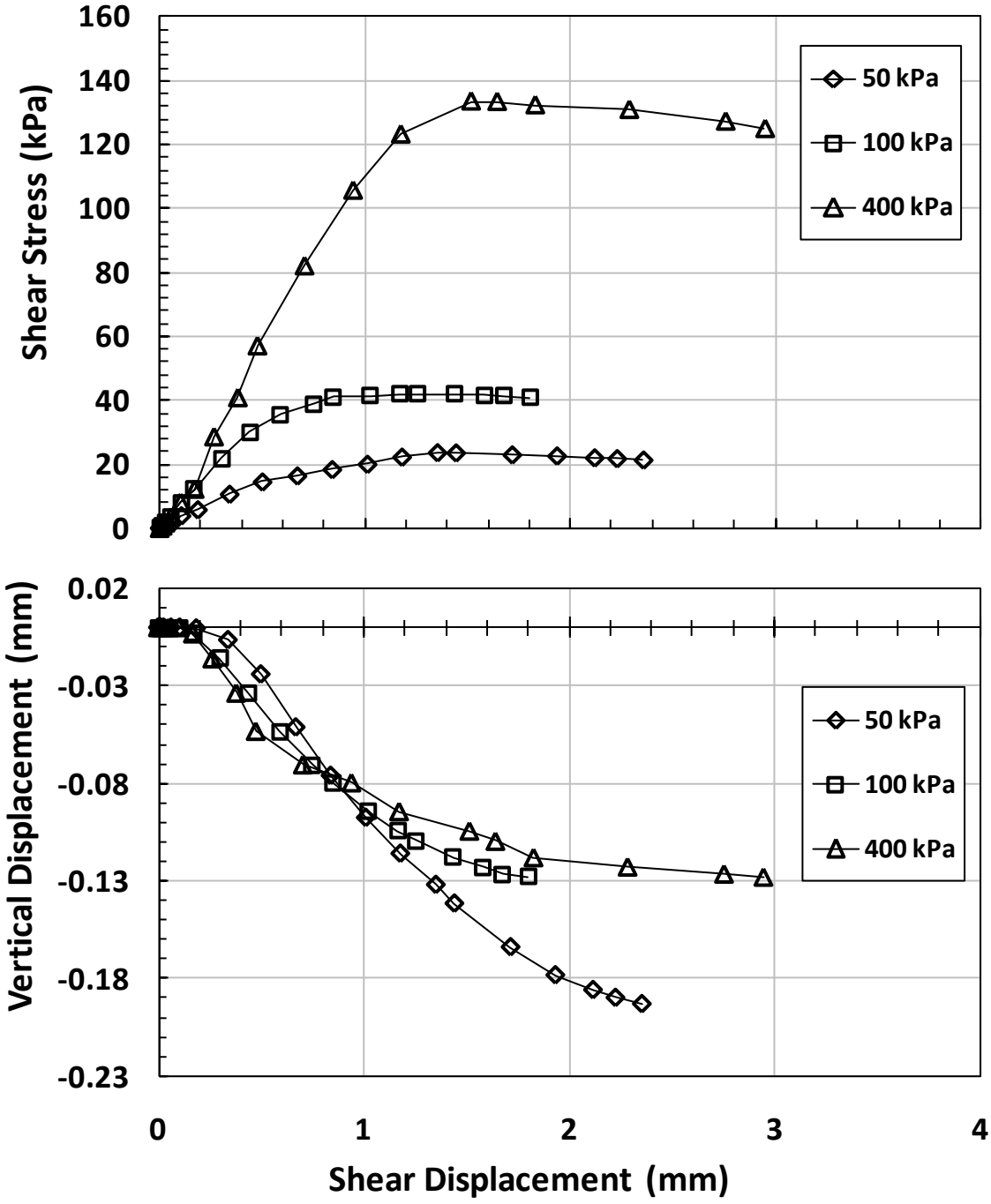

Figure D-10. Fully softened ring shear test result of shear surface sample of Madisette clay (Los Angeles, Calif.).